②

AFWL-TR-88-79

AFWL-TR-
88-79

AD-A199 564

EXPERIMENTAL STUDIES OF COAXIAL PLASMA GUN CURRENT

D. W. Price

September 1988

Final Report

Approved for public release; distribution unlimited.

DTIC
ELECTE
OCT 1 8 1988
S
E
D

AIR FORCE WEAPONS LABORATORY
Air Force Systems Command
Kirtland Air Force Base, NM 87117-6008

88 10 18 148

This final report was prepared by the Air Force Weapons Laboratory, Kirtland Air Force Base, New Mexico, under Job Order 57972501. Dr. David W. Price (AWPP) was the Laboratory Project Officer-in-Charge.

When Government drawings, specifications, or other data are used for any purpose other than in connection with a definitely Government-related procurement, the United States Government incurs no responsibility or any obligation whatsoever. The fact that the Government may have formulated or in any way supplied the said drawings, specifications, or other data, is not to be regarded by implication, or otherwise in any manner construed, as licensing the holder, or any other person or corporation; or as conveying any rights or permission to manufacture, use, or sell any patented invention that may in any way be related thereto.

This report has been authored by an employee of the United States Government and is copyright (c) by David Wayne Price. This material may be reproduced by and for the U.S. Government for Government purposes pursuant to a nonexclusive, paid-up license throughout the world granted by the author.

This report has been reviewed by the Public Affairs Office and is releasable to the National Technical Information Service (NTIS). At NTIS, it will be available to the general public, including foreign nationals.

If your address has changed, if you wish to be removed from our mailing list, or if your organization no longer employs the addressee, please notify AFWL/AWPP, Kirtland AFB, NM 87117-6008 to help us maintain a current mailing list.

This report has been reviewed and is approved for publication.

DAVID W. PRICE
Project Officer

J. DOUGLAS BEASON
Major, USAF
Chief, Advanced Concepts Branch

FOR THE COMMANDER

WILLIAM L. BAKER
Chief, Advanced Technology Division

DO NOT RETURN COPIES OF THIS REPORT UNLESS CONTRACTUAL OBLIGATIONS OR NOTICE ON A SPECIFIC DOCUMENT REQUIRES THAT IT BE RETURNED.

REPORT DOCUMENTATION PAGE

1a. REPORT SECURITY CLASSIFICATION	1b. RESTRICTIVE MARKINGS
Unclassified	

2a. SECURITY CLASSIFICATION AUTHORITY	3. DISTRIBUTION/AVAILABILITY OF REPORT
	Approved for public release; distribution
2b. DECLASSIFICATION/DOWNGRADING SCHEDULE	unlimited.

4. PERFORMING ORGANIZATION REPORT NUMBER(S)	5. MONITORING ORGANIZATION REPORT NUMBER(S)
AFWL-TR-88-79	

6a. NAME OF PERFORMING ORGANIZATION	6b. OFFICE SYMBOL (If applicable)	7a. NAME OF MONITORING ORGANIZATION
Air Force Weapons Laboratory	AWPP	

6c. ADDRESS (City, State, and ZIP Code)	7b. ADDRESS (City, State, and ZIP Code)
Kirtland Air Force Base, NM 87117-6008	

8a. NAME OF FUNDING/SPONSORING ORGANIZATION	8b. OFFICE SYMBOL (If applicable)	9. PROCUREMENT INSTRUMENT IDENTIFICATION NUMBER

8c. ADDRESS (City, State, and ZIP Code)	10. SOURCE OF FUNDING NUMBERS			
	PROGRAM ELEMENT NO.	PROJECT NO.	TASK NO.	WORK UNIT ACCESSION NO
	62601F	5797	25	01

11. TITLE (Include Security Classification)

EXPERIMENTAL STUDIES OF COAXIAL PLASMA GUN CURRENT

12. PERSONAL AUTHOR(S)
Price, David W.

13a. TYPE OF REPORT	13b. TIME COVERED	14. DATE OF REPORT (Year, Month, Day)	15. PAGE COUNT
Final	FROM Nov 85 TO Dec 87	1988 September	392

16. SUPPLEMENTARY NOTATION

Dissertation

17. COSATI CODES			18. SUBJECT TERMS (Continue on reverse if necessary and identify by block number)
FIELD	GROUP	SUB-GROUP	Plasma Guns; Plasma Sources, Plasma Accelerators, Plasma
20	09		Sheaths; Plasma Jets; Coaxial Geometry, Megampere Currents

19. ABSTRACT (Continue on reverse if necessary and identify by block number)

In this investigation of a coaxial plasma gun, plasma sheath currents and related behavior are examined. Plasma behavior in the gun affects gun characteristics. Plasma gun applications are determined by the plasma behavior.

The AFWL PUFF capacitor bank (72 μF, 29 nH, 120 kV) drives the plasma gun using a deuterium fill gas. The gas breakdown site is isolated from the dielectric/vacuum interface in the AFWL system. Two gas valves deliver gas in the system. The first delivers gas from the gun breech and the second optional valve delivers gas to the gun muzzle.

Currents and voltages are measured by Rogowski coils, $\dot{B}$ probes and capacitive voltage probes. Rogowski coils monitor current from the capacitor bank and to the plasma gun. $\dot{B}$ dot probes monitor current inside the plasma gun. Voltage probes monitor voltage delivered to the gun. Silver activation neutron detectors monitor fusion product neutrons.   (over)

20. DISTRIBUTION/AVAILABILITY OF ABSTRACT	21. ABSTRACT SECURITY CLASSIFICATION
☒ UNCLASSIFIED/UNLIMITED ☐ SAME AS RPT ☐ DTIC USERS	Unclassified

22a. NAME OF RESPONSIBLE INDIVIDUAL	22b. TELEPHONE (Include Area Code)	22c. OFFICE SYMBOL
Dr. David W. Price	(505) 844-1851	AWPP

DD FORM 1473, 84 MAR   83 APR edition may be used until exhausted.   SECURITY CLASSIFICATION OF THIS PAGE
All other editions are obsolete.

19. ABSTRACT (Continued)

A 0-D slug model is used to predict the current, inductance, gun voltage and plasma sheath velocity. The slug model assumes the sheath transits the gun with all mass in the sheath.

In the snowplow mode, the plasma sheath is thin with a sharp current rise and drop. In the deflagration mode, the plasma sheath is diffuse over a large volume. Our system operated in a transition mode between the snowplow and deflagration modes with early snowplow behavior and late deflagration behavior. Neutrons are produced in a plasma pinch at the gun muzzle, indicating snowplow behavior. The slug theory models overall gun behavior to experimental accuracy. Sheath thickness estimates show sheaths of at least 25% the gun length.

Experimental results are compared to four theories for plasma sheath velocities: the Alfvén collisionally limited model, the Rosenbluth model, the Fishbine saturated model and a single particle drift model. Experimental velocities vary from 10^5 to 10^6 m/s. Only the single particle drift and the slug model calculations are of the right magnitude (8×10^5 m/s). The Fishbine and the Rosenbluth models predict slower velocities (2×10^5 m/s). The Alfvén model is not applicable to this system.

Accession For

NTIS GRA&I	☒
DTIC TAB	☐
Unannounced	☐
Justification	

By

Distribution/

Availability Codes

Dist	Avail and/or Special
A-1	

DT .
COPY
INSPECTED
1

CONTENTS

CONTENTS (CONTINUED)

CONTENTS (CONTINUED)

CONTENTS (CONTINUED)

CONTENTS (CONCLUDED)

FIGURES

FIGURES (CONTINUED)

FIGURES (CONTINUED)

FIGURES (CONCLUDED)

TABLES

1.0 INTRODUCTION

1.1 HISTORIC PERSPECTIVE

Mechanically simple, but dynamically complex, coaxial plasma guns have been investigated and used in plasma physics experiments since the early 1960's. A schematic of a simple coaxial plasma gun is shown in Figure 1. Coaxial plasma guns consist of an inner and outer electrode and an annular region between. At one end, the two electrodes are separated electrically, usually by a dielectric material. The annular region is evacuated by vacuum pumps and a gas is inserted (near the end of the coaxial plasma gun where the insulator is located). An electrical potential is applied across the annular region by biasing the inner and outer electrodes. The gas, electrically stressed past its breakdown voltage (determined by the physical and chemical components of the individual gas and by the electrode geometry), breaks down (ionizes and carries electrical current) and allows a radial current J_r to flow between the electrodes.

The gas breakdown is characterized by a Paschen gas breakdown curve. The Paschen curve shows a function of gas dielectric strength (measured by the breakdown voltage) as a function of the gas fill pressure. The pressure can range from 10^{-7} Torr to tens of atmospheres. At the extreme low end of the gas pressure curve, the fill gas acts like a vacuum with its resultant high dielectric breakdown strength. At the high end of the gas pressure curve, the fill gas has its characteristic breakdown voltage. In the region between, where the gas pressure is

1

neither high nor low, the gas sustains a breakdown at a reduced voltage. (The smallest breakdown voltage for any fill gas and given geometry is defined to be the Paschen minimum.) While this generalized behavior is both electrode geometry and fill gas dependent, the trend remains the same for all gases.

This radial current J_r creates an azimuthal magnetic field B_θ. The radial current interacts with the self-produced magnetic field B_θ to create a driving force F defined by the vector cross product of J_r and B_θ given in equation (1.1.1).

$$F = J_r \times B_\theta \qquad\qquad (1.1.1)$$

The driving force F accelerates the plasma down the axial length of the coaxial plasma gun toward the gun muzzle (the open end of the plasma gun) with an acceleration a determined by the driving force and the accelerated mass.

The coaxial plasma gun operates in several regimes or modes. One of these modes is the snowplow mode [1]. Another mode is the deflagration mode [2]. The transition region of operation between snowplow and deflagration modes can be considered an intermediate mode [3].

The snowplow mode occurs when a plasma sheath sweeps up gas as it travels in the coaxial plasma gun. The snowplow mode occurs in a coaxial plasma gun when a thin plasma sheath is formed by the electric breakdown of a gas, usually at an insulator/vacuum interface in the gun.
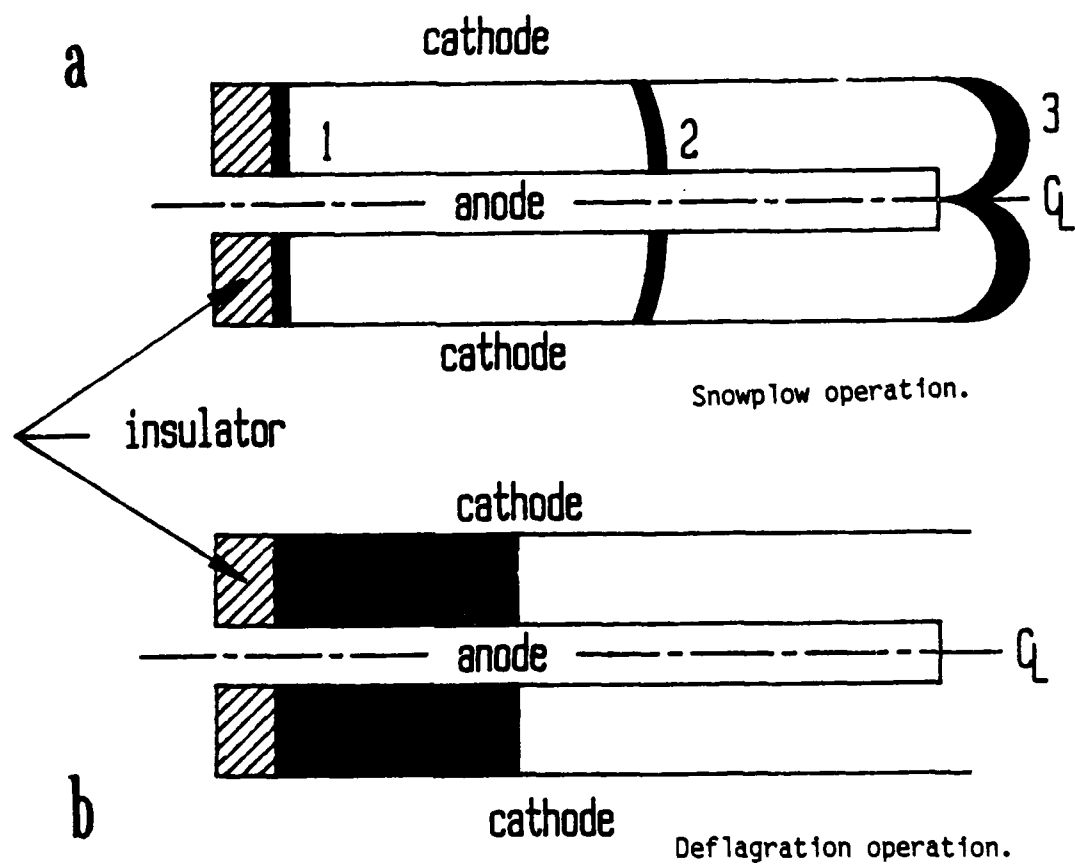
Figure 1. Coaxial plasma gun operation.

(This is indicated by the number 1 in Figure 1a.) The sheath "lifts off" or separates from the insulator and drives it from the electrode/vacuum interface down the length of the coaxial gun by the $J \times B$ force. (This is indicated by the number 2 in Figure 1a.) The snowplow mode drives mass ahead of the sheath and carries it with the sheath until the plasma sheath and the entrained mass reach the end of the gun. This accumulation and forcing a mass of gas ahead of the sheath, like a snowplow pushing a snow mass, give the snowplow mode its name. The snowplow coaxial plasma gun produces a plasma that is denser and thermally hotter than the deflagration mode. The snowplow mode is the mode used to produce the plasma focus (PF) behavior at the end of the plasma gun. (This is indicated by the number 3 in Figure 1a.) A great deal of research has been performed on the snowplow mode. This work includes different research aspects done in the Marshall/Mather coaxial geometry [4-23] and in the Filippov geometry [24-26].

The deflagration mode of the coaxial plasma gun occurs when a discharge is formed near the insulator end of the gun annulus and does not lift off the insulator surface. (A deflagration mode is indicated in Figure 1b.) A thick plasma discharge forms a stationary or quasi-stationary plasma sheath. The plasma sheath grows as mass is inserted. The deflagration mode was so named by Cheng [27] when he compared it with the motion of chemical combustion or deflagration. The deflagration mode produces a plasma less dense than the snowplow mode. The deflagration mode plasma produces a cooler plasma than the snowplow mode, but the plasma is more directed. Being less dense and more susceptible to magnetic field diffusion into the plasma, the

4

deflagration mode is used to produce plasmoids (plasma slugs) with embedded magnetic fields. Experimental and theoretical work on the deflagration mode of coaxial plasma guns has been performed by different researchers [28-31].

The transition mode is neither the snowplow mode or the deflagration mode, but has characteristics of both. In the experimental series reported by Len [3], transition modes occurred infrequently. Transition behavior starts off with snowplow characteristics and becomes more like the deflagration mode.

Coaxial plasma guns must be supplied with gaseous material. Gas can be supplied to the plasma gun prior to gun operation. The static fill (prefill) mode occurs when gas is provided to the gun on time scales much longer than the gun operation, so fill gas is quiescent in the coaxial gun annulus. The puffed gas mode occurs when the gas in provided to the plasma gun through a fast opening gas valve. Although not generally used for experimentation, gas can be provided to the plasma gun continuously. The prefill mode generally produces the snowplow mode. Depending on the gas arrival time and the gas density in the gun annulus, the puffed fill gas operation produces either snowplow or deflagration mode characteristics. The continuous gas fill generally produces the deflagration mode.

The coaxial plasma gun is similar to the pulsed dielectric erosion accelerator [32-42]. Behavior of the erosion accelerator has been shown to manifest aspects of both snowplow and deflagration behavior. The

difference between the pulsed dielectric erosion accelerator and the coaxial plasma gun is the dielectric erosion accelerator uses an electrically stressed and ablated solid insulator as the sole plasma source; the coaxial plasma gun uses a gas supplied to the gun. Because of the nature of the breakdown and evolution of the dielectric, it is probable the pulsed dielectric erosion accelerator will produce a snowplow mode.

The plasma focus is a product of the coaxial plasma gun operating in the snowplow mode [43-72]. The plasma sheath traveling the length of the gun converges (pinches) upon itself at the muzzle forming a dense plasma. The mechanisms for plasma equilibration in a PF are complex, involving the radial collapse of the sheath, the conversion of plasma sheath kinetic and magnetic energy into thermal energy and the chaotic turbulence created in these processes. When deuterium (D_2) gas or a deuterium gas mixture is used in the snowplow mode, high energy neutrons are formed as a result of the D-D nuclear fusion reactions. The PF can thus serve as an intense neutron source. The PF work is reported in this dissertation in its relation with the operation and behavior of the coaxial plasma gun and the total nuclear fusion neutron output. The actual physics of a plasma focus is beyond the scope of this dissertation and is not examined.

The coaxial plasma gun has a long history going back to the early 1960's. Related work had been done prior to that time. Electromagnetic shock tubes [73-84] have been used to create plasmas. These shock tubes can be used to create plasmas with high Mach numbers. Theta pinch guns

[85-87], both straight and conical, have been used to generate plasmas.
The behavior of z-pinches [88-96] where a current flows along the length
of the plasma is similar to the behavior of coaxial plasma guns. As
Fishbine [97] notes, the coaxial plasma gun in the snowplow mode is
topologically equivalent to a z-pinch. While this related work is
interesting and deserving of further study, it is also beyond the scope
of this dissertation. It is mentioned to give a flavor of devices
similar to the coaxial plasma gun.

1.2   INDIVIDUAL AND ADMINISTRATIVE PERSPECTIVE

From 25 November 1983 to 16 January 1984, coaxial plasma gun experiments
were performed by members of the Experimental Section, Plasma Physics
Branch, Simulation Division, Nuclear Technology Office of the Air Force
Weapons Laboratory (AFWL) on Kirtland AFB NM. There were a total of 177
firings (shots) of the PUFF bank into a coaxial plasma gun load. The
personnel performing the experiments were: Capt Charles W. Beason, Dr.
James H. Degnan, Lt Michael P. Snell, Lt Stephen W. R. Warren and the
author. These Air Force Weapons Laboratory personnel were assisted by
Airman Peter J. Lagomarsino, Dale L. Ralph and Brian N. Woolweber of the
Air Force Weapons Laboratory and Jack D. Graham and Emmanuel A. Lopez of
Maxwell Laboratories Inc. of Albuquerque. This particular series of
experiments was subsequent to an experimental series on the PUFF
capacitor bank performed in February 1983 by Dr. Degnan, Lt Warren and
Robert J. Richter-Sand, all of the Air Force Weapons Laboratory.

The initial results from this series of experiments were reported in 1984 [98-101]. An overview of the experimental effort was published in 1987 by Degnan et al. [102]. Calculated high energy photon spectra from these experiments were published by Beason [103] and Warren et al. [104]. In this dissertation, the coaxial plasma gun current and magnetic field behavior is specifically discussed and analyzed.

The data given here deal with the subset of the PUFF experimental effort from 29 December 1983 to 12 January 1984. In this series, small $\dot{B}$ loops, Rogowski coils and capacitive voltage monitors were used to analyze the flow of plasma current down the length of the coaxial plasma gun. Although Rogowski coils and capacitive voltage probes were used for the total experimental effort, only in this experimental subset were the $\dot{B}$ probes used. In this portion of the experimental series there was a total of 51 shots. Of these 51 data shots, 12 were shots where the circuit was shorted, either because the gas valve did not fire properly or because there was a breakdown at various regions of the transmission line/insulator/vacuum interfaces. The remainder of the shots yielded data sufficient for data analysis of the coaxial plasma gun. On that data is this dissertation produced.

1.3 APPLICATIONS OF COAXIAL PLASMA GUNS

Coaxial plasma guns have been studied and considered for several differing kinds of applications. Even if coaxial plasma guns are not completely understood, they have been proposed for and are used in various applications. While the applications are not vast, they do vary

considerably. These include use in aerospace and extraterrestrial transport [105-110], excitation of gas lasers [111-116], plasma insertion into experimental systems [117-133], fueling for proposed thermonuclear reactors [134-138], breeding fissionable material [139, 140] and treatment of metallic surfaces [141-143].

1.4 RATIONALE FOR STUDY

Although many researchers feel the flow of the plasma in a coaxial plasma gun is well-understood and not worthy of investigation, it is not clear this is the case. Len's work shows complexities do exist in the operation of the plasma gun. Other researchers, aside from observing that current flows in a plasma sheath and the plasma sheath can be parabolic in the radial-axial plane (see, for example, the sheath profiles in references 69 and 144), little research has been devoted to understanding the behavior of the plasma internal to the coaxial gun. It is not clear the plasma sheath is not also a function of gas breakdown and coaxial gas gun insulator effects. Few published studies have been performed that monitor the specific behavior of the plasma sheath in the gun. Whether this is due to greater interest in the behavior of the plasma focus or not, the behavior of the current sheath generally is assumed and analysis proceeds from that point. The work described here indicates the current sheath behavior may show characteristics that an assumed current sheath behavior does not address.

Additionally, the AFWL gun differs from the previously reported coaxial

plasma guns in several respects. Although the details are reported in

subsequent sections, these distinctives are stated here. The first

difference is the insulator is distant and isolated from the gas

breakdown, i.e., the gas does not (usually) breakdown at an

insulator/vacuum interface. The gas insertion point is obscured from

the coaxial gun insulator by means of anodized helical baffled

electrodes. The second difference is the voltage regime of operation.

The charge voltage for the coaxial plasma gun ranges from 60 to 70 kV in

the experimental sequence described here. Most reported work on coaxial

plasma guns has been at voltages of 40 kV or less. The stored energy

delivered to the coaxial plasma gun from the PUFF capacitor bank ranges

from 130 to 176 kJ. The energy used in many other coaxial plasma guns

ranges from 10 kJ up to 1 MJ. Related to this, the inductance of the

AFWL PUFF capacitor back delivering energy to the coaxial gun is

approximately 9 nH, less than most coaxial gun systems. (The electrodes

and the coaxial gun connections increase the system inductance to 29

nH.) A third difference is the AFWL plasma gun uses a rod array for an

outer electrode. This is a "squirrel cage" geometry. Many other

reported coaxial plasma guns have solid outer electrodes. Another

difference between the AFWL PUFF coaxial plasma gun and other coaxial

plasma guns is the gas fill mechanism. In many other guns, the gas is

injected at the central anode near the vacuum/dielectric insulator

interface or the gun is filled in a static mode. In the AFWL gun, the

gas is inserted in the gun through a fast gas valve away from the

vacuum/dielectric interface. In other experiments, where $\dot{B}$ probes have

been reported as being inserted in the plasma, they generally are

10

inserted through the outer electrode. In this study, these probes are inserted through the inner electrode.

1.5 PURPOSE AND TECHNICAL OBJECTIVES OF THE CURRENT STUDIES

This purpose for this study is to analyze the current behavior of a coaxial plasma gun. This analysis will be based on the experimental data taken from detailed magnetic field and current measurements of the AFWL coaxial plasma gun driven by the 72 μF PUFF capacitor bank. Both the total current and the current within the coaxial plasma gun will be analyzed. Additionally, the D-D nuclear fusion product neutrons resulting from the experiment will be compared to standard plasma focus current scaling.

The stated purpose gives rise to four technical objectives addressed in this dissertation:

1) Observe the plasma sheath behavior in the AFWL PUFF coaxial plasma gun;

2) Provide a simple model of the plasma sheath behavior;

3) Correlate the plasma sheath behavior with independent observable behavior in the AFWL PUFF coaxial plasma gun, including the observables of the probe voltage, the neutron yield and the system inductance; and

11

4) Characterize the behavior of the plasma sheath within the accuracy of the experimental data.

1.6 OVERVIEW OF THE CURRENT STUDIES

This dissertation is divided into sections. Each section details a major portion of these studies. Section 1 provides introductory material outlining the context of these studies. Section 2 provides a discussion of the experimental considerations of the data reported here. Section 3 provides the details of the AFWL coaxial plasma gun. Section 4 details the methods and results of the experimental analysis. Section 5 provides the summary and conclusions of the experimental results. Appendices with related information follow the main body of the dissertation.

2.0 EXPERIMENTAL CONSIDERATIONS

The experimental hardware used in this series of experiments is discussed in this section. Both the experimental equipment and the diagnostic hardware are discussed here.

As an overview, Figure 2 shows a photograph of the PUFF coaxial gun experiment. The PUFF bank is so named because it was built to perform experiments with injected or puffed gas. The upper portion of one of the capacitor bank modules is seen in the left rear of the picture. The transmission line and insulating Mylar film is seen in the middle. At the center of the transmission line is the vacuum vessel containing the coaxial plasma gun. At the top of the vacuum vessel is the gas line for the upper gas valve used in some of the experimental series described here. Lead bricks and lead sheets are mounted on the transmission line to keep the transmission line and the electrodes from being damaged by the mechanical shock created by the system current at discharge (on the order of 1.2 to 3.0 MA when the total bank voltage is 60 kV).

A schematic of the PUFF coaxial gun system is given in Figure 3. The coaxial gun consists of the anode and cathode structures. Except for the rod structure of the cathode (24 rods), the coaxial plasma gun is azimuthally symmetric along the center line. A fast gas valve feeds a flow volume of about 25 cm^3 (2.5×10^{-5} m^3) in the hollow center of the anode, entering the gun annulus through holes drilled in the anode. Where it enters the plasma gun, the gas will electrically break down when it is stressed beyond its dielectric strength. When it is used,

13

Figure 2. AFWL PUFF capacitor bank system.

14
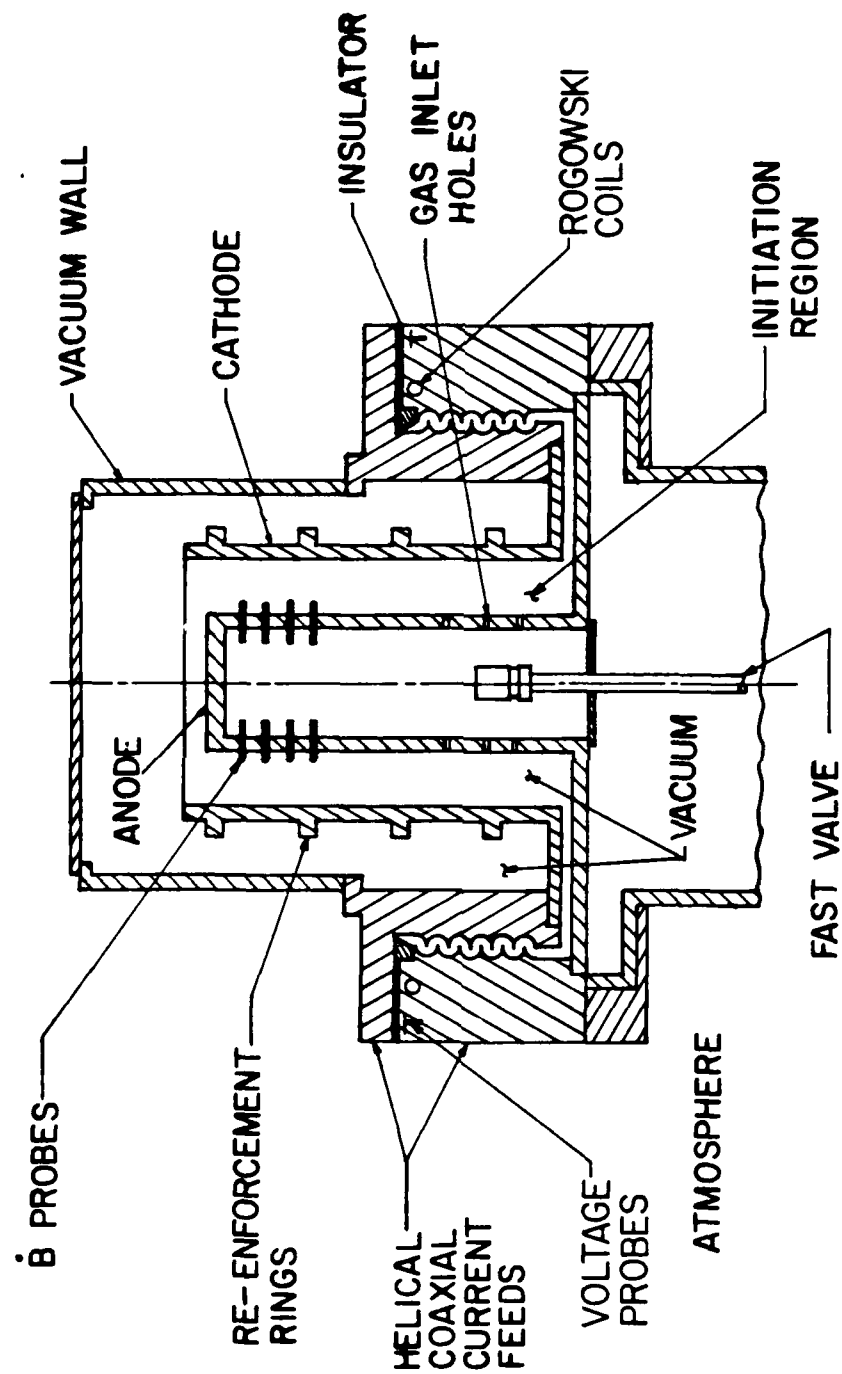
Figure 3. Coaxial gas gun schematic.

VACUUM WALL

CATHODE

INSULATOR

GAS INLET HOLES

ROGOWSKI COILS

INITIATION REGION

ANODE

VACUUM

B̊ PROBES

RE-ENFORCEMENT RINGS

HELICAL COAXIAL CURRENT FEEDS

VOLTAGE PROBES

ATMOSPHERE

FAST VALVE

15

the upper gas valve feed is mounted above the anode (along the centerline) atop the vacuum vessel. The current and voltage are fed to the plasma gun by helical coaxial feed electrodes. (These electrodes were used by Turchi et al. in AFWL SHIVA experiments [145].) The anode is attached, mechanically and electrically, to the lower helical electrode. The cathode is similarly attached to the upper helical electrode. The electrodes are helically baffled to reduce the incidence of insulator breakdown from exposure to ultraviolet light created by electrical discharges. The calculated inductance of the helical baffle structure is 10.1 nH from the transmission line to the base of the plasma gun electrodes.

A polyethylene insulator electrically separates the two electrodes in the vacuum region. The insulator is sloped according to Milton's findings [146] to reduce the possibility of insulator/vacuum interface voltage breakdown. A vacuum vessel surrounds the coaxial plasma gun and is attached to the upper helical electrode. Prior to the feed gas insertion, the coaxial gas gun is evacuated to about 10^{-5} Torr. At the time of the capacitor bank discharge, slow gas valve leaks raise the background vacuum vessel pressure to about 10^{-4} Torr.

2.1 AFWL PUFF CAPACITOR BANK

The AFWL PUFF capacitor bank consists of two modules made of capacitors and rail gap switches. Each module consists of 24 capacitors and 4 rail gap switches. The total effective capacitance of the PUFF bank is 72

µF. The modules feed a parallel plate transmission line connected to
the load.

The modular capacitor bank consists of capacitors in a series/parallel
configuration. Twelve capacitors (in parallel configuration) are
connected to the upper transmission line through four rail gap switches.
The other twelve capacitors are connected to the lower transmission line
through four rail gap switches. Since the upper polarity is negative
and the lower polarity is positive, the effective voltage delivered to
load is twice the charging voltage.

The capacitors are all Maxwell Laboratories high energy density
capacitors, model number 32184 [147]. These have a nominal capacitance
of 6 µF. They are rated to 60 kV (10.8 kJ stored electrical energy)
with up to 65% voltage reversal. They are rated to a peak current of
230 kA and a life of over 10,000 (charge and discharge) cycles. The
approximate inductance for a single capacitor is 35 nH.

The rail gap switches are all Maxwell Laboratories rail gap switches,
model number 40200 [148]. They are rated for switching voltages from 60
to 120 kV. Each rail gap is rated to conduct a maximum of 750 kA and up
to 10 C of charge. Switch jitter is less than 2 ns. Typical single
switch inductance is 20 nH. Minimum rated switch life is 5000 shots.

Experimental inductance for each module (including the 24 capacitors and
the four rail gap switches) is 12 to 14 nH. Since the two modules are
in parallel, the total PUFF inductance is 6 to 7 nH.

17

In this series of experiments, one leg of the transmission line has an inductance of 3.3 nH. Since both legs of the transmission line are in parallel, the total transmission line inductance is 1.7 nH. Excluding the load, the PUFF system inductance is 8 to 9 nH.

2.2 TRANSMISSION LINE

The transmission line has three parts. Two identical parts attach to one of the two switch outputs. These are 6' 4" (1.930 m) wide and 3' 6" long (1.067 m) aluminum plate pairs. The third part of the transmission line (also an aluminum plate pair) connects the other two portions of the transmission line to the helical coaxial gun feed electrodes. The dimensions of this third transmission line portion are 6' by 6' (1.829 by 1.829 m) excluding the area required by the helical feed electrodes. The helical feed electrodes are in the center of the transmission line. These electrodes have a diameter of about 2' (0.6 m). The transmission line has a total capacitance of 62.5 nF for the whole transmission line, from the switches to the feed electrodes. This assumes a dielectric constant of 2.3 for the Mylar (polyethylene erephthalate) insulation and a transmission line electrode separation of 92.2 mils (2.34×10^{-3} m).

2.3 COAXIAL PLASMA GUN

The coaxial gun consists of the two electrodes, the inner anode and the outer cathode. The anode outer diameter is 5.125" (0.1302 m). The cathode inner diameter is 7.0" (0.1778 m). The coaxial gun is 24.75"

(0.6287 m) long. Using the formula for coaxial transmission line
inductance

$$L = \frac{\mu_0 z}{2 \pi} \ln \left(\frac{b}{a} \right)$$

where L is inductance in Henries, μ_0 is permeability of free space
($4\pi \times 10^{-7}$ Henries/meter), z is length of the coaxial region, b is outer
radius and a is inner radius. The coaxial gun inductance is about 39.2
nH. From the base of the helical feed electrodes to the center of the
gas feed holes in the anode, the inductance is 15.3 nH.

The capacitance of the coaxial gun can be derived from the relation

$$C = \frac{2\pi \varepsilon_0 z}{\ln \left(\frac{b}{a} \right)}$$

where ε_0 is permittivity of free space (8.854×10^{-12} Farads/meter) and a,
b and z are previously defined. The coaxial plasma gun capacitance is
0.11 nF. This is small compared to the PUFF bank capacitance (72 μF)
and is neglected.

Two views of the inner electrode can be seen in Figures 4 and 5. In
Figure 4, the inner electrode is not attached to the gas gun prior to
mounting on the lower electrode. The array of 96 gas inlet holes can be
seen on the electrode. These gas inlet holes are 0.25" (6.35×10^{-3} m) in
diameter. The gas inlet holes cover a length of 1 1/2" (3.81×10^{-2} m)
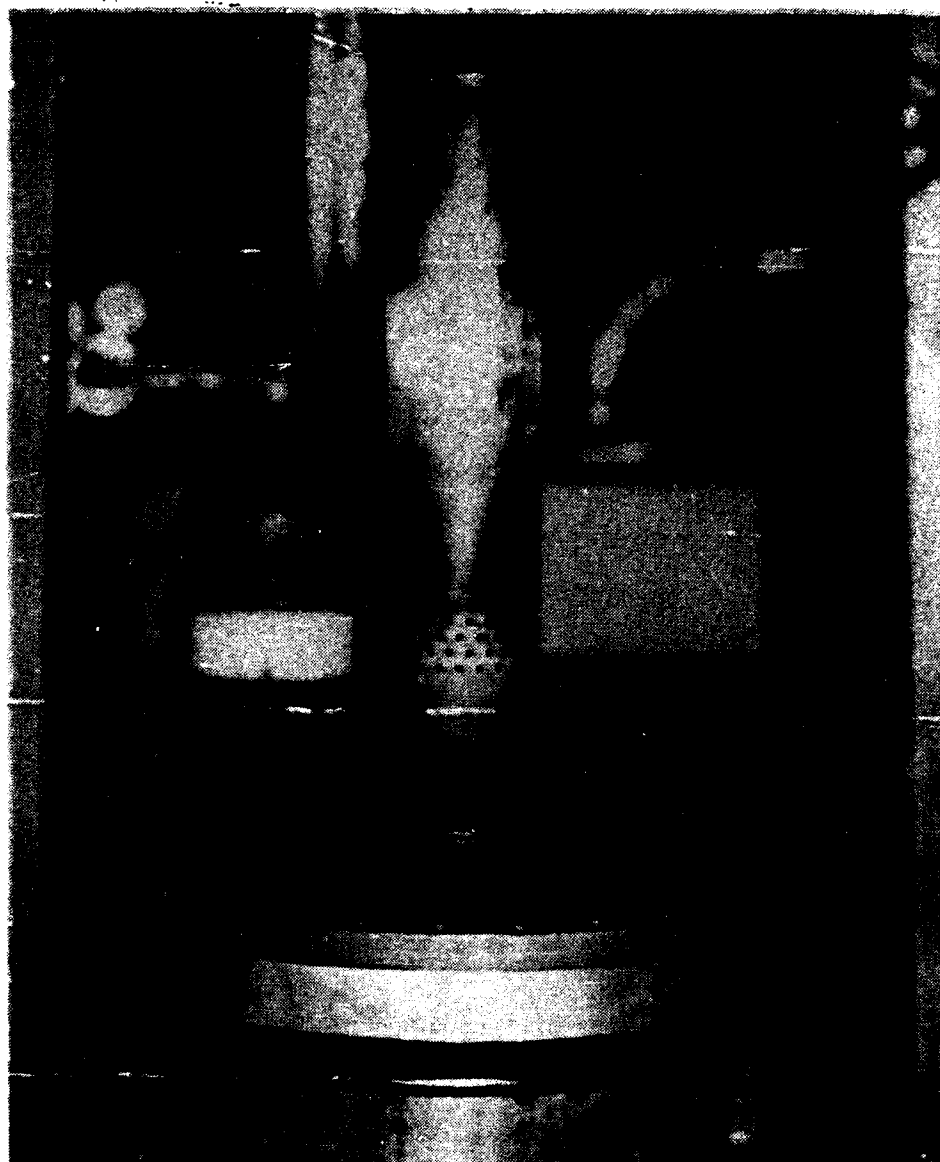
Figure 4. PUFF plasma gun inner electrode (unmounted).
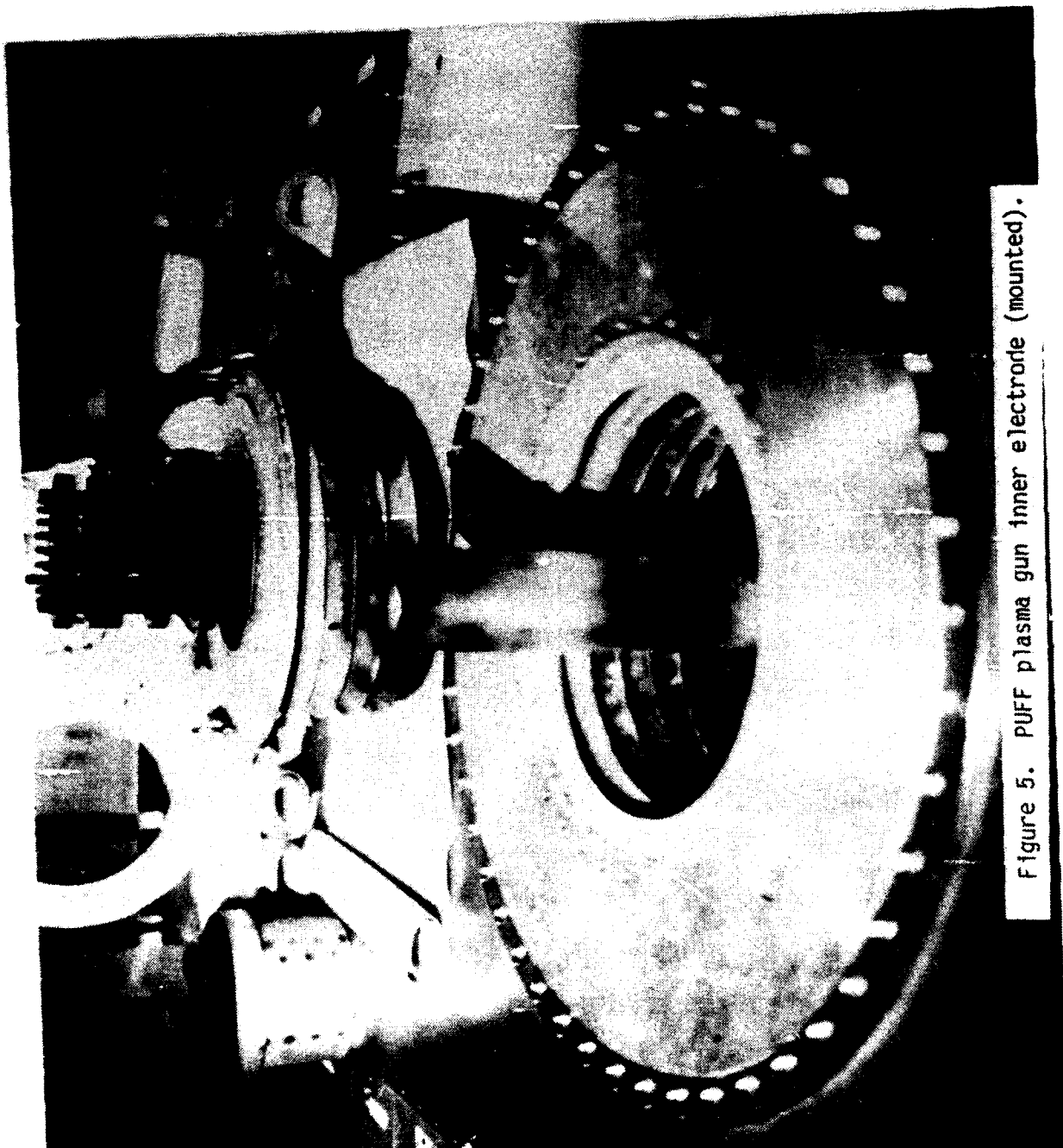
Figure 5. PUFF plasma gun inner electrode (mounted).

from the center of the top ring of gas inlet holes to the center of the
bottom ring. The distance from the bottom of the electrode to the
bottom ring of gas inlet holes is 5 3/4" (0.1461 m). The holes in the
upper portion of the anode are for the insertion of $\overset{\circ}{B}$ probes into the
annular region of the plasma gun. In Figure 5, the anode is mounted in
the transmission line and the cathode is in the background.

The outer electrode consists of 24 copper rods. These rods are 1/2"
(1.27×10^{-2} m) in diameter. The electrode array is reinforced with
machined disks of steel for mechanical stability. A side view of these
electrodes is shown in Figure 6. Both the upper and lower coaxial gun
copper electrodes are mounted on the upper helical feed electrode. It
can be seen the cathode rods are about 1" (2.5×10^{-2} m) shorter than the
anode. The visual distinction between the electrodes and the support
rings is lost since both are covered with powdery residue from the
experimental series.

2.4 FEED GAS VALVES

Two gas valves are used in this experimental series. The first (primary
or lower) gas valve feeds gas to the plasma gun annulus. The primary
gas valve is used in every shot in the series. The second (secondary or
upper) gas valve feeds gas to the centerline region of the anode tip
(coaxial gun muzzle). This valve inserts additional gas into the
coaxial plasma gun. We examine the effects of additional gas loading on
the plasma in the coaxial plasma gun.
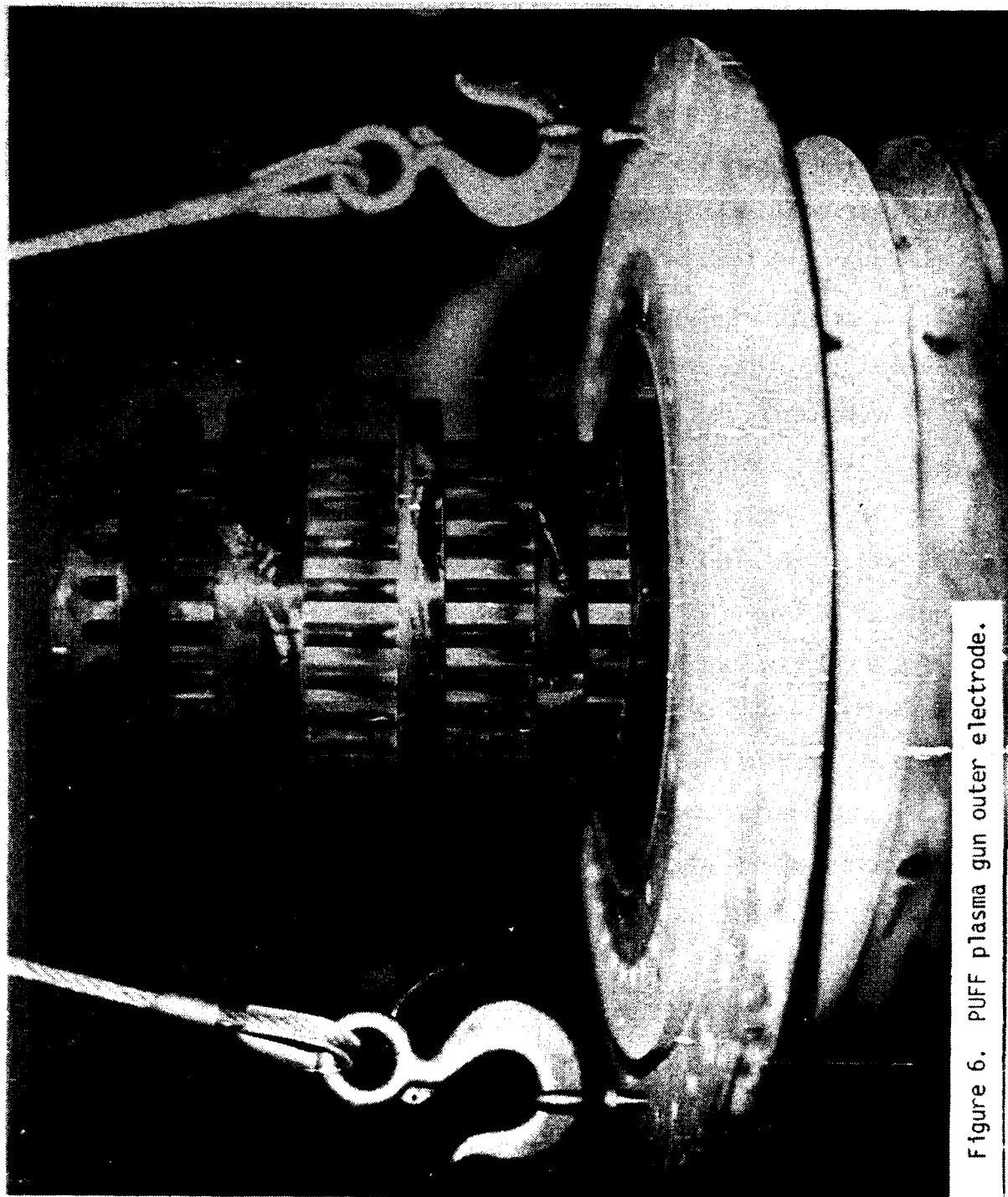
Figure 6. PUFF plasma gun outer electrode.

23

In the experiments described here, the feed gas is deuterium (heavy hydrogen). The gas arrival is measured in the gun by using fast ion gauges [149, 150]. These ion gauges are 6AH6 vacuum tubes with the protective glass cover removed. Oscilloscope traces for typical calibration shots with the 6AH6 tubes are shown in Figure 7.

2.4.1 Lower Gas Valve

The lower gas valve is based on the design of Henins and Marshall [151, 152]. The valve assembly is seen in Figure 8. This Los Alamos National Laboratory designed gas valve releases a gas volume of 3.2 cm^3 at ambient temperature and 900 psia (6.2×10^6 Pascals). This yields a mass of 32.9 mg of deuterium (D_2) gas. The feed gas line is on the side of the valved assembly. A pneumatic jack, at the base of the valve assembly, is used to compress a Lexan (polycarbonate plastic) rod in the extended portion of the assembly. The rod is about 30" (0.76 m) long. The hydraulic jack provides compression through the phenolic plastic base and a wooden plug to the Lexan rod. The operating compression of the hydraulic jack is 2000 psi (1.4×10^7 Pascals).

The phenolic base above the jack keeps a wooden plug in contact with (and maintain compressional stress on) the valve rod. The wooden plug is 1/2" (1.27×10^{-2} m) diameter and has a small hole drilled along the axial centerline. A small diameter magnet wire is inserted through this hole. Several drops of water are inserted into the hole and sealed in the plug with paraffin wax. The wooden plug is exploded by a current discharge generated by the capacitor bank through the wire. The water

Z = 0"

0.5V/Div

0.1V/Div

Z = 4"
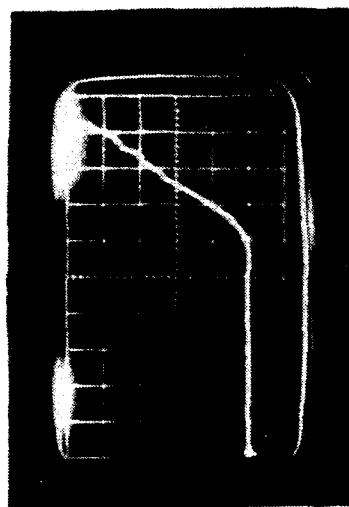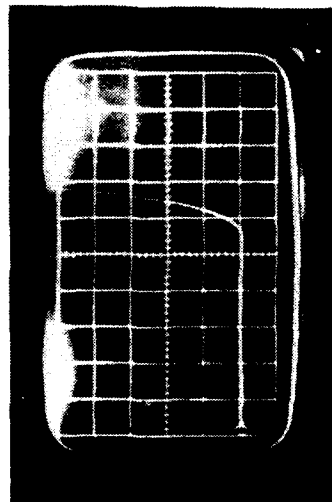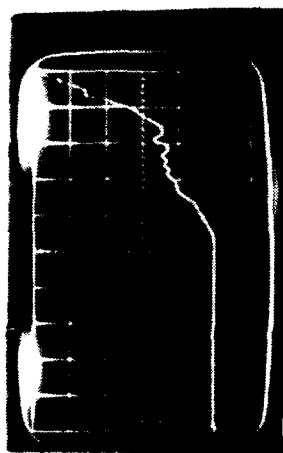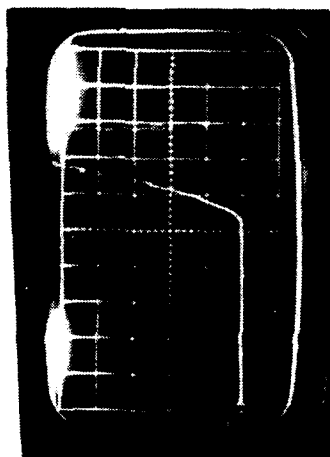
Figure 7. Typical PUFF gas injection data.

D_z, 800 psig   200 μsec/Div

~0.8 Torr/Volt
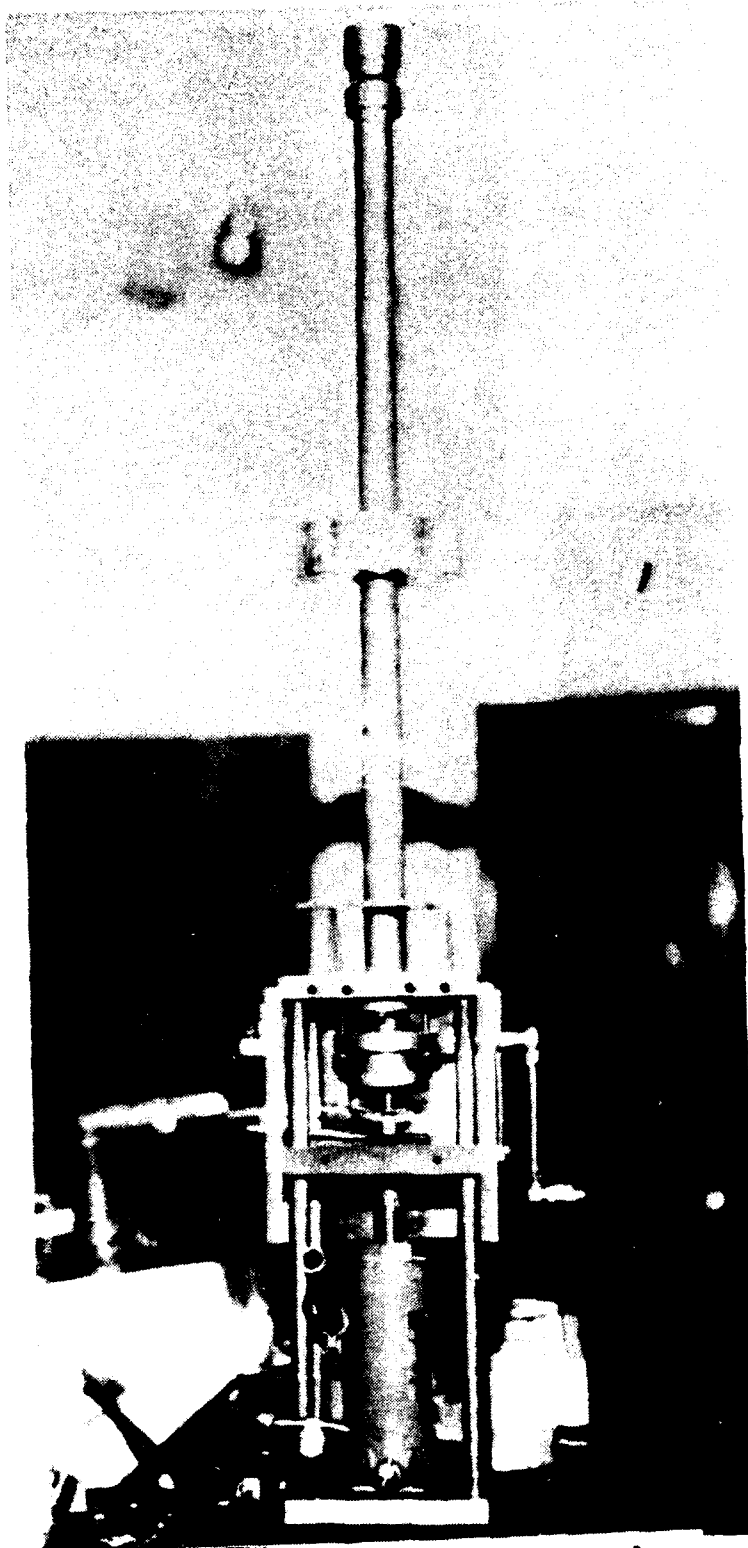
Figure 8. Lower (primary) gas valve.

in the plug assists the exploding wire in the plug destruction. When
the wooden plug explodes, a compressional longitudinal wave propagates
through the Lexan rod, allowing the gas into the internal anode region.

The lower valve discharge circuit consists of a 12 μF capacitor bank
charged to 5 kV. The rise time for the discharge circuit is 5 μs. As
might be expected, the gas delay into the coaxial plasma gun is weakly
dependent on the charging voltage. (The destruction of the plug
provides the compressional shock to the Lexan rod. Once the voltage
plateau where the plug is destroyed is reached, additional voltage adds
little to the effect.) However, since it is the compressional
longitudinal wave in the Lexan that allows the gas to enter the gun, rod
compression is a consideration. The fitted relation of experimental
parameters is

$$T_d = 2080 - 0.4881 \times P$$

where T_d is time delay of the gas into the coaxial plasma gun annular
region in μs and P is jack compressional pressure in psi. This relation
yields time delays accurate to ±3.5%. Typical operating delays range
from 1100 to 1300 μs. With too small compressional pressures (generally
1000 psi and below), the plug firing becomes unreliable because physical
contact is not assured between the plug and the valve. Above 2250 psi,
the wooden plug tends to fracture (and become useless) prior to firing.

The gas valve time delay has two parts. The first is determined by the
Lexan rod compressional velocity; this is about 600 to 700 μs. The

27

second delay is determined by the gas acoustical speed from the valve to the gun annulus. For a 400 to 700 μs acoustic gas delay, this yields an acoustic velocity on the order of 200 m/s for the D_2 fill gas.

The gas valve time delays were selected in a series of experiments performed prior to those described in this dissertation. These experiments optimized the time delays according to the current delivered to the gun as measured by the chamber Rogowski coil and the neutron production at the gun muzzle. The neutron yield is a positive monotonic increasing function of the current delivery to the gun muzzle; thus, the greater the neutron yield, the greater the current that has been delivered to the end of the coaxial plasma gun.

In this series of experiments, the gas valve time delays were selected to allow energy delivery when the deuterium fill gas reaches a Paschen breakdown. (This is different from the case where energy delivery occurs after the fill gas has reached an equilibrium state). After the gas valve is fired, gas is released and streams into the plasma gun annulus. The leading edge (or density front) of this gas delivery causes Paschen breakdown to occur. This gas breakdown carries the initial current delivered to the plasma gun.

2.4.2   Upper Gas Valve

The secondary or upper gas valve is an electromagnetic hammer valve of Lawrence Livermore National Laboratory design [153, 154]. The secondary valve was used after the eighth shot of 10 January 1984 and for every

28

shot thereafter in this series. The disassembled upper valve is shown in Figure 9. The valve consists of a solenoidal coil, a restoring spring and a valve rod that passes through the solenoid. The solenoid volume can be identified by the white electrical insulation surrounding it and the gas input feed line connection at its end. Gas is fed into the valve plenum through the feed connection. Voltage is applied to the solenoid through electrical connections at the valve end. Once a voltage is applied to the solenoid, the gas valve rod is drawn (lectromagnetically) into the solenoid and opens the seated valve-flange connection, allowing gas to escape. When the upper valve is no longer energized, the restoring spring reseats and reseals the valve.

The upper valve is mounted inside the vacuum chamber. The external connections are seen in Figure 10. The upper gas valve is located about 4" (10 cm) from the anode surface. The gas feed line is at the center of the vessel vacuum top plate. The electrical connections are on either side of the gas feed line. The upper gas valve touches the vacuum vessel plate. Since the gas in the gas valve is deuterium and the vacuum vessel was biased (when the PUFF bank was energized) to -30 kV, the Mylar sheet and electrical insulation on the electrical lines are provided to reduce the chance for an electrical discharge to the electrical lines or the gas line. The results of a spark ignition of the gas is both dangerous and damaging.

The upper valve releases a gas volume of 3 cm^3 at ambient temperature and 45 psia pressure. This yields a mass of 1.54 mg of D_2 gas. The upper gas valve is very sensitive to the capacitor discharge voltage. A

29
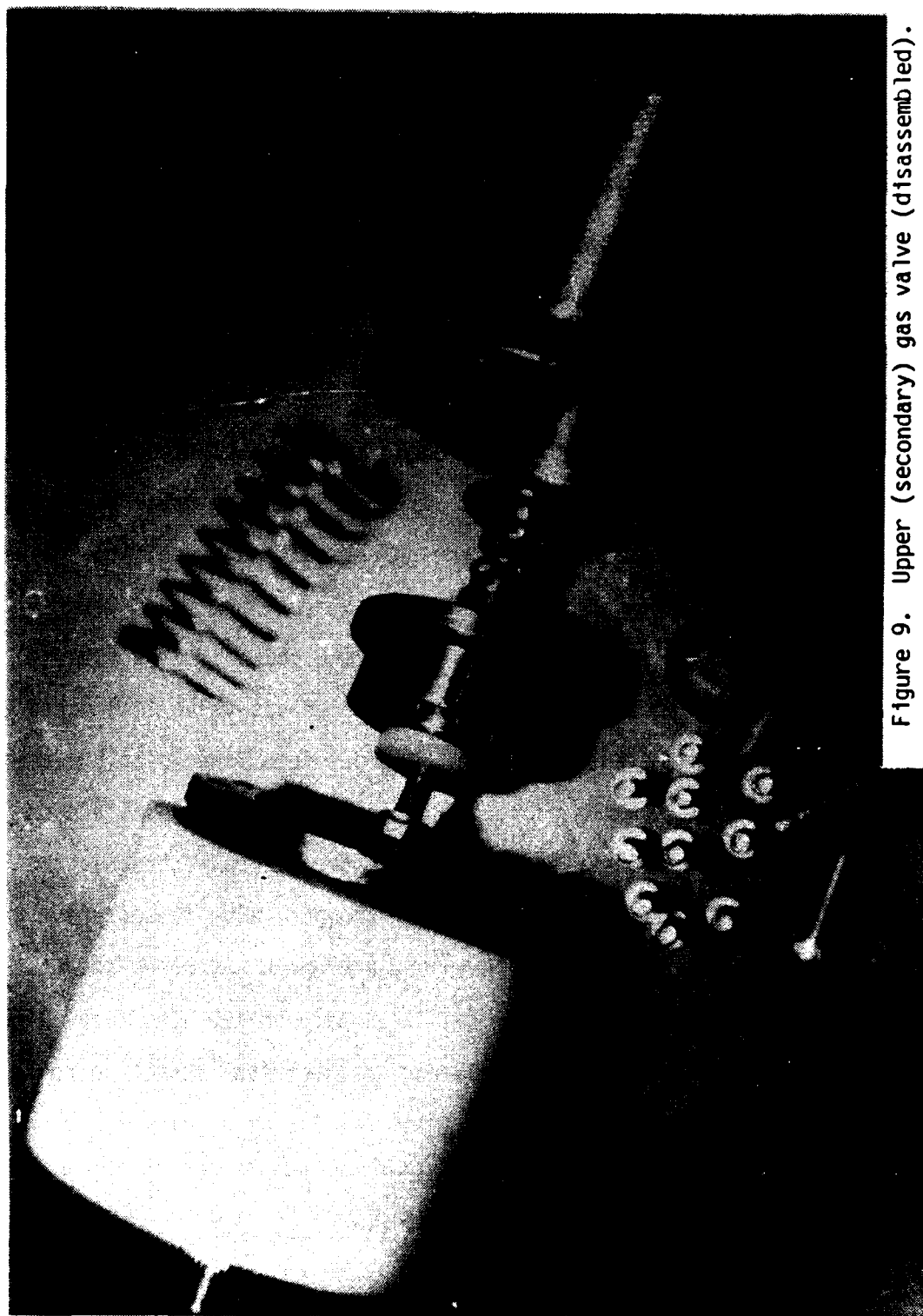
Figure 9. Upper (secondary) gas valve (disassembled).

30
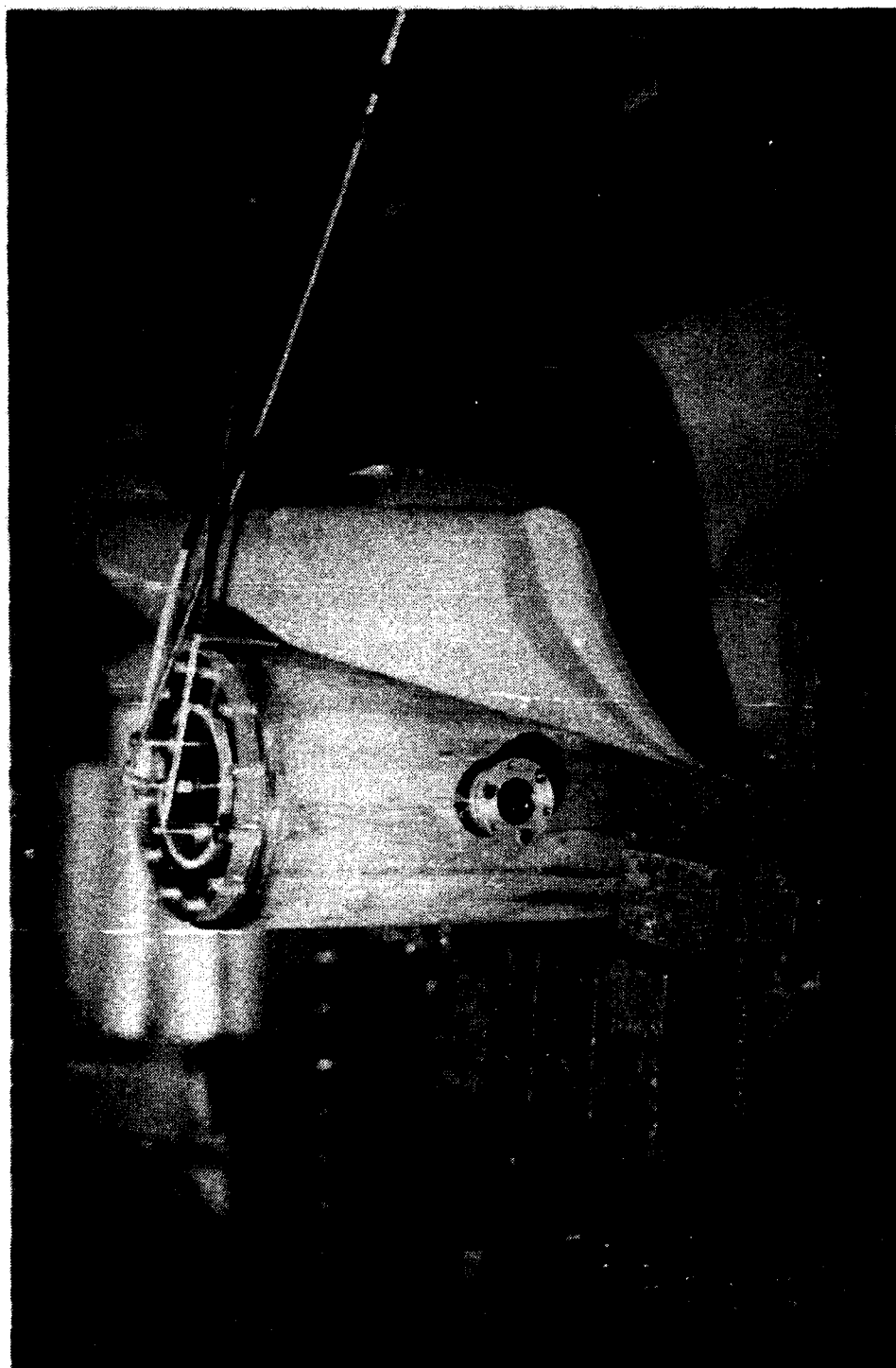
Figure 10. Mounted upper gas valve with electrical and gas connections.

31

voltage regulator is required to stabilize the discharge voltage and the quantity of gas released by the upper valve. The time delay between energizing the upper valve and firing the PUFF capacitor ranges from 3.75 to 3.90 ms. Most of this delay is required to energize the valve solenoid inductance. Although the two gas valve delays differ by some 2.6 ms, the gas from the two valves is inserted into the plasma gun at approximately the same time.

An electrically disrupted diaphragm valve was tried prior to using the secondary electromechanical valve. When a voltage pulse is applied to this valve, a resistive metal foil diaphragm separating a high pressure plenum ruptured. This valve did not completely vaporize the diaphragm and scattered debris into the coaxial plasma gun. For this reason, this valve design was abandoned. It is presented here for the sake of completeness.

2.5 EXPERIMENTAL DIAGNOSTIC DEVICES

In this section, the diagnostic devices used in these experiments will be described. General principles of operation will be given and the specifics of each diagnostic device will follow. Applications to this experimental series described here will be emphasized.

2.5.1 Rogowski Coils

Rogowski coils are the diagnostic devices for measuring the current from the transmission line and the delivered coaxial plasma gun current.

Three Rogowski coils are used. Two Rogowski coils (wound in opposite directions) are used to measure the transmission line current. These are located in the transmission line outside the helical feed electrodes and are the counter-rotating Rogowski coils. The third Rogowski coil is located at the base of the anode electrode. This is the center or chamber Rogowski coil.

2.5.1.1 Rogowski Coil Theory. Since Rogowski and Steinhaus's paper in Archiv für Elektrotechnik in 1912, Rogowski coils have been used to measure current [155]. A Rogowski coil measures the total current passing through an area surrounded by the coil. Several comparatively recent papers [156, 157] have been written on Rogowski coil theory. However, the theory is relatively simple.

Two of Maxwell's equations are required to show the relation between the input current I (observed by a Rogowski coil) and the induced voltage V. These equations are:

$$\nabla \times \mathbf{H} = \mathbf{J} + \frac{\partial \mathbf{D}}{\partial t} \qquad (2.5.1.1.1)$$

and

$$\nabla \times \mathbf{E} = - \frac{\partial \mathbf{B}}{\partial t} \qquad (2.5.1.1.2)$$

If the dielectric source term ($\frac{\partial \mathbf{D}}{\partial t}$) is negligible compared to the current source term, i. e. ($\frac{\partial \mathbf{D}}{\partial t} \ll \mathbf{J}$), the remaining relation is

33

$$\nabla \times H = J \qquad (2.5.1.1.1a)$$

Using the constituitive relation between B and H, that is, $B = \mu_0 H$, we have

$$\nabla \times B = \mu_0 J \qquad (2.5.1.1.3)$$

If we take the surface integral over a closed surface, we then have

$$\int (\nabla \times B) \cdot dS = \mu_0 \int J \cdot dS = \mu_0 I \qquad (2.5.1.1.4)$$

where I is defined to be the total current passing through the volume defined by the closed curve. Transforming the surface integral on the left hand side of equation (2.5.1.1.4) into a line integral using Stokes' theorem, we have

$$\int B \cdot dl = \mu_0 I \qquad (2.5.1.1.5)$$

We can then transform the differential length dl into an equivalent relation with a differential normal vector dn or a differential normal cross-sectional area dA,

$$\frac{dl}{L} = \frac{dn}{N} = \frac{dA}{A} \qquad (2.5.1.1.6)$$

where L is length of Rogowski coil, N is number of turns in the Rogowski coil and A is Rogowski coil cross-sectional area. The Rogowski coil

34

characteristics (L, N and A) are constant in this analysis. Using equations (2.5.1.1.5) and (2.5.1.1.6), we have

$$I = \frac{1}{n\mu_o} \int B \cdot dn = \frac{1}{n\mu_o A} \int B \cdot dA \qquad (2.5.1.1.7)$$

where n is defined to be (N/L), linear turn density. Defining a magnetic flux Φ passing through a coil of cross-sectional area A, we have

$$\Phi = \int B \cdot dA \qquad (2.5.1.1.8)$$

and equation (2.5.1.1.8) becomes

$$I = \frac{\Phi}{n\mu_o A} \qquad (2.5.1.1.9)$$

We invoke equation (2.5.1.1.2) to apply equation (2.5.1.1.9) to the experiment. Integrating the surface integral of equation (2.5.1.1.2) yields

$$\int (\nabla \times E) \cdot dS = - \int \frac{\partial B}{\partial t} \cdot dS \qquad (2.5.1.1.10)$$

Since the differential surface is independent of time, we can remove the time differential from the integral

$$\int (\nabla \times E) \cdot dS = - \frac{\partial}{\partial t} \int B \cdot dS \qquad (2.5.1.1.10a)$$

35

Transforming the left hand side of this equation into a line integral with Stokes' theorem, we have

$$\int \mathbf{E} \cdot d\mathbf{l} = - \frac{\partial}{\partial t} \int \mathbf{B} \cdot d\mathbf{S} \qquad (2.5.1.1.11)$$

Defining an induced voltage V to be the line integral on the left hand side and noting the magnetic flux Φ is equal to the integral on the right hand side, this equation becomes

$$V = - \frac{\partial \Phi}{\partial t} \qquad (2.5.1.1.12)$$

Defining the magnetic flux Φ as a function only of time, equation (2.5.1.1.12) becomes

$$V = - \frac{d\Phi}{dt} \qquad (2.5.1.1.12a)$$

This relation is Lenz's rule from electrodynamics. Substituting equation (2.5.1.1.12a) into the equation (2.5.1.1.10), we have

$$V = - n\mu_o A \frac{dI}{dt} \qquad (2.5.1.1.13)$$

If the Rogowski coil is not self-integrating and needs to be integrated (in our case, by a passive RC integrator), we have

$$V = - \frac{n\mu_o A}{RC} I \qquad (2.5.1.1.14)$$

The relation between the induced voltage V and the current I passing through the Rogowski coil then becomes

$$V = - \frac{K_R}{RC} I \qquad (2.5.1.1.14a)$$

where K_R, the Rogowski coil calibration factor, is equal to $n\mu_0 A$ and RC is the passive integrator time constant. If other integration methods are used, this is reflected in an equivalent relation.

The response of a Rogowski coil is independent of the Rogowski coil length (assuming each coil turn is effectively the same). The important term is n, the number of turns on the Rogowski coil (N) divided by the length (L). The greater the number of turns per unit length the larger the induced voltage for a given current.

2.5.1.2   Rogowski Coil Construction.   The AFWL Rogowski coils are constructed of 50 Ω UT-47c coaxial cable. The nominal cable capacitance is 29.3 pF/foot (96.1 pF/m). UT-47c cable has a copper inner conductor of 11.3 mils diameter (2.87×10^{-4} m). The inner cable conductor is surrounded by a 37 mil (9.40×10^{-4} m) outer diameter plastic insulator. The outer conductor is copper. The outer conductor and the cable have an outer diameter of 47 mils (1.19×10^{-3} m). The outer conductor is etched to form a helical winding. The number of turns per unit length etched in the coil depends on the desired sensitivity of the Rogowski coil. Typical values are 1 turn/inch and 2 turns/inch (39 and 79 turns/meter). The lower sensitivity coils are used on higher current

37

experiments (such as the larger 1313 µF AFWL SHIVA Star capacitor bank).
Etching the solid outer conductor allows magnetic field to diffuse into
the Rogowski coil. The inner electrode is electrically connected to the
outer electrode at one end of the coil. A Microdot coaxial connector
(AMP Inc. catalog number 2-329037-2) is soldered at the other end.
After the cable connections are made, the whole coil (from the soldered
inner/outer conductor connection to the Microdot connector) is sealed in
heat shrink insulation material. Since the Rogowski coils are
constructed within AFWL, they are made to any length.

2.5.1.3   Rogowski Coil Calibration. Although the Rogowski coil
calibrations can be calculated from the theory from Section 2.5.1.1,
reliance upon the theory is not recommended for experimental analysis.
The Rogowski coils are calibrated under experimental conditions.

The calibration method uses an RLC circuit to produce a current. The
current produces a voltage in the Rogowski coil. A schematic of the RLC
circuit used is shown in Figure 11. A typical result of a calibration
shot is shown in Figure 12.

In the circuit of Figure 11, we can use Kirchhoff's two circuit laws to
calculate the circuit response. Kirchhoff's first law states that, at a
node, the sum of the currents in equals the sum of the currents out.
Since the circuit being examined is a closed loop, the same current I
will pass through all the circuit elements. Kirchhoff's second law
states, in a circuit loop, the sum of the voltages is 0. Using these
relations, we can now proceed to examine the calibration circuit.

38
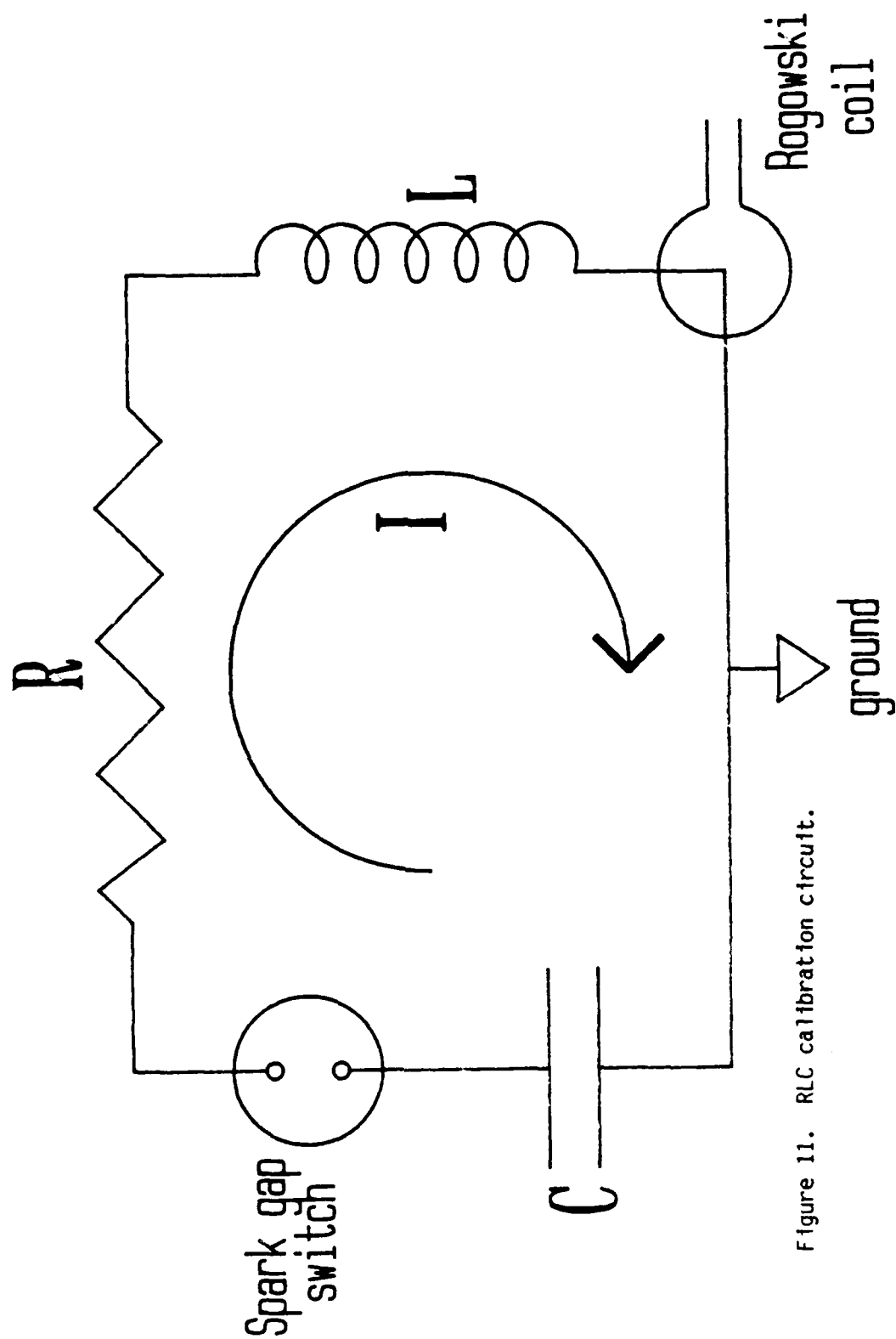
Figure 11. RLC calibration circuit.
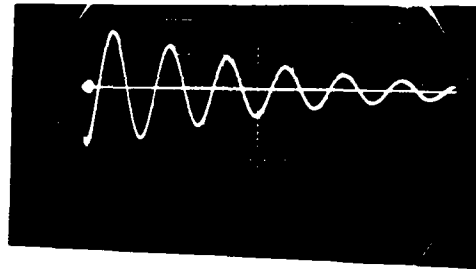
Figure 12. Typical RLC calibration oscilloscope record.

(Shot taken 24 January 1984 for $\overset{\bullet}{B}$ probe J.
C = 1.922 μF   V = 11.5 kV
0.5 V/div   2 μs/div)

The voltages are summed to equal

$$V_0 = V_C + V_R + V_L \qquad (2.5.1.3.1)$$

where V_0 is initial charge voltage, V_C is capacitor voltage, V_R is resistor voltage and V_L is inductor voltage. Relating the voltages to the current in each of the circuit elements, we have

$$V_0 = \frac{1}{C} \int I\, dt + IR + L\frac{dI}{dt} \qquad (2.5.1.3.2)$$

Using Laplace transforms, we have

$$\frac{V_0}{s} = \frac{I}{Cs} + IR + LsI \qquad (2.5.1.3.3)$$

where s is the transform variable corresponding to frequency (inverse time). In the transform equation, the same variable names are used for ease in identification, but they have been transformed from the time domain to the frequency domain.

For the transform equation (2.5.1.3.3), the transformed current is solved for in terms of the circuit elements

$$I = \frac{V_0}{L}\; \frac{1}{(s^2 + \frac{Rs}{L} + \frac{1}{LC})} \qquad (2.5.1.3.4)$$

41

Completing the squares and casting equation (2.5.1.3.4) in standardized Laplace form, we have

$$I = \frac{V_0}{L} \frac{1}{(s + \alpha)^2 + \omega^2} \qquad (2.5.1.3.5)$$

where $\alpha = \frac{R}{2L}$ and $\omega = [\frac{1}{LC} - (\frac{R}{2L})^2]^{1/2}$.

Using the inverse Laplace transform, we then have the solution of the circuit in the time domain

$$I = \frac{V_o}{L\omega} e^{-\alpha t} \sin \omega t \qquad (2.5.1.3.6)$$

Were the Rogowski coils integrated, this relation would suffice for calibration. Since the calibrations were done without integration, we need a relation for the time differential of the calibration current. Differentiating equation (2.5.1.3.6) and performing the appropriate algebraic and trigonometric manipulations, we have

$$\frac{dI}{dt} = \frac{V_o}{L} \frac{(\alpha^2 + \omega^2)^{1/2}}{\omega} e^{-\alpha t} \cos (\omega t + \theta) \qquad (2.5.1.3.7)$$

where α and ω have been defined previously and θ is the arctangent of (α/ω).

If $\alpha \ll \omega$, we can then approximate equation (2.5.1.3.7) to

$$\frac{dI}{dt} = \frac{V_0}{L} e^{-\alpha t} \cos(\omega t) \qquad (2.5.1.3.7a)$$

This approximation is valid for these calibrations (seen in Figure 12).

Having derived the relation describing the behavior of the calibration circuit, it is easy to relate the experimental data to a calibration constant K_R. The discharge voltage V_0 is known from the charging circuit. The circuit parameters α and ω can be calculated from the oscilloscope record of the voltage trace. Knowing the time base speed and the oscilloscope voltage setting, the voltages and the corresponding times are known. Once the oscilloscope data is known, several basic algebraic and trigonometric properties are invoked to solve for the calibration constant K:

1) The difference between two adjacent extrema (positive/negative peaks) is given by $t = (\pi/\omega)$.

2) The difference between two adjacent zeroes is $t = (\pi/\omega)$.

3) The absolute values of the extrema (where $(\omega t + \theta) = \pm n\pi$, n an integer, so $\cos(\omega t + \theta) = \pm 1$) will obey the relation $V = v e^{-\alpha t}$, v is a constant.

By using the time differences relations of 1) and 2), an average frequency ω is calculated. The circuit damping constant α can be calculated from the extrema as specified in 3). Knowing the circuit

43

parameters α and ω, the circuit values for the inductance L and the resistance R can be calculated. Because the frequency ω is generally taken to be $(1/LC)^{1/2}$ (with the effect of the resistance R ignored), the values of L and R may need to be iterated to be consistent with the calculated values of α and ω. (The system capacitance C is known.) The voltage on the Rogowski coil V_r at time $t = 0$ can be derived by using the information in 3) and extrapolating the initial voltage from the absolute value of the extrema voltage beginning with the second peak. Using the first peak would be easy, but yields erroneous results, since the plasma arc needs a finite (though small) time to ignite.

From equation (2.5.1.3.7a), we know the value for $\frac{dI}{dt}$,

$$\lim_{t \to 0} \frac{dI}{dt} = \frac{V_0}{L} e^{-\alpha t} \cos(\omega t) = \frac{V_0}{L} \qquad (2.5.1.3.7b)$$

We know the relation for the Rogowski coil is

$$V_r = K_R \frac{dI}{dt}$$

yielding the calibration constant K_R to be

$$K_R = \frac{V_0}{LV_r} \qquad (2.5.1.3.8)$$

where V_0 is charge voltage, L is circuit inductance and V_r is extrapolated initial Rogowski voltage.

44

A 1.922 μF capacitor is used for the circuit capacitance C. Any other system or stray capacitance is assumed negligible. The capacitor is discharged through the self-breakdown of an air switch and a current flows in the circuit. The resistance R and the inductance L are assumed to be a function only of the circuit and relatively constant in time. The spark gap resistance is not constant, but when it is sufficiently small (as it is in the case of these calibrations), the time variation can be ignored. The resistance and the inductance are not negligible, but they can be calculated from the voltage response of the Rogowski coil.

Using the relation given in equation (2.5.1.1.14), we can calculate the expected calibration constant K_R for the AFWL Rogowski coils. With a turns ratio of 2 turns/inch (79 turns/m) and an effective area of 1.00×10^{-6} m^2, the calibration constant K_R becomes

$$K_R = n\mu_o A = 1.01 \times 10^{-10} \frac{Vs}{A}$$

This compares to the calculated Rogowski coil response constants of $(7.4 \pm 1.4) \times 10^{-11}$ Vs/A for the counter-rotating Rogowski coils and $(1.03 \pm 0.24) \times 10^{-10}$ Vs/A for the center (chamber) Rogowski. The error bars are taken from the standard deviation of the current calibration factors. This wide standard deviation is due to the stochastic variation in the calibration circuit spark gap breakdown voltage. The actual calibration breakdown voltage was not as accurately monitored as it should have been.

The effective Rogowski coil outer radius is a function of both the inner radius of the outer conductor and the skin (penetration) depth δ where $\delta = (2/\sigma\mu_0\omega)^{1/2}$. Here, σ is electrical conductivity, μ_0 is permeability of free space and ω is frequency of the electromagnetic radiation penetrating the conductor. For our case, $\delta = 9.6\times10^{-5}$ m with $\sigma = 5.8\times10^{7}/\Omega m$ (the conductivity of copper) and $\omega = 3.0\times10^{6}/s$ (the characteristic frequency of the 1.922 μF capacitor calibration circuit).

2.5.2 $\overset{\bullet}{B}$ Probes

Just as Rogowski coils are the diagnostic devices used in analyzing the total current delivery to the coaxial plasma gun, $\overset{\bullet}{B}$ probes are diagnostic devices for analyzing the internal coaxial plasma gun current. A series of 16 $\overset{\bullet}{B}$ probes is inserted through the inner anode surface to observe the plasma in the plasma gun annulus. This mounting from the internal electrode is similar to that of Len [158]. The 16 $\overset{\bullet}{B}$ probes are mounted at four different axial positions and four different azimuthal positions.

2.5.2.1 $\underline{\overset{\bullet}{B} \text{ Probe Theory}}$. The theory for the $\overset{\bullet}{B}$ probes is similar to that of the Rogowski coils. Instead of repeating the derivations from Section 2.5.1.1, portions of that presentation will be recalled only as they apply.

A distinction needs to be drawn in comparing the Rogowski coil and the $\overset{\bullet}{B}$ probes. The Rogowski coil measures the total current (or the time rate of change of current) passing through its interior. The Rogowski coil

46

does not reflect the local variation of the current it measures. As long as the current geometric effects are minimized, the Rogowski coil measures all the current passing through it. However, the $\dot{B}$ probe measures the magnetic field due to a current at a point and can reflect some local variation of the current. If the current does not exhibit large azimuthal variations, the distinction is minor.

From equation (2.5.1.1.5), we have the relation between the current and the induced magnetic field (in non-magnetic materials). This is

$$\int \mathbf{B} \cdot d\mathbf{l} = \mu_0 I \qquad (2.5.1.1.5)$$

If we assume cylindrical geometry where a current I is axial and exhibits no radial or azimuthal variation, a closed curve can be used to describe the line integral. Realizing a circle of radius r is the simplest closed curve about a point, we then have

$$B_\theta (2\pi r) = \mu_0 I \qquad (2.5.2.1.1)$$

For this coaxial geometry, the azimuthal magnetic field will be

$$B_\theta = \frac{\mu_0 I}{2\pi r} \qquad (2.5.2.1.2)$$

This relation differs from that of the Rogowski coil (2.5.1.1.7) in the inverse variation of current with radial distance from the source.

47

Using Lenz's rule,

$$V = - \frac{d\Phi}{dt} \qquad (2.5.1.1.12a)$$

The magnetic flux Φ measured by the $\dot{B}$ probe coil is given by

$$\Phi = NAB$$

where N is number of turns and A is effective cross-sectional area. The induced voltage V_B in the $\dot{B}$ probe is

$$V_B = - \frac{\mu_0 NA}{2\pi r} \frac{dI}{dt} \qquad (2.5.2.1.3)$$

(The effective area is used in the derivation since the magnetic flux Φ uses the vector dot product.

$$\Phi = \int \mathbf{B} \cdot d\mathbf{S}$$

This can vary from the actual cross-sectional area of the $\dot{B}$ probe.) The $\dot{B}$ probes used in this series of experiments were not self-integrating. They were passively integrated with RC integrators (mentioned previously in Section 2.5.1.1). The actual response for the $\dot{B}$ probes becomes

$$V_B = - \frac{\mu_0 NA}{2\pi r} \frac{I}{RC} \qquad (2.5.2.1.3a)$$

48

where RC is the integrator time constant. This derivation assumes the number of turns N, the effective area A and the radius of the $\overset{\smile}{B}$ probe are fixed in time. This is true in both the calibration and experimental series.

2.5.2.2 $\overset{\bullet}{B}$ Probe Construction. The author constructed and calibrated the $\overset{\bullet}{B}$ probes used in this experiment. The $\overset{\bullet}{B}$ probe base and mounts were designed within AFWL. A sketch of a $\overset{\bullet}{B}$ probe base and mount is shown in Figure 13.

The $\overset{\bullet}{B}$ probe mount and base are made from an insulating phenolic plastic material. The phenolic plastic, chosen because it is easily machined, has relatively strong physical strength and exhibits a high dielectric breakdown strength. The mount has a 1.5" (3.81×10^{-2} m) long arm. At the arm end is a 50 mil (1.27×10^{-3} m) cylinder. The $\overset{\bullet}{B}$ probe is formed on this cylinder. Four or five turns of insulated 32 gauge magnet wire are wound around the cylinder. This yields a typical turns-area product (NA) of 10^{-5} turns-m^2. The wire is sealed into place on the phenolic cylinder with Vacseal high vacuum leak sealant. The leads from the coils are twisted and brought out along the length of the support arm. (The twisted leads reduces unwanted voltage pickup.) These leads were then connected to a coaxial cable.

The support arm is wedged into the alignment fin slot so the support arm extends some 0.5" (1.27×10^{-2} m) from the surface of the alignment fin. (The curved surface of the alignment fins fixes the $\overset{\bullet}{B}$ probe in a preferred orientation.) This $\overset{\bullet}{B}$ probe mount cylinder is oriented up (0°

Figure 13. β probe mount.

50
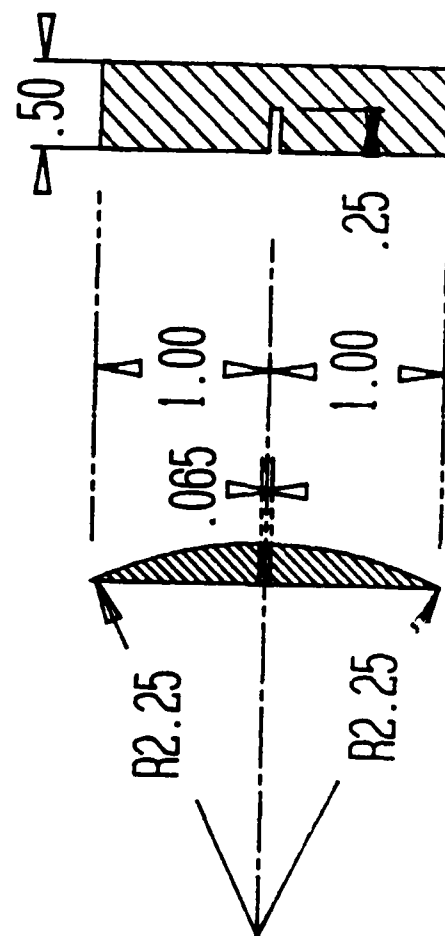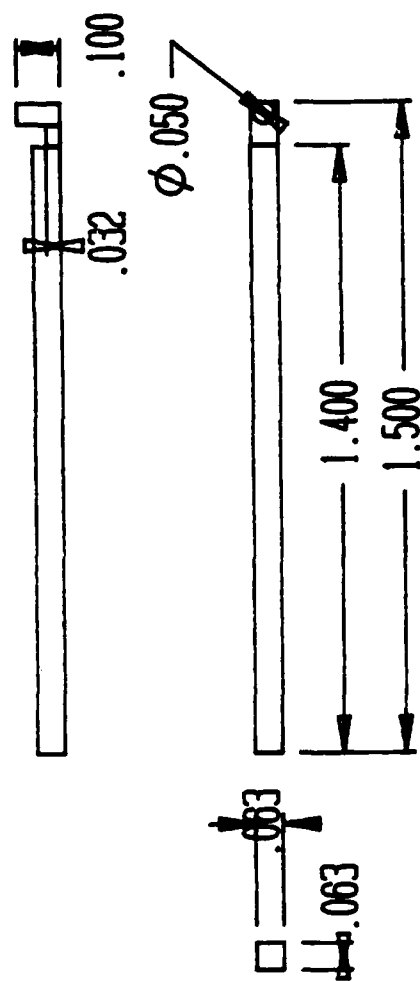
with respect to the system axis of symmetry), down (180°), right (90°) and left (270°). The $\dot{B}$ probe is operates when oriented right or left. With the alignment fin, the $\dot{B}$ probe has orientation errors no larger than ±5°, leading to a maximum error of [cos(0°) - cos(5°)] or ±0.4%. After the support arm is mounted on the alignment fin and the electrical leads are taken through the alignment fin slot, the $\dot{B}$ probe and the support arm are sealed with Torr Seal low vapor pressure resin epoxy.

A ceramic sheath is placed over the $\dot{B}$ probe after sealing with Torr Seal (and before the Torr Seal dries). The material for the sheath is molded or extruded alumina rod. It is about 0.25" (6.4×10^{-3} m) in outer diameter and about 30 mils (7.6×10^{-4} m) thick. The end of the probe sheath is closed with a hemisphere of the same ceramic.

After the epoxy on the $\dot{B}$ probe (rod, alignment fin and the ceramic sheath) has dried, the $\dot{B}$ probe leads are mated to a coaxial connector and a RG-58/U coaxial cable. The connections are then tested for continuity. Once continuity is verified, the $\dot{B}$ probes are tested for an appropriate resistance. After the complete construction of the $\dot{B}$ probes, the probes are mounted inside the anode. The $\dot{B}$ probes extend through the anode some 0.25" (6.4×10^{-3} m) into the plasma gun annular gap. The $\dot{B}$ probe electrical leads are connected to oscilloscopes for data recording.

2.5.2.3 $\underline{\dot{B} \text{ Probe Calibration}}$. The same calibration system is used for both $\dot{B}$ probes and Rogowski coil calibration. The same system of

51

calibration derivations can be used. Using equation (2.5.1.3.7b) and the relation

$$V_B = K_B \frac{dI}{dt}$$

we derive the $\overset{\circ}{B}$ probe calibration response constant K_B such that

$$K_B = \frac{V_o}{LV_B} \qquad (2.5.2.3.1)$$

where K_B is $\overset{\circ}{B}$ probe calibration constant, V_o is capacitor charging voltage and L is calibration circuit inductance.

The calibration system fixes the $\overset{\circ}{B}$ probe radius at 6.5" (0.165 m). The $\overset{\circ}{B}$ probe alignment errors in the calibration system are no worse than $\pm 10°$. This leads to an error no worse than $[\cos(0°) - \cos(10°)]$ or $\pm 1.5\%$.

For a typical turns-area product (NA) of 10^{-5} turns-m^2 and $\overset{\circ}{B}$ probe radius (r) of 7.1×10^{-2} m, a calibration constant for the $\overset{\circ}{B}$ probe is

$$\frac{1}{K_B} = \frac{2\pi r}{\mu_o NA} = 3.55 \times 10^{10} \frac{Vs}{A}$$

This compares well to the $\overset{\circ}{B}$ probe calibrations in Table 1.

Table 1 calibrations are made from physical measurements and actual calibrations prior to $\overset{\circ}{B}$ probe insertion in the plasma gun. Three $\overset{\circ}{B}$ probes (E, H' and Q) were apparently damaged in insertion. Comparison with other probes at the same level yield the revised calibrations reported in Table 1a.

Attempts were made to calibrate the $\overset{\circ}{B}$ probes in the plasma gun in situ. This involved shorting the anode and the cathode rods at the gun muzzle. These attempts did not produce reliable results. Arcing occurred because of poor electrical contact of the current shunt. The gun current in the in situ calibrations was asymmetric. After four or five unsuccessful attempts to calibrate the $\overset{\circ}{B}$ probes in situ, the efforts were abandoned and the earlier calibrations were used.

When a $\overset{\circ}{B}$ probe is used, there is a frequency effect that limits the probe response. This frequency limitation is a result of the probe inductance and the effective system resistance. The effective system resistance R is the 50 Ω termination resistance. The probe inductance L is given by Grover [159]

$$L = 10^{-3} \ F \ d \ N^2$$

where L is probe inductance in µH, F is a form factor (a function of the coil length/diameter ratio), d is coil diameter in cm and N is number of turns.

Table 1. Calibrated Characteristics of the AFWL $\overset{\bullet}{B}$ probes

Probe Name	Probe Radius (10^{-2} m)	Turns-Area (10^{-6} m^2)	Calculated Response (10^{10} A/Vs)
B	7.127 ± 0.089	10.85 ± 2.29	3.28 ± 0.69
C	7.082 ± 0.066	10.87 ± 0.51	3.26 ± 0.16
D	7.109 ± 0.064	9.57 ± 0.67	3.71 ± 0.26
E	7.084 ± 0.038	11.38 ± 0.69	3.11 ± 0.19
F	7.082 ± 0.048	10.39 ± 0.38	3.41 ± 0.13
G'	7.137 ± 0.043	9.28 ± 0.86	3.85 ± 0.36
H'	7.099 ± 0.043	9.36 ± 0.71	3.79 ± 0.29
J	7.122 ± 0.056	11.19 ± 0.78	3.18 ± 0.22
L	7.112 ± 0.048	8.57 ± 0.93	4.15 ± 0.45
M	7.112 ± 0.048	9.03 ± 1.42	3.94 ± 0.62
N	7.112 ± 0.041	11.32 ± 0.71	3.14 ± 0.20
O	7.178 ± 0.061	10.92 ± 1.45	3.29 ± 0.44
P	7.135 ± 0.038	10.67 ± 1.47	3.34 ± 0.46
Q	7.130 ± 0.041	8.90 ± 0.65	4.01 ± 0.29
R'	7.122 ± 0.041	11.12 ± 1.13	3.20 ± 0.33
S	7.132 ± 0.038	9.04 ± 0.94	3.94 ± 0.41

Table 1a. Recalibrated Characteristics of Several AFWL $\overset{\bullet}{B}$ probes

Probe Name	Probe Radius (10^{-2} m)	Turns-Area (10^{-6} m^2)	Calculated Response (10^{10} A/Vs)
E	7.084 ± 0.038	8.4 ± 2.4	4.2 ± 1.2
H'	7.099 ± 0.043	3.9 ± 0.6	9.1 ± 1.4
Q	7.130 ± 0.041	11.8 ± 1.4	3.02 ± 0.37

With a turns-area product of 10^{-5} turns-m^2 and 4 to 5 turns, the coil diameter ranges from 1.6×10^{-3} to 1.8×10^{-3} m. The coil length is about 2.5×10^{-4} m. The form factor F ranges from 17.2 to 18.0. The coil inductance ranges from 52 nH to 69 nH. The calculated L/R quotient is about 1 to 1.4 ns. Any phenomena occurring on a time scale shorter than the time constants is severely attenuated and is not observed by the $\overset{\circ}{B}$ probes.

2.5.3 Capacitive Voltage Probes

Voltage diagnostics are used to analyze the gun voltage. The voltage diagnostics used are capacitive voltage probes. These voltage probes consist of two capacitors in series. The input voltage is seen by the capacitor stack (consisting of the two capacitors). The resultant output voltage (presented by only one of the capacitors) is recorded.

The capacitive voltage divider is used because the voltages are on the order of tens of kilovolts. Directly applied, these voltages can induce electrical breakdown in electrical components, even in such comparatively simple ones as coaxial cables. In more extensive and complex systems (such as oscilloscopes), the damage from overvoltages is more consequential. To reduce the deleterious effects of measuring high voltages, series of circuit elements (resistors, inductors or capacitors) are used.

The voltage probes are mounted on the underside of the transmission line outside the coaxial plasma gun electrodes and the vacuum/insulator

interface. Two voltage probes are used, one mounted to the north and one mounted to the south of the coaxial plasma gun.

Capacitive voltage probes have several advantages not exhibited by resistive probes:

1) Resistive probes drain current from the voltage source. The current drain distorts the measured voltage. Capacitive voltage probes do not drain current. Rather, capacitive voltage probes measure the polarization charge induced by the dielectric stress on the insulator.

2) Resistive voltage probes may explosively fragment with the application of high voltages (unless specifically designed to dissipate high power levels). Capacitive voltage probes drain no power from the voltage source and do not exhibit this behavior.

3) Resistive voltage probes, if designed for large power dissipation, can have time varying resistances (as in aqueous metallic salt solution resistors) complicating the voltage analysis. If the voltage probes are time invariant, they tend to be expensive and susceptible to mechanical shock. Our capacitive voltage probes maintain the same response for the same probe geometry. Our capacitive voltage probes are robust.

2.5.3.1 <u>Capacitive Voltage Probe Theory</u>. The simplified circuit model
for the capacitive voltage is shown in Figure 14. There are two
capacitors in series: C_1 which taps the source voltage V_o and C_2 which
goes from the C_1 point voltage to ground. The capacitor stack measures
the voltage from V_o to ground. A current I flows through both
capacitors C_1 and C_2.

Applying Kirchhoff's second law to the circuit, we have

$$V_o = V_{C_1} + V_{C_2} \qquad (2.5.3.1.1)$$

where V_{C_1} is voltage on the first capacitor and V_{C_2} is voltage on the
second capacitor.

The voltage seen by the recording device V_m becomes

$$V_m = V_{C_2} \qquad (2.5.3.1.2)$$

Using the relationship for the capacitor voltage and current, we have

$$V_C = \frac{1}{C} \int I_C \, dt \qquad (2.5.3.1.3)$$

where V_C is capacitor voltage and I_C is capacitor current. Substituting
equation (2.5.3.1.3) in equations (2.5.3.1.1) and (2.5.3.1.2), we have
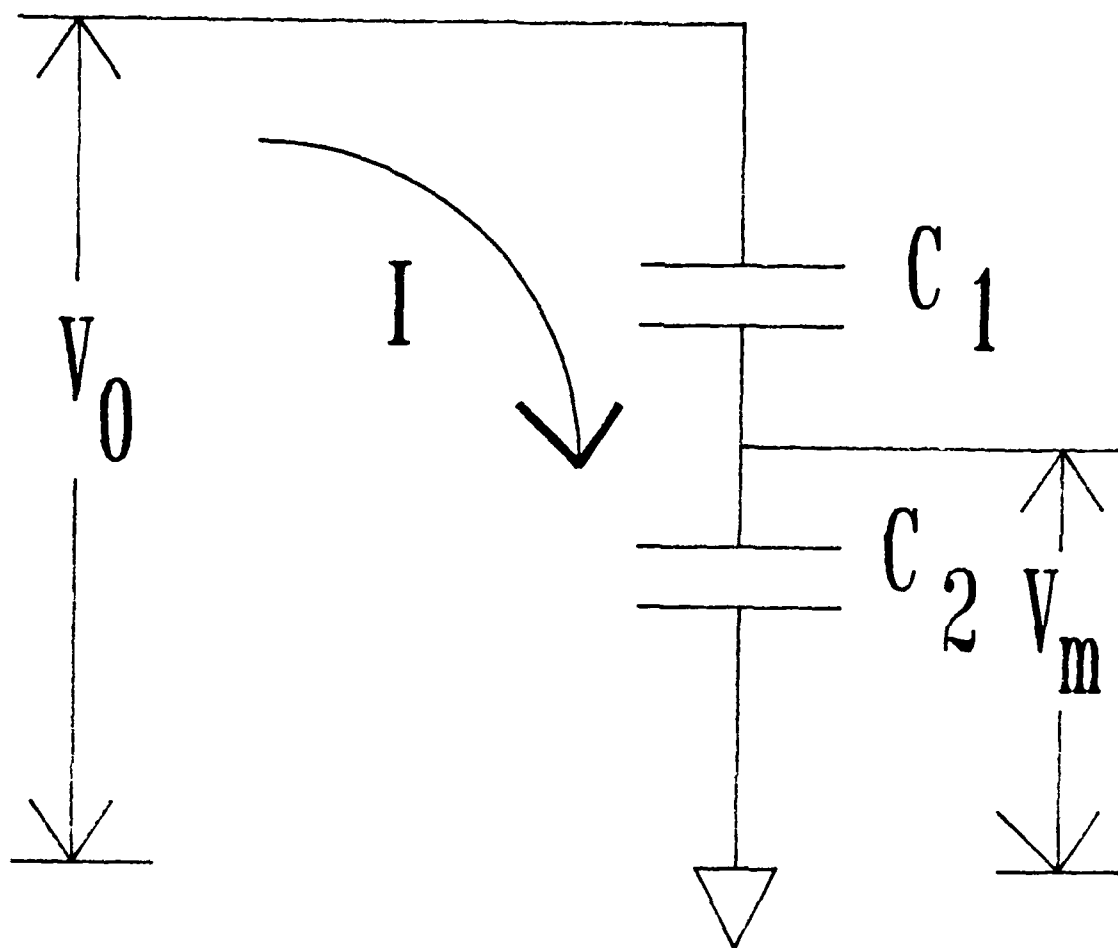
Figure 14. Capacitive voltage monitor circuit.

$$V_o = \frac{1}{C_1} \int I \, dt + \frac{1}{C_2} \int I \, dt \qquad (2.5.3.1.1a)$$

and

$$V_m = \frac{1}{C_2} \int I \, dt \qquad (2.5.3.1.2a)$$

Now, if rather than solving for the ratio of V_m/V_o, we take the time differentials of equations (2.5.3.1.1a) and (2.5.3.1.1.b) and have

$$\frac{dV_o}{dt} = I \left(\frac{1}{C_1} + \frac{1}{C_2} \right) \qquad (2.5.3.1.1b)$$

and

$$\frac{dV_m}{dt} = I \left(\frac{1}{C_2} \right) \qquad (2.5.3.1.2b)$$

Solving for the current I in both equations (2.5.3.1.1b) and (2.5.3.1.2b), we arrive at the relationship

$$\frac{dV_m}{dt} = \frac{C_1}{C_1 + C_2} \frac{dV_o}{dt} \qquad (2.5.3.1.4)$$

If we integrate equation (2.5.3.1.4), we arrive at the relation between the voltages

$$V_m = \frac{C_1}{C_1 + C_2} V_o \qquad (2.5.3.1.5)$$

Equation (2.5.3.1.5) is the basis for our capacitive voltage probes.

Unless the capacitance C_1 is much less than C_2, V_m can be very large. To reduce the probe voltage, the output capacitor voltage is passively integrated with an RC integration circuit.

This analysis does not address stray capacitance from the probe to ground potential. It is presumed negligible. The analysis also does not fully address the time dependence of the voltage probe. If we include these frequency effects, the probe response will produce the voltage response V [160],

$$V = \frac{V_0 \omega \tau}{1 + \omega^2 \tau^2} (\cos \omega t + \omega \tau \sin \omega t - e^{-t/\tau})$$

where V_0 is input voltage, ω is frequency variation of the voltage (exhibiting the behavior $V_0 \sin \omega t$), τ is capacitive voltage probe time constant $= R_t C_p$, R_t is termination resistance and C_p is the probe capacitance.

Using the effect of the voltage frequency yields a voltage V of

$$V(t) = \alpha \cos \omega t + \beta \sin \omega t - \alpha e^{-t/\tau}$$

where α and β are values determined by the frequency ω and the time constant τ. The value for α is

60

$$\alpha = V_0 \frac{\omega\tau}{1 + \omega^2\tau^2}.$$

The value for β is

$$\beta = V_0 \frac{\omega^2\tau^2}{1 + \omega^2\tau^2}.$$

If, for all times of interest t, $\omega\tau \ll 1$ and $t \gg \tau$, then the recorded voltage V_p is [161]

$$V_p \cong \tau \dot{V}$$

where $\dot{V}$ is the time differential of the voltage probe and is

$$\dot{V} = V_0 \, \omega \, \cos \omega t.$$

The voltage seen by the probe is then the time rate of change of the measured voltage V_0. In the limit where $\omega\tau \ll 1$ and $t \gg \tau$, the previous analysis should be valid.

With the termination resistance $R_t = 50 \, \Omega$ and the probe capacitance $C_p \cong 1 \, \text{pF}$, the characteristic time $\tau = 50 \, \text{ps}$ and the time $t \gg \tau$. If we note the system quarter-cycle rise time $T_{1/4} \cong 2.0 \, \mu\text{s}$, then the characteristic frequency $\omega \cong 8 \times 10^5 \, \text{s}^{-1}$ and $\omega\tau \cong 4 \times 10^{-5} \ll 1$ satisfying the constraining inequalities.

2.5.3.2 <u>Capacitive Voltage Probe Construction</u>. The capacitive voltage

probes used on the AFWL PUFF bank are made in-house. The capacitive

voltage probes have brass and aluminum housings and use polyethylene as

a dielectric material. These probes consist of two concentric cylinders

separated by the polyethylene dielectric.

The outer probe housing is a hollow aluminum cylinder of 1.75"

$(4.45 \times 10^{-2}$ m) outer diameter and 1.25" $(3.18 \times 10^{-2}$ m) inner diameter. A

shaped polyethylene dielectric insulator is fitted inside the hollow

cylinder. The second electrode fits inside the polyethylene cylinder.

A brass end cap covers the hollow aluminum cylinder and brings out the

electrical connections from the inner probe electrode.

The outer probe housing is in electrical contact with the lower

transmission line. The outer electrode is at the bias of the lower

transmission line.

The inner probe electrode is capacitively coupled to the upper

transmission line biasing the inner electrode to its potential. The

capacitive coupling between the inner electrode and the upper

transmission line is the C_1 capacitance. The inner and the outer probe

electrodes are capacitively coupled with the C_2 capacitance.

2.5.3.3 <u>Capacitive Voltage Probe Calibration</u>. No direct calibrations

were performed on the capacitive voltage probes. The voltage probes

measured the voltage difference between the upper and the lower

transmission plates. Weights placed on the transmission line altered

62

the transmission line dielectric spacing and, consequently, the C_1 coupling between the probe and the upper transmission line. Altering the coupling changes the voltage division of the probe. The coupling voltage division was sensitive to weight as light as a person on the upper transmission plate. Since some personnel went on top of the transmission line for every shot, direct voltage calibrations were not made. It was decided to rely on the relative amplitude and shape of the voltage trace for each shot. The time average amplitude in the early portion of the voltage trace can be related to the voltage on the capacitor bank V_o times an inductive ratio ν. This inductive ratio ν is defined to be

$$\nu = \frac{L_{02}}{L_{01} + L_{02}}$$

where L_{02} is inductance from the probe to the load, L_{01} is inductance from the capacitor bank to the probe. $L_{01} + L_{02}$ is the system inductance from the capacitor bank to the load.

2.5.4 Passive RC Integrators

RC integrators integrate the output voltage from the diagnostic devices (Rogowski coils, $\dot{B}$ probes and voltage probes). The RC terminology refers to the resistor R and the capacitor C forming the integration circuit. Passive integrators do not use any circuit elements that use current gain or positive feedback mechanisms.

63

2.5.4.1 <u>Passive RC Integrator Theory</u>. The simplified circuit for the passive RC integrator used in integrating voltage sources (Rogowski coils, $\dot{B}$ probes and capacitive voltage probes) is shown in Figure 15.

Using Kirchhoff's first and second laws, we have

$$V_o = IR + \frac{1}{C} \int I \, dt \qquad (2.5.4.1.1)$$

and

$$V_m = \frac{1}{C} \int I \, dt \qquad (2.5.4.1.2)$$

Using Laplace transforms, equations (2.5.4.1.1) and (2.5.4.1.2) are transformed to

$$V_o = IR + \frac{I}{Cs} \qquad (2.5.4.1.1a)$$

and

$$V_m = \frac{I}{Cs} \qquad (2.5.4.1.2a)$$

Performing the algebraic manipulations, the transfer relation becomes

$$V_m = V_o \, \frac{1}{RC} \, \frac{1}{s + \frac{1}{RC}} \qquad (2.5.4.1.3)$$

64
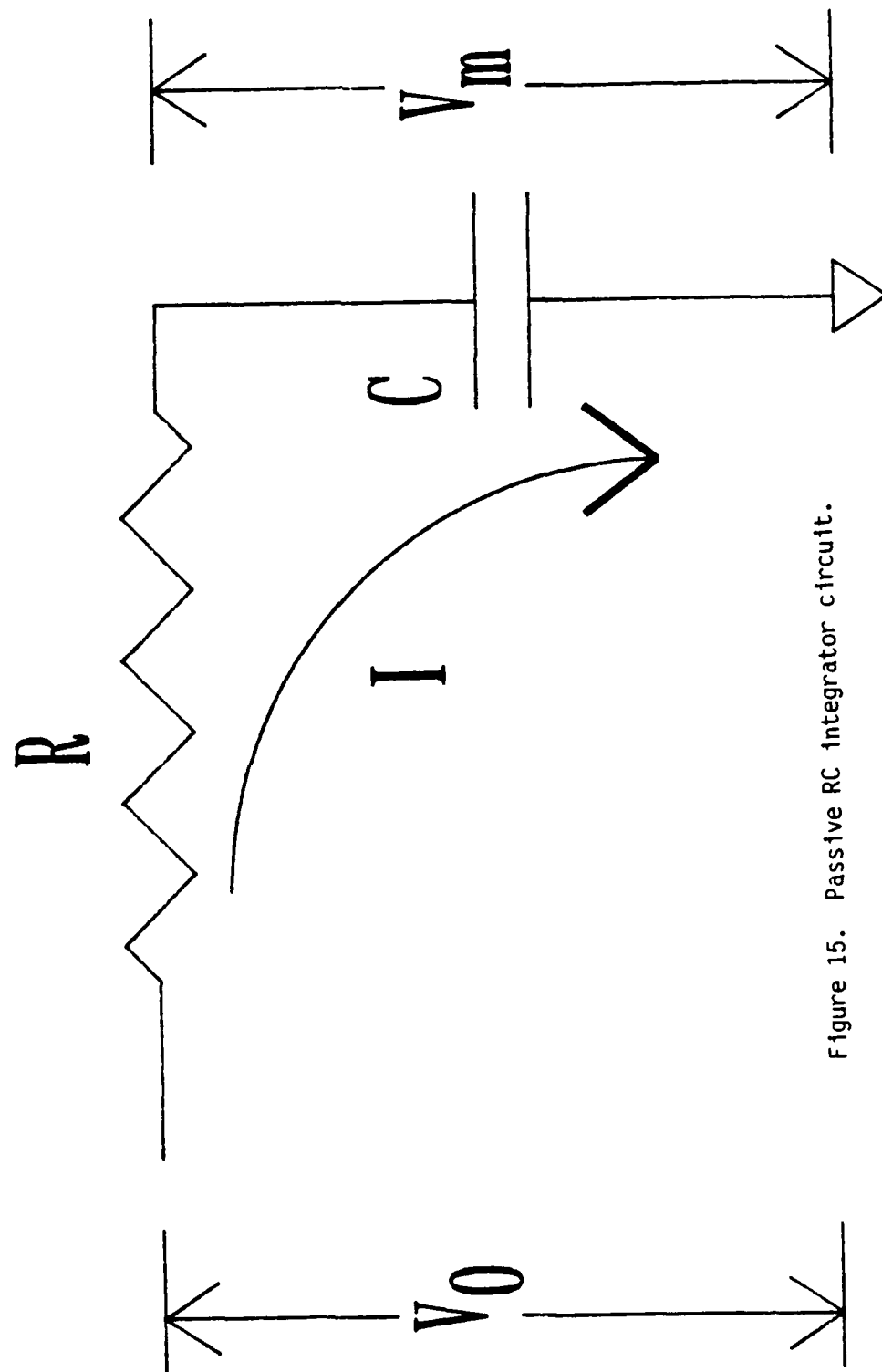
Figure 15. Passive RC integrator circuit.

Using inverse Laplace transforms, this relation becomes

$$V_m = \frac{1}{RC} \, \Gamma\left[\frac{V_0}{s + \frac{1}{RC}}\right] \qquad (2.5.4.1.4)$$

where Γ indicates the inverse Laplace transform.

If we note the Laplace transform variable s corresponds to frequency or inverse time, i.e.,

$$s \propto \omega \text{ and } s \propto \frac{1}{\tau}$$

where ω is a characteristic system response frequency and τ is a characteristic time of the system, we can perform some asymptotic analysis of the transfer relation in equation (2.5.4.1.4)

$$V_m = V_0 \qquad \text{for } s \ll \frac{1}{RC} \; (\tau \gg RC) \qquad (2.5.4.1.4a)$$

$$V_m = \frac{1}{RC} \int V_0 \, dt \qquad \text{for } s \gg \frac{1}{RC} \; (\tau \ll RC) \qquad (2.5.4.1.4b)$$

With these two asymptotic relations, we predict the integrator response. If the characteristic system time is much greater than the RC time constant, the input voltage equals the output voltage. If the characteristic system time is much less than the RC time constant, the output voltage is the time integral of the input voltage divided by RC.

66

The requirement that the characteristic time τ be much less than the time constant RC implies

$$\tau \leqslant 6RC$$

to have valid integration of the voltage to the integrator.

To observe the effect of the RC integrator, assume a unit step function input, $u(t)$ (where $u(t) = 0$ if $t < 0$ and $u(t) = 1.0$ if $t \geqslant 0$)

$$V_{\circ} = V_0 \, u(t)$$

the recorded voltage V_m becomes

$$V_m(t) = \frac{V_0}{RC} \, e^{-t/RC} \qquad\qquad (2.5.4.1.5)$$

This implies the integrator voltage is bled off by the resistor R in the integrator circuit. If the characteristic time is small compared to RC, the resultant error is small.

Having introduced an error with the RC integrator, it would be desirable if a correction could be made. This can be done by using the transfer function, equation (2.5.4.1.3). If we multiply the voltage V_m by (RCs + 1) which is the multiplicative inverse of the transfer function, we have

67

$$V_{cor} = V_m (RCs + 1) \qquad (2.5.4.1.6)$$

where V_{cor} is the corrected voltage and V_m is the measured voltage. Performing the Laplace inverse, we have

$$V_{cor} = RC \frac{dV_m}{dt} + V_m \qquad (2.5.4.1.7)$$

This corrects the integrated measured voltage traces. Except for possible numerical errors, this correction is exact.

2.5.4.2 Passive RC Integrator Construction. The passive integrators are constructed with coaxial connections; one end has a male connection and the other has a female connection. They measure about 2" (5×10^{-2} m) long. The capacitors used in the integrators are nominally 0.5 µF. The RC time constants vary from 10 µs to 50 µs.

2.5.4.3 Passive RC Integrator Calibration. RC integrators can be calibrated in several ways. Two methods are discussed here. The first method compares the input and output signals when a step or square wave function is the input signal. The second method compares the input and output signals when driven by an adjustable sinusoidal wave generator of adjustable frequency.

In the first method, a known voltage is applied to the RC integrator. This voltage is measured with an oscilloscope picture. The output of the RC integrator is recorded on another oscilloscope picture. Using

68

equation (2.5.4.1.5), a comparison of the input and output signals can be made and the RC time constant derived.

In the second method, we use the transfer function from equation (2.5.4.1.3). In a more appropriate form, this is

$$\frac{V_m}{V_o} = \frac{1}{RCs + 1} \qquad (2.5.4.1.3a)$$

Realizing s corresponds to the frequency ω of the driving oscillator, we can compare the input/output ratio as a function of frequency. If the product $RC\omega$ is sufficiently large (i.e., $RC\omega \gg 1$), the ratio is inversely proportional to frequency so that

$$\frac{V_m}{V_o} \cong \frac{1}{RC\omega}$$

By measuring the slope $(\frac{1}{RC})$, the RC time constant can be calculated. Even should the product $RC\omega$ not be sufficiently large, a curve fit can be used to derive the RC time constant. The results for the RC calibration series are displayed in Table 2. A single standard deviation is reported as the error.

Not all the RC integrators could be calibrated. When they were being used, the integrators could not be removed for calibration. After the experimental series was completed, these integrators were borrowed by Los Alamos National Laboratory personnel. Unfortunately, not all of the

69

integrators were returned to AFWL. For these integrators, the nominal
RC time constant is assumed. The error is assumed to be ±10%.

Table 2. RC Integrator Time Constants

Probe Name	Time Constant (μs)
B	10 ± 1
C	10.27 ± 1.13
D	10 ± 1
E	9.93 ± 0.32
F	9.45 ± 0.26
G'	9.32 ± 0.34
H'	10 ± 1
J'	10 ± 1
L	10 ± 1
M	10 ± 1
N	25 ± 3
O	22.91 ± 1.83
P	26.18 ± 1.32
Q	25 ± 3
R'	25 ± 3
S	25 ± 3

2.5.5 Time of Flight Photon and Neutron Detectors

Photon and neutron detectors are used to analyze the high energy photons
and neutrons produced in the experiment. The high energy photons and
the neutrons are products of the D-D nuclear fusion reaction. The

detectors provide a voltage response proportional to the energy deposited by the photons or neutrons.

The D-D fusion reaction is

$$D + D \rightarrow He^3 + n + 3.26 \text{ MeV}$$
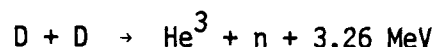
with the neutron having 2.44 MeV and the He^3 nucleus having 0.82 MeV energy.

The time of flight method measures the time difference between the photon and the neutron, hence the nomenclature. For a given distance ℓ from the source to the detector, the time delay t_{ℓ_1} for the photon is

$$t_{\ell_1} = \frac{\ell}{c}$$

where c is the speed of light (2.998×10^8 m/s). In this analysis, the fusion reaction products are assumed to be produced in a time scale much less than the characteristic time of flight.

For the same distance ℓ, the time delay for the neutron t_{ℓ_2} is

$$t_{\ell_2} = \frac{\ell}{v}$$

where v is the velocity of the neutron. Since the D-D fusion product neutrons are on the order of several MeV, they are non-relativistic and the energy of the neutron E_n is

$$E_n = \frac{1}{2} m_n v^2$$

where m_n is mass of the neutron (1.675×10^{-27} kg). Knowing the velocity spectrum, an energy spectrum of the neutron can be generated to diagnose the D-D neutron interaction mechanisms.

For our case, the distance d is on the order of several meters. The time delay t_{ℓ_1} is on the order of tens of nanoseconds. For the microsecond time scales of the experiment, this time is practically instantaneous. As such, the photons measured by the time of flight detectors are used as a time reference.

The detectors used are E G & G model number NPM54X detectors. These sealed integral units are based on a 2.25" (5.72×10^{-2} m) diameter 2.25" long NE111 plastic scintillator. The scintillator is optically coupled to the XP2020 photomultiplier. The detector assembly is surrounded by a 0.1875" (4.76×10^{-3} m) aluminum jacket except for a window made of other materials. The detectors are wrapped in a thickness of 0.625" (1.59×10^{-2} m) lead to reduce sensitivity to photons and neutrons not traveling directly (line of sight) into the detectors. A detector is shown in Figure 16. Knowing the different detector responses and the filter material attenuation, the photon spectrum can be determined using
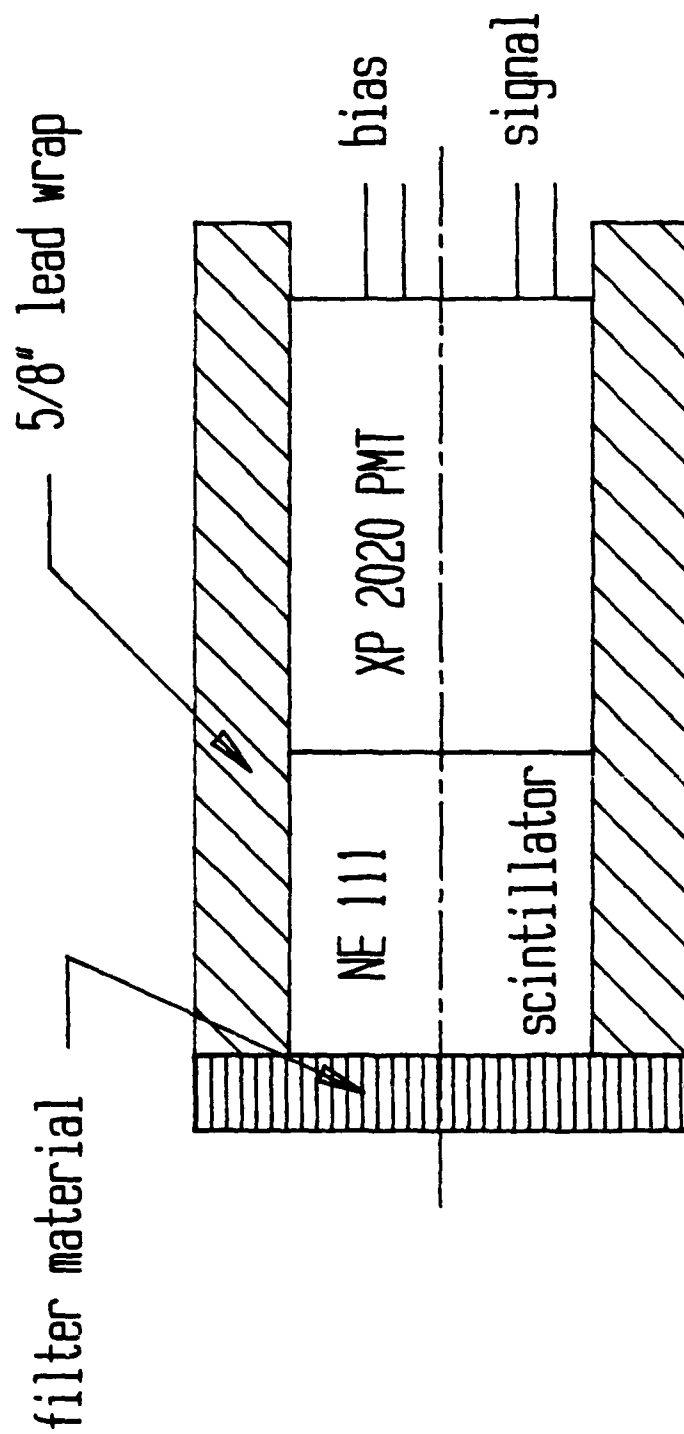
Figure 16. Scintillation photomultiplier.

73

the Degnan deconvolution technique [162]. Particular results from the AFWL PUFF coaxial plasma gun are dealt with in greater detail by Beason [103] and Warren et al. [104].

2.5.6   Silver Geiger-Müller Counter Neutron Detectors

The D-D nuclear reaction products were detected using Geiger-Müller tubes. These tubes detect nuclear (n, γ) reactions through neutron activation of natural silver (Ag). The detection method follows that of Lanter and Bannerman from Los Alamos [163, 164].

Natural silver (instead of isotopically pure silver) is used for the thermalized neutron detection. The characteristics for the naturally occurring silver isotopes are reported in Table 3.

Table 3. Characteristics of Natural Silver Isotopes

Isotope	Natural Abundance [165]	Neutron Cross-Section (b) [166]	Product Isotope	Half Life [165]
Ag-107	51.839±.005	38	Ag-108	2.37 ± 0.01 min
		0.35	Ag-108m	127 ± 2.7 yr
Ag-109	48.161±.005	87	Ag-110	24.6 ± 0.2 sec
		4.6	Ag-110m	249.76 ± 0.04 day

One minute count times are used. The major activation products of concern are Ag-108 and Ag-110; the metastable isomeric states have little effect on the count rate. Major Ag-108 products are 1.65 MeV β^-

74

particle (with 96% occurrence), 1.02 MeV β^- (with 1.7% occurrence) and 0.88 MeV β^+ (with 0.3% occurrence) [166]. The particulate occurrence does not add to 100% because the Ag-108 isotope exhibits a 2% electron capture [166]. Major Ag-110 products are the 2.89 MeV β^- (with 95% occurrence) and 2.22 MeV β^- (with 5% occurrence) [166]. Both isotopes exhibit fractional numbers of γ-rays. With the multiplicity of product particles, each with an independent Geiger-Müller collection efficiency, a complete physical description is complex. Instead of attempting a complex description (which would be beyond the range of this dissertation), the presentation of Lanter and Bannerman is followed. Their empirical relations are used and an effective decay constant derived (with the values reported in Table 3). This approach can be repeated since the AFWL system is nearly identical to theirs. The effective decay constant is 2.114×10^{-2}/s in good agreement with the value of 2.14×10^{-2}/s of Lanter and Bannerman.

The Geiger-Müller tubes are Victoreen type 1B85 detector tubes. They operate at a bias voltage of about +900 V. They are ensheathed by 20 mil natural silver. A methyl methacrylate plastic tube, 3 1/8" (7.94×10^{-2} m) long, 1 1/8" (2.86×10^{-2} m) outer diameter and a wall thickness of about 160 mils (4.05×10^{-3} m) surrounds the detector. These tube ensembles are mounted in a 12 × 12 × 6" (0.3048 × 0.3048 × 0.1524 m) polyethylene block. The polyethylene thermalizes the fusion reaction neutrons for absorption in the silver sheet. One large area side (12×12") of the polyethylene block faces the neutron source. On the opposite side of the polyethylene block, the tube assemblies are
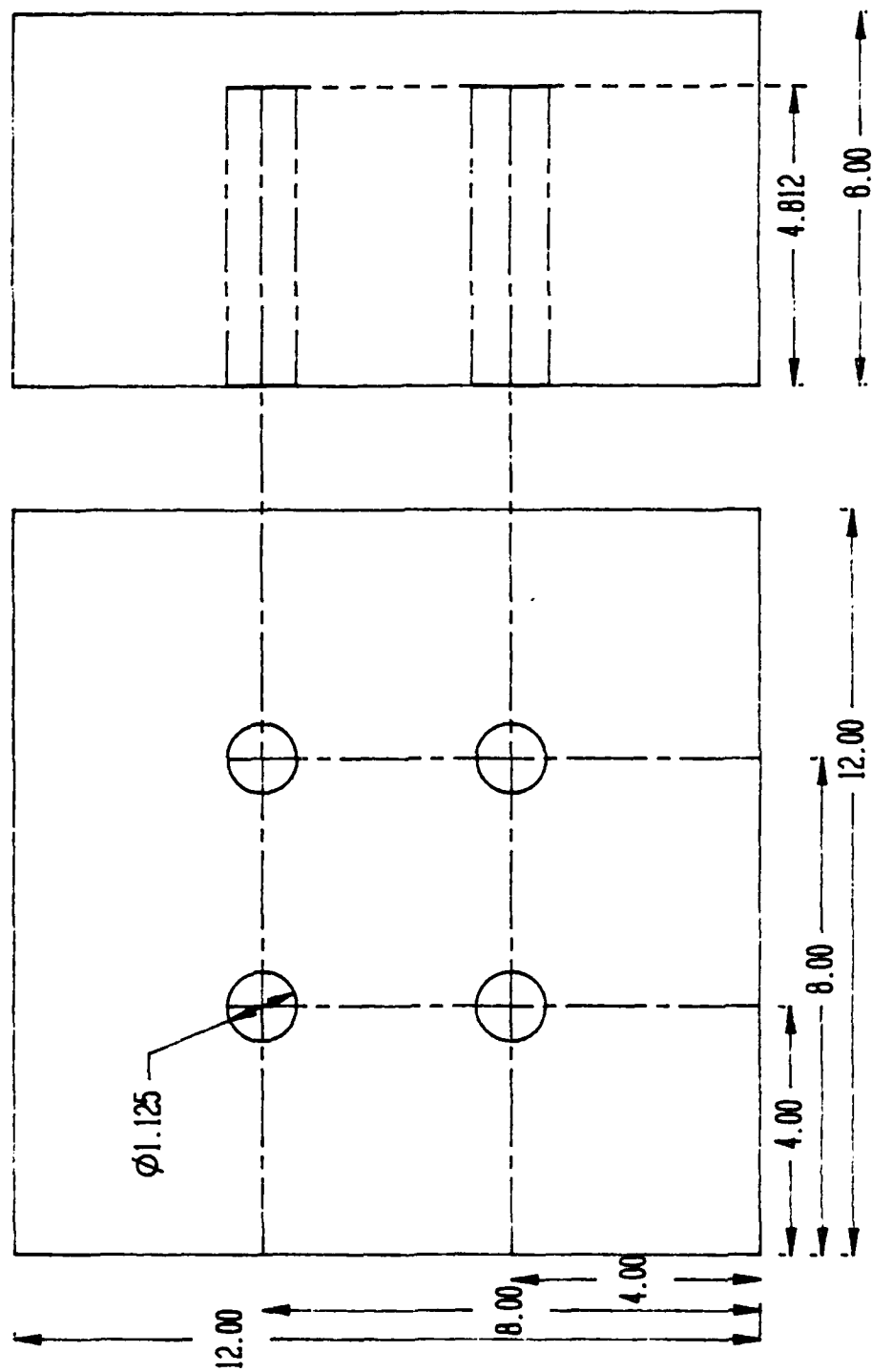
Figure 17. Mount and moderator for silver Geiger-Müller neutron detector.

inserted some 4 13/16" (0.1222 m) into the block. Four tube assemblies are placed in the block. The tube assemblies placement is shown in Figure 17.

The major difference between the Los Alamos and the AFWL detectors is the silver sheet thickness used to surround the Geiger-Müller tubes. Lanter and Bannerman used 10 mil (2.54×10^{-4} m) silver sheet; we use 20 mil (5.08×10^{-4} m) thickness sheet. With Ag density of 10.5 g/cm^3 (1.05×10^4 kg/m^3), the macroscopic nuclear cross-section increases from 3.61 cm^{-1} to 7.22 cm^{-1}. Increasing the macroscopic cross-section increases the fractional neutron absorption from 0.0876 to 0.1676. This increases the neutron absorption by 1.912. However, the Geiger-Müller tube β absorption also decreases with the increased silver sheet thickness.

Using the relation reported by Price [167], material beta absorption is approximated by

$$\text{fraction of } \beta\text{'s absorbed} = 1 - e^{-\mu_m \rho x}$$

where μ_m is averaged mass absorption coefficient, ρ is mass density and x is length of β transport. The mass absorption coefficient is reported by Price [167] to be approximately

$$\mu_m = \frac{17}{E_m^{1.14}}$$

where μ_m is in units of cm^2/g and E_m is MeV. With the natural isotopic silver abundance and the particulate occurrence as weighting factors, the mean silver mass absorption coefficient is 7.44 cm^2/g. Doubling the silver sheet thickness causes the fractional β absorption to increase from 0.8625 (in the 10 mil sheet) to 0.9811 (in the 20 mil sheet).

This analysis assumes the β particle is produced at the outer edge of the silver sheet. A more reasonable assumption assumes an effective β production site is located at the nuclear reaction centroid location.

The centroid of the silver sheet is determined by the integral

$$\bar{r} = \frac{\int r\,f(r)\,dr}{\int f(r)\,dr}$$

where radial position is used because of the tube cylindrical symmetry. The weighting function $f(r)$ is

$$f(r) = e^{-\Sigma r}$$

where Σ is neutron absorption cross section. The limits on the integration go from r_0 (the inner silver sheet radius) to $r_0 + \delta$ (the outer silver sheet radius).

Performing the integration, we obtain the relation for the centroid position $\bar{r}$

$$\bar{r} = \frac{(r_0 + \frac{1}{\Sigma}) - e^{-\Sigma r}(r_0 + \delta + \frac{1}{\Sigma})}{1 - e^{-\Sigma r}}$$

Using $r_0 \cong 0.375$ inch (9.525×10^{-3} m), $\Sigma = 7.22$ cm^{-1} (7.22×10^2 m^{-1}) and δ of 10 or 20 mil (2.54×10^{-4} or 5.08×10^{-4} m), the centroid position $\bar{r}$ is 0.3798 inch (9.647×10^{-3} m) for the 10 mil sheet and 0.3844 inch (9.865×10^{-3} m) for the 20 mil sheet. The radial position difference between r_0 and the centroid position $\bar{r}$ is the mean distance the β particles have to cross the silver sheet. This yields the fractional β absorption from 0.3858 (for the 10 mil sheet centroid) to 0.8451 (for the 20 mil sheet centroid).

Noting the relation between the fractional β transmission T and the fractional β absorption A

$$T = 1 - \text{fractional } \beta \text{ absorption} = 1 - A$$

and comparing the response of the 20 mil (AFWL) detector to the 10 mil (Los Alamos) detector, all other factors being equal, the AFWL system produces a count 0.482 times the Lanter and Bannerman value.

Lanter and Bannerman derive the neutron production N from the relation

$$N = F \, C_t$$

79

where F is a geometry factor and C_t is the true count rate (the first one minute count less background and corrected for dead time) of the system. For D-D fusion nuclear reactions, they quote F to be

$$F = 30 (5.3 + D)^2$$

where D is the distance from the neutron source to the moderator in inches. Lanter and Bannerman state this relation is good to ±15%. We calculate the AFWL silver detector neutron response to be

$$N = 62.2 (5.3 + D)^2 C_t$$

Following Lanter and Bannerman and assuming a Geiger-Müller tube recovery time of 125 μs, we have the true count rate C_t to be

$$C_t = 2.72 \times 10^5 \frac{(e^{2.64 \times 10^{-6} C} - 1)}{(1 - 0.281 \ e^{2.64 \times 10^{-6} C})}$$

where C is count rate corrected for background. Lanter and Bannerman caution their derivation is not valid for cases where $C_t > 1.2C$ limiting the maximum count rate to be 72,500 counts per minute for one tube or 290,000 counts per minute for all four tubes.

2.5.7   Open Shutter Camera

One concern with visible light photography for diagnosing the plasma behavior has been noted by Mather--visible light output does not necessarily correlate with plasma behavior [168]. Visible light production mechanisms do not necessarily reflect plasma mechanisms. Plasma sheath velocity does not necessarily relate to visible light velocity. While visible light photography does yield qualitative plasma information, it is not readily converted to useful quantitative data.

An open shutter cameras took time integrated pictures of visible light processes within the plasma gun, but it was of limited use. With only three available ports, access to the plasma gun is limited. There are two 2" (5.08×10^{-2} m) ports on either side of the vacuum vessel covering the plasma gun. (One of these is seen in Figure 2.) A typical plasma gun visible light output during a pinch is shown in Figure 18. The other access is from the top of the vacuum vessel. The top of the vacuum vessel is more limited than the 2" ports. Mounting a camera to observe the vacuum vessel top involved the use of a tripod mount. The tripod was prone to vibration so open shutter photographs smear due to vibration as well as due to the time integration. When the upper or secondary gas valve is used, it requires a connection to allow gas to penetrate the vacuum interface. This valve requires a skirt or shield for successful operation. (A photograph of the underside of the valve and the skirt is shown in Figure 19.) The skirt reduces the energy load to the upper valve by dissipating it over a larger area. Without the skirt, the upper valve is sealed open or closed.
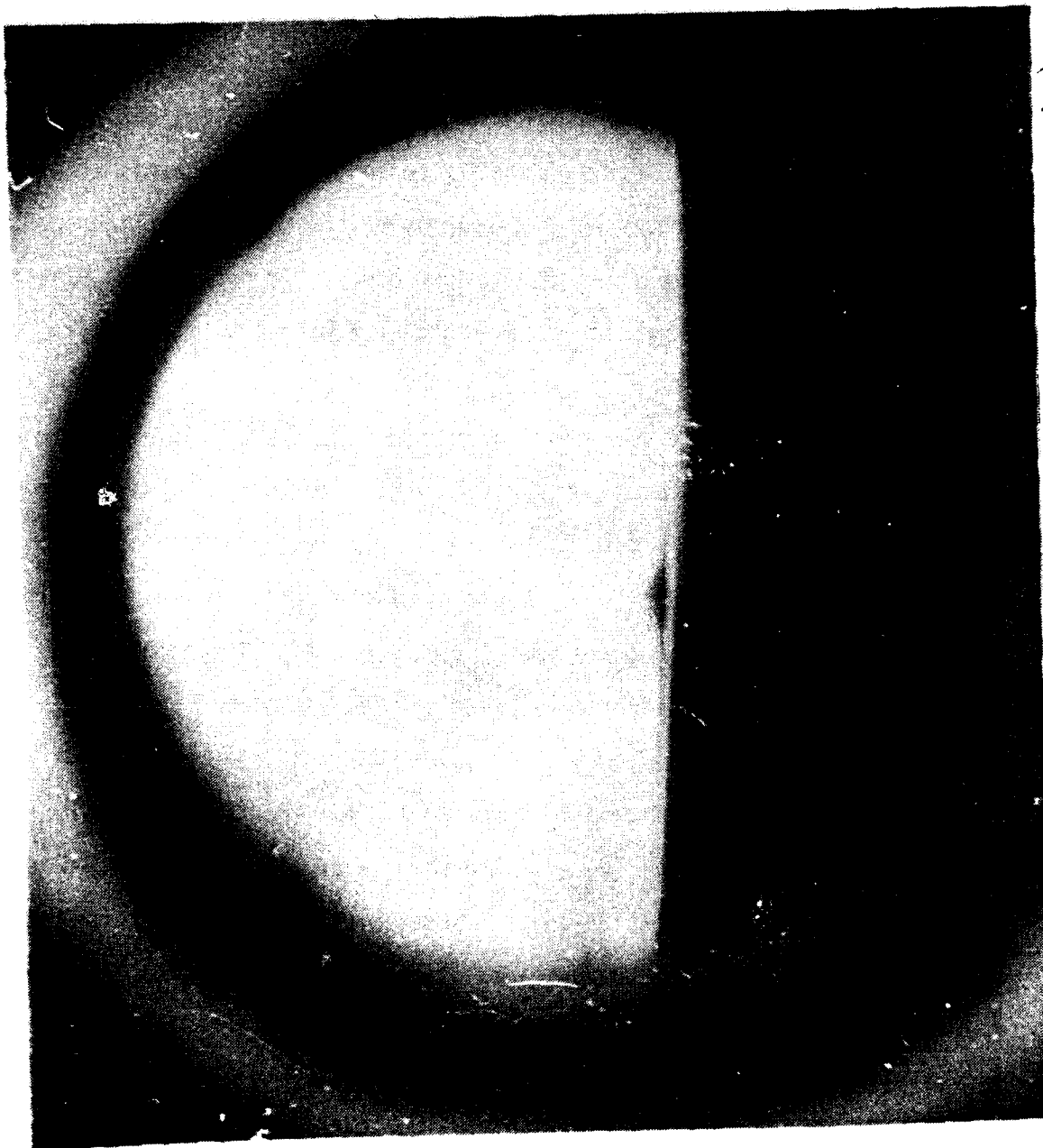
Figure 18. Open shutter photograph of gun muzzle (side view).
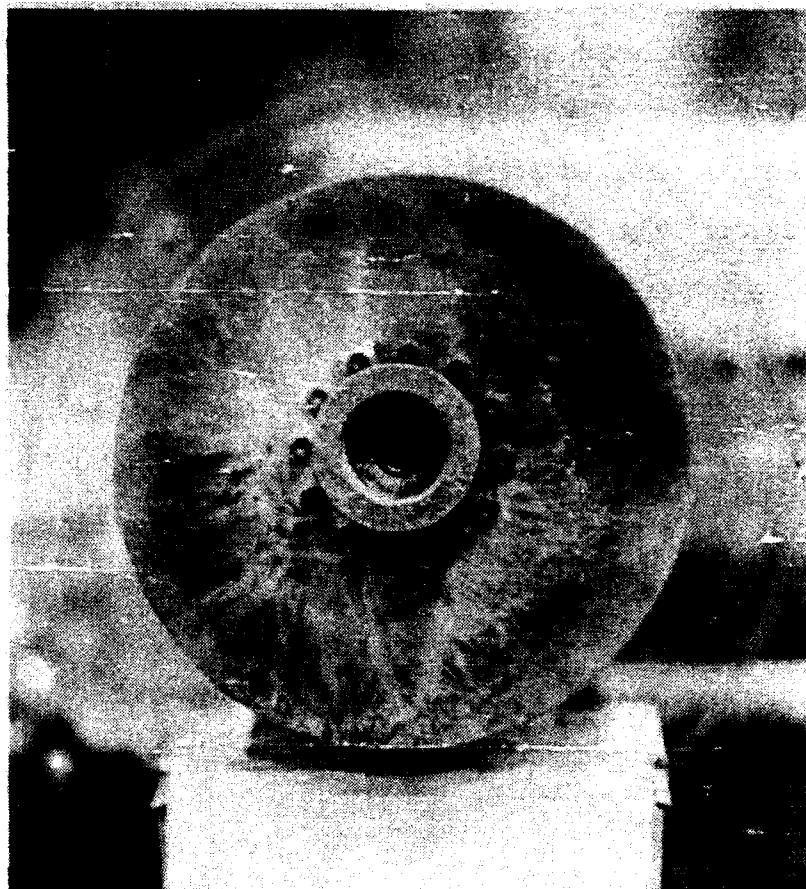
Figure 19. Upper (secondary) gas valve with skirt.

2.5.8 Framing Camera

A framing camera takes a short time photograph. The time allowed for each photographic image (a frame) can be set. The time between the frames is also adjustable (within the limits of the camera). The image can be recorded for times as short as tens of nanoseconds. The time between images can be of the same order as the frame time. A framing camera may use light amplification to enhance the photographic image. Our framing camera did not.

We used a framing camera focused on the gun muzzle. Since the upper gas valve was not in place, the muzzle could be photographed. Because of problems with timing and the pulsed electromagnetic environment, only one useful framing photograph was obtained. This was reported in the paper by Degnan et al. [102] and is shown as Figure 20. In that photograph, the visible light intensity increased significantly during the discharge. Since we did not use light intensification techniques, imaging was a problem.

An end view of the gun muzzle is shown in Figure 20. There are three frames of the coaxial gun discharge running sequentially from bottom to top. Each frame shows a 50 ns exposure. The time between frames (from the start to start of each frame) is 100 ns. The first frame is under-exposed. The second frame shows the plasma lighting the 24 cathode rods in the plasma gun annulus. The third and final frame shows the plasma coming off the gun muzzle. The large light output may be due to fast plasma impinging on the upper Lexan cover and inducing luminescence.

84
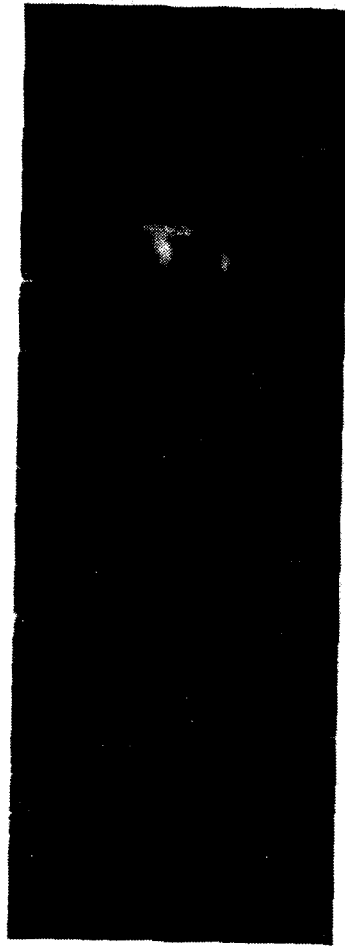
Figure 20.   Framing camera photograph of gun muzzle (end view).

2.5.9 Attempted Experimental Diagnosis

This section discusses additional diagnostic techniques that were
attempted, even if they yielded less than fully successful results.
This provides a more complete listing of the attempted diagnostic
devices applicable to the reported coaxial plasma gun system.

2.5.9.1 Interferometry. Interferometry is used to measure electron
density n_e over an optical path length through the plasma. Specifying a
monotonic radiation source (such as a maser or laser) and using a Fabry-
Perot interferometer, the governing relation is

$$2n\ell = m\lambda$$

where n is index of refraction, ℓ is the optical path length, λ is
characteristic radiation wavelength and m an integer.

Assuming the plasma is unmagnetized and consists of normal matter
(electrons and ions, instead of mesonic matter or antimatter), the
relation for the index of refraction is

$$n^2 = 1 - \frac{f_p^2}{f^2}$$

where f_p is plasma frequency and f is characteristic wavelength of the
probing electromagnetic radiation.

From [169], we have

$$f_p = 8.98 \times 10^3 \, n_e^{1/2} \text{ Hz}$$

where n_e is number density of electrons in cm^{-3}. For singly ionized plasmas, the ion density n_i is approximately equal to the electron density, i.e., $n_i \cong n_e$.

If we realize the ratio, $\dfrac{f_p}{f}$, is very small ($\dfrac{f_p}{f} \ll 1$), we approximate the index of refraction n by

$$n \cong 1 - \frac{f_p}{2f}$$

Noting the interferometer measures change through destructive interference of the electromagnetic radiation (fringes), we have

$$2\ell\Delta n = \lambda\Delta m$$

where Δn is change in the index of refraction and Δm an integer.

We then have the relation for the electron density n_e

$$n_e = \frac{1.115 \times 10^3 \, \Delta m}{\ell\lambda}$$

There is a limit to the interferometer effectiveness when the plasma electron density becomes too dense for the radiation to penetrate the plasma. This limiting condition occurs when the characteristic radiation frequency ω equals the plasma frequency ω_p, i.e.,

$$\omega = 2\pi f = \omega_p = (\frac{n_e e^2}{m_e \epsilon_0})$$

A listing of the limiting electron densities for various different radiation sources is given in Table 4.

In our experiment, we used a helium neon (HeNe) laser. However, any interferometric data was masked by excessive electromagnetic noise.

The previous discussion assumes the effect of density gradients is negligible. With large gradients, the laser light would be refracted out of the optical path length [170] according to the reported relation

$$\frac{1}{R} = \frac{1}{n} \nabla n \cdot \mathbf{n}$$

where R is radiation radius of curvature from the optical path, n is local refractive index, ∇n is gradient of the local refractive index and $\mathbf{n}$ is a local unit normal. In our experiments, the optical light paths are not be particularly large (on the order of several meters), but the density gradients can be very large.

Table 4. Limiting Plasma Electron Densities for Various Sources

Electromagnetic Radiation	Wavelength		Plasma Electron Density (cm^3)
3 GHz microwave	10	cm	1.1×10^{11}
30 GHz microwave	1	cm	1.1×10^{13}
300 GHz microwave	1	mm	1.1×10^{15}
3 THz microwave	0.1	mm	1.1×10^{17}
CO_2 laser	10.6	μm	9.9×10^{18}
CO laser	5	μm	4.5×10^{19}
InGaAsP diode laser	1.550	μm	4.6×10^{20}
NdYAG laser	1.32	μm	6.4×10^{20}
HeNe laser	594	nm	3.2×10^{21}
ArF excimer laser	193	nm	3.0×10^{22}

The density gradient and derivative of the density gradient form the basis of Schlieron and shadowgraph diagnostic techniques [171]. Although laser shadowgraphy was successfully used on the AFWL SHIVA device, Schlieron and shadowgraphy techniques were not used on the experiments described here.

2.5.9.2   Streak Camera.   The streak camera takes a time integrated photograph of an object [172], smearing the image as a function of time. However, this time smearing is controlled. The image is moved at a

fixed rate so the image can be known as a function of time through the corresponding position on the photograph.

The available ports for viewing the images did not accommodate using a streak camera. A streak camera would have been ideal for examining the plasma sheath flow along the length of the gun, but this would have involved remachining the experimental hardware. This could not be accommodated by the available time and funding.

2.5.10 Experimental Limitations

The series of experiments discussed here are limited. It is not the purpose of this section to minimize the effect of these limitations; some of them are significant. The discussion is provided for identifying the effect of the limitations on the data and results that follow. If some procedure were not followed or some method not used, this section should provide some illumination as to the rationale.

2.5.10.1 Time Limitations. Time on the AFWL PUFF capacitor bank was limited by management concerns. Maximum system use was required. Since the coaxial plasma gun required priming or clearing with an initial shot, gun operation over many days requires more time and energy for gun preparation than if the shots were performed in rapid succession. As a result, many shots were performed in a relatively short time.

This limitation allowed little time for the examination of data and for reflection on experimental results. After the experimentation was

completed, no amount of reflection and analysis would have provided the personnel and funding to continue. Had more time been available, the experimental series would have most certainly been more comprehensive, thorough and complete.

A third constraint, not directly relating to the experimentation, limited the timely reporting of the results. Following experimentation, recorded data (oscilloscope pictures) are required to be digitized into numerical form suitable for analysis. Having up to 20 voltage traces for each data shot and each data trace must be digitized, taking from 10 to 60 minutes per trace. The data needs to be made acceptable, i.e., high frequency noise required smoothing, baseline corrections needed to be made (where digitization introduced slope errors) and conversion factors were used to convert voltage traces into system voltages, currents and magnetic fields. Correction of a single digitized trace requires over an hour. With 711 oscilloscope traces, data conversion is time and labor intensive. Only part-time efforts could be devoted to completing the analysis.

2.5.10.2 Equipment Limitations. Two major experimental limitations should be noted: the screen room used to house the oscilloscopes was not completely effective, giving rise to excessive amounts of noise on the data, and fiducial signals were not superimposed on the data traces. Other experimental limitations can be compensated for or corrected; these two could not be totally compensated for or corrected.

After completion of the experimental series, it was discovered the isolation feedthrough connections (connecting the signal sources and the oscilloscopes) were installed in the screen room backward. This caused the screen room (ideally a Faraday cage) to be incompletely grounded and allowed a high frequency noise from the capacitor discharge in the data.

In terms of data analysis, the second restriction is more stringent. Having no time fiducials introduced timing errors. Data analysis yielding sheath velocities, current simultaneity at an axial position, azimuthal sheath symmetry and the current as a function of both time and position, was more difficult than otherwise would have been the case. Certain assumptions have been made in data extraction. While these assumptions are reasonable, they are not without qualification.

2.6 NOMENCLATURE USED IN THIS EXPERIMENTAL SERIES

In the experimental series, a standardized designation for different shots and data traces is maintained. This notation is followed throughout this dissertation.

The format followed for naming traces is

M DD SS I N

where M, DD, SS, I and N are one or two character alphanumeric fields.

M is a one character alphabetic field representing the month of the particular shot. It was N if the month of the shot were November; D if it were December; and J if it were January.

DD is a two character numeric field representing the day of the month of the particular shot. DD varies from 01 to 31.

SS is a two character numeric field representing the number of the particular shot. SS begins at 01.

I is a one character alphabetic field representing the type of detector. If the identifier were I, it represents a current; if it were B, it represents a magnetic field; if it were V, it represents a voltage probe; and if it were N, it represents a neutron detector.

N is a one character alphanumeric field further characterizing the identifier I. N is explained in Table 5.

$\dot{B}$ probes are classified according to position. Details are given in Section 3. There are four $\dot{B}$ probes in each level and at each azimuthal position.

The notation J0703BP represents the signal for the $\dot{B}$ probe P for the third shot on January 7. Similarly, D2901VN is the north voltage probe signal for the first shot on December 29. J1111IC is the chamber current signal for the eleventh shot of January 11.

Table 5. Identification of Probe Nomenclature

Probe Type	Identifier I	Identifier N	Particular Probe
Rogowski coil	I	C	chamber or center Rogowski
	I	R	counter-rotating Rogowski
Voltage	V	N	north voltage probe
	V	S	south voltage probe
$\dot{B}$ probe	B	B	$\dot{B}$ probe B
	B	C	$\dot{B}$ probe C
	B	D	$\dot{B}$ probe D
	B	E	$\dot{B}$ probe E
	B	F	$\dot{B}$ probe F
	B	G	$\dot{B}$ probe G'
	B	H	$\dot{B}$ probe H'
	B	J	$\dot{B}$ probe J'
	B	L	$\dot{B}$ probe L
	B	M	$\dot{B}$ probe M
	B	N	$\dot{B}$ probe N
	B	O	$\dot{B}$ probe O
	B	P	$\dot{B}$ probe P
	B	Q	$\dot{B}$ probe Q
	B	R	$\dot{B}$ probe R'
	B	S	$\dot{B}$ probe S
Neutron detector	N	B	bare (unfiltered) scintillator photomultiplier detector

3.0 AFWL COAXIAL PLASMA GUN

In this section, the specifics of the AFWL PUFF coaxial plasma gun are examined. Specifically discussed are the placement of $\overset{\circ}{B}$ probes, Rogowski coils and capacitive voltage probes and their effect on the experimental data.

3.1 COAXIAL PLASMA GUN THEORY

Although the plasma gun theory is discussed in Section 2, this section discusses the coaxial plasma gun in greater detail. This discussion addresses the PUFF coaxial plasma gun specifics.

3.1.1 Plasma Formation in the Coaxial Plasma Gun

Before a plasma gun can operate, a plasma must be formed. Before plasma formation, matter must be inserted into the gun for ionization to the plasma state. One means, ideally the primary means, for delivering matter to the coaxial plasma gun is neutral gas injection. However, other means exist for inserting matter in the coaxial plasma gun. Dielectric (insulator) material can ablate as a function of its dielectric strength and the applied voltage. Physically adsorbed or physically embedded gas molecules can evolve with application of high voltages. When reactive gases are used in the plasma gun, chemically absorbed molecules can be released. When adsorbed or chemisorbed molecules are released, they are subject to the same dielectric stress of the injected gas.

In most coaxial plasma guns, a non-ionized gas dissociates into electrons and ions according to the gas dielectric strength (given by the gas Paschen curve) when high voltage is applied. In these guns, gas generally dissociates at the vacuum/dielectric interface. With spark formation of the breakdown, ultraviolet light and soft X-rays are emitted. These high energy photons release electrons through the photoelectric mechanism. The photoelectron evolution is photon spectrum and materials dependent.

In the PUFF coaxial plasma gun, the dielectric/vacuum interface is remote from the gun. Since the dielectric is isolated from ultraviolet and soft X-radiation produced by the plasma formation, it does not influence the plasma formation in the gun. Paschen gas breakdown predominates the plasma formation and the plasma is formed near the gas outlet in the gun annulus. The evolution of gas (through release of embedded, adsorbed and chemisorbed material) from plasma gun surfaces is a factor in the plasma formation in the AFWL plasma gun. In terms of the total plasma formation, it is generally a small factor, but it is nevertheless a real factor. This is evident by the need to precondition the plasma gun with clearing shots.

Depending on the coaxial gun plasma density distribution, a current carrying plasma sheath is formed. If the plasma sheath is narrow, indicating a higher conductivity in the plasma than in the surrounding gas, the plasma is driven along the plasma gun. The sheath may drive mass ahead of it; this is the snowplow mode. If this narrow sheath does not appreciably accrete mass, this would be a washer or slug mode. This

washer or slug mode is a limiting case of the snowplow. If the current
sheath is diffuse, the plasma remains relatively stationary. This is
the deflagration mode. In our plasma gun, the sheath appears to be a
combination of the slug/washer and the deflagration modes. There is no
analog to the sheath lift-off of other coaxial plasma guns in the AFWL
plasma gun.

3.1.2   Sheath Velocity Theory

There are several models for the coaxial plasma gun sheath velocity.
Four of these models are discussed here. The first model is the
collisionally dominated model of Alfven [173], a theory promoted by
Axnäs [174-177] and Raadu [178, 179] of Sweden. The second model is
that of Rosenbluth [180], developed for analysis of a toroidal z-pinch.
The third model is a single particle drift velocity. The fourth model
is the limited or saturated velocity model reported by Fishbine [181].

3.1.2.1   Alfven Sheath Velocity Model. The Alfven model assumes a
weakly ionized magnetized plasma in a sea of neutral particles. In this
model, the critical velocity is limited by charged-neutral particle
collisions. At the neutral particle ionization energy, neutral
particles are ionized and absorb energy from the plasma. A resonance
absorption is formed when the energy of the neutrals, E_n, equals the
ionization energy of the plasma

$$E_n = \frac{1}{2} m_n u_c^2 = eV_i$$

97

where m_n is mass of the neutral particle, u_c is Alfvén critical velocity, e is electronic charge and V_i is ionization potential of the neutral gas. This is

$$u_c = (\frac{2eV_i}{m_n})^{1/2} .$$

The Alfvén critical velocity depends only on the neutral gas.

Using our experimental conditions, the Alfvén critical velocity can be derived. With a D_2 ionization potential of 15.46 eV (2.477×10^{-18} J) and a mass of 6.695×10^{-27} kg for a D_2 molecule, the Alfvén critical velocity is 2.7×10^4 m/s.

3.1.2.2   Rosenbluth Sheath Velocity Model. The Rosenbluth sheath velocity v_s is derived from theory for the Perhapsatron toroidal z-pinch device. The applicable equation, in SI units, becomes

$$v_s = (\frac{\varepsilon_o c^2 E^2}{\rho})^{1/4}$$

where ε_o is electrical permittivity of free space, c is speed of light in a vacuum, E^2 is square of the electric field and ρ is density of the ionized material.

In our geometry, the electric field is a function of radius. The electric field strength E becomes

$$E = \frac{2V_o}{r} \frac{1}{\ln\left(\frac{b}{a}\right)}$$

where V_o is potential difference from a charged transmission plate to ground potential. (The total potential difference across the gun becomes $2V_o$.) Radial position is represented by r. The coaxial gun inner and outer electrode radii are respectively a and b.

To calculate the Rosenbluth sheath velocity in our system, some assumptions about the charged particle density are made. If the gas is uniformly dispersed in the coaxial plasma gun annulus, the mass load is the total gas load from the upper gas valve (32.9 mg of D_2) and is completely ionized, the charged particle mass density is 4.5×10^{-3} kg/m^3. With inner diameter (2a) of 5.125" (0.1302 m), outer diameter (2b) of 7" (0.1778 m) and applied voltage ($2V_o$) 60 kV, the sheath velocity ranges from 1.2×10^5 m/s at the outer gun surface (r = b) to 1.4×10^5 m/s at the inner gun surface (r = a).

Assuming a total charged particle mass of 0.1 mg in a 1 mm thick sheath in the gun, the sheath velocity ranges from 1.0×10^5 m/s (at r = b) and a sheath velocity of 1.2×10^5 m/s at the gun surface (at r = a). For a 1 cm thick sheath for the same mass, the sheath velocity is 1.8×10^5 m/s (r = b) and 2.1×10^5 m/s (r = a). If the sheath thickness is 1 1/2" (the width of the gas inlet holes) for the same mass, the sheath velocities are 2.5×10^5 m/s (r = b) and 2.1×10^5 m/s (r = a).

For these charged particle mass densities (ranging from 2.3×10^{-4} to 8.7×10^{-3} kg/m^3), the Rosenbluth sheath velocity varies from 2.5×10^5 to 10^5 m/s. The factor of 2.5 variation in the sheath velocity for a factor of 40 in density is a result of the $\rho^{-0.25}$ velocity scaling.

3.1.2.3 <u>Single Particle Drift Velocity Model</u>. The single particle drift velocity model assumes the sheath velocity can be approximated by the single particle drift velocity. It ignores the effects of particle interactions. While not providing the detail of a self-consistent multidimensional magnetohydrodynamic (MHD) treatment, it serves to benchmark the sheath velocity.

In Section 2, we see the magnetic field generated in the annular region ($a \leq r \leq b$) is

$$B = \frac{\mu_o I}{2\pi r} \mathbf{a}_\theta$$

From Section 3.1.2.2, the electric field in the plasma gun annulus is

$$E = \frac{2V_o}{r} \frac{1}{\ln \left(\frac{b}{a}\right)} \mathbf{a}_r$$

Defining the single particle drift velocity v_D, we have

$$v_D = \frac{E \times B}{B^2}$$

and

$$v_D = \frac{4\pi V_o}{\mu_o I \ln(\frac{b}{a})} a_z$$

This formulation depends on applied voltage ($2V_o$), current (I) and coaxial plasma gun radii a and b. Unlike the Rosenbluth velocity, there is no radial dependence. This formulation is limited to the condition a≤r≤b. Assuming collisional effects are small, this drift velocity can apply to both the snowplow and the deflagration modes of the coaxial plasma gun.

For the coaxial gun dimensions, applied voltage ($2V_o$) of 60 kV and gun current of 1.4 MA, the single particle drift velocity v_D is 6.9×10^5 m/s.

3.1.2.4   Limited or Saturated Sheath Velocity Model. Assuming a limited sheath velocity exists, simple physics can be used to calculate this limited or saturated sheath velocity v_ℓ. Such limitations can result from mass accretion ahead of the sheath (and thus applicable to the snowplow mode). Particle collisions can also provide a limiting mechanism for the limited or saturated sheath velocity.

Following Fishbine [181],

$$F = \frac{dp}{dt} = \frac{d(mv)}{dt}$$

101

$$F = \int P \cdot n \, dS$$

where F is applied force, p is linear momentum, m is total mass and v is the linear velocity of the mass. In this analysis, all velocities are non-relativistic. The pressure P acts normally on the area dS.

In this analysis, a cylindrical geometry is assumed. The area dS is

$$dS = \pi \, (r^2_{i+1} - r^2_i)$$

where r_i is inner radius and r_{i+1} is outer radius. The mass of the gas m becomes

$$m = \rho \, t \, dS$$

where ρ is sheath material density and t is axial sheath thickness. Equating the two relations for force F, we have

$$\frac{d}{dt} \, (\rho \, t \, dS \, v) = \int P \cdot n \, dS$$

Assuming the pressure P is approximately constant over the area dS, the relation becomes

$$\int P \cdot n \, dS = P \, dS$$

102

where P now represents the average scalar pressure. For a cylindrical geometry and only an axial velocity, we have

$$\frac{d}{dt} \left(\rho\, t\, dS\, \frac{dz}{dt} \right) = P\, dS$$

for the axial position z.

For a complete snowplow analysis, the quantities ρ, t, dS and $\frac{dz}{dt}$ are all functions of time. The mass density ρ changes by mass accretion and leakage (if applicable). The thickness t changes as a result of mass accretion. Changes in ρ and t depend on the mass ahead of the sheath, mixing processes in the sheath and whether material ahead of the plasma sheath impacts the sheath elastically or inelastically. The area dS changes through plasma sheath tilting in the coaxial gun annulus. Because of these time variations, complete sheath analysis generally is not possible. However, for an estimated saturation velocity v_ℓ, a complete analysis is not required.

If we assume the sheath thickness t to be equal to the axial dimension z (such as is the case in the early stages of a snowplow mode or in a deflagration mode), we then have the relation

$$\rho\, dS\, \frac{d}{dt} \left(z\, \frac{dz}{dt} \right) = P\, dS$$

Since this model assumes steady state conditions, the acceleration a $(\frac{d^2z}{dt^2})$ is zero and we have

$$\rho \left[z \frac{d^2z}{dt^2} + (\frac{dz}{dt})^2 \right] = P = \rho \ (\frac{dz}{dt})^2$$

or

$$v_s = \frac{dz}{dt} = (\frac{P}{\rho})^{1/2}$$

Up to this point, no assumptions have been made about the pressure P profile or the mass density ρ profile. If we assume a magnetic piston (i.e., a pressure wave created by the magnetic field B) drives along the plasma gun and any other pressures can be ignored, we can derive a limiting sheath velocity v_s for the AFWL coaxial plasma gun conditions. The magnetic pressure P_m is

$$P_m = \frac{1}{2\mu_0} B^2$$

and we have

$$v_\ell = \left[\frac{B^2}{2\rho\mu_0} \right]^{1/2}$$

Except for a factor of $2^{1/2}$, the limited or the saturation velocity is identical to the Alfven velocity $(B/(\mu_0\rho)^{1/2})$.

104

Using the **B** field relation from Section 3.1.2.3, we have

$$v_\ell = \left[\frac{\mu_o}{2\rho}\right]^{1/2} \frac{I}{2\pi r}$$

Using the assumptions about mass density (ρ) from Section 3.1.2.2 and assuming a current I of 1.4 MA, we can calculate sheath velocities v_ℓ for our plasma gun conditions. These results are summarized in Table 6.

It can be seen that the limited or saturated velocity v_ℓ varies from 2.1×10^4 to 1.8×10^5 m/s depending on the mass density ρ and the radius r. The saturated velocity v_ℓ is inversely proportional to radius and the square root of total mass density.

Table 6. Calculated Limited or Saturation Sheath Velocity

Density (kg/m^3)	Mass Distribution of Sheath	Radius (m)	Velocity v_ℓ (m/s)
4.5×10^{-3}	32.9 mg mass isotropically distributed	0.0651	4.0×10^4
4.5×10^{-3}	32.9 mg mass isotropically distributed	0.0889	2.9×10^4
8.7×10^{-3}	0.1 mg mass in 1 mm thick sheath	0.0651	2.9×10^4
8.7×10^{-3}	0.1 mg mass in 1 mm thick sheath	0.0889	2.1×10^4
8.7×10^{-4}	0.1 mg mass in 1 cm thick sheath	0.0651	9.1×10^4
8.7×10^{-4}	0.1 mg mass in 1 cm thick sheath	0.0889	6.7×10^4
2.3×10^{-4}	0.1 mg mass in 1 1/2" thick sheath	0.0651	18.0×10^4
2.3×10^{-4}	0.1 mg mass in 1 1/2" thick sheath	0.0889	13.2×10^4

3.1.3 Plasma Physics at the Gun Muzzle

Although a complete description of the physics of the sheath exiting the
gun muzzle is beyond the scope of this dissertation, two effects should
be noted. The first is the plasma exits the coaxial gun with a directed
forward velocity. The second is the radial convergence of mass at the
gun muzzle. This focused radial convergence, or pinching, can lead to
the turbulent plasma behavior and an increase in plasma density. This
plasma pinch can be a source of radiation and fusion reactions.

3.2 COAXIAL PLASMA GUN PERSPECTIVE

Coaxial plasma guns are classified by geometry, by polarity, by gas
loading or by plasma gun energy delivery. A great deal of work has been
performed on coaxial plasma guns. An overview of the field will be
either be extensive and lengthy or short and general. In this section,
the AFWL coaxial plasma gun is placed within the general framework of
past coaxial plasma gun work.

Coaxial plasma gun geometries divide them into the Mather/Marshall
plasma and the Filippov geometry. In the Mather/Marshall plasma gun,
the ratio of the outer to inner coaxial gun radius (b/a) is on the order
of 1.3 to 3. The length ℓ of the Mather/Marshall gun is several times
larger of the radii a or b and the annulus (b - a). In the Filippov
geometry, the ratio of the outer to inner coaxial gun radius (b/a) is on
the order of 1.02 to 1.2. The Filippov gun length ℓ is short compared
to the radial dimensions a and b. The Mather/Marshall gun can be used

106

in either the snowplow or deflagration modes. The Filippov gun is used more in the snowplow mode, since the aspect ratio radially focuses the plasma in a pinch at the gun muzzle than ejecting it. The PUFF coaxial plasma gun is a Mather/Marshall gun. The outer to inner electrode radius ratio (b/a) is 1.4. The length ℓ to the inner electrode radius ratio (ℓ/a) for the AFWL plasma gun is 7.1.

Variations on the standard geometries include varied or altered electrodes or simultaneous multiple coaxial guns. Alterations include sloped or tapered electrodes to achieve a geometric plasma focusing to a point. Coaxial plasma gun electrodes can be perforated to allow for diagnostic access. Plasma gun electrodes can be made of rods or tubes instead of solid metal; the rod structure allows diagnostic access the solid metal electrodes would not allow, as well as producing plasma effects not found in solid electrode plasma guns. These effects include the potential for reflexing or scattering plasma particles. The AFWL coaxial plasma gun uses non-tapered electrodes, a solid inner electrode and a 24 rod outer electrode structure.

In the coaxial plasma gun, the inner electrode is either positive or negative. The polarity is an important factor since dielectric breakdown and the gas breakdown are both geometry and polarity dependent. In our coaxial plasma gun, the inner electrode is the anode (of positive polarity). The outer rod structures are the cathode (of negative polarity).

Plasma gun gas loading can be continuous or in single charges. In the continuous mode, the plasma is formed (after gun arcing occurs in the gas) and gas is constantly fed into the gun. Continuous gas feed is used for gun deflagration mode operation and is used for industrial processes [141-143]. Single shot gas loading is used in experimental systems. Single shot gas charge timing is related to the function of the coaxial plasma gun. The gas is inserted into the gun and, after a suitable delay, a voltage is applied. A short time delay (so gas is not distributed uniformly) gives rise to a sharp current front and the plasma gun initially operates in a snowplow mode. In a long time delay between gas insertion and applied gun voltage (a static prefill), the plasma gun initially operates in a deflagration mode. The size of the gas loading determines the plasma behavior after initial discharge occurs. Coaxial gun plasma formation is dependent on applied voltage (including polarity effects), gas chemistry (including ionization potentials), gas density distribution (including the effects of density gradients and plasma conductivity) and gun surfaces (including surface gas evolution and plasma site formation). If filamentary currents form at gas breakdown and coalesce into a narrow plasma sheath, this becomes a snowplow mode. If the plasma formation is diffuse, deflagration develops. Our plasma has a single gas charge. The time delay between gas input and application of voltage to the gun is varied. Initially, our gun has strong snowplow characteristics, but because a sharp plasma density gradient is not maintained after discharge, the gun develops deflagration characteristics.

108

The stored energy is used to classify coaxial plasma guns. Experimental systems have energy sources varying several orders of magnitude. Many coaxial plasma guns have delivered energies less than 10 kJ. Experimental work has reported delivered energies greater than 100 kJ [181] including work approaching 1 MJ [182]. Delivered gun energy is important for the deuterium plasma focus where the neutron yield Y_N is seen to be a function of energy E so that

$$Y_N \propto E^\beta$$

where β is a number on the order of 2. Increases in delivered energy produce a much larger increase in the neutron yield. Our coaxial plasma gun operated at 130 kJ (although the potential system energy delivery exceeds 500 kJ).

Applied voltage corresponds to the delivered energy in a coaxial plasma gun. Many plasma gun have applied voltages of 30 kV or less. The AFWL gun uses an applied voltage of 60 kV or more.

From simple circuit theory, the initial voltage across an inductor V_L is

$$V_L = L \frac{dI}{dt}$$

where L is inductance and $\frac{dI}{dt}$ is time differential of the current. From this relation, for a given voltage V_L, the smaller the inductance L, the larger the current rise. In the PUFF bank, the system inductance is 29

nH. Many coaxial gun systems have larger inductances. For an applied voltage ($2V_0$) of 60 kV, the initial current rise $\frac{dI}{dt}$ is 2×10^{12} A/s.

Mather [183] and Fishbine [184] both discuss coaxial plasma guns as plasma focus devices. They note the ratio $Z_0/\dot{L}$, where Z_0 is effective gun current source impedance ($Z_0 = (\frac{L}{C})^{1/2}$, L is initial system inductance and C is system capacitance) and $\dot{L}$ is the time rate of change of inductance in the coaxial plasma gun. Reported values vary from less than 1.0 to greater than 5.0. The lower the ratio $Z_0/\dot{L}$, the more the source acts as a constant voltage device. The higher the ratio, the more the source acts as a constant current device. $Z_0/\dot{L}$ for our gun is 1.1. This is typical of most reported coaxial plasma gun systems.

3.3 COAXIAL PLASMA GUN DIAGNOSTIC DEVICES

The location of the different plasma gun diagnostic devices is discussed in this section. Since the theory was discussed in Section 2, it is not dealt with here.

3.3.1 Rogowski Coil Discussion

There were three Rogowski coils in place during the experimental sequence. There were two Rogowski coils placed in the transmission line outside the helical feed electrodes. The third Rogowski coil was mounted in the base of the anode electrode. (The etched ring in the

110

base of the anode for the chamber or center Rogowski coil can be seen in Figure 4.)

The two Rogowski coils mounted outside of the helical electrodes are the counter-rotating Rogowski coils. One of the Rogowski coils was irreparably damaged prior to the described experiments. It was decided to rely on the operational counter-rotating Rogowski coil to measure the PUFF system current external to the dielectric/vacuum interface.

The third Rogowski coil (in the anode base), the center or chamber Rogowski, measured the current delivered to the plasma in the coaxial plasma gun. Small differences (±5%) in the results between the counter-rotating and the chamber Rogowski coils can be ascribed to calibration errors. Where the larger errors (>20%) occur, current was incompletely delivered from the transmission line to the plasma gun. This indicates a dielectric/vacuum breakdown. When the discrepancies are very large (when the counter-rotating current rises as the chamber current simultaneously falls), the breakdown has crowbarred the circuit, i.e., it has isolated the plasma gun from the rest of the PUFF capacitor bank circuit.

3.3.2 $\dot{B}$ Probe Discussion

The $\dot{B}$ probes are mounted from the inside of the anode electrode outward. Their relative positions are seen in Figures 21 and 22. The $\dot{B}$ probe tips protrude some 0.25" (6.4×10^{-3} m) into the plasma gun annulus. The relative protrusion of the $\dot{B}$ probes into the coaxial plasma gun annulus

111

is shown in Figure 21. The $\dot{B}$ probes are expected to perturb the plasma, since the protrusion is greater than 25% of the annular gap.

The $\dot{B}$ probe axial position is seen in Figure 22. There are four axial levels in the plasma gun: bottom, mid-bottom, mid-top and top. Each level is 4" (0.1016 m) distance from adjacent levels. The bottom level is centered 10.25" above the anode base and 3.75" (9.35×10^{-2} m) from the centerline of the gas outlet holes (where gas from the primary gas valve entered the coaxial plasma gun.) The bottom level is 14.5" (0.3683 m) from the anode top. The mid-bottom level is centered 14.25" (0.3620 m) from the anode base, 7.75" (0.1969 m) from the gas outlet centerline and 10.5" (0.2667 m) from the anode top. Similarly, the mid-top level is 18.25" (0.4636 m) from the anode base, 11.25" (0.2858 m) from the gas outlet centerline and 6.5" (0.1651 m) from the anode top. The top level is 22.25" (0.5652 m) from the anode base, 14.25" (0.3620 m) from the gas outlet centerline and 2.5" (6.35×10^{-2} m) from the anode top.

The $\dot{B}$ probe positions are summarized in Tables 7, 8 and 9. $\dot{B}$ probe position are given at each level and each azimuthal position. The azimuthal positions are NE, SE, SW and NW.

The $\dot{B}$ probes are encased in ceramic sheaths. These ceramic sheaths protect the $\dot{B}$ probes from destruction and from giving rise to signals from the high electric fields associated with plasmas. As the plasma impinges on the sheath, the sheaths may ablate surface material. To calculate the effects of this ablation, some derivations and estimates are made.

112

CATHODE ROD

ANODE

B-dot probe

R3.50

Ø5.125

Ø.500
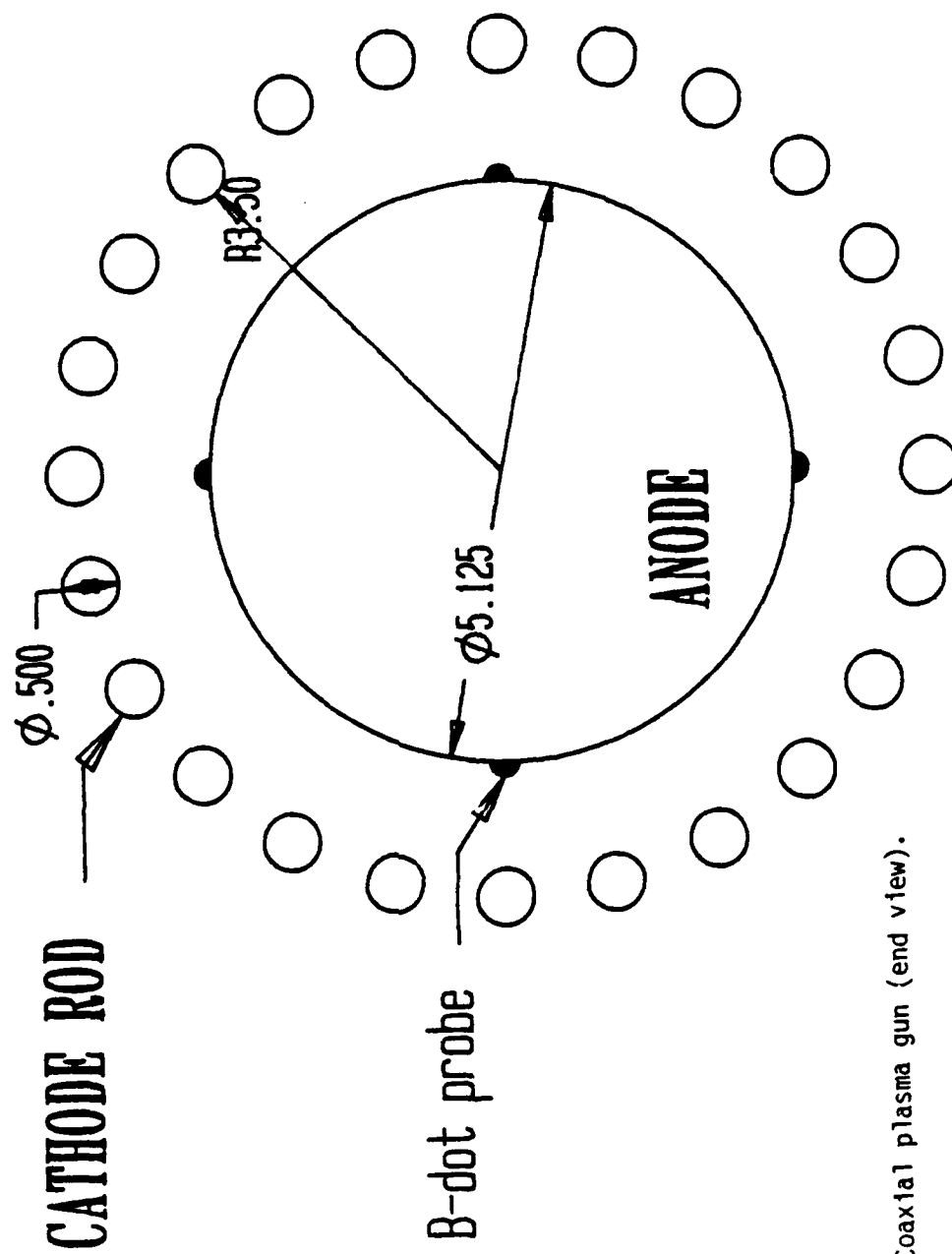
Figure 21. Coaxial plasma gun (end view).
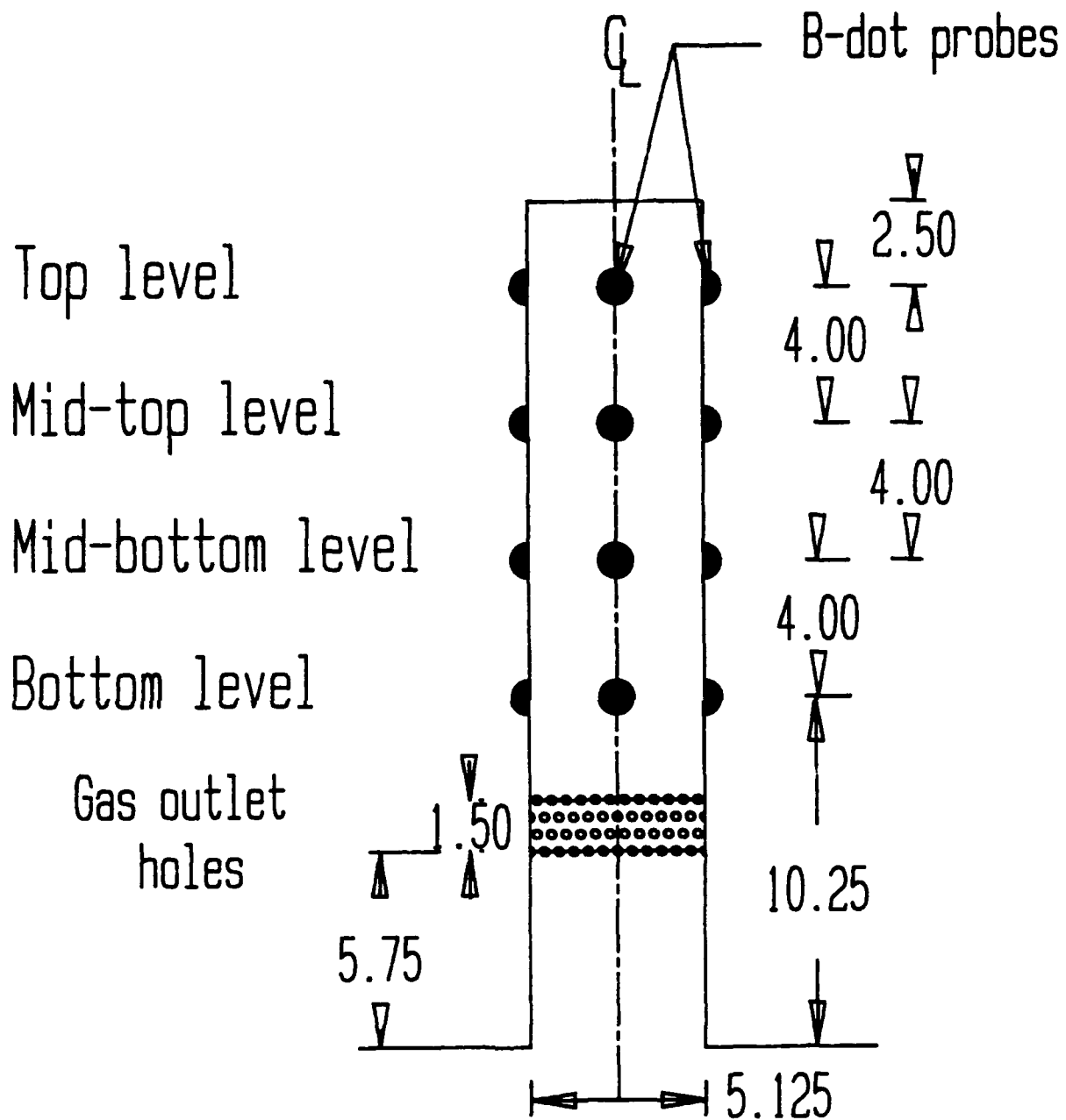
Figure 22. Coaxial plasma gun (side view) with $\dot{B}$ probes.

Table 7. $\dot{B}$ Probe Position in Coaxial Plasma Gun

$\dot{B}$ probe	Axial Position	Azimuthal Position
B	top	NW
C	top	SW
D	top	SE
E	top	NE
F	mid-top	NE
G'	mid-top	SE
H'	mid-top	SW
J'	mid-top	NW
L	mid-bottom	NE
M	mid-bottom	SE
N	mid-bottom	SW
O	mid-bottom	NW
P	bottom	NE
Q	bottom	SE
R'	bottom	SW
S	bottom	NW

Table 8. Axial Levels of $\overset{\circ}{B}$ Probes

Axial Level	$\overset{\circ}{B}$ Probes in Level			
top level	B	C	D	E
mid-top level	F	G'	H'	J'
mid-bottom level	L	M	N	O
bottom level	P	Q	R'	S

Table 9. Azimuthal Positions of $\overset{\circ}{B}$ Probes

Azimuthal Positions	$\overset{\circ}{B}$ Probes at Azimuthal Position			
NE	E	F	L	P
SE	D	G'	M	Q
SW	C	H'	N	R'
NW	B	J'	O	S

To begin, we invoke three of Maxwell's equations. These equations are:

$$\nabla \times \mathbf{H} = \mathbf{J} + \frac{\partial \mathbf{D}}{\partial t} \qquad (2.5.1.1.1)$$

$$\nabla \times \mathbf{E} = - \frac{\partial \mathbf{B}}{\partial t} \qquad (2.5.1.1.2)$$

$$\nabla \cdot \mathbf{B} = 0 \qquad (3.3.2.1)$$

Recalling the constituitive relations and a generalized Ohm's law, we have

$$<\varepsilon> \mathbf{E} = \mathbf{D} \qquad (3.3.2.2)$$

$$<\mu> \mathbf{H} = \mathbf{B} \qquad (3.3.2.3)$$

$$<\sigma> \mathbf{E} = \mathbf{J} \qquad (3.3.2.4)$$

where $\mathbf{E}$ is electric field, $\mathbf{B}$ is magnetic field strength and $\mathbf{J}$ is current density. The dielectric permittivity ε is a tensor quantity, ε is the magnetic permeability μ and the electrical conductivity σ.

117

Several assumptions simplify these relations. The medium under consideration is considered isotropic so the tensors simplify to scalar quantities: $\langle\varepsilon\rangle = \varepsilon$; $\langle\mu\rangle = \mu$; and $\langle\sigma\rangle = \sigma$. Assuming the time differential of the displacement current $\frac{\partial D}{\partial t}$ is small compared to the current density J (i.e. $\frac{\partial D}{\partial t} \ll J$), we have

$$\nabla \times B = \mu \, J = \mu \, \sigma \, E \qquad (3.3.2.5)$$

$$\nabla \times E = - \frac{\partial B}{\partial t} \qquad (3.3.2.6)$$

Taking the curl of the equation (3.3.2.5), we have

$$\nabla \times \nabla \times B = \mu \, \sigma \, \nabla \times E = - \mu \, \sigma \, (\frac{\partial B}{\partial t}) \qquad (3.3.2.7)$$

Using the definition of the curl of a curl of vector field, we have

$$\nabla (\nabla \cdot B) - \nabla^2 B = - \mu \, \sigma \, (\frac{\partial B}{\partial t}) \qquad (3.3.2.7a)$$

Using equation (3.3.2.1), we have the relation

$$\nabla^2 B = \mu \, \sigma \, (\frac{\partial B}{\partial t}) \qquad (3.3.2.8)$$

118

Realizing the spatial derivative $\nabla^2 B$ is roughly equivalent to $\dfrac{B}{R^2}$ and the time derivative $\dfrac{\partial B}{\partial t}$ is roughly equivalent to $\dfrac{B}{\tau}$, where R is spatial scale length and τ is time scale length, we have the time scale τ

$$\tau = \mu \, \sigma \, R^2$$

so the time τ a magnetic field diffuses through a material is related linearly to the magnetic permeability μ, the conductivity σ and the square of the scale length R.

Plasma magnetic permeability equals to the permeability of free space μ_0. The ablation scale length is on the order of the sheath protrusion into the gun annulus, i.e., the scale length R is on the order of 0.25" (6×10^{-3} m). The ablatant plasma conductivity σ is to be determined.

If the plasma sheath is of temperature T, the ablatant plasma is of a lesser temperature since the plasma expends energy to ablate material.

Plasma conductivity σ is estimated from the Spitzer formulation [185]. Chen [186] reports the Spitzer resistivity η to be

$$\eta_{||} = 5.2 \times 10^{-5} \, \frac{\ln \Lambda}{T^{1.5}}$$

119

where the || subscript represents resistivity parallel to the B field, η is resistivity in Ω-m, T is plasma temperature in electron volts (eV) and ln Λ is the Coulomb logarithm.

The Spitzer resistivity of interest is that perpendicular to the magnetic field $\eta_\perp$. This is calculated by

$$\eta_\perp = 2\eta_{||} \, (1 + \omega_c^2 \tau_e^2)$$

where ω_c is electron cyclotron frequency and τ_e is electron collision time.

The Coulomb logarithm, ln Λ, is approximated by the relation [187]

$$\ln \Lambda = 23 - \ln(\frac{n_e^{1/2}}{T^{1.5}}) \text{ where } T_e \gtrsim 10 \text{ eV}$$

where n_e is electron density in cm^{-3} and T_e electron temperature in eV.

The electron cyclotron frequency ω_e is

$$\omega_e = (\frac{eB}{m_e})$$

where e is electronic charge (1.6022×10^{-19} C), B is magnetic field strength in Tesla (Webers/m^2) and m_e is electron mass (9.1095×10^{-31} kg).

The electron collision time τ_e is [188]

$$\tau_e = 3.44 \times 10^5 \frac{T_e^{1.5}}{n_e \ln \Lambda}$$

with n_e in cm^{-3} and T_e in eV.

Assuming plasma gun current (I) of 1.4 MA, the magnetic field strength varies from 4.30 Tesla at the the inner gun electrode (r = a) to 3.14 Tesla at the the outer gun electrode (r = b). The electron cyclotron frequency ω_c becomes 7.56×10^{11} s^{-1} at r = a and 5.52×10^{11} s^{-1} at r = b.

Using the density (ρ) profiles of Sections 3.1.2.2 and 3.1.2.4, we convert to particle density. The particle densities range from 3×10^{16} to 1×10^{18} particles/cm^3. For a deuterium fill gas with a charge state of 1, ion density n_i and electron density n_e are assumed equal. If ablation and photoelectric effects do not change the ion and electron number densities, this assumption is valid. Calculated results for the effective resistivities $\eta_\perp$ are displayed in Tables 10a and 10b.

From the data in Tables 10a and 10b, several observations can be made. The Coulomb logarithm, $\ln \Lambda$, varies from 7.2 to 7.5 for our plasma gun conditions. This is less than the generalized value of 10 that Chen cites [189] and smaller than the range of 10 to 20 of the NRL Formulary [187]. The collisional range of the plasma sheath is limited under these conditions because the density is relatively high and the temperature relatively low.

121

Table 10a. Calculated Resistivities for Coaxial Plasma Gun

Density (cm^{-3})	T (eV)	B (Tesla)	$\ln \Lambda$	ω_{c_1} (s^{-1})	τ_e (s)	$\eta_{||}$ (Ωm)	$\eta_{\perp}$ (Ωm)
3.0×10^{16}	1	3.14	4.0	5.5×10^{11}	2.9×10^{-12}	2.1×10^{-4}	7.4×10^{-4}
1.0×10^{17}	1	3.14	3.4	5.5×10^{11}	1.0×10^{-12}	1.8×10^{-4}	4.7×10^{-4}
7.0×10^{17}	1	3.14	2.5	5.5×10^{11}	2.0×10^{-13}	1.3×10^{-4}	2.6×10^{-4}
1.0×10^{18}	1	3.14	2.3	5.5×10^{11}	1.5×10^{-13}	1.2×10^{-4}	2.4×10^{-4}
3.0×10^{16}	2	3.14	5.1	5.5×10^{11}	6.4×10^{-12}	9.4×10^{-5}	2.5×10^{-3}
1.0×10^{17}	2	3.14	4.5	5.5×10^{11}	2.2×10^{-12}	8.3×10^{-5}	2.0×10^{-4}
7.0×10^{17}	2	3.14	3.5	5.5×10^{11}	4.0×10^{-13}	6.4×10^{-5}	1.3×10^{-4}
1.0×10^{18}	2	3.14	3.3	5.5×10^{11}	2.9×10^{-13}	6.1×10^{-5}	1.3×10^{-4}
3.0×10^{16}	3	3.14	5.7	5.5×10^{11}	1.0×10^{-11}	5.7×10^{-5}	3.6×10^{-3}
1.0×10^{17}	3	3.14	5.1	5.5×10^{11}	3.5×10^{-12}	5.1×10^{-5}	4.8×10^{-4}
7.0×10^{17}	3	3.14	4.1	5.5×10^{11}	6.2×10^{-13}	4.1×10^{-5}	9.2×10^{-5}
1.0×10^{18}	3	3.14	3.9	5.5×10^{11}	4.6×10^{-13}	3.9×10^{-5}	8.3×10^{-5}
3.0×10^{16}	5	3.14	6.4	5.5×10^{11}	2.0×10^{-11}	3.0×10^{-5}	7.3×10^{-3}
1.0×10^{17}	5	3.14	5.8	5.5×10^{11}	6.6×10^{-12}	2.7×10^{-5}	7.6×10^{-4}
7.0×10^{17}	5	3.14	4.9	5.5×10^{11}	1.1×10^{-12}	2.3×10^{-5}	6.3×10^{-5}
1.0×10^{18}	5	3.14	4.7	5.5×10^{11}	8.2×10^{-13}	2.2×10^{-5}	5.3×10^{-5}
3.0×10^{16}	10	3.14	7.5	5.5×10^{11}	4.8×10^{-11}	1.2×10^{-5}	1.7×10^{-2}
1.0×10^{17}	10	3.14	6.9	5.5×10^{11}	1.6×10^{-11}	1.1×10^{-5}	1.7×10^{-3}
7.0×10^{17}	10	3.14	5.9	5.5×10^{11}	2.6×10^{-12}	9.7×10^{-6}	5.9×10^{-5}
1.0×10^{18}	10	3.14	5.7	5.5×10^{11}	1.9×10^{-12}	9.4×10^{-6}	3.9×10^{-5}

Table 10b. Calculated Resistivities for Coaxial Plasma Gun

Density (cm^{-3})	T (eV)	B (Tesla)	$\ln \Lambda$	$\omega_c \tau_e$ (s^{-1})	τ_e (s)	$\eta_{||}$ (Ωm)	$\eta_{\perp}$ (Ωm)
3.0×10^{16}	1	4.30	4.0	7.6×10^{11}	2.9×10^{-12}	2.1×10^{-4}	2.5×10^{-3}
1.0×10^{17}	1	4.30	3.4	7.6×10^{11}	1.0×10^{-12}	1.8×10^{-4}	5.7×10^{-4}
7.0×10^{17}	1	4.30	2.5	7.6×10^{11}	2.0×10^{-13}	1.3×10^{-4}	2.7×10^{-4}
1.0×10^{18}	1	4.30	2.3	7.6×10^{11}	1.5×10^{-13}	1.2×10^{-4}	1.2×10^{-4}
3.0×10^{16}	2	4.30	5.1	7.6×10^{11}	6.4×10^{-12}	9.4×10^{-5}	4.6×10^{-3}
1.0×10^{17}	2	4.30	4.5	7.6×10^{11}	2.2×10^{-12}	8.3×10^{-5}	6.3×10^{-4}
7.0×10^{17}	2	4.30	3.5	7.6×10^{11}	4.0×10^{-13}	6.4×10^{-5}	1.4×10^{-4}
1.0×10^{18}	2	4.30	3.3	7.6×10^{11}	2.9×10^{-13}	6.1×10^{-5}	1.3×10^{-4}
3.0×10^{16}	3	4.30	5.7	7.6×10^{11}	1.0×10^{-11}	5.7×10^{-5}	6.7×10^{-3}
1.0×10^{17}	3	4.30	5.1	7.6×10^{11}	3.5×10^{-12}	5.1×10^{-5}	8.2×10^{-4}
7.0×10^{17}	3	4.30	4.1	7.6×10^{11}	6.2×10^{-13}	4.1×10^{-5}	1.0×10^{-4}
1.0×10^{18}	3	4.30	3.9	7.6×10^{11}	4.6×10^{-13}	3.9×10^{-5}	8.7×10^{-5}
3.0×10^{16}	5	4.30	6.4	7.6×10^{11}	2.0×10^{-11}	3.0×10^{-5}	1.4×10^{-2}
1.0×10^{17}	5	4.30	5.8	7.6×10^{11}	6.6×10^{-12}	2.7×10^{-5}	1.4×10^{-3}
7.0×10^{17}	5	4.30	4.9	7.6×10^{11}	1.1×10^{-12}	2.3×10^{-5}	7.8×10^{-5}
1.0×10^{18}	5	4.30	4.7	7.6×10^{11}	8.2×10^{-13}	2.2×10^{-5}	6.1×10^{-5}
3.0×10^{16}	10	4.30	7.5	7.6×10^{11}	4.8×10^{-11}	1.2×10^{-5}	3.2×10^{-2}
1.0×10^{17}	10	4.30	6.9	7.6×10^{11}	1.6×10^{-11}	1.1×10^{-5}	3.3×10^{-3}
7.0×10^{17}	10	4.30	5.9	7.6×10^{11}	2.6×10^{-12}	9.7×10^{-6}	9.5×10^{-5}
1.0×10^{18}	10	4.30	5.7	7.6×10^{11}	1.9×10^{-12}	9.4×10^{-6}	5.8×10^{-5}

It should also be noted the perpendicular resistivity $n_\perp$ is strongly affected by the azimuthal magnetic field. The greater the $\omega_c^2 \tau_e^2$ product, the greater the perpendicular resistivity. The greater the resistivity, the greater the magnetic field penetration into the plasma. Since the ablating plasma expands radially and the magnetic field is azimuthal, the appropriate resistivity is the resistivity perpendicular to the magnetic field.

Since the $\dot{B}$ probes are located at the plasma gun inner surface (r = a), the data in Table 10b applies. The perpendicular resistivity $n_\perp$ varies from 5.8×10^{-5} to 3.2×10^{-2} Ωm. Using the scaling formula, the scaling time for magnetic field penetration into the plasma is

$$\tau = \mu_o \sigma R^2 \approx \mu_o R^2 / \eta$$

The magnetic diffusion time ranges from 1.4 ns to 0.780 μs. Only if the plasma is in the lower ranges of the resistivity (10^{-4} Ωm or less) is limitation of the magnetic diffusion into the $\dot{B}$ probe a concern. If the scaling time τ represents one e-folding of the magnetic field into the plasma, a minimum of three e-folding times τ would be required for 95% of the field to penetrate a distance L into the plasma.

Assuming an ablatant plasma temperature (T_e) of 5 eV or less and the lower end of the density range, the time to diffuse 95% of the magnetic field through the ablatant plasma is tens of nanoseconds. Although magnetic field diffusion into the $\dot{B}$ probe could still present a problem, it is less a problem than reported by Degnan et al. [102].

124

3.3.3 Capacitive Voltage Probe Discussion

Two capacitive voltage probes were used in the experimental series.
Both were mounted on the underside of the bottom transmission plate
outside the helical feed electrodes. One voltage probe was mounted
north of the coaxial plasma gun; the other was mounted south of the
coaxial plasma gun. The voltage probes measured only the coaxial plasma
gun feed voltage, not the plasma gun voltage itself. They do not
reflect the increased gun voltage due to the $(I \frac{dL}{dt})$ coaxial gun
voltage spike as a result of increased inductance.

To go from measured probe voltage V_m to plasma gun voltage V_p, we use
the relation

$$V_p = V_m + [L(t) - 8.2 \text{ nH}] \frac{dI}{dt} + I \frac{dL}{dt} + IR$$

where $L(t)$ is total system inductance (both fixed and time varying), $\frac{dI}{dt}$
is time differential of the current I, $\frac{dL}{dt}$ is time differential of
inductance and R is total circuit resistance. Generally, the resistance
is assumed to be small. For our experiment, we assumed a time invariant
resistance of 1 mΩ. (The 8.2 nH inductance is subtracted from the total
system inductance since it is already reflected in the measured probe
voltage V_m.)

As noted in Section 2, the capacitive voltage probes were not calibrated
since changes on the transmission line changed the coupling capacitance

between the probes and transmission line. A voltage trace is obtained in the experiment. (A typical voltage trace is given in Figure 23.) It is digitized in a method discussed in Section 4. After the voltage trace is digitized and smoothed, it is corrected for RC droop. After the numerical correction, the voltage trace is ready for analysis. A baseline portion of the trace, where the voltage trace is zero, precedes the voltage signal. On application of the voltage (through the discharge of the capacitors through the rail gap switches), the voltage exhibits high frequency ringing. This ringing is probably due to some impedance mismatch the transmission line and the plasma gun load. After the initial voltage rise, the voltage tends to stabilize at a nearly constant value for some time. (In Figure 23, the voltage plateau is over 1 μs.) Using this voltage plateau, the voltage is averaged to yield a voltage V_{ave}. This averaged voltage V_{ave} is the basis for the individual probe calibration for an individual shot.

There is a total inductance of 29 nH from the capacitor to the end of the coaxial plasma gun. Of the 29 nH inductance, 8.2 nH is the inductance from the capacitor bank to the voltage monitor position. The voltage appearing at the voltage monitor is 71.7% (20.8/29.0) of the capacitor bank voltage. The voltage monitor calibration constant K_V is defined by the relation

$$V_{ave} = K_V (2V_o) (\frac{20.8}{29.0})$$

where V_{ave} is defined by the plateau voltage on the voltage trace and

126
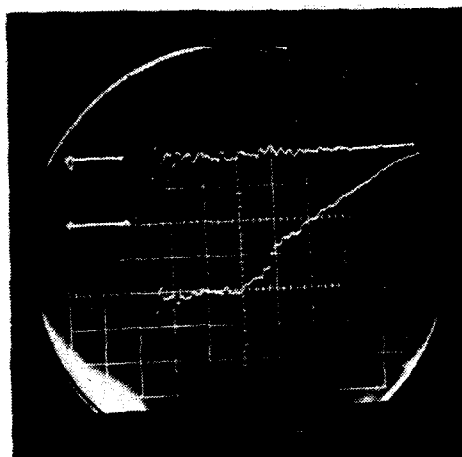
Figure 23.   Typical voltage trace.

(Shot taken 11 January 1984.
0.2 V/div   0.5 μs/div)

$2V_o$ is the applied voltage to the plasma gun. The inductance ratio (20.8/29.0) reduces the voltage appearing on the voltage monitor. For our experiments, the calibration constant K_V includes the effect of the passive RC integrator. For a typical result, the calibration constant K_V for voltage trace J1108VN is 9.59×10^{-7} V/V.

3.3.4 Silver Activation Detector Discussion

The silver activated neutron detector described in Section 2.5.6 is inherently geometry dependent. The number of neutrons detected varies inversely as the square of the source distance. This variation reflects the fact the solid angle subtended by the detector to the source varies as the detector is moved.

The silver detector front face was 8 7/8" (0.2254 m) from the anode center on all shots up to and including shot J1008. After that shot (from shot J1009 on), the detector front face was placed 24" (0.6096 m) from the anode center. The anode center is taken as the neutron source since it is presumed the plasma pinch occurs there.

The analysis presented in Section 2.5.6 does not include fast neutron scattering and absorption by the vacuum cover. The vacuum cover absorbs few fast neutrons since the cross-section is small. The cover scatters the neutrons instead. The scatter reduces the detector response for a given number of neutrons. The number of scattered neutrons measured by the detector will be low. This effect has been ignored.

The results reported by Degnan et al. [102] do not include the effects of the thicker silver sheet in the AFWL detector. The results also do not include the effects of the increased distance after shot J1008. Before shot J1009, the reported detector response is low by 52%; the reported results should be corrected by a factor of 2.07. After shot SJ1008, the reported detector results are low by a factor of 8.86. (This factorization is not exact since Degnan's analysis assumes a background of 150 counts/minute. A more correct background is 164 ± 14 counts/minute. The corrected values are used in this analysis.)

3.4 AFWL PUFF COAXIAL GUN OPERATING PROCEDURES

Operation of the AFWL PUFF capacitor bank is an involved process. It involved no fewer than three people at any one time. The number was generally four to six, depending on the diagnostic devices being used and the data collection requirements.

The AFWL PUFF capacitor bank can provide high voltages at lethal current levels. Standard Air Force policy requires no less than two people on location when hazardous operations are under way.

The specific operating procedures for the AFWL PUFF coaxial plasma gun are provided in Appendix A.

4.0 EXPERIMENTAL ANALYSIS

The data taken in the experimental series is analyzed in this section. This includes discussion on the simple 0-dimensional (0-D) slug model used to predict the behavior of the plasma sheath flow through the coaxial plasma gun annulus. A discussion of the overall AFWL PUFF coaxial gun experimental behavior follows. A more detailed analysis of three particular shots follows. The detailed analysis contains comparison with the theory.

4.1 COMPUTATIONAL MODELING

The model used for simulating the coaxial plasma gun behavior is discussed. The model physics and how it applies to the AFWL PUFF coaxial plasma gun is discussed. Model limitations are dealt with and a discussion why other modeling was not performed is presented.

4.1.1 Slug Model Assumptions

A 0-D model is chosen to simulate the coaxial plasma gun behavior. The slug model makes several assumptions about the plasma sheath:

1) All the mass is assumed concentrated in the plasma sheath. No mass is swept up in the plasma sheath since there is no mass outside the sheath. This is a plasma slug/washer assumption.

2) The current density is assumed to be isotropic, azimuthally and radially symmetric. The only plasma sheath variation occurs as it is accelerated axially along the coaxial plasma gun.

3) The plasma sheath is assumed to be infinitesimally thick and uniformly accelerated across the area of the sheath. This is not a necessary requirement. The model could just as well assume a small, finite thickness. The sheath position would then represent the mid-plane of the plasma sheath. Uniform plasma sheath acceleration is assumed to avoid azimuthal and radial variations. This is physically equivalent to assuming the sheath is mechanically rigid and rotationally fixed.

4.1.2 Physics of the Slug Model

The driving circuit is assumed to consist of lumped circuit elements. The diagram for the circuit is given in Figure 24. The capacitance of the system C is 72 μF. There are three inductors in the system. There is the system inductance L_{01} prior to the voltage probes (that monitor the probe voltage V_p). The system inductance L_{02} after the voltage probes is L_{02}. The load inductance L_{load} is the third inductance. Both the system inductances (L_{01} and L_{02}) are fixed. The load inductance varies as a function of time. The lumped plasma sheath resistance R also includes the system resistances. The resistance R is assumed to be time invariant. There is a time-varying current I flowing through all the circuit elements. The initial capacitor voltage is V_0. Initial
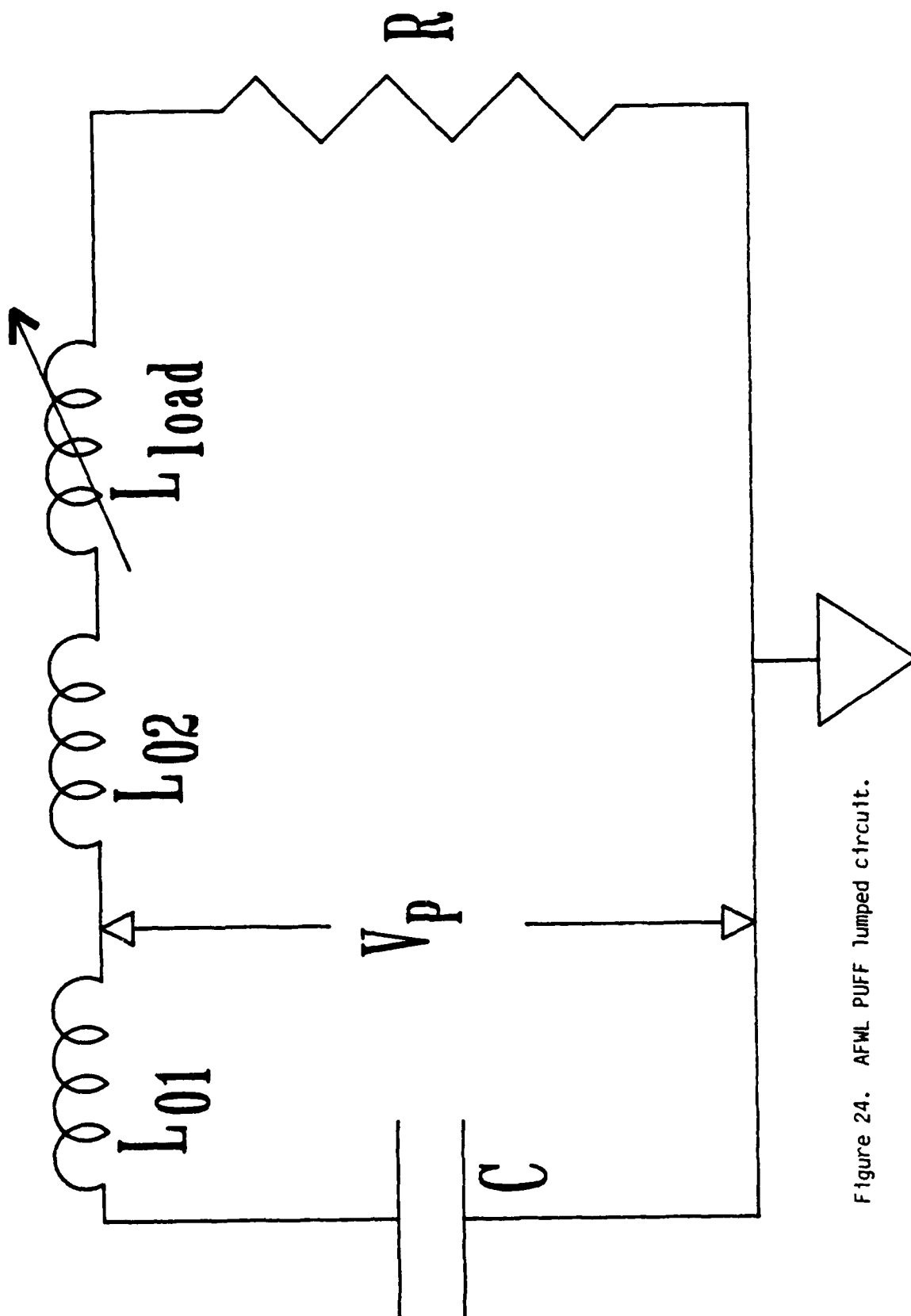
Figure 24. AFWL PUFF lumped circuit.

current I is 0. The capacitor bank voltage V_C is

$$V_C = (L_{01} + L_{02} + L_{load}) \ast \frac{dI}{dt} + (\frac{d(L_{load})}{dt} + R) \ast I$$

where $\frac{dI}{dt}$ is time differential of the current and $\frac{d(L_{load})}{dt}$ is time differential of the time-varying load inductance.

The voltage at the voltage probe V_p is

$$V_p = V_C - L_{01} \ast \frac{dI}{dt} = (L_{02} + L_{load}) \ast \frac{dI}{dt} + (\frac{d(L_{load})}{dt} + R) \ast I$$

. The load voltage V_{load} is

$$V_{load} = L_{load} \ast \frac{dI}{dt} + (\frac{d(L_{load})}{dt} + R)$$

The Newtonian force relation

$$F = ma$$

describes the plasma sheath acceleration a. The driving force F drives the plasma sheath mass m. The acceleration is produced by the magnetic force generated by the current flowing in the coaxial plasma gun. The acceleration a becomes

133

$$\mathbf{a} = \mu_0 \ln(\frac{b}{a})\, I^2/(4\pi m)\, \mathbf{a}_z$$

where a and b are coaxial plasma gun inner and outer radii and I is gun current.

The velocity v is produced by time integration of the acceleration. By time integrating the velocity, the axial position of the sheath z is calculated. For the initial conditions where $v(0) = 0$ and $z(0) = z_0$, we obtain a closed series of equations.

4.1.3 Slug Model Restrictions

There are several restrictions in this slug model. Since the slug model is 0-dimensional, it does not allow for any spatial variation of the mass or the coaxial plasma gun. Although the restriction on the coaxial plasma gun does not affect the modeling of the AFWL PUFF coaxial plasma gun, the assumption of mass in the sheath only is not physically realizable. The mass only assumption is, at best, an approximation to the real plasma sheath behavior.

Another slug model restriction is that the calculation terminates when the sheath reaches the plasma gun muzzle. Much interesting physics occurs in the pinch region and beyond the muzzle. However, the investigation of those phenomena is beyond the range of this study.

A final restriction relates to the sheath behavior. The slug model does not deal with the microscopic behavior of the sheath, only the gross macroscopic behavior. Where azimuthal variation occurs (as in the spokes or vortices described at length by Bostick and his co-workers) or when the sheath varies radially, this model does not offer adequate sheath simulation. Only when the aspect ratio of outer to inner radius $(\frac{b}{a})$ is small can the radial variation be assumed to be negligible.

More complete modeling of the plasma in the coaxial plasma gun was contemplated, but such modeling was beyond the resources allocated to this effort. A multi-component multidimensional MHD approach could offer much insight into the behavior of the plasma sheath in the coaxial plasma gun, especially in the region where the sheath shows the effects of turbulence, filamentation or other chaotic behavior.

4.1.4 Computer Coding of the Slug Model

The slug is computationally modeled with the FORTRAN computer program CLIN. The program source code is provided in Appendix B. The program is short. Much of the program is dedicated to comments for the user. A sample input file is also provided in Appendix B. The input file gives the value for the AFWL PUFF coaxial plasma gun system. Since the code is reported in Appendix B, the interested reader is referred there for more detail about the actual FORTRAN coding.

Slug model results are displayed in Figures 25 through 30. These
results show results of the slug model for PUFF plasma gun conditions.
Inner gun radius (a) is 2 9/16" (6.51×10^{-2} m), outer gun radius (b) is
3.5" (8.89×10^{-2} m) and effective plasma gun length (from the gas outlet
holes to the end of the gun) is 18.25" (0.4636 m). The system
inductances are L_{01} of 8.2 nH and L_{02} of 20.8 nH. The mass of the
plasma sheath is assumed to be 0.1 mg (10^{-7} kg). The total fixed system
resistance is assumed to be 1 mΩ. The system capacitance is 72 μF. The
initial capacitor bank voltage is 60 kV. It should be noted that, for
all Figures of graphically displayed data, the ordinate (x-axis)
exponent is in the lower right corner of the graph. The abscissa (y-
axis) exponent is in the upper left corner.

In Figure 25, the plasma sheath axial position as a function of time is
displayed. The plasma sheath begins at the initial position at the gas
outlet holes. It slowly separates from the initial position until it
reaches the end of the plasma gun (where the calculation terminates).

In Figure 26, the instantaneous and time averaged plasma sheath
velocities are displayed. The instantaneous velocity rises from 0 to a
maximum of 79 cm/μs (7.9×10^5 m/s). The time averaged sheath velocity is
28 cm/μs (2.8×10^5 m/s).

In Figure 27, the load inductance is displayed. It varies linearly
with the axial position. It rises from 0 to a maximum of 28 nH. This
value is different from the earlier quoted total coaxial gun inductance
since only part of the coaxial gun is in the circuit.

136

Figure 25. Slug calculation, axial position of plasma sheath.

Figure 26. Slug calculation, plasma sheath velocities.

138

Figure 27. Slug calculation, load inductance.

139
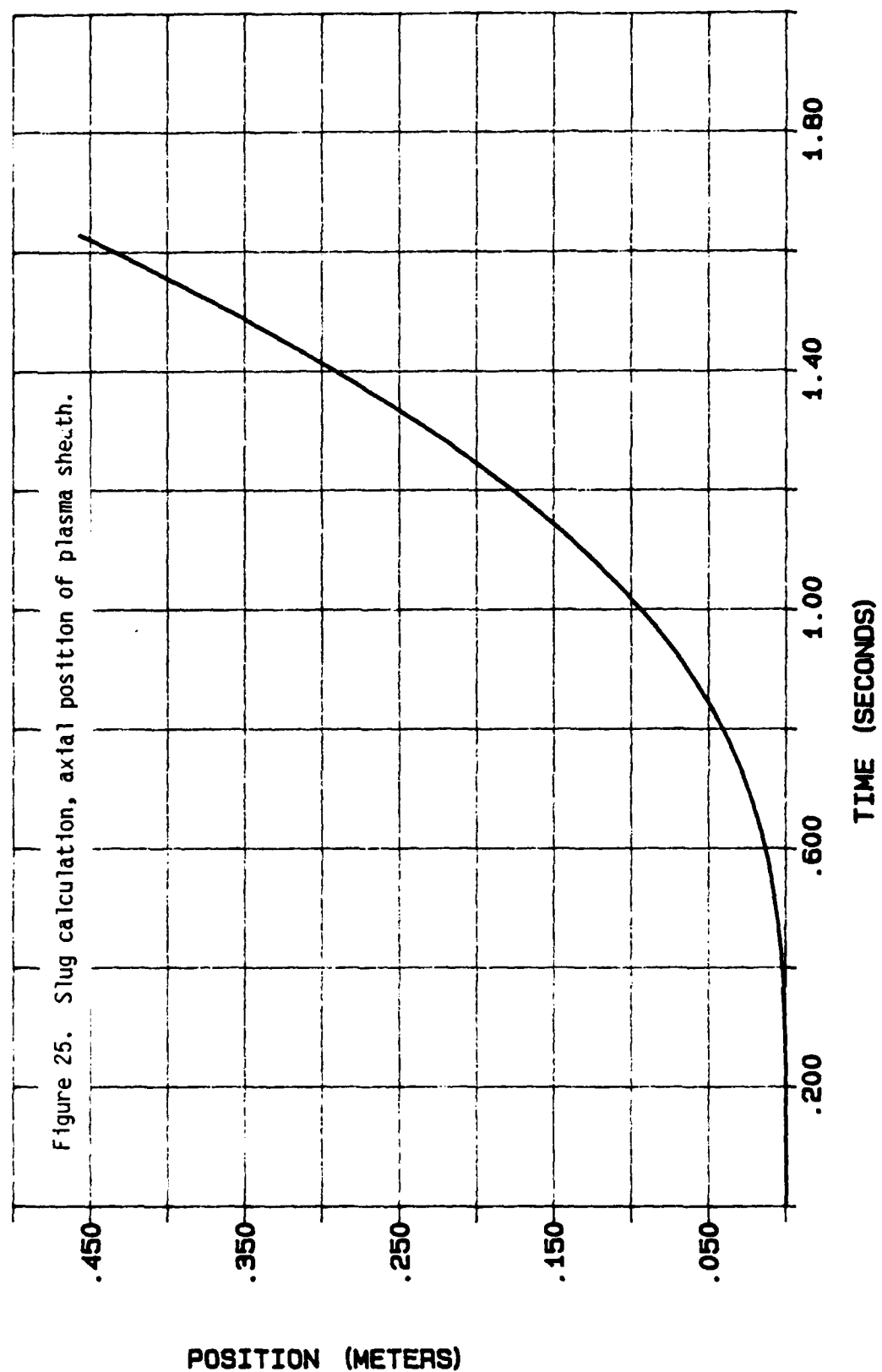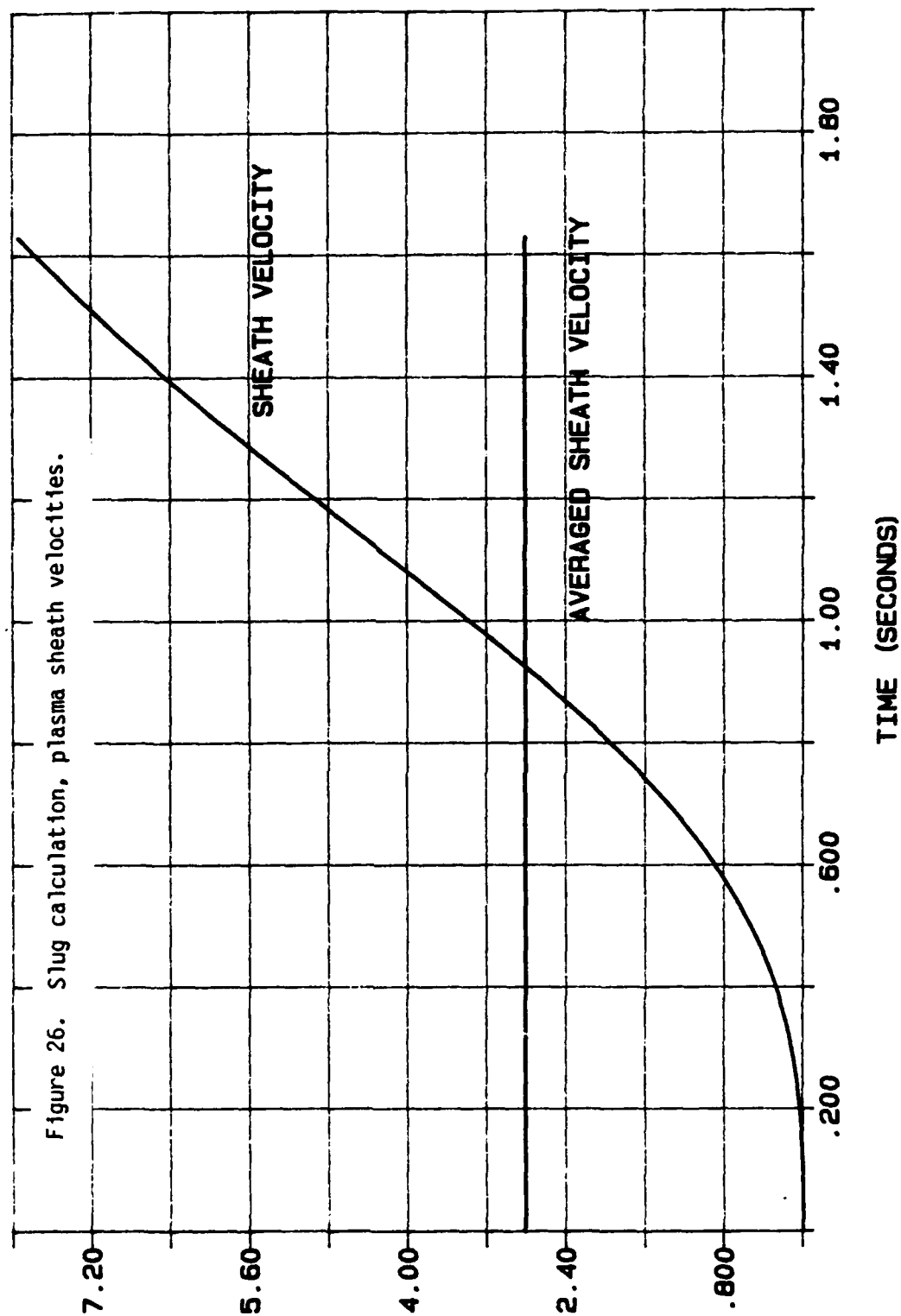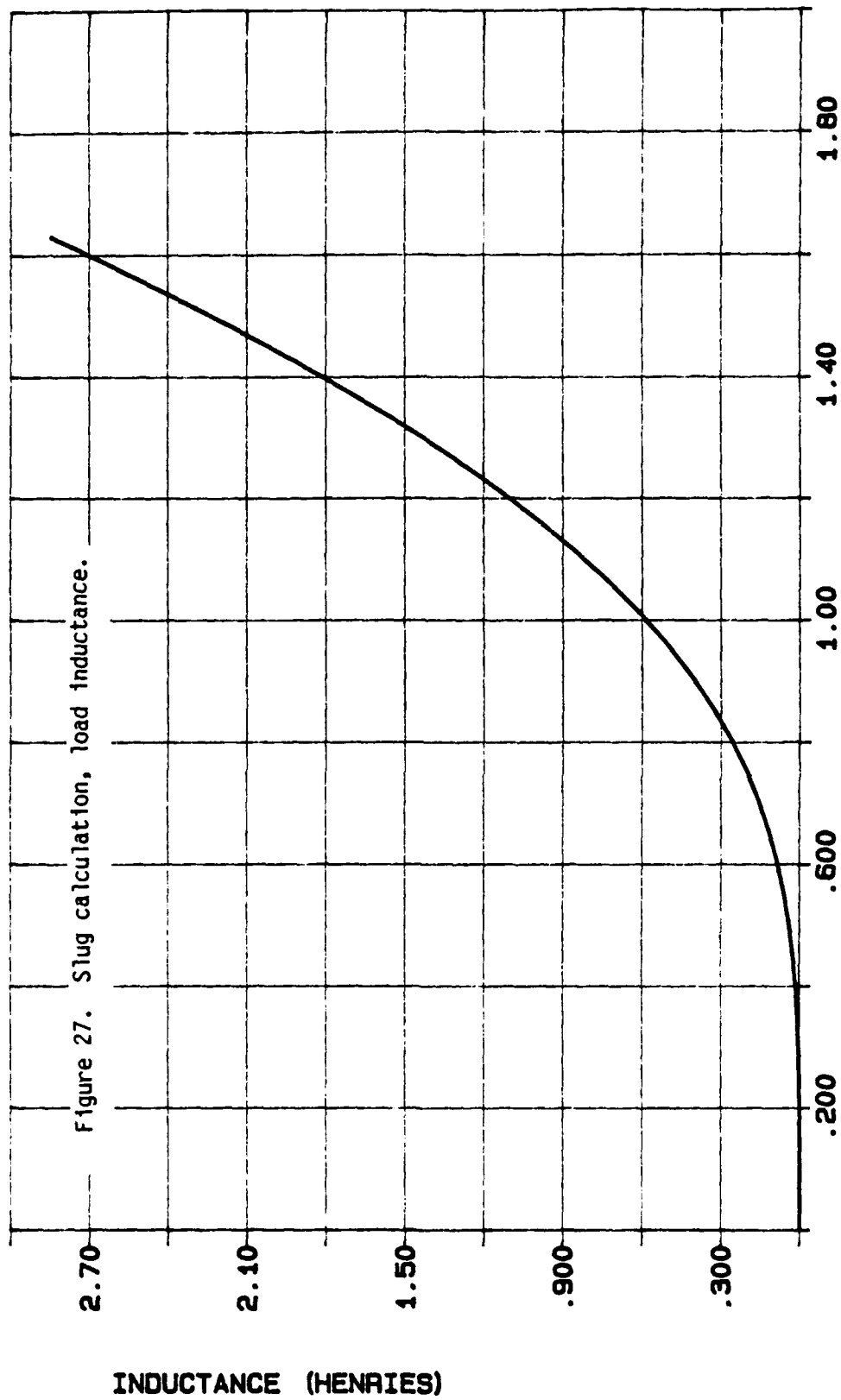
In Figure 28, the calculated coaxial plasma gun current is displayed.
It rises from 0 to a maximum of 1.59 MA at about 1.1 μs. It then drops
to about 1.4 MA at the end of the calculation at 1.62 μs.

In Figure 29, the calculated load voltage is displayed. It rises from 0
to a maximum of 53.3 kV at about 1.46 μs. It then drops to a slightly
smaller value at the end of the calculation.

In Figure 30, the calculated probe voltage is displayed. It begins at
43.0 kV. It remains flat to 10% over the entire calculation. The probe
voltage drops to 42 kV at 0.53 μs and then rises to 44.6 kV at 1.12 μs.

4.2 NUMERICAL CONVERSION

Before proceeding with analysis of the experimental results, some
discussion of the digitization procedures is required. Since no
information about these procedures is available, the experimental
analysis would be incomplete without some documentation.

4.2.1 Digitization Procedures

Two different computer routines are used to convert the analog data from
an oscilloscope picture to a data form suitable for digital conversion
and computer storage. Both procedures were developed by AFWL/AWPP
military personnel. The first was developed under the oversight of Capt
Steven S. Payne. The second was developed by Capt J. Michael
Westerfield.

Figure 28. Slug calculation, gun current.

E-6

141

Figure 29. Slug calculation, load voltage.

TIME (SECONDS)

E-6

VOLTAGE (VOLTS)

E 4

142

Figure 30. Slug calculation, probe voltage.

E-6

143
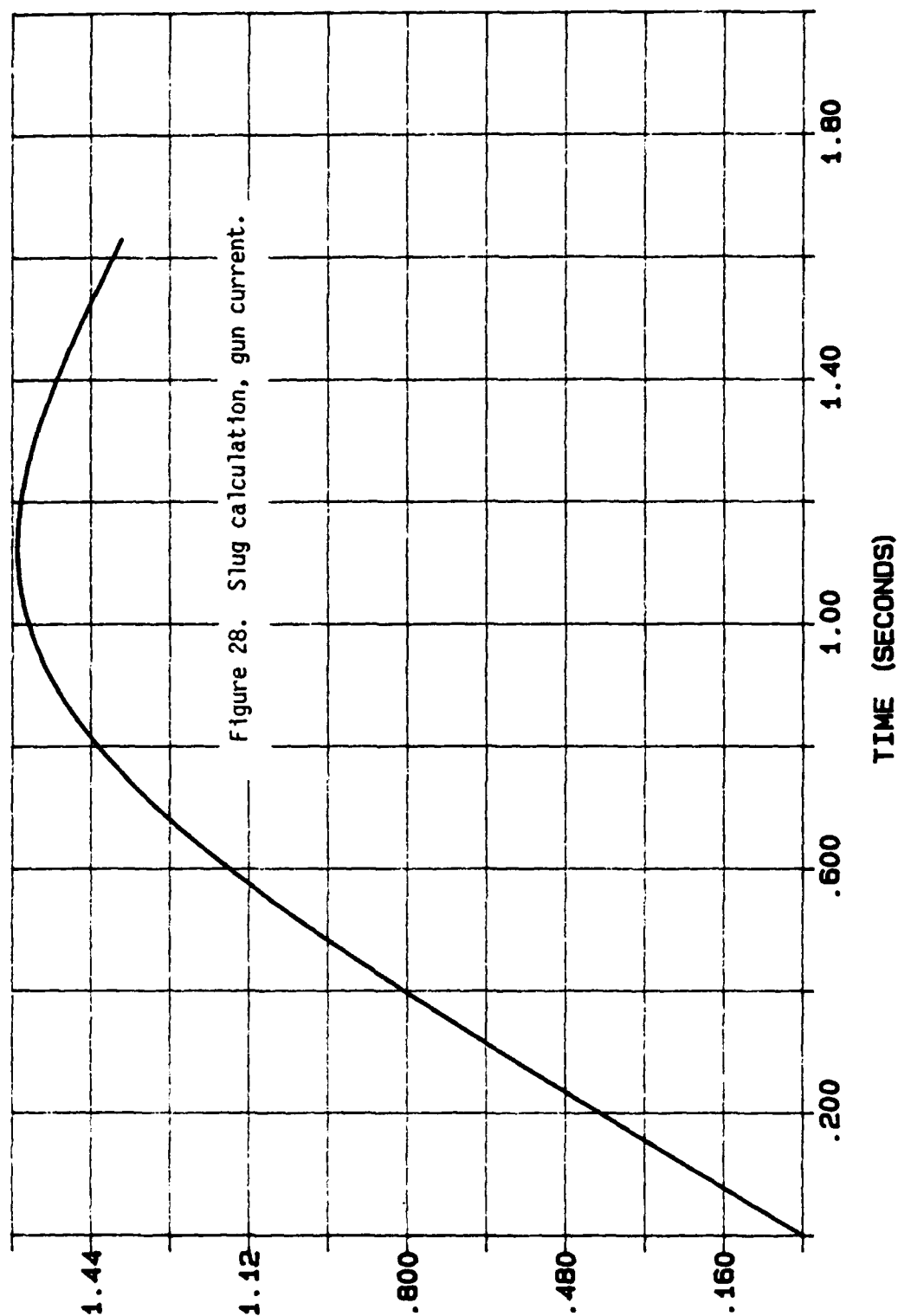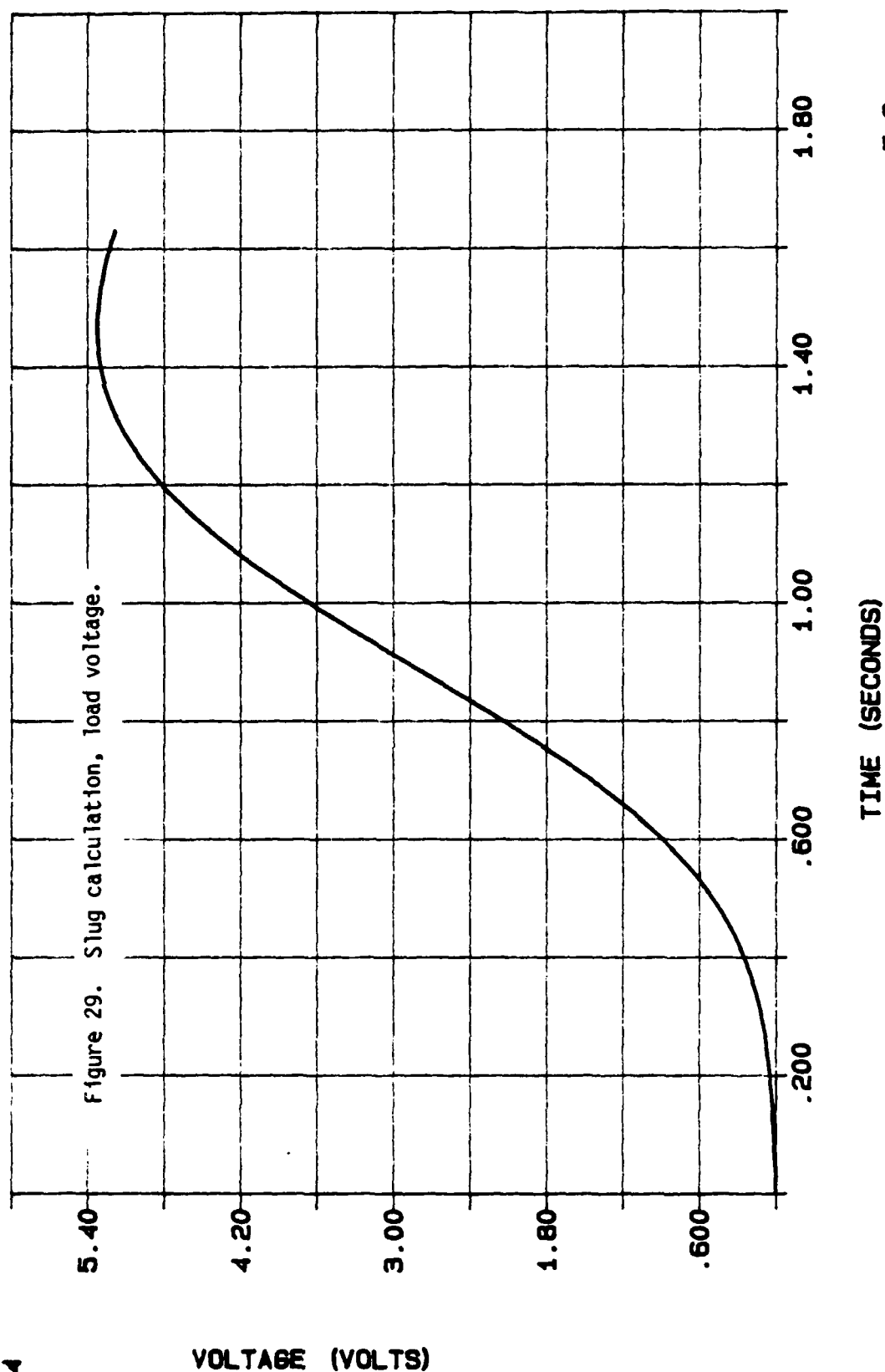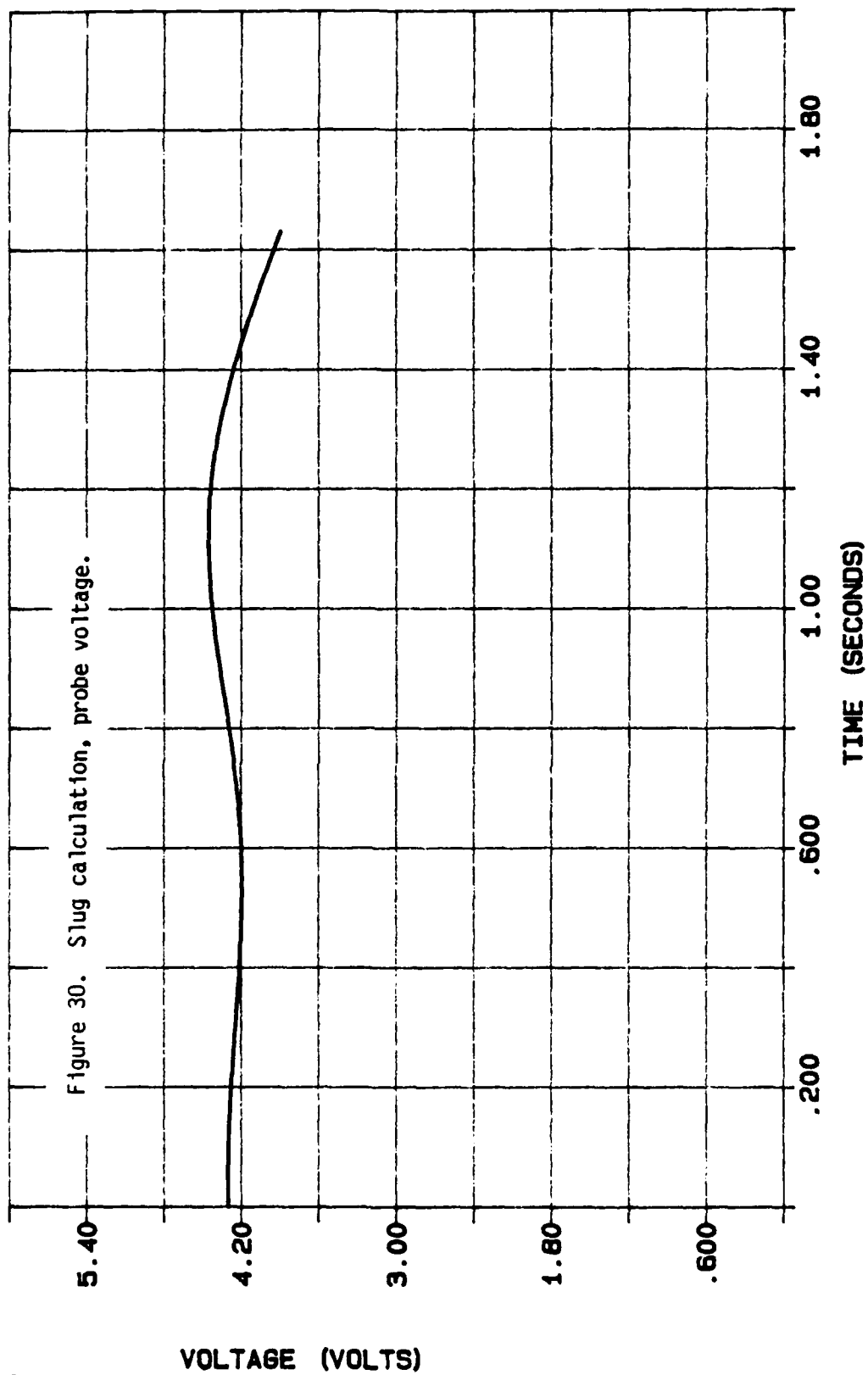
4.2.1.1 COMTAL Digitization Procedure. The first digitization procedure involves the COMTAL image processing system. It is interfaced with the AFWL/AWPP VAX 11/750 computer and involves a customized FORTRAN computer program to transfer COMTAL images to the VAX system for storage and analysis. The method captures an oscilloscope image with the COMTAL system. The trace is stored on the COMTAL system and is converted into an array of numerical (x,y) data pairs. Since the COMTAL digitization procedure is no longer being actively supported by AFWL/AWPP personnel and is not used for data conversion, further discussion is not warranted. Generalized comments about this digitization procedure are given in the discussion about the second digitization procedure.

4.2.1.2 BONES and TURTLE Digitization Procedures. Because of the need to convert increasing amounts of analog oscilloscope data from the Plasma Physics Branch (AFWL/AWPP), Capt Westerfield was tasked to create a procedure to convert oscilloscope data into numerical data. Capt Westerfield created two programs to be hosted by the Zenith 100 microcomputer. The first program, BONES, creates digitized data from analog oscilloscope traces. The second program, TURTLE, allows display and manipulation of the output hexadecimal digitized data created by the BONES program. The TURTLE program allows the data to be output in the ASCII format discussed in Section 4.2.2.

There are four steps in the BONES digitization procedure. Using an RCA video camera, the BONES program captures a video image in a 501 by 256 array. In this first step, each element in the array contains a brightness level from 0 to 7. In the second step, the BONES program

144

converts the brightness level for each pixel (picture element) in the array into either 0 or 7 (fully black or fully white). The brightness cutoff (between fully black and fully white) is adjustable by the BONES program user. It is typically set at a brightness level of 3 or 4.

The third step in the BONES program is functional thinning. This step performs the actual calculations to convert the pixel array into a functional display. The program begins searching from the first bottom pixel. (This is the pixel located at position (1,1) in the array.) The program then proceeds upward until a fully white pixel is found. (This upward search goes through pixels (1,1) to (1,n), n is pixel position of the first fully white pixel.) The program proceeds upward in the data array until the fully white pixels end. This range of fully white pixels is averaged to a mid-range pixel. This mid-range pixel is used as the first functional data point. The program searches in the general area of the previously calculated fully white pixel range. (The program searches around the area of pixel (2,m) to find a fully white pixel range, where (1,m) is the position of the averaged pixel.) If no fully white pixel range is found, the program searches sequentially from (2,1) to (2,256) to (501,1) to (501,256) until a fully white range is found. Once a fully white range is found, the procedure continues until the search and averaging procedures are completed. If no fully white pixel range is found, the program yields a zero trace.

In the fourth step of BONES, the program scales the data taken in the third step. Given an x-range from 0 to 10 and a y-range frcm -4 to 4, the user gives three graticule positions on the video image. These

graticule positions correspond to the baseline edges and a perpendicular distance above the baseline. The user assigns a position value for the baseline and the distance above it: x-value for the left baseline edge, x-value for the right baseline edge, y-value for the baseline and y-value for the position above the baseline. Using these assigned values, the BONES program converts the relative numbers obtained from the third step into calibrated numbers. The 8 level brightness (501,256) array is converted into a single string of 501 hexadecimal numbers ranging from -4 to 4.

Once the BONES program converts the oscilloscope image to the string of numbers, the TURTLE program converts the string into a functional image displayed on the host computer. The TURTLE program allows rescaling of the data file. The TURTLE programs also allows data to be numerically manipulated (adding, subtracting, multiplying or dividing by a constant, smoothing the data with 5-point, 7-point or fast Fourier transforms and numerical differentiation and integration). The program allows functional manipulation (adding, subtracting, multiplying or dividing traces by each other). The TURTLE program outputs the data in hexadecimal or ASCII forms accepted by other computer programs. The BONES program performs the actual digitization; the TURTLE program scales the data to experimental values.

4.2.2 Data File Format

All the numerical data files have the same format. The files are in ASCII format and have the following structure:

TITLE--an alphanumeric string of up to 132 characters representing
the title line of a data file for reference. All of the title
occurs on one line. A portion of all the character string may not
be input/output.

N--an integer equalling the number of data points. The number must
be on a separate line from the title and the numbers that follow.

X-ARRAY--an array of x (ordinate) data points going in order from
X(1) to X(N). A total of N x data points must be provided. Some
programs require one x data point per line. All programs require
the X array to have all N x data points in order.

Y-ARRAY--an array of y (abscissa) data points going in order from
Y(1) to Y(N). A total of N y data points must be provided. Some
programs using this data format require on y data point per line.
All programs require the Y array to have all N y data points in
order.

COMMENTS--may follow the data file. These comments are not read by
the programs and are lost in file transformation. Comments
identify and provide extra information about the file.

4.3 Computational Treatment of Numerical Data

The method for handling the numerical data is discussed here. Since no
fiducials were used in the oscilloscope data, an explanation of the

147

method for dealing with timing issues must be provided. Voltage and time bases were calibrated in the oscilloscopes, so voltage and time scales are not in question. Without a reference time, oscilloscope triggering is problematic. Reference timing would have been obtained from a superposition of a fiducial signal and a diagnostic probe signals. From the experimental data, it is evident some oscilloscopes tended to trigger inconsistently. These times could vary as much as 2.0 µs, but the time variation is typically less than 0.2 µs. Without fiducials, it is impossible to ensure signal times from different oscilloscopes (or even the different signals from the same dual-trace oscilloscope) are simultaneous to ±0.1 µs.

4.3.1 Manipulating Data Traces

In all cases, the data traces needed to be manipulated. In some cases, the manipulation is used to correct the data trace. In some cases, calibration factors are used to convert the voltage signals to appropriate units (be they voltage probe voltages, Rogowski coil currents or $\dot{B}$ probe magnetic fields). Numerical manipulation is required when traces were to be added, subtracted, multiplied, divided, differentiated or integrated. A FORTRAN computer program is written to perform these data manipulations. The logic of the computer program in manipulating data is discussed here.

4.3.1.1 Data Manipulation for Correction. In the oscilloscope data, there are often high frequency signals imposed on the diagnostic signal trace. The smoothing method involves differentiation of the data trace,

148

numerical smoothing of the differential and integration of the differential. The smoothing methods used were seven-point smoothing or a fast Fourier transform. Seven point smoothing yields a running average of the data. Fast Fourier transforms filter out high frequency data components. Smoothing the original trace degrades the signal contained in the digitized data; smoothing the differential reduces this signal degradation and reduces the high frequency noise.

When there is a flat baseline preceding the voltage trace, one or several techniques are used to obtain better data (data more accurately representing actual results). One routine assumes the baseline can be fitted by least squares and the baseline is subtracted from the data trace. Another routine allows a correction for angular rotation. A third computer routine allows "RC droop" to be corrected (using the method discussed in Section 2).

In the rare cases where digitization produces spurious data points, correction procedures are used. This sometimes involves redigitizing an oscilloscope trace or editing the data file and removing the spurious data points. If the data is not pathological, these smoothing methods are sufficient to deal with the problems.

4.3.1.2 <u>Data Manipulation for Calibration</u>. Corrected data traces were multiplied by the calibration factors reported in Section 2. Current data taken with Rogowski coils and $\dot{B}$ probes are multiplied by the appropriate calibration factors. Since the voltage probes vary from shot to shot, the data is individually averaged to assume an averaged

149

plateau value. This averaged plateau voltage value is used to calculate the individual voltage probe value. (The FORTRAN source code for the data manipulation program is given as Appendix C.)

4.3.1.3 Data Manipulation for Multiple Traces. When two or more traces are operated (addition, averaging, subtraction, multiplication or division), several things must be done: trace conversion to continuous functional relations, common start and end points and trace correction.

Each data array can be thought of a discontinuous function with a finite number of data points. Data from another trace cannot operate on the given trace if the data is inconsistent. To deal with this, a third order spline fit is applied to both traces to establish numerical continuity.

When data traces of different endpoints operate on each other, the largest beginning time (ordinate) and the smallest ending time are used. Outside the stated time, data arrays are undefined. Linear data extrapolation outside the defined time range was considered and discarded when the results became unacceptable.

Finally, trace operations needed to allow for the finite (discontinuous) mathematics of the host computer. Values produced as a result of trace operations would not exceed $\pm 10^{36}$ (numerical overflow). Absolute values for trace operations would not become smaller than 10^{-36} (numerical underflow). Checks for these numerical problems and modification of data arrays are used.

4.3.1.4 <u>Data Manipulation for Common Timing</u>. Because no timing
fiducials were used, a method of dealing with data time variations is
required. Time variations of tens of nanoseconds may be due to
digitization. Errors in oscilloscope triggering have been noted. The
following assumptions are used for common time extrapolation:

1) Current rise is assumed the same for the Rogowski coils
   (counter-rotating and chamber). This assumption <u>a priori</u> masks
   any information obtained from Rogowski coil current timing.

2) Beginning of current is assumed the same for all $\dot{B}$ probes at
   any axial level. Azimuthal variation information is lost.

3) A "zero time", that is, a time for measuring the signal rise
   can be extrapolated from voltage rise. This extrapolated zero
   time is used as an artificial fiducial.

The extrapolated zero time derives maximum signal trace V_s. The signal
trace between 10% of V_s and 25% of V_s is linearly least-squares fit to
extrapolate zero time t_0 (where the linear least squares signal value is
0.0). The limits of 10% and 25% are chosen because all the data traces
have a signal rise between these limits. Having the same percentage
limits for each data trace (regardless of magnitude), extrapolation to
t_0 is computationally made. The few special cases where the 10%/25%
limits did not apply required individualized attention.

Having obtained the extrapolated zero time value t_o for each signal trace, the zero times value are averaged. The resultant averaged zero time became the artificial fiducial time. Every signal trace in a set is referenced to this artificial fiducial. Each resultant data trace begins at the same reference time, the averaged extrapolated zero time.

4.3.1.5 <u>Data Manipulation for Derived Data</u>. Data files are manipulated to derive data. In all data calculations, the fundamental data traces are voltage V(t) and current I(t). The voltage trace is the voltage average from both voltage probes. The current trace is the smaller of the counter-rotating or chamber Rogowski coil traces.

The integrated current trace IC(t) is derived by time integrating the current I(t).

$$IC(t) = \int I(t) \, dt$$

The integrated voltage IV(t) is obtained by time integrating the averaged voltage V(t).

$$IV(t) = \int V(t) \, dt$$

The impedance Z(t) is given by

$$Z(t) = \frac{IV(t)}{IC(t)}$$

Integrated values are used because integrated data is smoother than the digitized data. Unless the integrated current IC(t) contains a functional pole or the integrated voltage IV(t) a functional zero, Z(t) should have enough accuracy for this analysis. Since the voltage V(t) is voltage at the voltage probe positions, the impedance is the system impedance at the voltage probe, not the plasma sheath impedance.

The power P(t) at the voltage probes is

$$P(t) = I(t) * V(t)$$

The energy E(t) at the voltage probes is

$$E(t) = \int P(t) \, dt$$

The impedance L(t) at the voltage probe is

$$L(t) = \frac{1}{I(t)} \int [V(t) - R * I(t)] \, dt$$

The sheath resistance R is constant. An integral method for calculating inductance is chosen (as opposed to calculating time differentials) since the integral is numerically smoother.

153

4.4 EXPERIMENTAL SUMMARY

An summary of each shot in this experimental series is provided in
Appendix D. This summary details the major characteristics found on
each shot.

Some definitions are in order. A clearing shot is the first shot of the
day. The clearing shot prepares the electrodes for subsequent shots. A
clearing shot evolves adsorbed gases from gun surfaces. (In our system,
deuterium gas was used.) A prefire shot is a shot where the capacitor
bank or a gas valve discharged prior to the trigger. A short shot is a
shot where the PUFF system current (and energy) is decoupled from the
plasma gun. When a short shot occurs, current in the plasma gun is not
driven by transmission line current. A prefire shot is a short shot,
but a short shot is not necessarily a prefire.

In the summary, all currents are accurate to ±25% and reported times are
accurate to ±0.1 µs. The neutron information is accurate to ±15%.

Some observations can be made based on the experimental data summary.
The peak coaxial plasma gun currents are about 1.6 MA or less, the slug
model maximum current. Rogowski coil calibration errors are ±25%; this
accounts for some of the variation in the experimental results. Where
the current variation is larger (e.g., shots J0702, J0903, J1001 and
J1103), transmission line current is also significantly higher,
indicating a larger charging voltage. When the gun current peaks are

154

1.6 MA or less, current peaks occur at about 1.1 μs indicating good
agreement between the slug model and the experimental data.

When a short occurs, total current is 3 to 4 MA. This indicates a lower
system inductance implying no current transfer to the plasma gun. When
the peak transmission line current occurs much later (2 to 3 μs) than
the plasma gun current peaks, the results indicate gun current isolation
from the driving current.

Neutron output increases an order of magnitude when both gas valves are
used. Since there is limited plasma gun optimization, the insertion of
cold D_2 gas into the pinched deuterium plasma shows potential for
increasing the neutron yield of the plasma focus.

Coaxial plasma gun operation using $\dot{B}$ probes became more consistent as a
function of time. This is due, in part, to increased capability of the
experimental personnel and to plasma gun conditioning from consistent
and repeated use.

In most of the coaxial plasma experiments, the behavior is predominantly
transition mode. Following Len [3], this behavior begins with a
snowplow mode characterized by a sharp $\frac{\Delta I}{\Delta z}$ (delta function-like) peak as
a function of time. This is discussed in detail in analyzing three
shots from the experimental series.

4.5 ANALYSIS OF SELECTED SHOTS

In this section, refined data from three shots is analyzed. These are D3004, J1006 and J1104. These shots are chosen because they exhibit good current separation at each axial plasma gun position. (The timing problems are as small as possible for these shots.) Other shots might have been chosen for analysis, but these shots best typify the characteristics applicable to the type of analysis developed in this dissertation. The three selected shots span the range of shots taken during the experimental series. There are snowplow characteristics shown in shots D3004 and J1006. Shot J1104 used both the upper and lower gas valves to deliver gas to the plasma gun; shots D3004 and J1006 did not. Shot J1006 shows a crowbarring of the driving current.

Both internal ($\dot{B}$ probe) and external driving circuit data are displayed in this particular shot analysis. Comparison is made with the slug model results. Any anomalous behavior is discussed.

4.5.1 Shot D3004

In shot D3004, charge voltage is 60 kV. The stored electrical energy in the capacitor bank is 1.30×10^5 Joules. The peak current in the transmission line is 1.56 MA at 3.6 μs after current begins. Peak plasma gun current is 1.24 MA at 1.3 μs after current begins. The shot produced 736 counts in the Ag detector in the first minute; this is 9.2×10^6 neutrons produced by the plasma pinch. One gas valve, the lower

valve, is used in this shot. The gas valve is energized 1075 μs before bank discharge. There are 14 active $\overset{\bullet}{B}$ probes in this shot.

Figure 31 shows a display of the current overlay of shot D3004. In this Figure, the driving current D3004IR is shown to exceed the plasma current D3004IC. At about 3 μs, the driving current decoupling from the gun current is essentially complete. At this time, the driving current is seen to oscillate with a frequency not characteristic of the PUFF system with the coaxial plasma gun in the circuit.

In Figure 31, current transport along the gun length is displayed. The current is transported from the bottom to the mid-bottom to the mid-top to the top levels. The current degrades along the length of the gun, probably due to the loss of particles to charged-neutral interactions.

Although plasma gun timing is a problem, plasma sheath velocity can be estimated. If a current of 0.5 MA is a tracer reference, the axial average of the $\overset{\bullet}{B}$ probes reaches the reference at the following times:

Bottom level average	1.867 μs
Bottom level correlated average	1.862 μs
Mid-bottom level average	2.213 μs
Mid-bottom level correlated average	2.209 μs
Mid-top level average	2.406 μs
Mid-top level correlated average	2.411 μs

Figure 31. Shot D3004 current overlay.

E-6

TIME (IN SECONDS)

CURRENT (IN AMPERES)

E 6

158
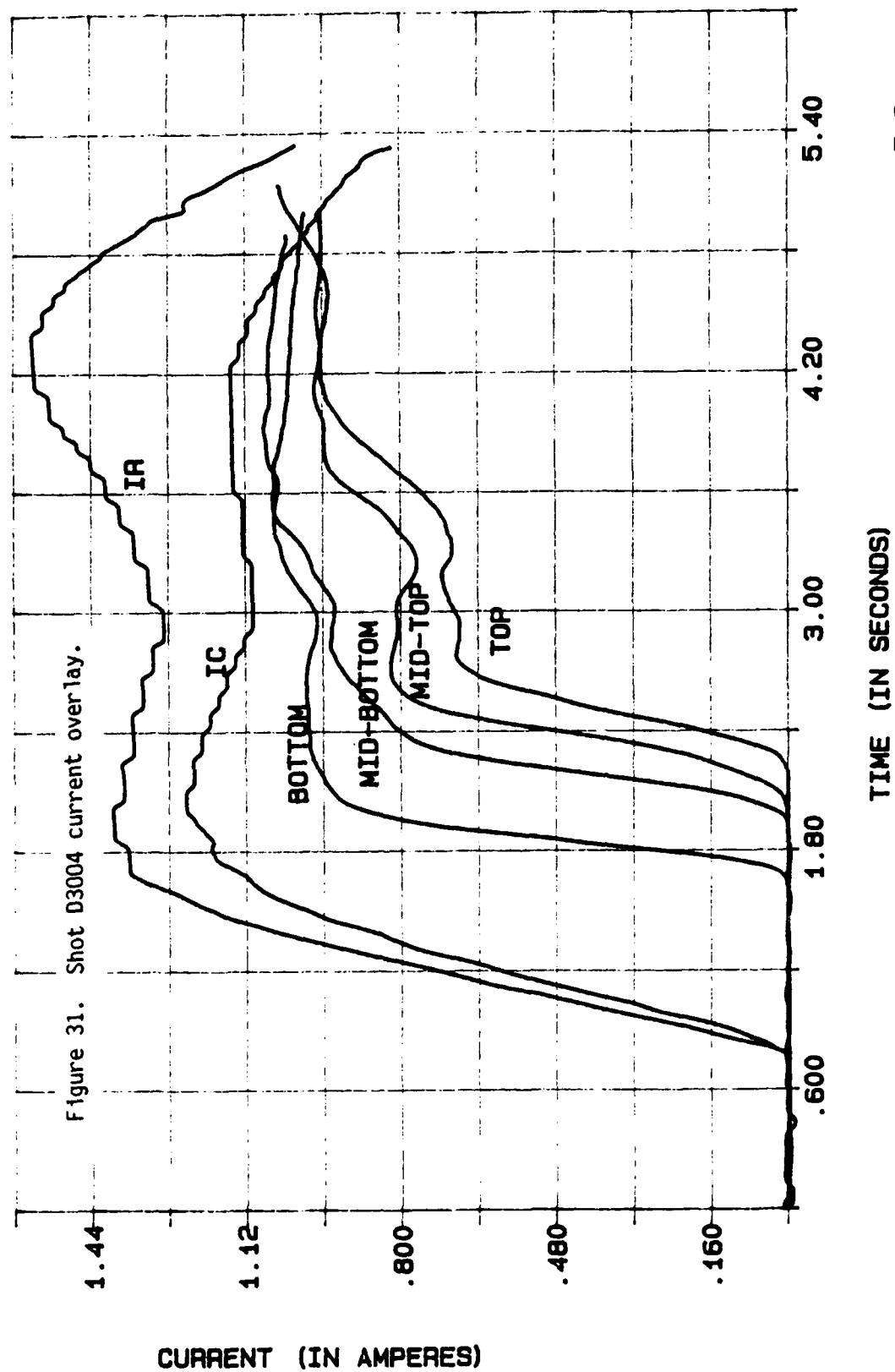
Top level average	2.573 µs
Top level correlated average	2.574 µs

Uncorrelated averages take trace data as digitized and corrected, but with no timing corrections. The correlated average takes data to be both digitized and corrected and, additionally, corrects the timing to an artificial zero, i.e., a place where a zero is extrapolated. Differences between uncorrelated and correlated timings give an indication of the timing variation for a particular shot.

Knowing the distance between each axial position (level) is 4" (0.1016 m), the plasma sheath velocity is calculated.

Velocity between the bottom and mid-bottom levels	2.9×10^5 m/s
Velocity between the mid-bottom and mid-top levels	5.1×10^5 m/s
Velocity between the mid-top and top levels	6.2×10^5 m/s

The velocity profile is similar to the slug model velocity profile; it increases as a function of time. The magnitude of the velocities indicates the Alfven critical velocity is not an accurate model for the sheath. It predicts a velocity a factor of 10 smaller than the calculated velocities given here. The Rosenbluth sheath velocity is of the right order of magnitude for the early velocity, but is too small for the later velocities. The single particle drift velocity (invoking $E \times B$ forces) is of the right order of magnitude. The limited sheath

velocity reported by Fishbine is too small. Of the four models, the most accurate modeling occurs to be the single particle drift velocity.

The azimuthal variation of the sheath as it transits the coaxial plasma gun can be seen in Figures 32 to 35.

At the bottom level, in Figure 32, the traces are simultaneous to ±0.1 μs. The amplitude of each trace agrees well (from 0.9 to 1.1 MA), easily within the calibration accuracy of the individual $\dot{B}$ probes. Current structures on different probes seem to be consistent on all probes at this level.

At the mid-bottom level, in Figure 33, the plasma sheath behavior is not as consistent. The plasma sheaths rise at approximately the same time, but there is a lack of simultaneity in the plasma sheath motion as it passes the $\dot{B}$ probes on this level. The variations of the current amplitude vary more than at the bottom level; however the variation is easily within the calibration accuracy of the $\dot{B}$ probes. At this level, there are more characteristic current features ("peaks" and "valleys" superimposed on the amplitude trace). This could indicate azimuthal spoking formation at this axial position.

In Figure 34, the mid-top current is displayed. The timing is only simultaneous to ±0.1 μs. Currents are flat (not tipped or canted) within the accuracy of the $\dot{B}$ probes. Characteristic current features are seen on all traces at the same approximate time.

Figure 32. Shot D3004 bottom current.

CURRENT (IN AMPERES)

TIME (IN SECONDS)

E-6

E 6

161

Figure 33.   Shot D3004 mid-bottom current.

E-6

E 6

162

Figure 34. Shot D3004 mid-top current.

163
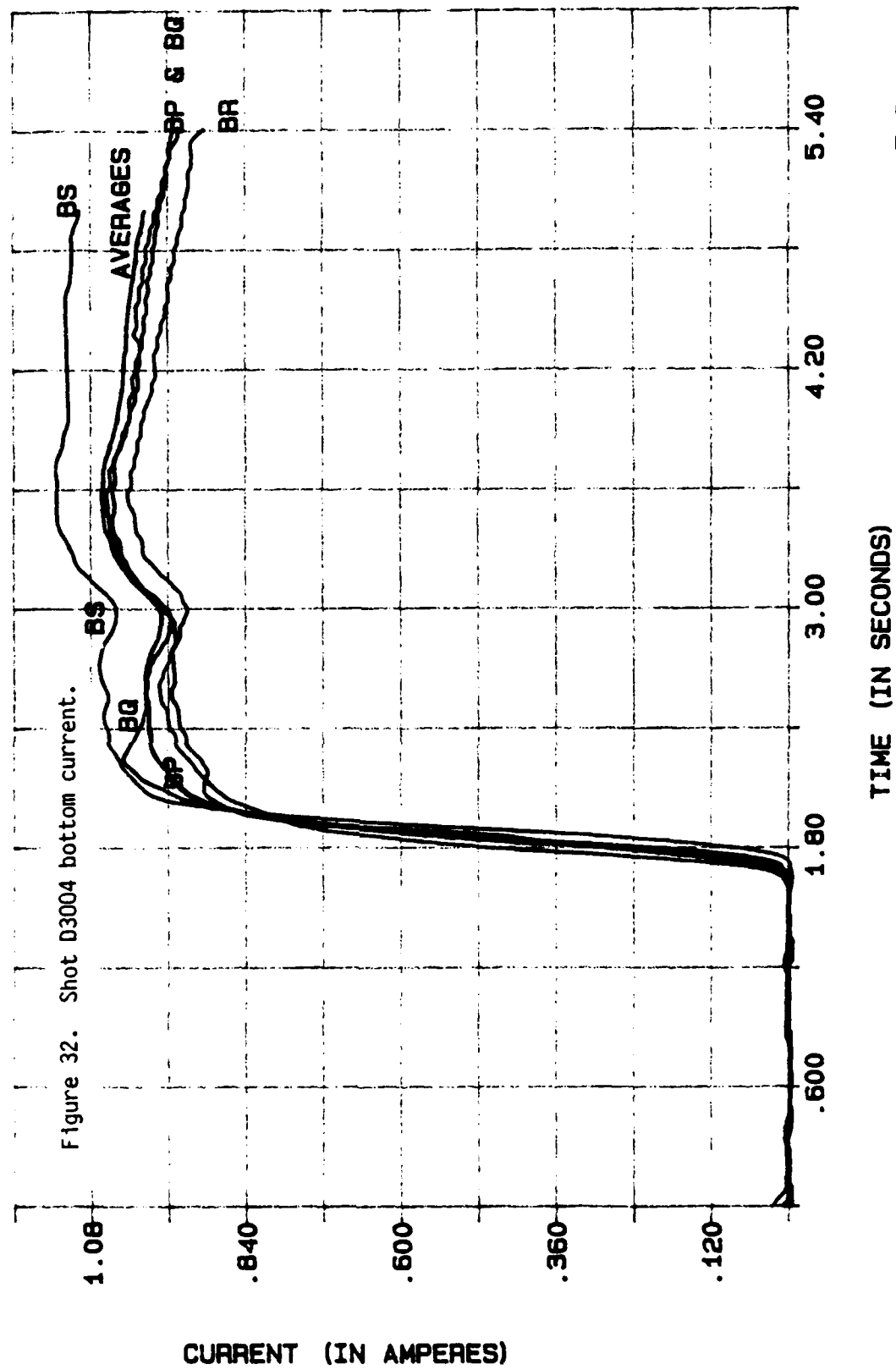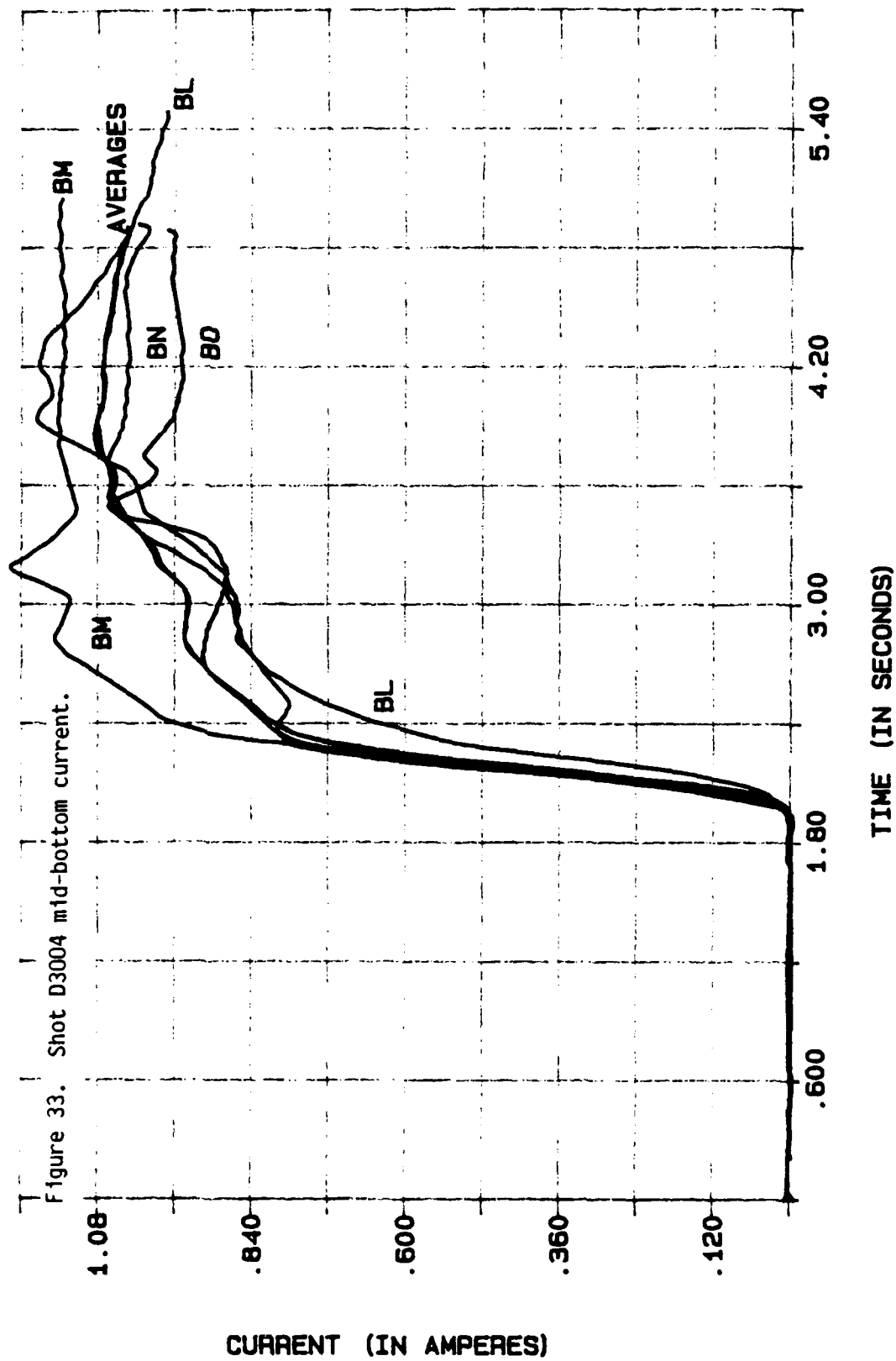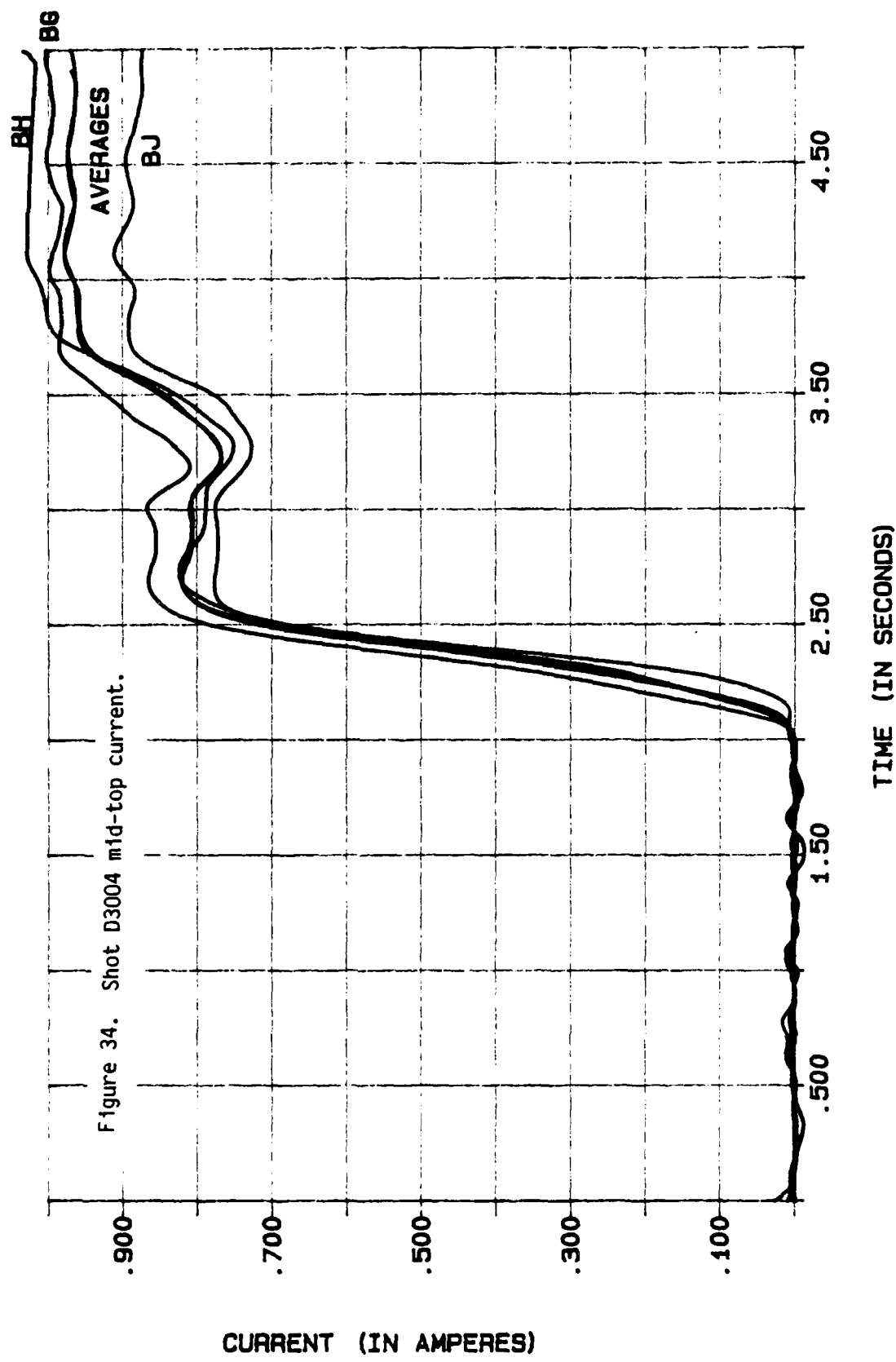
In Figure 35, the top current is displayed. As at the mid-top level, the timing accuracy is accurate to ±0.1 μs. The amplitude at the top level is flat within the accuracy of the $\overset{\bullet}{B}$ probes. There are more individual characteristic features on the top level than on the mid-top level.

In Figure 36, the gun current, D3004IC, is displayed with the calculated slug current. The gun current does not reach the calculated plasma sheath slug current. This is hardly surprising, since the driving current is decoupled from the plasma gun.

In Figure 37, the experimental probe voltage is displayed with the calculated voltage. The agreement is very good. As noted before, the probe voltage is the voltage at the transmission line prior to the coaxial plasma gun. The probe voltage does not measure the plasma voltage.

In Figure 38, the positional current derivative $\dfrac{\Delta I}{\Delta z}$ is displayed. There is a sharp snowplow component in the plasma gun at about 2.0 μs between the bottom and mid-bottom level, at about 2.3 μs between the mid-bottom and mid-top level and at about 2.5 μs between the mid-top and top level. After that time, the plasma sheath appears to operate in a deflagration mode. It appears this shot is operating in the transition mode identified by Len.

Figure 35. Shot D3004 top current.

E-6

165
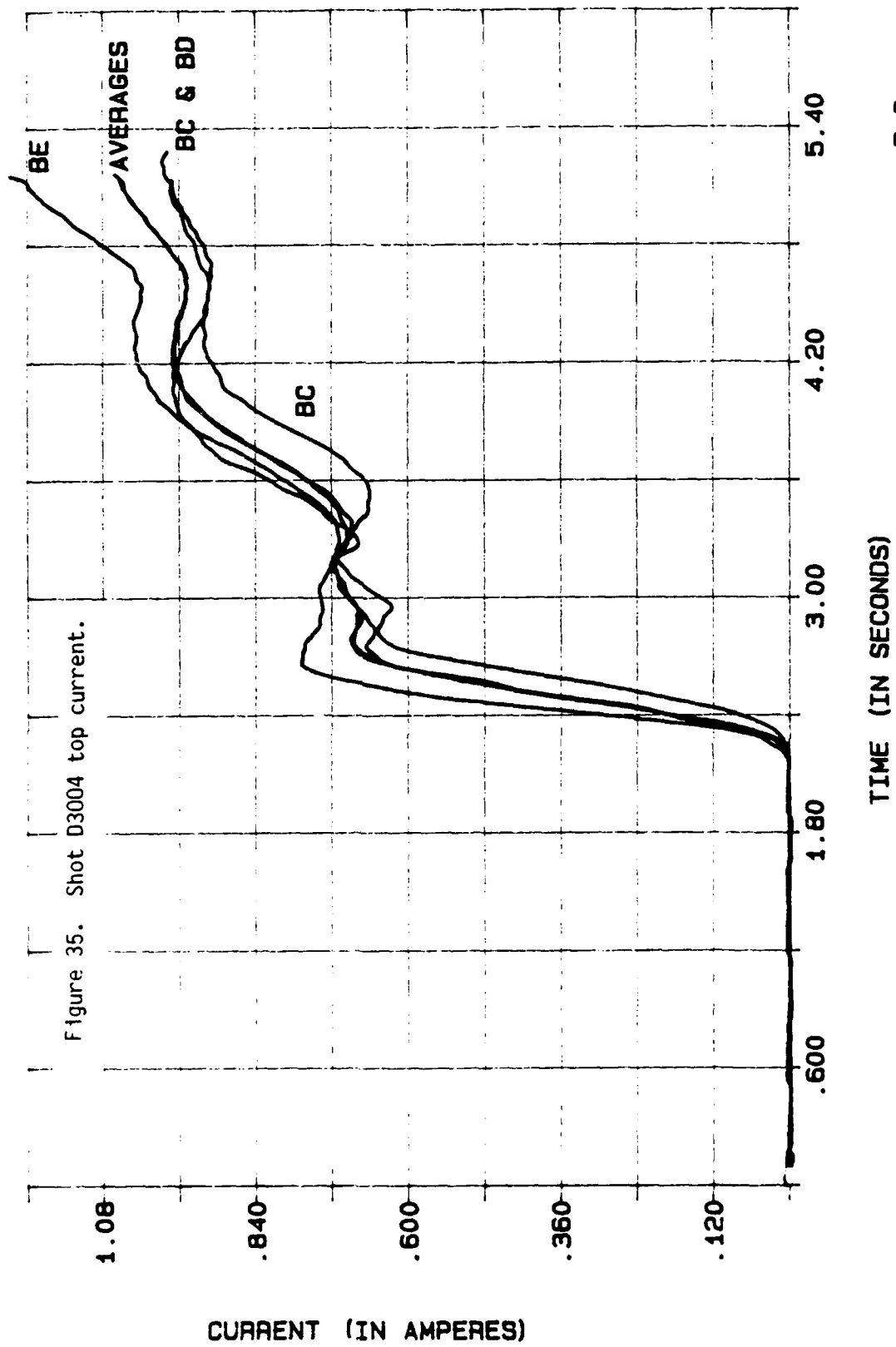
E 6
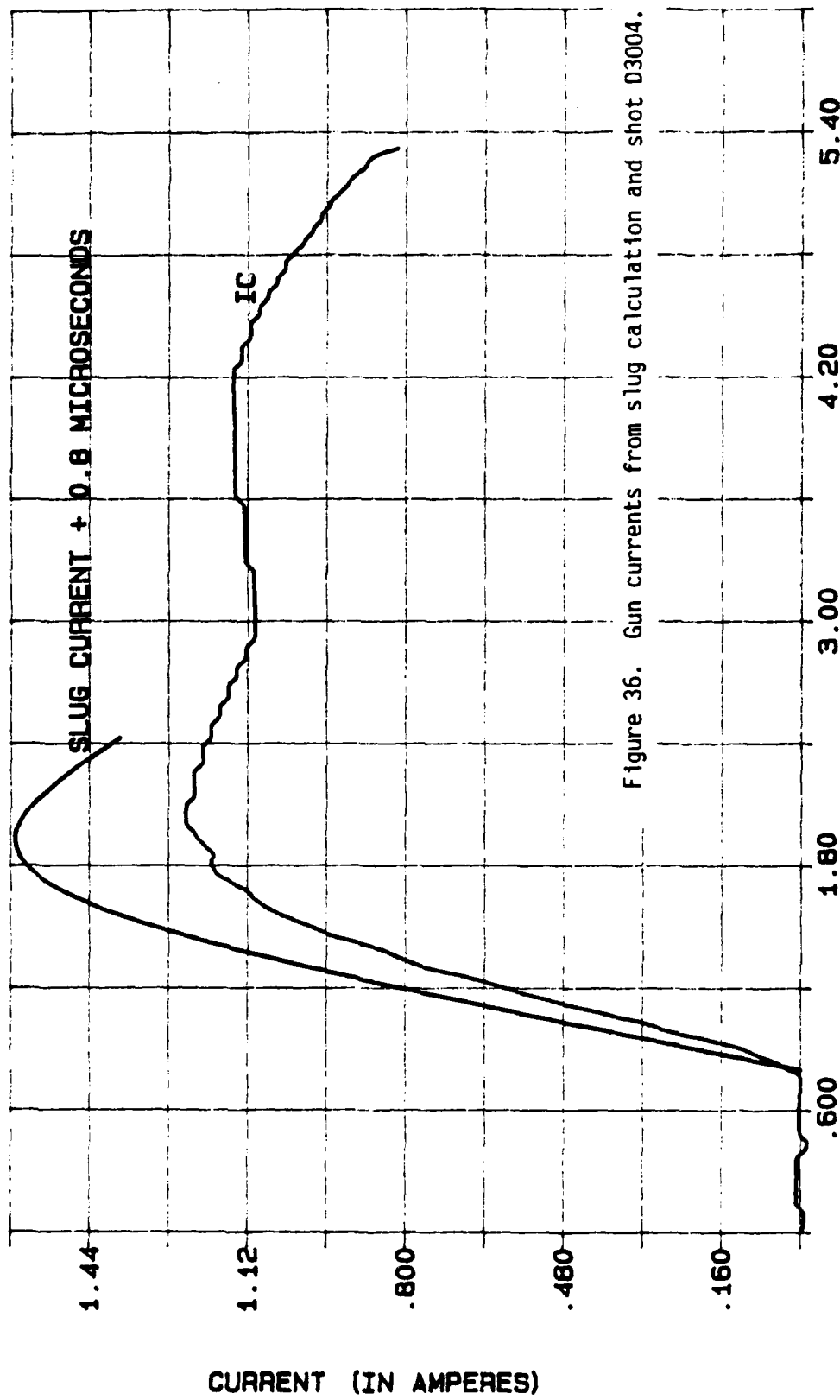
Figure 36. Gun currents from slug calculation and shot D3004.

166

Figure 37. Probe voltages from slug calculation and shot D3004.

167

Figure 38. Shot D3004 $\frac{\Delta I}{\Delta z}$.

BOTTOM AND MID-BOTTOM

MID-BOTTOM AND MID-TOP

MID-TOP AND TOP

TIME (IN SECONDS)

DI/DZ (AMPERES/METER)

E 6

E-6

168
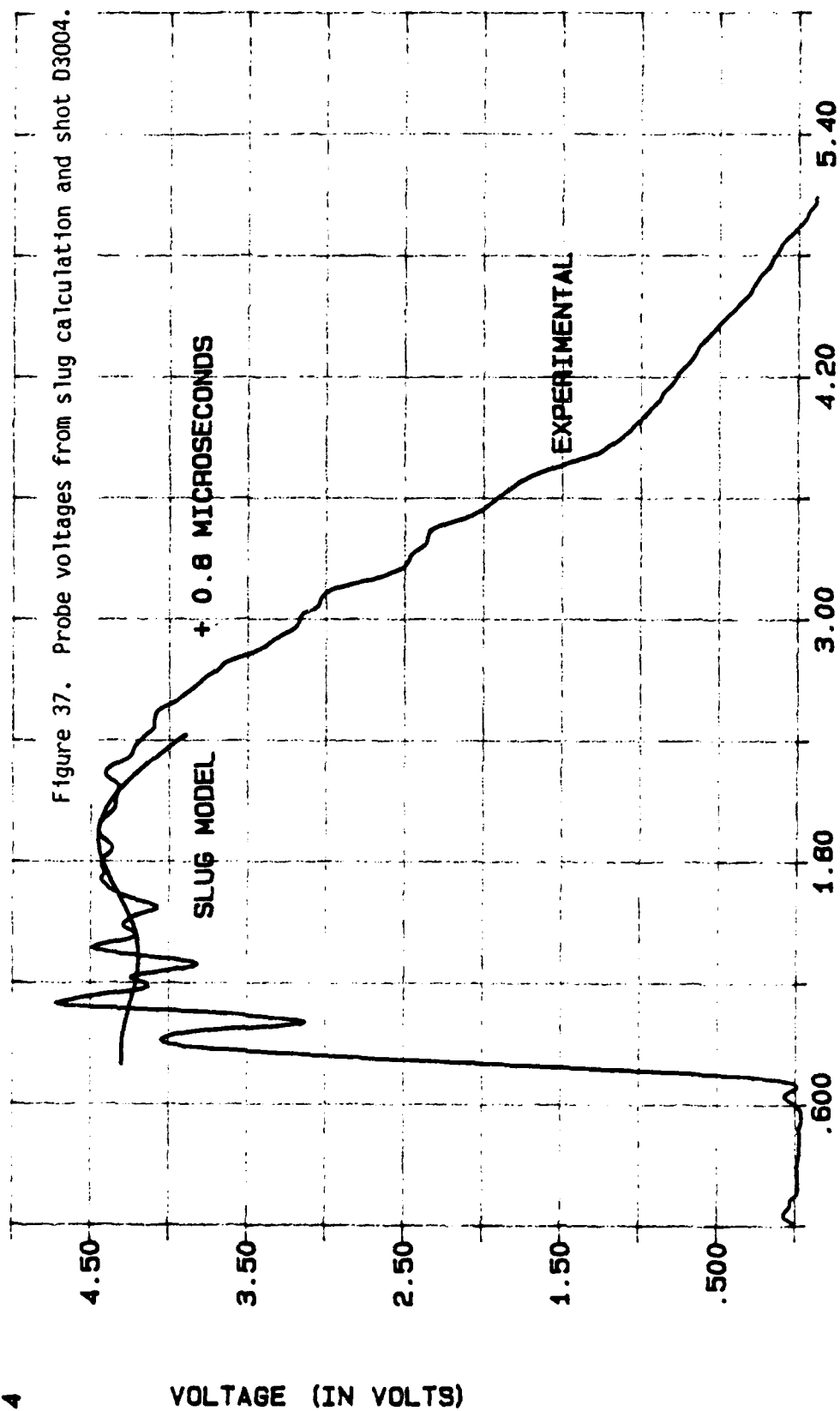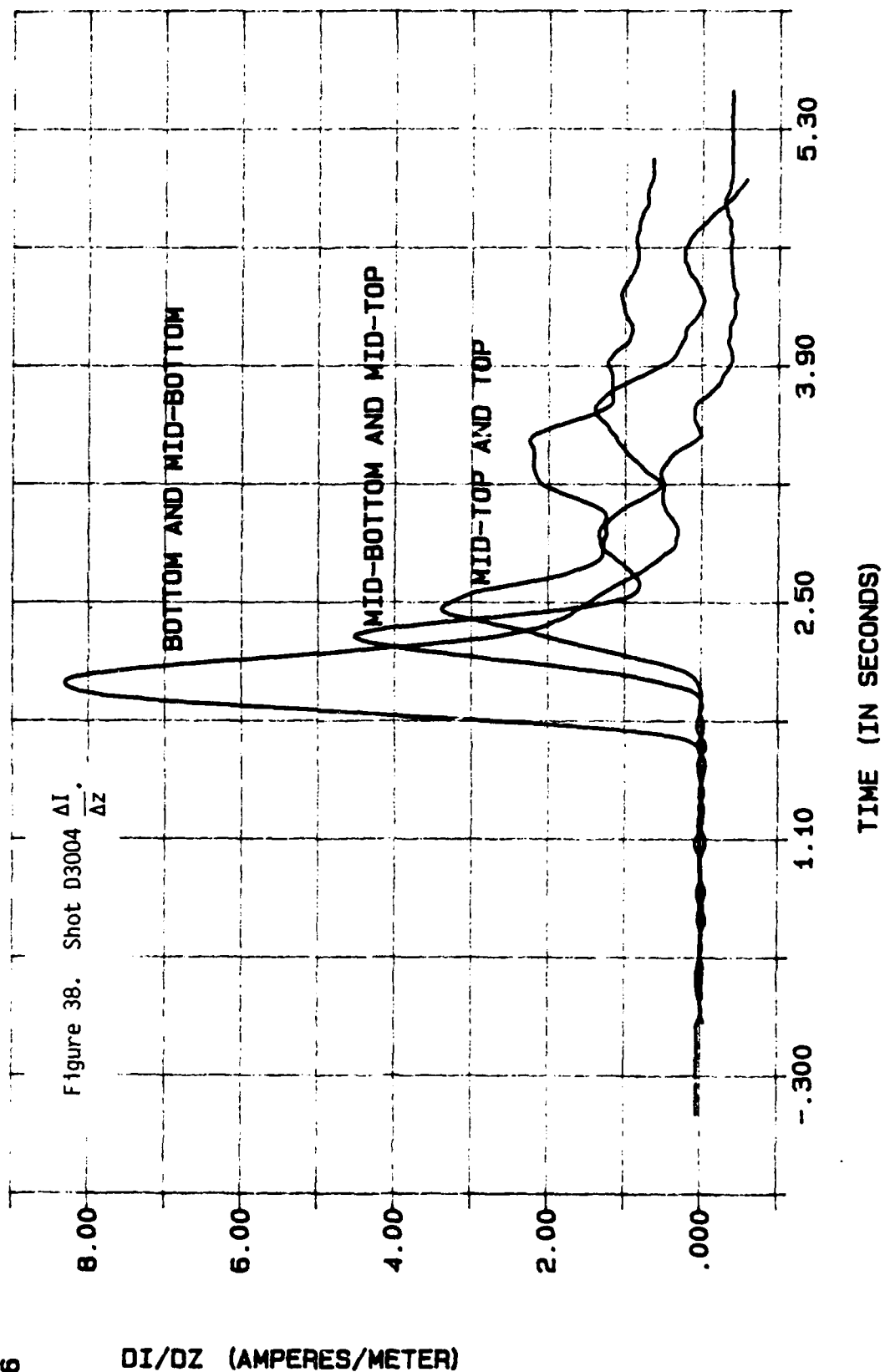
In Figure 39, the electrical power delivered past the voltage probe positions is displayed. Both the uncorrelated and correlated (where time shifting of the current and the voltage traces occur) power traces are displayed. Peak electrical power is about 55 GW at 2.2 µs.

In Figure 40, the time integral of electrical power is displayed. The total energy of the capacitor bank is 130 kJ; the total energy to the plasma gun (at the voltage probe position) is less than 120 kJ. This indicates a decoupling between the driving current and the gun current.

In Figure 41, the calculated inductances as seen by the voltage probe position are displayed. Overlaid on these inductance traces are those predicted by the slug model. The agreement is very good except for early time. Here, numerical problems prevent obtaining a physical result from the voltage and current traces. The uncorrelated and the correlated inductance traces only differ in timing, the magnitude is the same. The inductance drops drastically at about 4.75 µs. This unphysical result is due to the coding, set to artificially limit the magnitude of the inductances.

Examining the current rise at each different axial level, an estimate for current sheath thickness can be made. After calculating the maximum current, reference limits are chosen. These limits are some fraction of the maximum current. Finding times corresponding to the current limits, an incremental time is found. This incremental time is multiplied by a normalization factor (to represent the total current rise). The normalized incremental time for shot D3004 is given:

Figure 39. Shot D3004 electrical power at voltage probe.
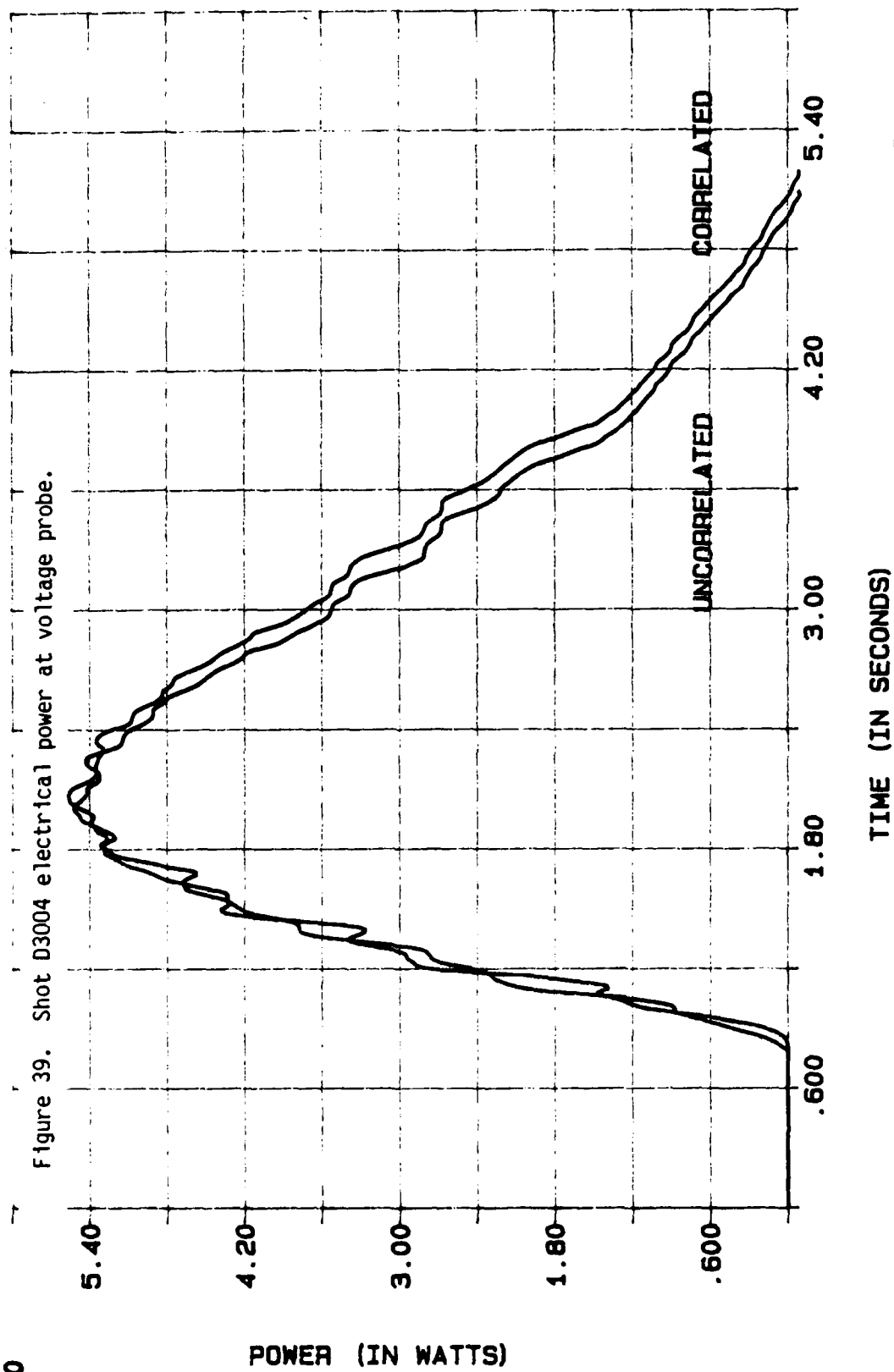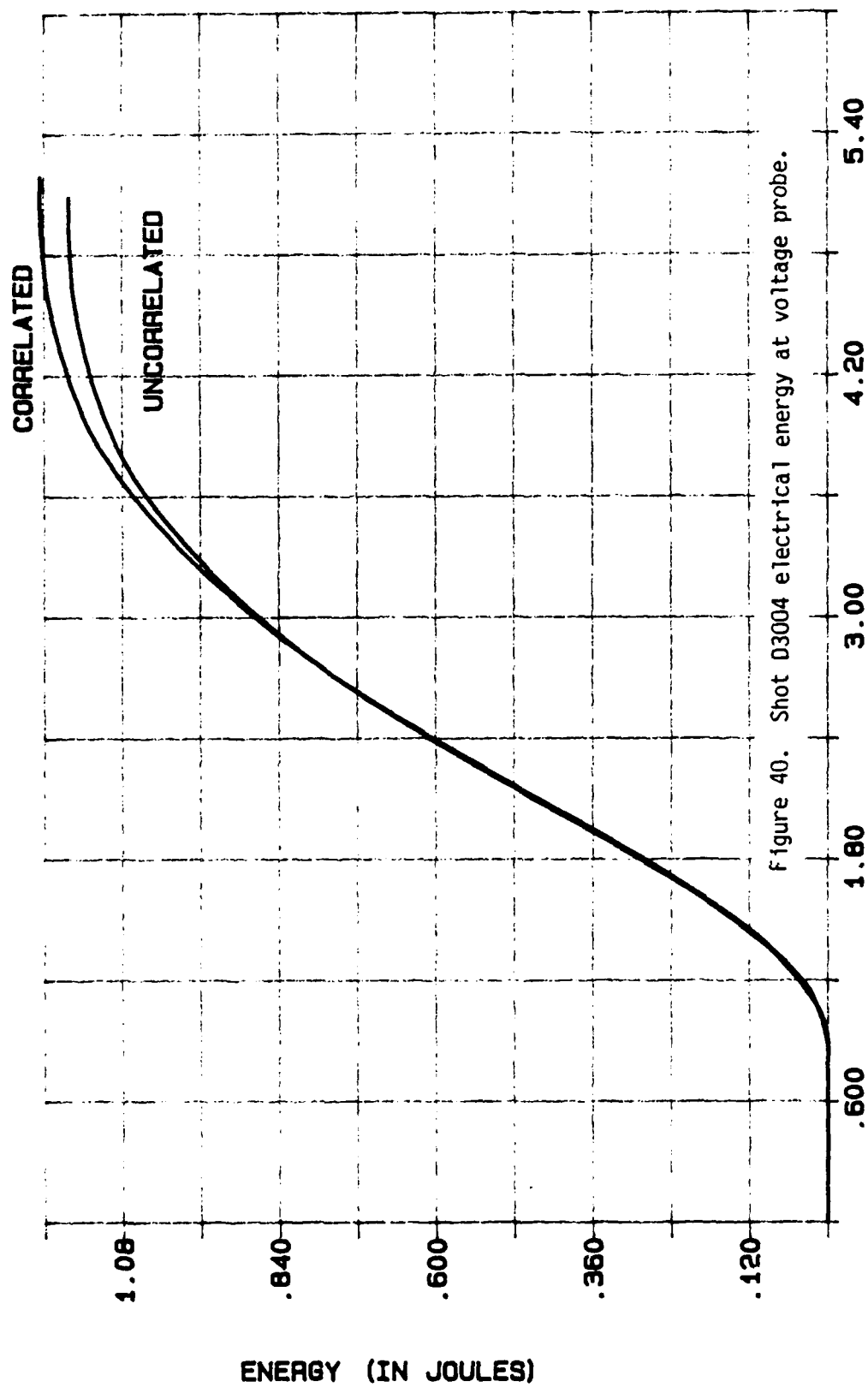
170

Figure 40.   Shot D3004 electrical energy at voltage probe.

171

Figure 41. Gun inductances from slug calculation and shot D3004.

172
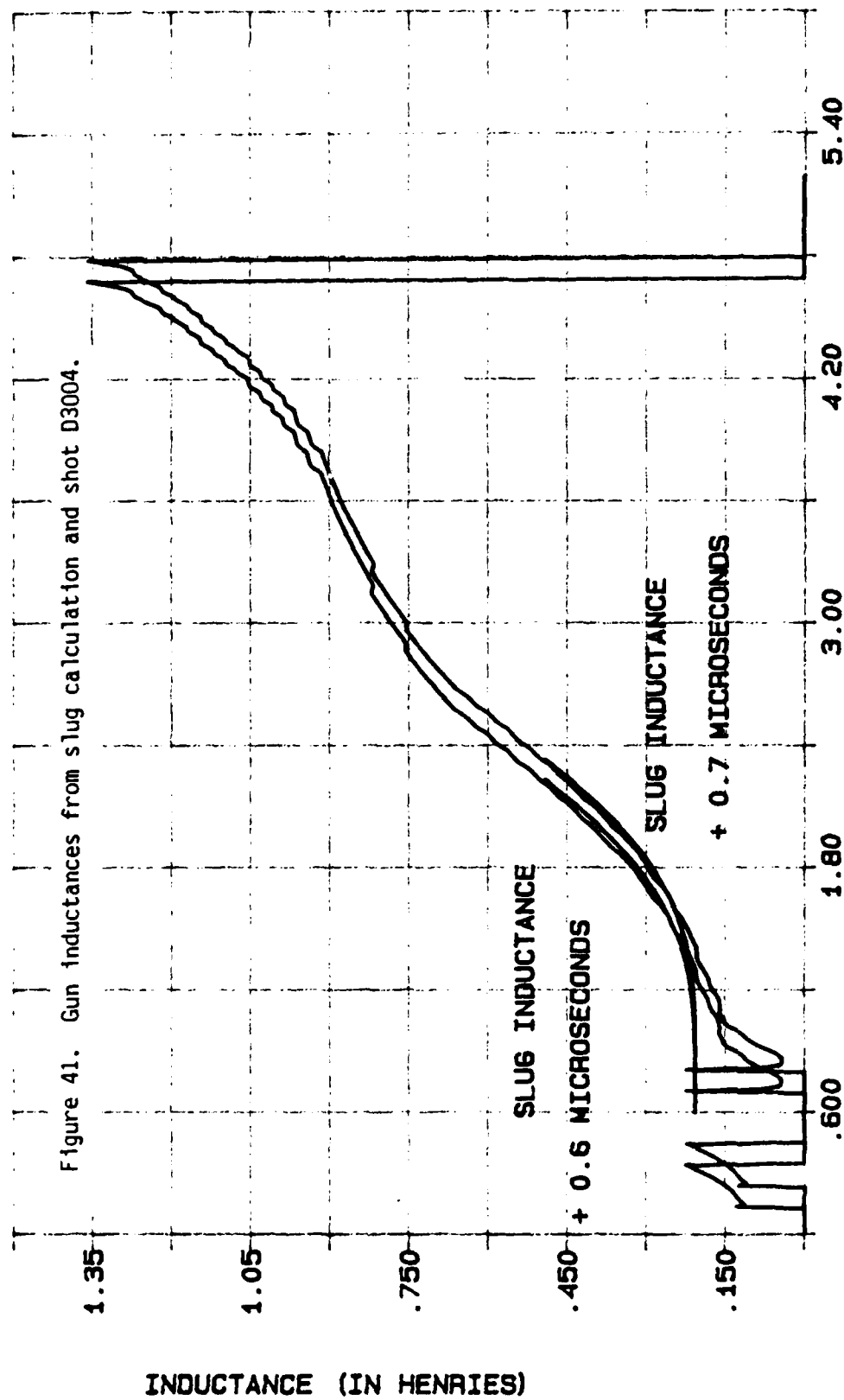
Bottom level normalized time increment $(4.09\pm0.80)\times10^{-7}$ s

Mid-bottom level normalized time increment $(5.07\pm0.72)\times10^{-7}$ s

Mid-top level normalized time increment $(6.22\pm1.44)\times10^{-7}$ s

Top level normalized time increment $(7.26\pm1.02)\times10^{-7}$ s

Errors on the normalized time increments result from using different fractional current limits and averaging different results.

With the normalized time increments and plasma sheath velocity, the plasma sheath thickness can be calculated. The time averaged sheath velocity is 2.81×10^{5} m/s. Position dependent plasma sheath velocities are obtained from the data displayed in Figures 25 and 26. The calculated slug bottom current (current at the bottom axial level) is 3.39×10^{5} m/s; calculated slug mid-bottom current is 5.24×10^{5} m/s; calculated slug mid-top current is 6.52×10^{5} m/s; and calculated slug top current is 7.49×10^{5} m/s. This produces the data shown in Table 11.

In analyzing the data in Table 11, the measured plasma sheath is thick, characteristic of a deflagration mode in the plasma gun. Using the time averaged velocity, the sheath thickness ranges from about 0.10 m at the bottom level to about 0.20 m at the top level. This is indicative of a sheath expansion as a function of position. Using the position dependent calculated slug velocities, the sheath thickness goes from about 0.14 m at the bottom level to 0.54 m at the top level. However,

173

since the effective length of the plasma gun is about 0.46 m, sheath thicknesses longer than this are suspect. The position dependent velocities also indicate a sheath expansion as it travels the plasma gun. This sheath expansion is consistent with the possibility of plasma components with different velocities in the sheath.

Table 11. D3004 Calculated Plasma Sheath Thickness

Level	Time Averaged Plasma Thickness (m)	Axial Level Plasma Thickness (m)
Bottom	$(1.15\pm0.22)\times10^{-1}$	$(1.39\pm0.27)\times10^{-1}$
Mid-bottom	$(1.42\pm0.20)\times10^{-1}$	$(2.66\pm0.38)\times10^{-1}$
Mid-top	$(1.75\pm0.41)\times10^{-1}$	$(4.06\pm0.94)\times10^{-1}$
Top	$(2.04\pm0.29)\times10^{-1}$	$(5.44\pm0.76)\times10^{-1}$

In summary, shot D3004 shows both snowplow and deflagration effects. It operates in what Len calls the transition region. The gross behavior of the plasma gun is modelled well by the 0-D slug model theory. The plasma sheath velocity scales as the simple $E \times B$ theory. The plasma sheath current is reduced as it transits the length of the coaxial

plasma gun. This reduction is probably due to charged-neutral particle interactions. The plasma sheath is thick indicating deflagration behavior.

4.5.2 Shot J1006

In shot J1006, the charge voltage is 60 kV. The stored electrical energy in the capacitor bank is 1.30×10^5 Joules. The peak current in the transmission line is 2.96 MA at 2.5 μs after current begins. Peak plasma gun current is 1.53 MA at 1.6 μs after current begins. The shot produces 351 counts in the first minute in the Ag detector; this is a total of 4.4×10^6 neutrons produced by the plasma pinch. One gas valve, the lower valve, is used. The gas valve is energized 1125 μs before the bank discharge. There are 14 active $\dot{B}$ probes.

Shot J1006 is somewhat anomalous in that it exhibits more snowplow behavior than other shots in the series. The driving current J1006IR separates early from the coaxial plasma gun system at about 1.0 μs after current begins. The D_2 gas regulator malfunctioned for this shot, giving a D_2 gas pressure of 925 psi (instead of 900 psi). Delivered mass to the system is increased to 33.8 mg (from 32.9 mg).

The J1006 current overlay is shown in Figure 42. The driving current greatly exceeds the gun current. After the transmission line current is decoupled from the plasma gun, it oscillates at a different frequency from the system with the coaxial plasma gun. The timing difference for start of current J1006IR and gun current J1006IC does not mean the

175

Figure 42. Shot J1006 current overlay.
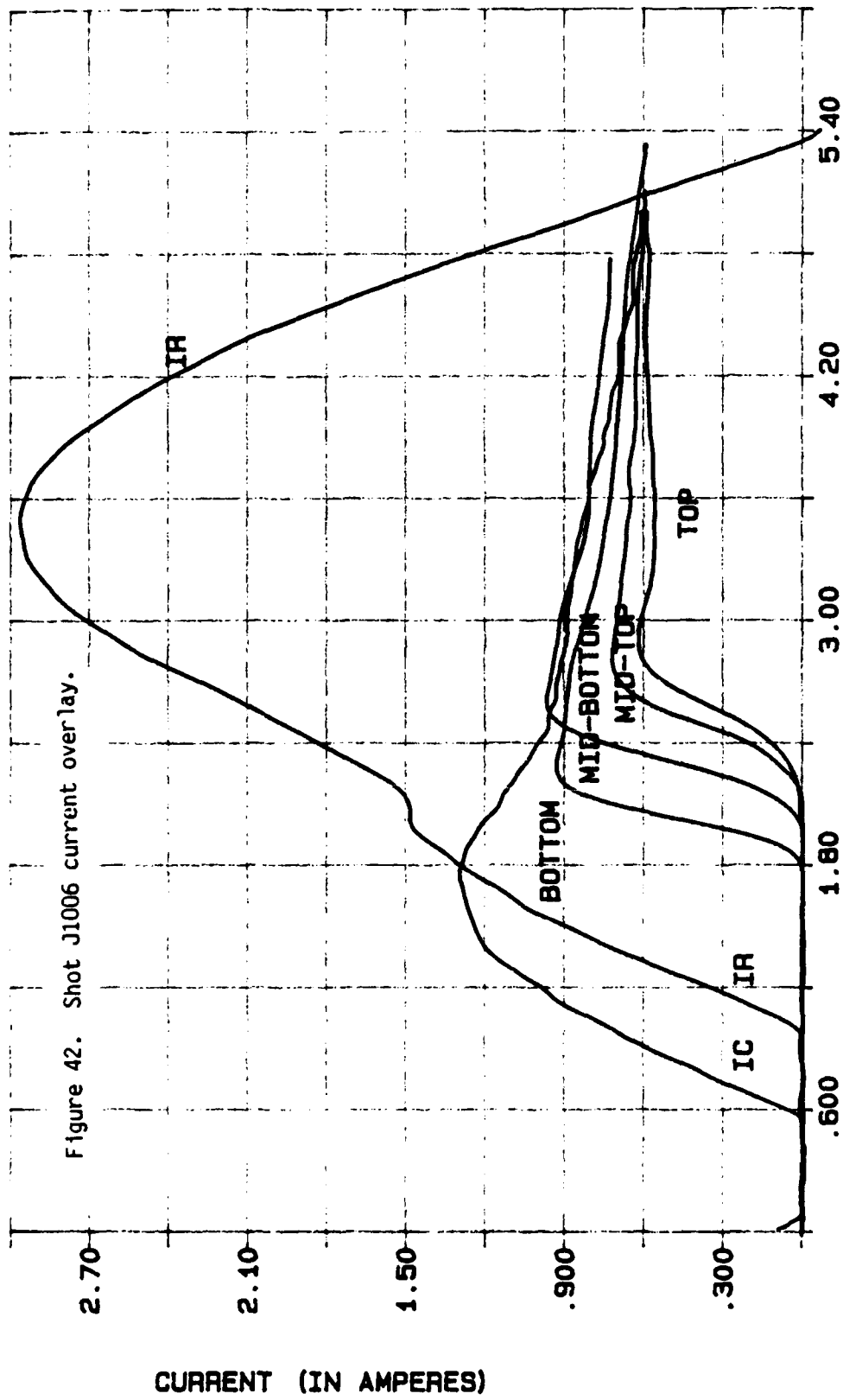
176

plasma gun current is generated <u>ex nihilo</u>, but the driving current oscilloscope trigger is off 0.4 µs on this shot. This triggering problem characterizes the problems we faced without a reliable timing fiducial. This timing problem is extreme. Typical timing errors are smaller (on the order of 0.1 µs).

Due to triggering problems, timing is a real concern. Plasma sheath velocity estimates can still be made, however. Using a 0.4 MA current as a reference, the $\dot{B}$ probes axial currents equal the current reference at the given times:

Bottom level average	2.003 µs
Bottom level correlated average	2.004 µs
Mid-bottom level average	2.268 µs
Mid-bottom level correlated average	2.273 µs
Mid-top level average	2.496 µs
Mid-top level correlated average	2.495 µs
Top level average	2.600 µs
Top level correlated average	2.613 µs

Differences between the uncorrelated and the correlated times estimate timing errors at each level.

Using the difference between each level of 4" (0.1016 m), the plasma
sheath velocity is estimated.

Velocity between the bottom and mid-bottom levels 3.8×10^5 m/s

Velocity between the mid-bottom and mid-top levels 4.5×10^5 m/s

Velocity between the mid-top and top levels 9.2×10^5 m/s

As with shot SD3004, the velocity profile is similar to the 0-D slug
model. Of the four sheath velocity models presented, only the single
particle model yields velocities of the right order of magnitude.

Azimuthal variation of the plasma sheath at different axial levels is
seen in Figures 43 to 46.

In Figure 43, at the bottom level, the traces are simultaneous within
±0.1 μs. There seems to be some sheath tilting so current is not flat
as a function of azimuth. The variations could be due to calibration
errors, but the consistency suggests an azimuthal sheath tilting. This
tilting of the plasma sheath is the variation of the arrival time as a
function of the azimuthal position. Since different $\dot{B}$ probes at each
level are at different azimuths, tilting can be distinguished if it is
larger than 0.25" (6.3×10^{-3} m, the diameter of the $\dot{B}$ probes).

Figure 43. Shot J1006 bottom current.

E-6

179
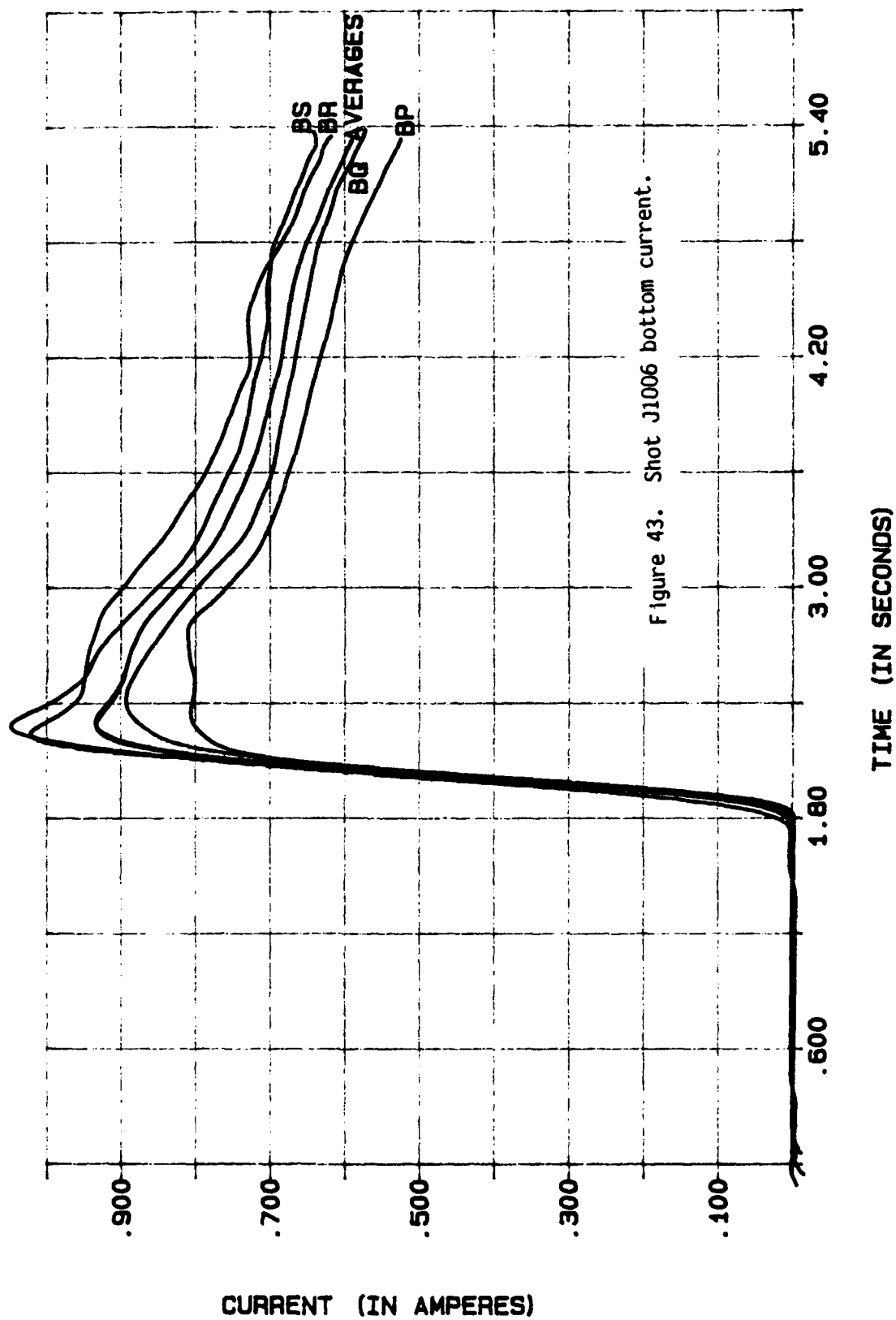
In Figure 44, the mid-bottom current is shown. There is a strong plasma sheath azimuthal variation. Total current errors are larger than the calibration errors. Lack of plasma sheath arrival simultaneity indicates timing variations larger than ±0.1 μs. At the mid-bottom level, the plasma sheath is tilted and indicates some spoking.

In Figure 45, the mid-top current is displayed. Since only two $\dot{B}$ probes are used, any information about timing or current behavior is limited.

In Figure 46, the top current is displayed. Plasma sheath tilting appears to have been continued from the mid-bottom level. Timing variations are greater than ±0.1 μs. Current distribution is spread over a range greater than what the calibration errors alone can account.

In Figure 47, gun current J1006IC is displayed with the calculated slug current. The gun current does not match the calculated plasma sheath current from the slug model, but the current rise does match the slug current reasonably well. The loss of the current driver explains the loss of the gun current, so it would not be expected to match the slug model current. The experimental current peaks at the same relative time of the slug model, about 1.1 μs after the current begins.

In Figure 48, the experimental voltage is displayed with the calculated probe voltage. The agreement is very good. As noted before, the probe measures only the voltage at the voltage monitor prior to the coaxial plasma gun.
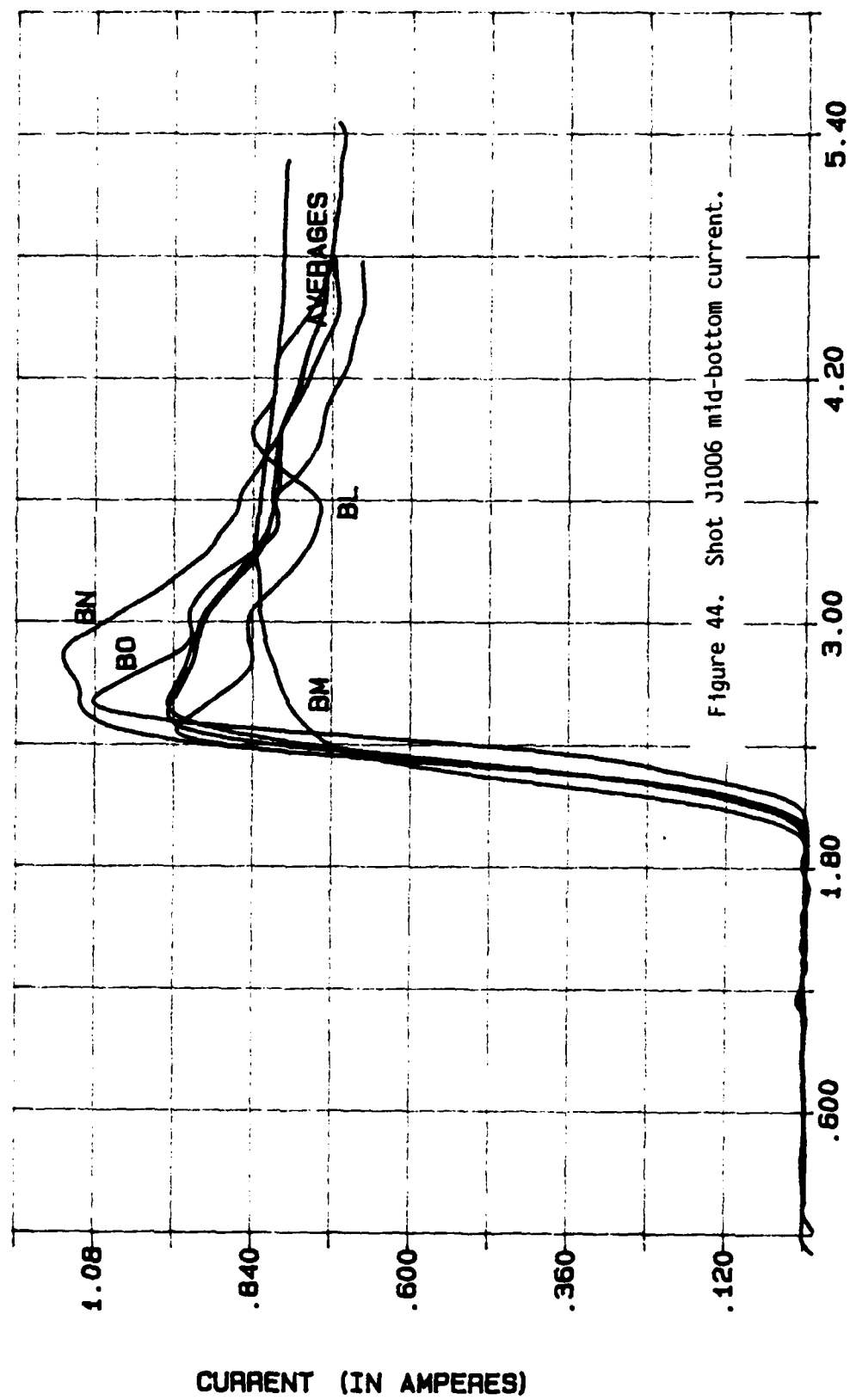
Figure 44. Shot J1006 mid-bottom current.

E-6

TIME (IN SECONDS)

CURRENT (IN AMPERES)

E 6

181

Figure 45. Shot J1006 mid-top current.

CURRENT (IN AMPERES)

TIME (IN SECONDS)

E-6

E 5

182

Figure 46. Shot J1006 top current.

183
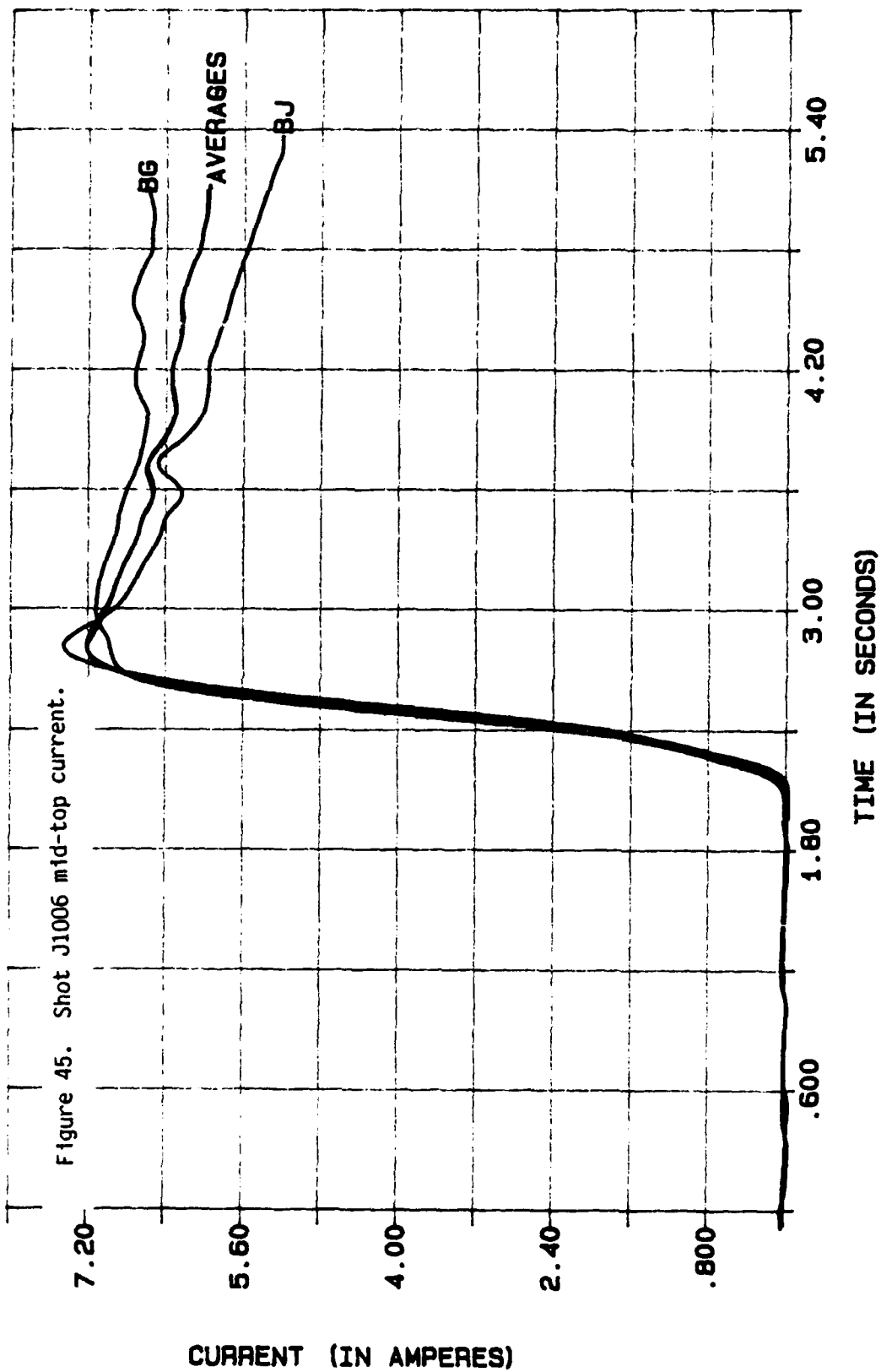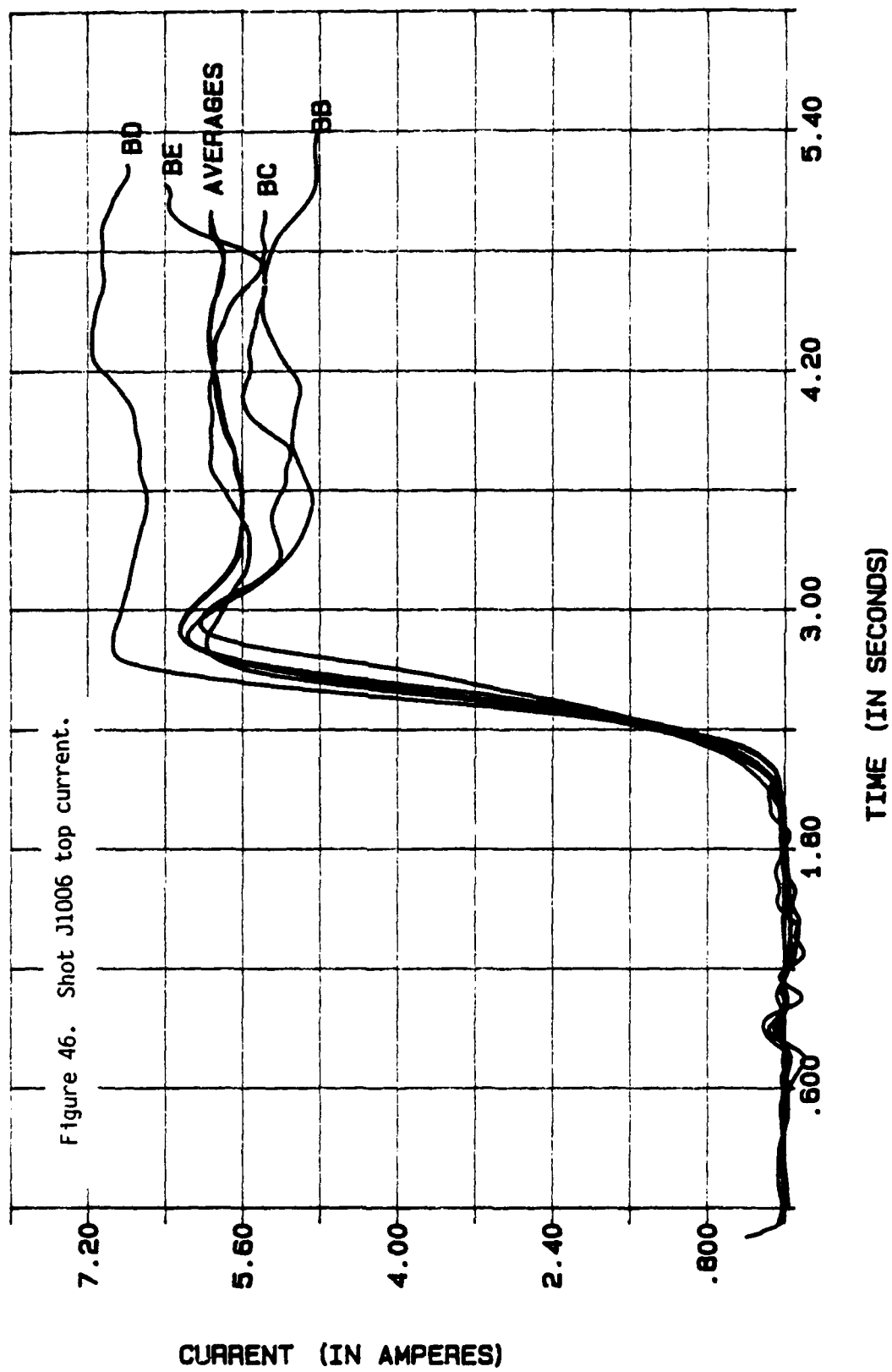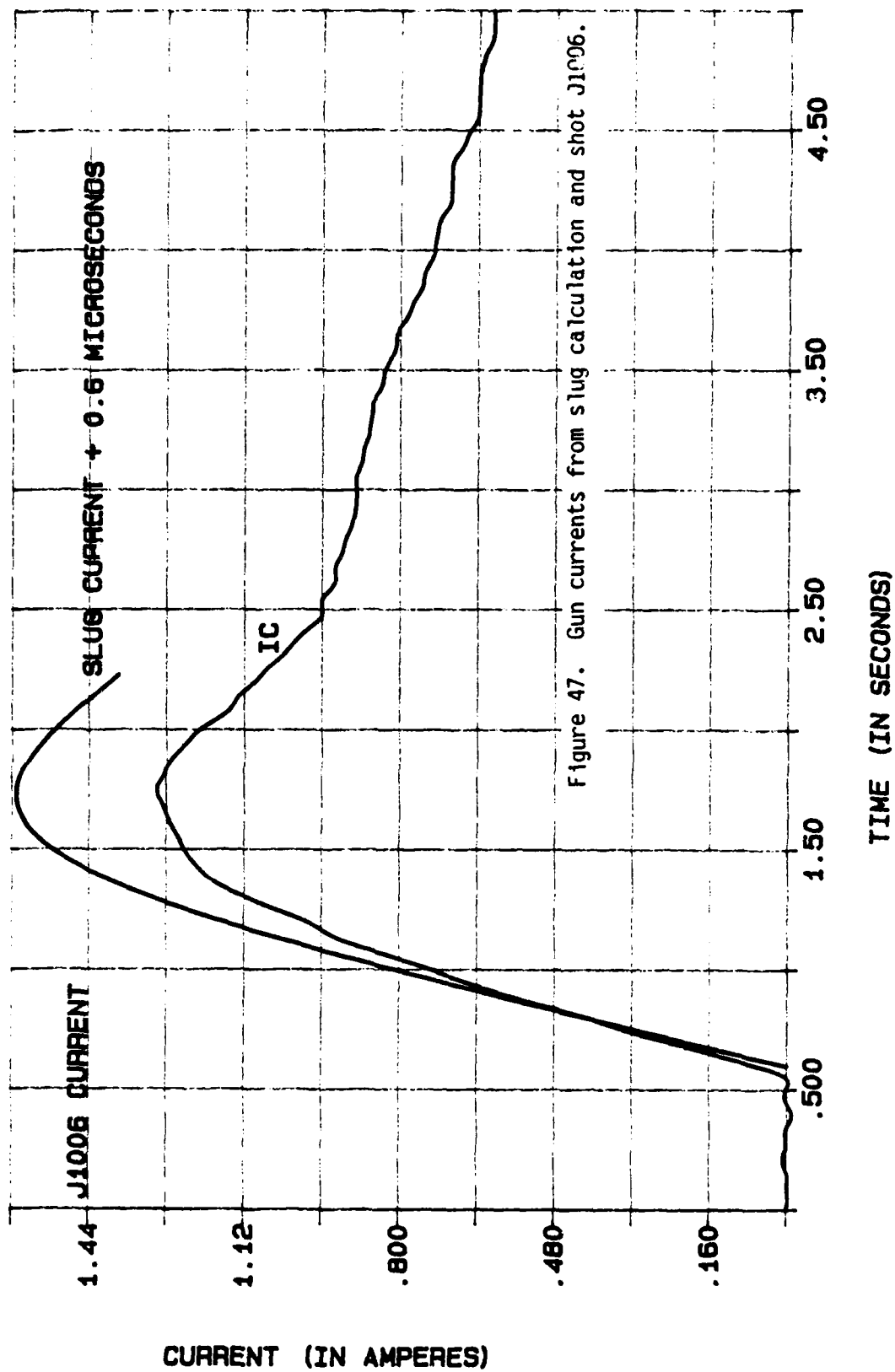
Figure 47. Gun currents from slug calculation and shot J1006.

E-6

Figure 48. Probe voltages from slug calculation and shot J1006.

185
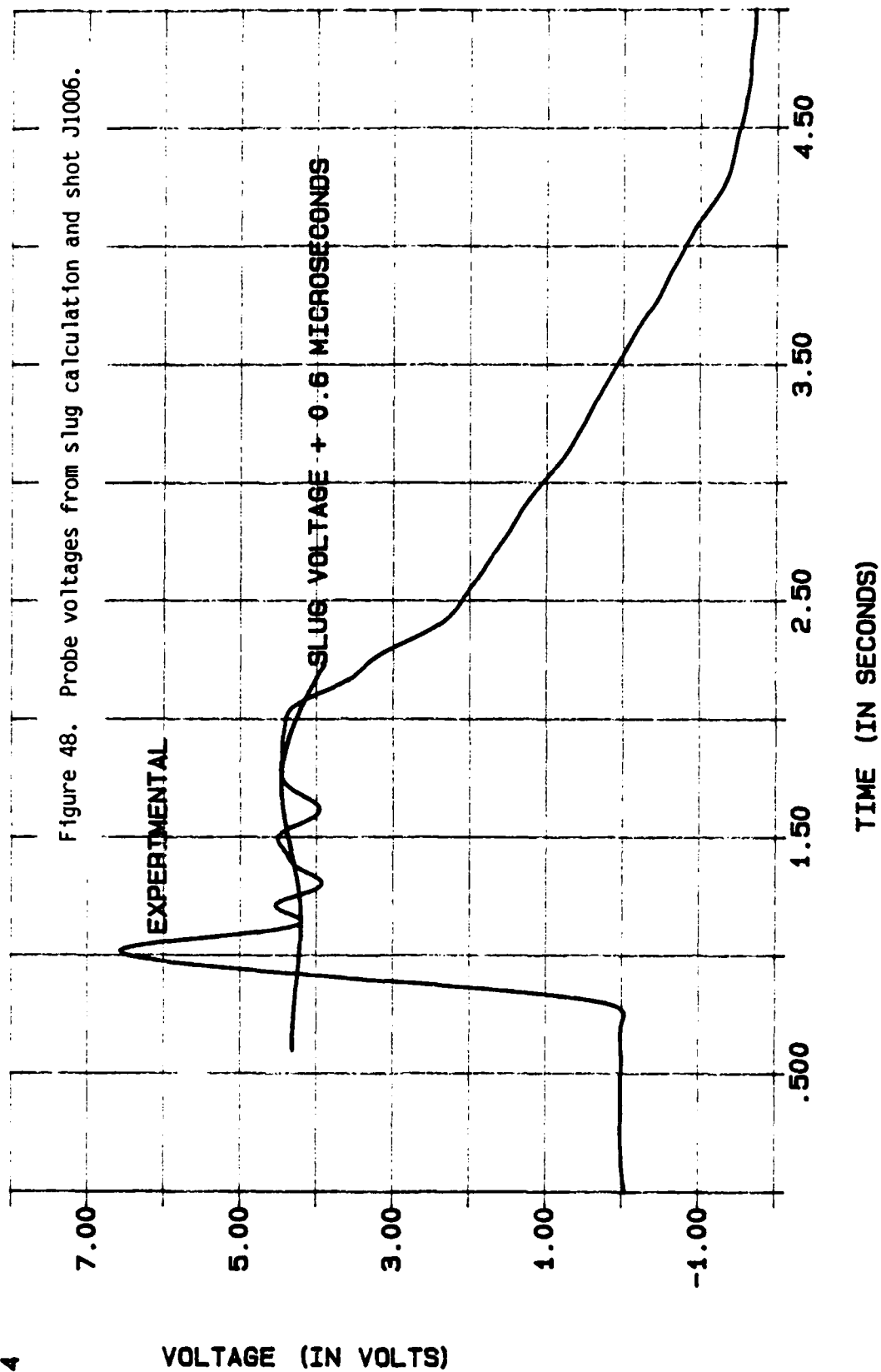
In Figure 49, the positional current derivative $\frac{\Delta I}{\Delta z}$ is displayed. There is a strong snowplow component at about 2.2 μs between the bottom and mid-bottom level, at about 2.4 μs between the mid-bottom and mid-top level and about 2.6 μs between the mid-top and top level. The behavior of the plasma sheath from the bottom level to the mid-top level appears to be snowplow-dominated. From the mid-top level onward, the deflagration mode appears to become more dominant. This shot, too, appears to operate in the transition mode.

In Figure 50, the electrical power delivered past the voltage probe positions is displayed. Timing differences can be seen in this Figure. The peak electrical power flowing past the voltage probe position is about 55 GW occurring at about 2.0 μs.

In Figure 51, the time integral of electrical power is displayed. Peak energy flowing past the voltage probe position is about 70 to 80 kJ. Since the system current decoupled from the plasma gun early, the energy loss is not unexpected.

In Figure 52, calculated inductances (seen at the voltage probe position) are displayed. Overlaid on these inductance traces are slug model inductance predictions. Agreement between the predicted and experimental inductances is good. The difference between uncorrelated and correlated inductances is only in timing, not in magnitude.

186

Figure 49. Shot J1006 $\frac{\Delta I}{\Delta z}$.

187

Figure 50. Shot J1006 electrical power at voltage probe.

188
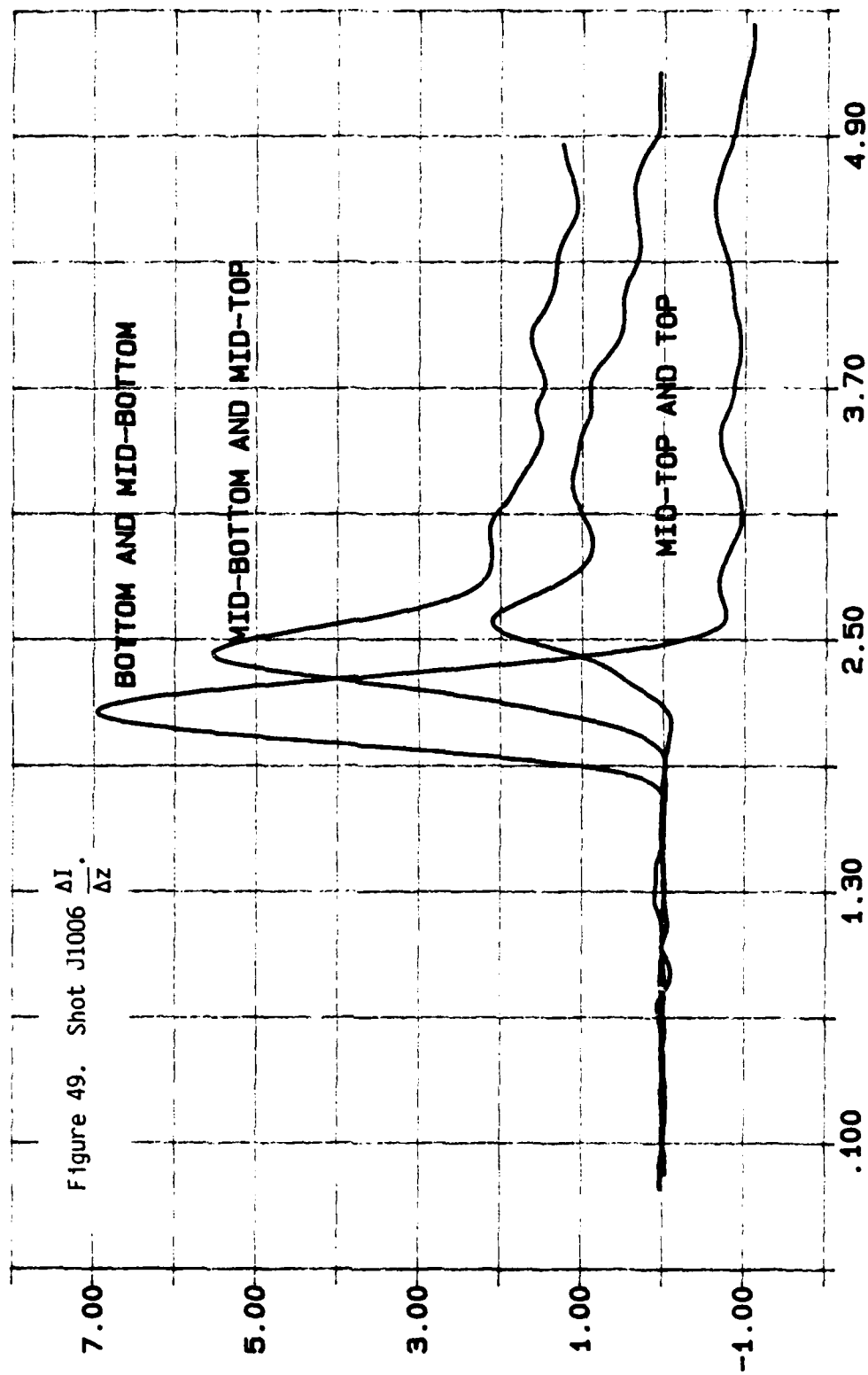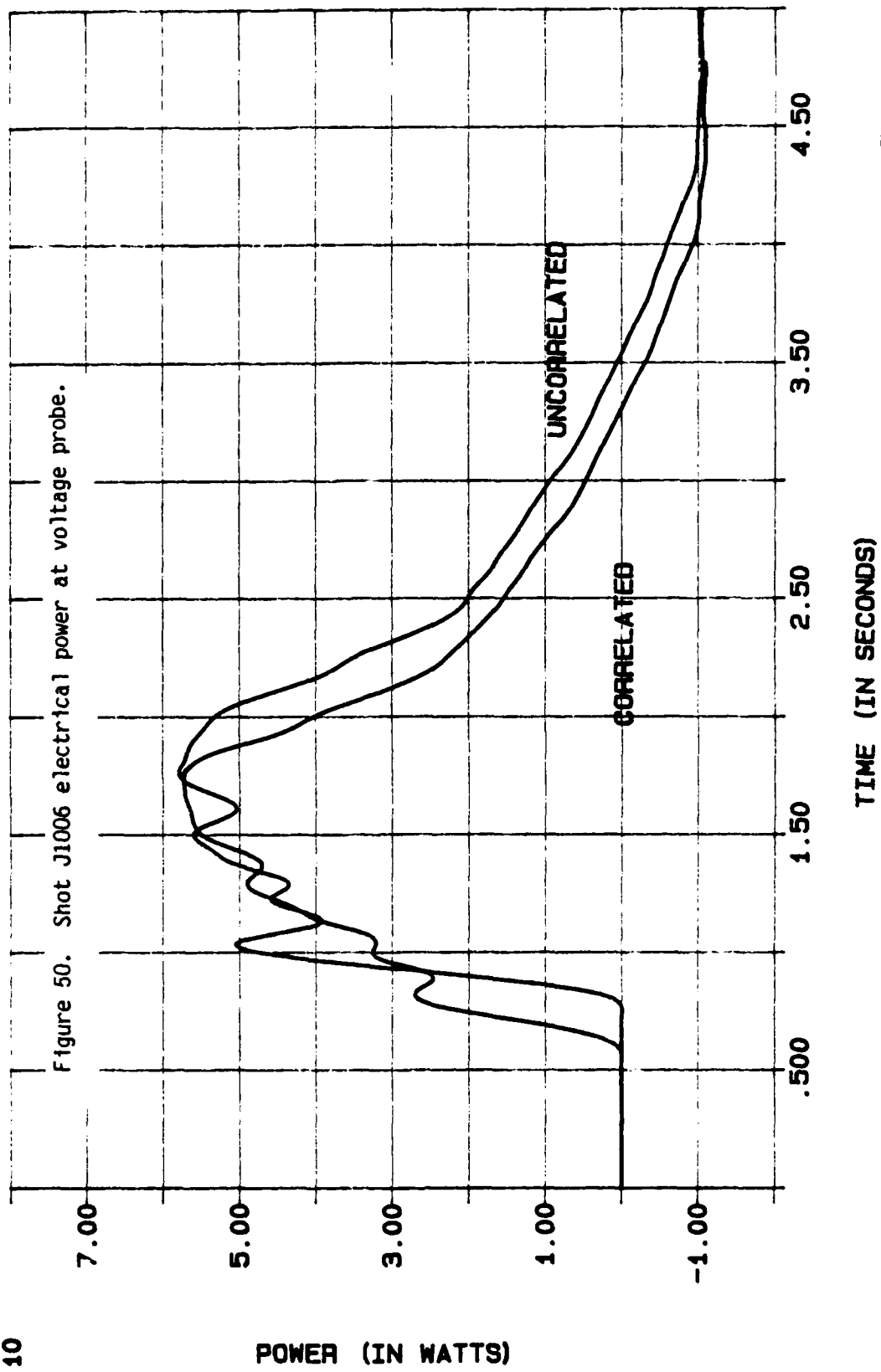
Figure 51. Shot J1006 electrical energy at voltage probe.

189

Figure 52. Gun inductances from slug calculation and shot J1006.

INDUCTANCE (IN HENRIES)

TIME (IN SECONDS)

E-7

E-6

190
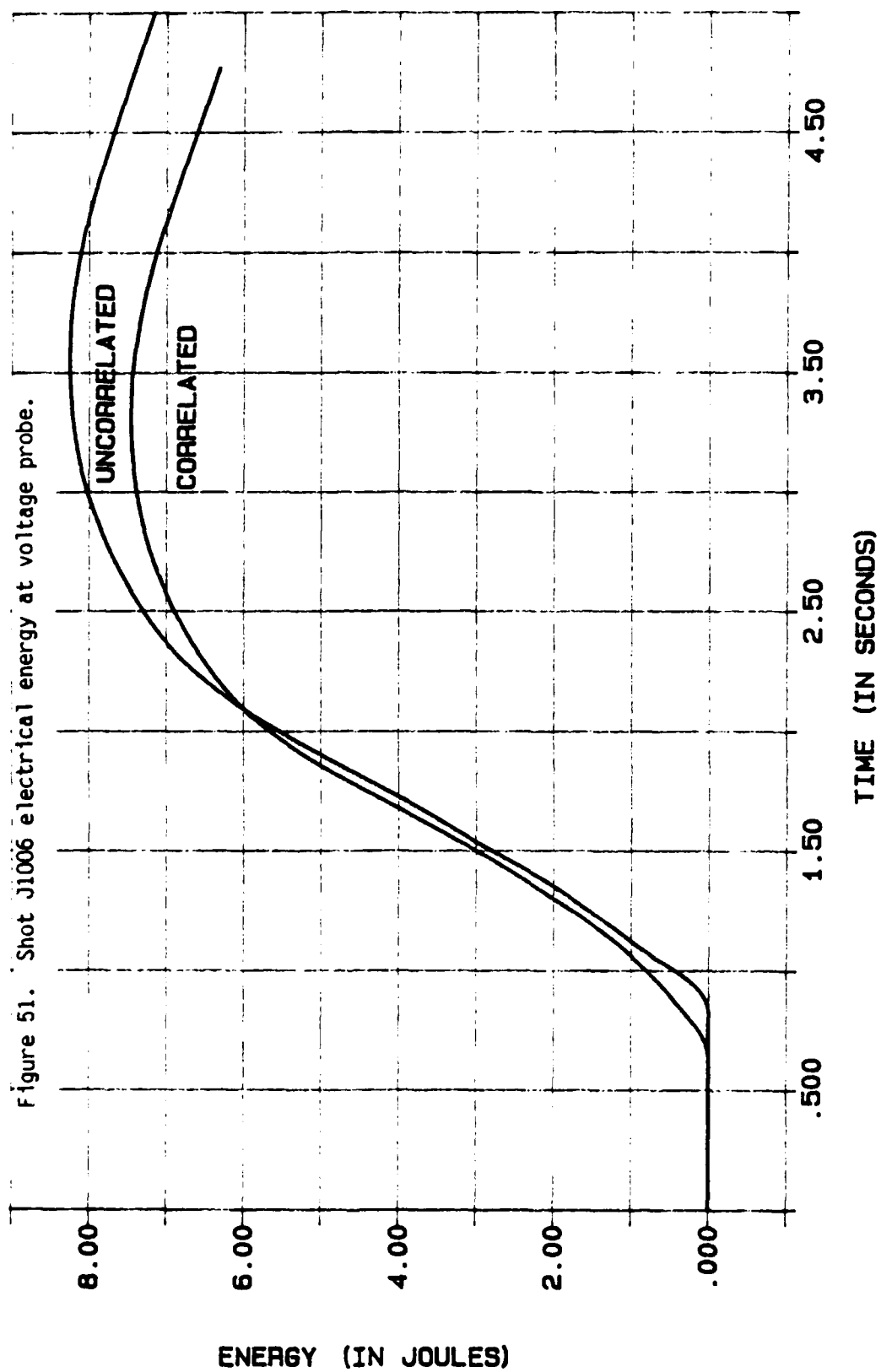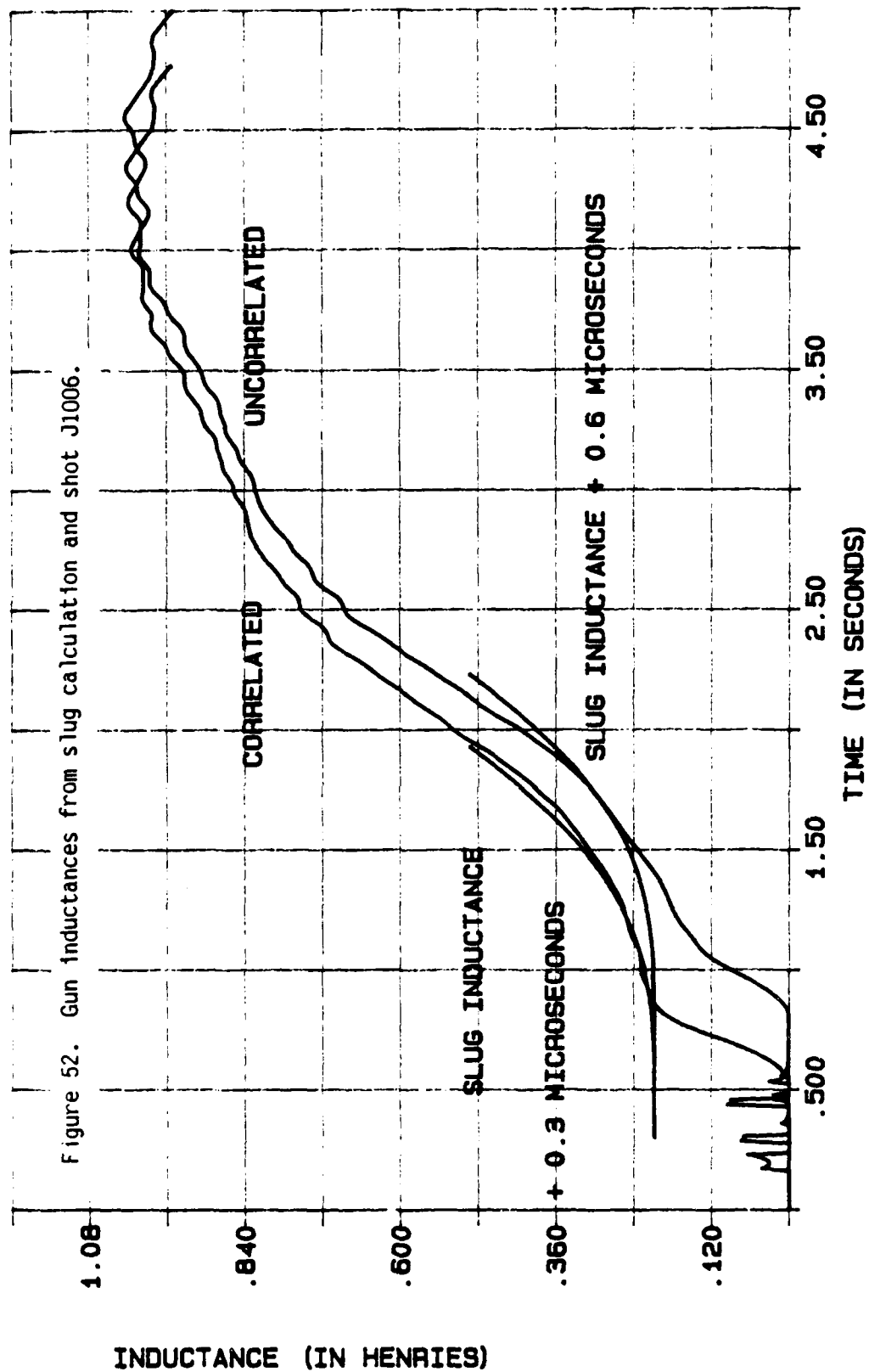
J1004 plasma sheath velocities are estimated in the same way as previously. Using the plasma sheath velocities cited in Section 4.5.1, the data in Table 12 is prepared.

Examining the Table 12 data, it can be seen the plasma sheath is thick. If the time averaged sheath velocity is used, the plasma sheath varies from about 0.12 m at the bottom level to 0.18 m at the top. This indicates plasma sheath expansion (but not as much as in shot D3004). If the position dependent sheath velocities are used, estimates for sheath velocities range from 0.15 m at the bottom to 0.49 m at the top level. Any sheath thickness longer than the length of the plasma gun (0.46 m) is probably spurious. Again, this sheath expansion is consistent with the possibility of multivelocity sheath components.

Table 12. J1004 Calculated Plasma Sheath Thickness

Level	Time Averaged Plasma Thickness (m)	Axial Level Plasma Thickness (m)
Bottom	$(1.21\pm0.25)\times10^{-1}$	$(1.46\pm0.30)\times10^{-1}$
Mid-bottom	$(1.51\pm0.30)\times10^{-1}$	$(2.83\pm0.55)\times10^{-1}$
Mid-top	$(1.68\pm0.42)\times10^{-1}$	$(3.90\pm0.98)\times10^{-1}$
Top	$(1.83\pm0.44)\times10^{-1}$	$(4.88\pm1.18)\times10^{-1}$

In summary, shot J1006 shows both snowplow and deflagration behavior. It, like shot D3004, appears to operate in the transition mode. The gross plasma behavior in the coaxial system is relatively well described by the 0-D slug model. The single particle $E \times B$ theory appears to best predict the sheath velocity; it is an order of magnitude better in predicting the sheath velocity than the other three reviewed theories. Estimates of the plasma sheath thickness show it is not thin, but it is on the order of 0.10 m thick.

4.5.3 Shot J1104

In shot J1104, the charge voltage is 60 kV. The stored electrical energy in the capacitor bank is 1.30×10^5 Joules. The peak current in the transmission line is 1.77 MA at 1.4 µs after current begins to rise. The peak plasma current is 1.70 MA at 1.5 µs after current rise. The shot produced 2094 Ag silver detector counts in the first minute; this corresponds to a total of 1.1×10^8 neutrons. Two gas valves are used in this shot. The lower gas valve is energized 1150 µs before the PUFF capacitor bank fires. The upper gas valve is energized 3750 µs before the capacitor bank fires. There are 14 active $\overset{\circ}{B}$ probes.

Figure 53 shows the J1104 current overlay. The driving current J1104IR and the plasma gun current J1104IC track well, except for the error in timing caused by triggering problems. Of the shots chosen for detailed analysis, this shot shows the best current transfer from the capacitor bank to the plasma gun.

192

Figure 53. Shot J11O4 current overlay.

E-6

E 6

193
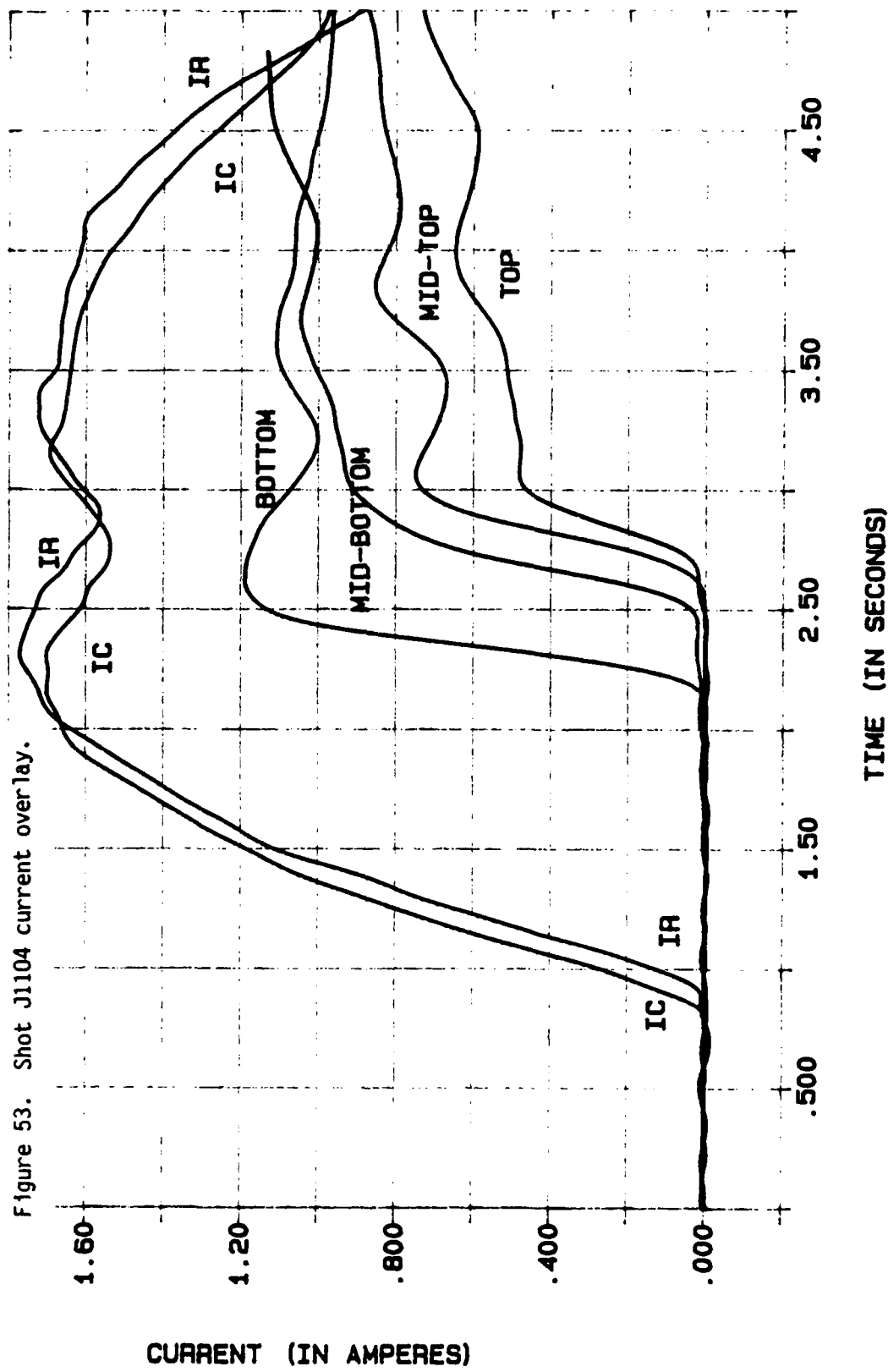
Using a reference current of 0.4 MA, the times for the plasma sheath to reach the reference are given.

Bottom level average	2.309 μs
Bottom level correlated average	2.308 μs
Mid-bottom level average	2.666 μs
Mid-bottom level correlated average	2.662 μs
Mid-top level average	2.821 μs
Mid-top level correlated average	2.821 μs
Top level average	2.940 μs
Top level correlated average	2.938 μs

Using the axial distance between each position of 4" (0.1016 m), the velocity of the plasma sheath is estimated.

Velocity between the bottom and mid-bottom levels	2.9×10^5 m/s
Velocity between the mid-bottom and mid-top levels	6.5×10^5 m/s
Velocity between the mid-top and top levels	8.6×10^5 m/s

The velocity profile is similar to the profile predicted by the slug model. Only the single particle drift theory predicts a sheath velocity of the right order of magnitude.

The azimuthal current variation is seen in Figures 54 to 57. These figures show the variation as a function of axial position.

The bottom currents are seen in Figure 54. The timing variation varies over a range of ±0.1 µs. After the plasma sheath crosses the bottom level of the $\dot{B}$ probes, the four azimuthal probes track well.

The mid-bottom currents are displayed in Figure 55. Except for $\dot{B}$ probe M (trace J1104BM) which shows an uncharacteristic signal superimposed, timing agreement is within 0.1 µs. Current variations are greater than the calibration errors. It is possible the sheath is somewhat tilted at this level. Late in the experimental series, the $\dot{B}$ probe M showed a voltage proportional to the driving current.

The mid-top currents are shown in Figure 56. With only two $\dot{B}$ probes, extracted information is limited.

The top currents are shown in Figure 57. The timing for the plasma sheath arrival is simultaneous within 0.1 µs. The different probes indicate a canted or tilted plasma sheath. A current depression occurs at about 4.5 µs.

The gun current J1104IC is shown in Figure 58. Calculated current tracks well with experimental current. The experimental current peaks some 0.2 µs later than slug model predictions. This could be caused by a sheath of finite thickness. Gun current is depressed at about 2.8 µs. This is due to the inductive rise of the plasma pinch at the gun muzzle.

Figure 54. Shot J1104 bottom current.

E 6

Figure 55. Shot J1104 mid-bottom current.

CURRENT (IN AMPERES)

TIME (IN SECONDS)

E-6

E 6

197

Figure 56. Shot J1104 mid-top current.

AVERAGES

BJ

B6

CURRENT (IN AMPERES)

E 5

8.00

6.00

4.00

2.00

.000

.500 1.50 2.50 3.50 4.50

TIME (IN SECONDS)

E-6

Figure 57. Shot J1104 top current.

199

Figure 58. Gun currents from slug calculation and shot J1104.

200
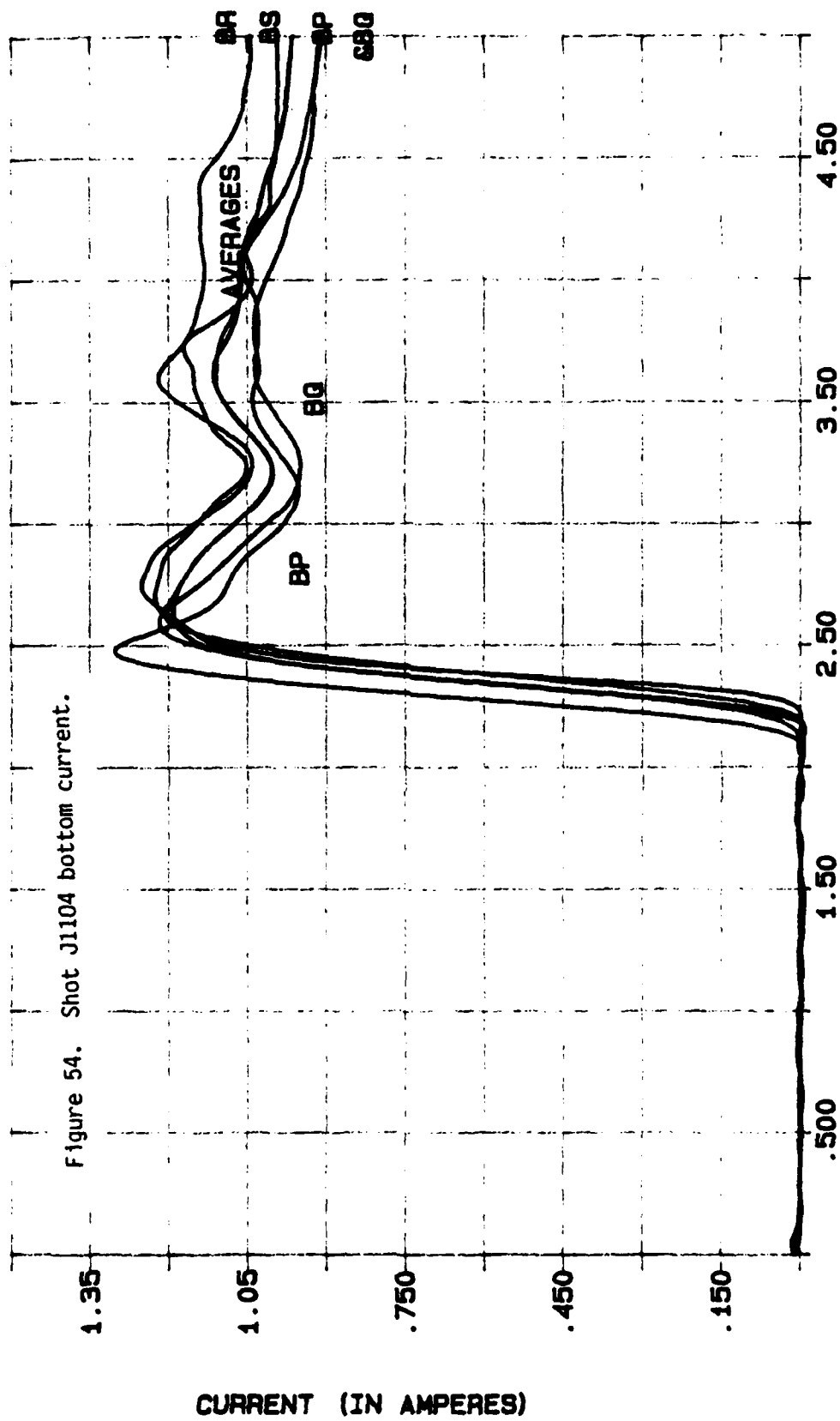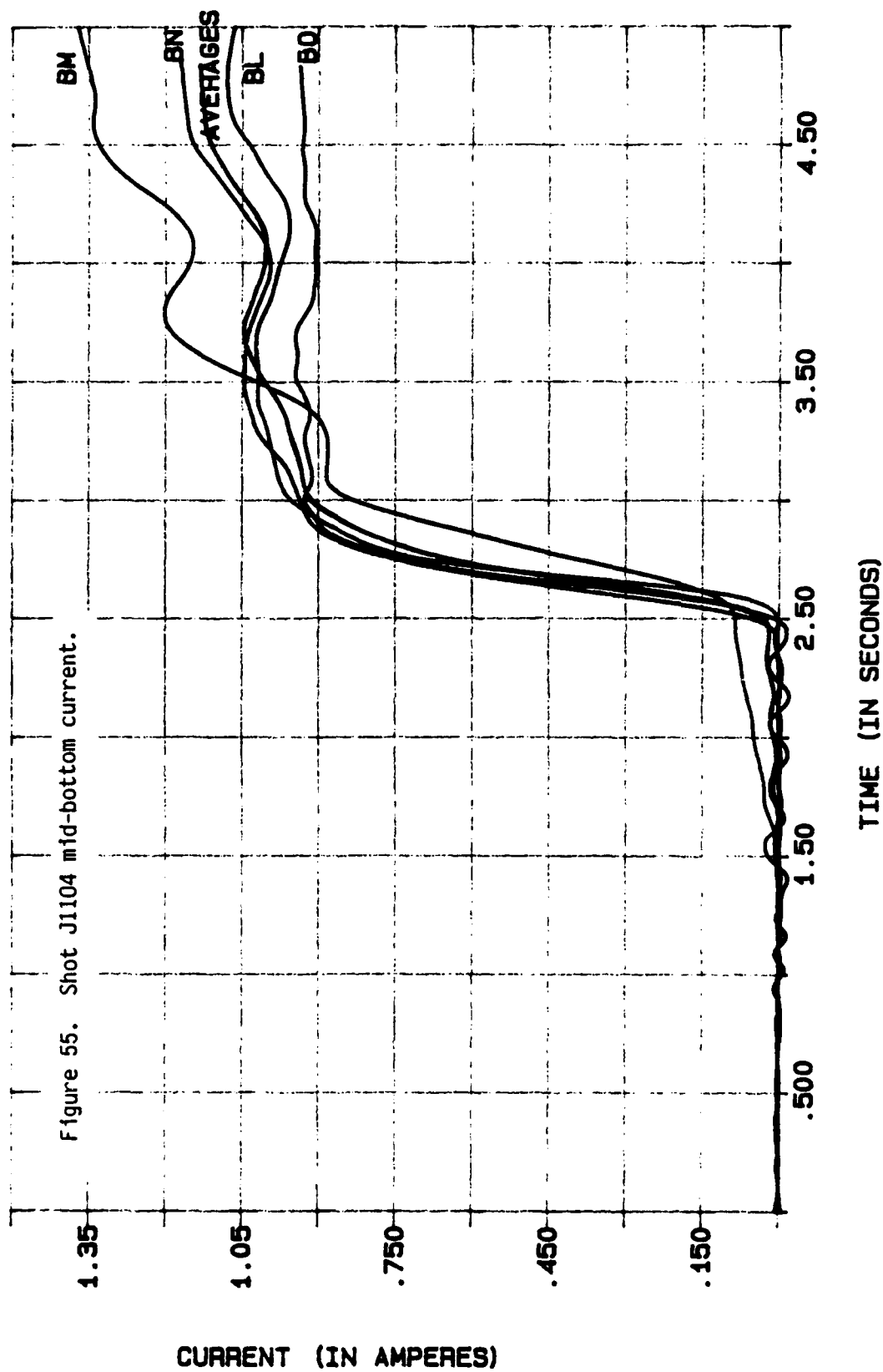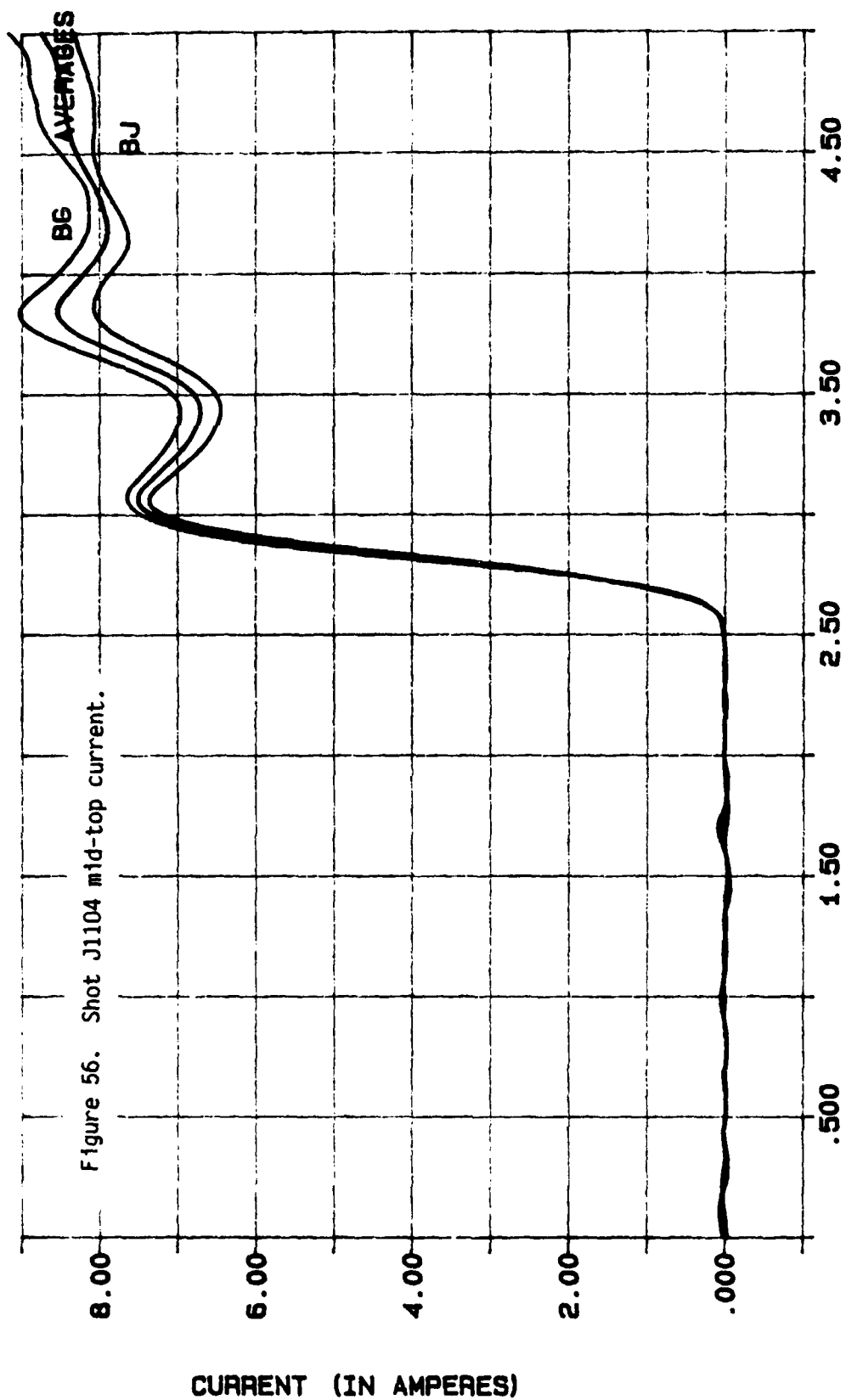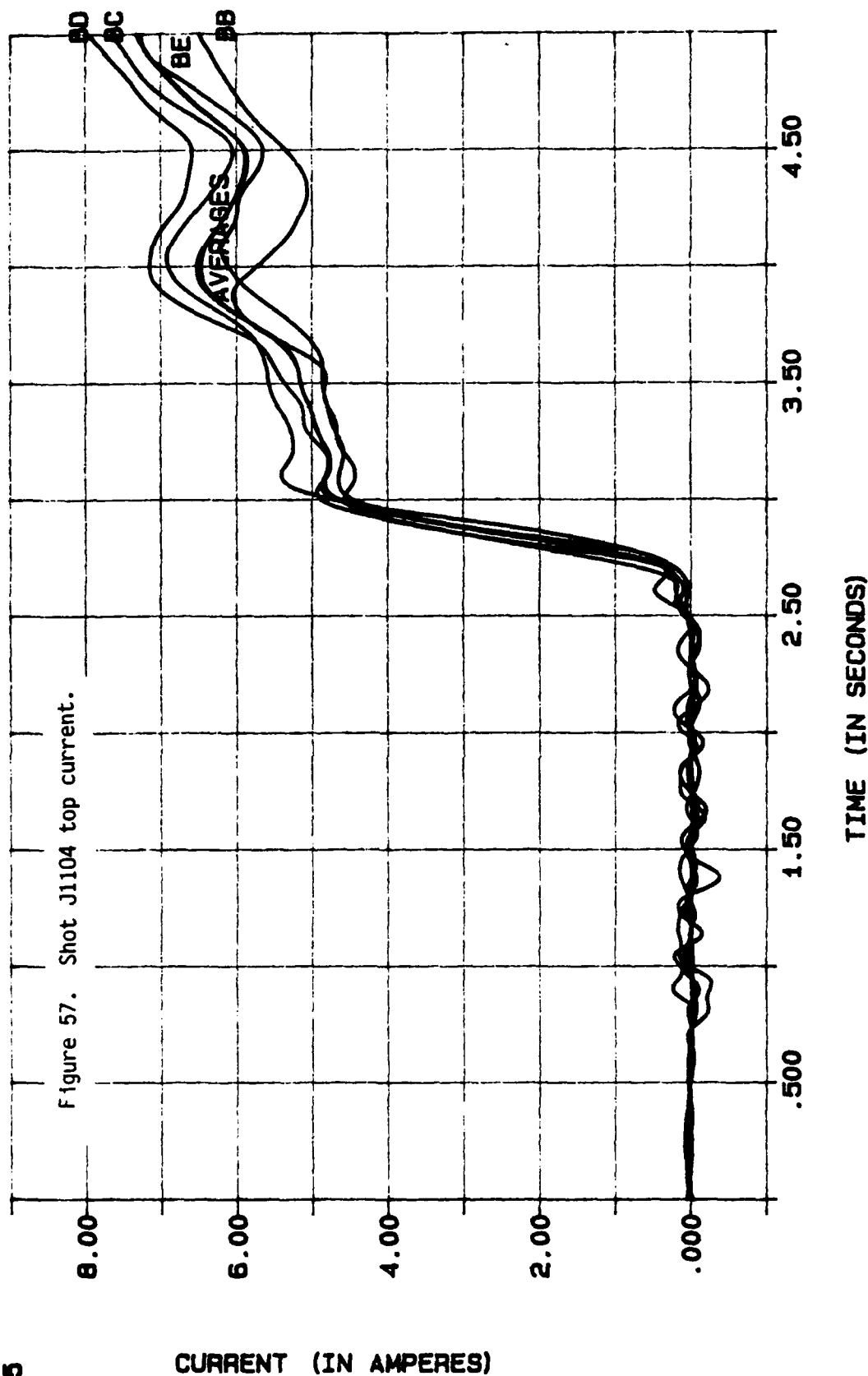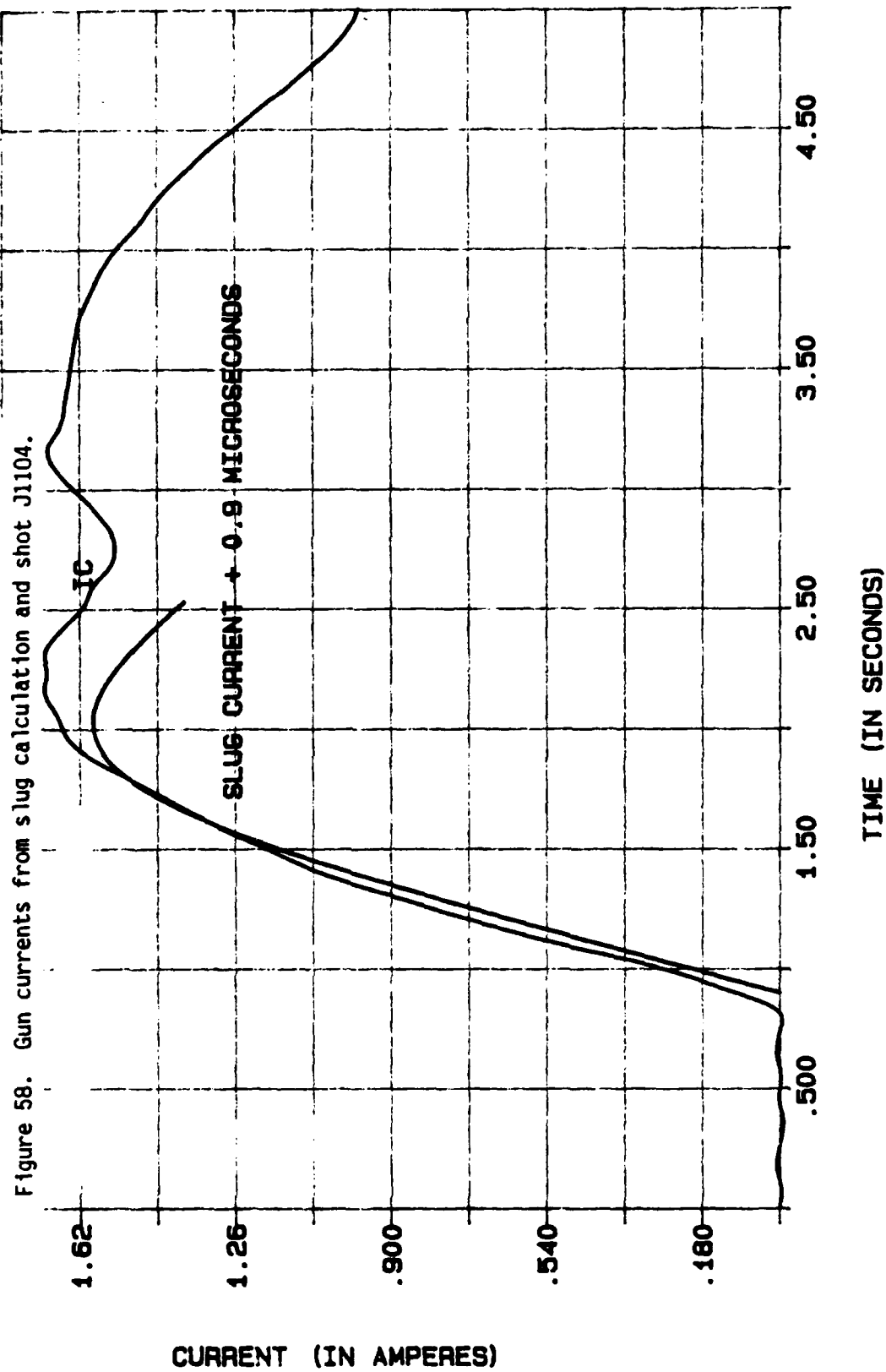
Increased plasma gun current is due to a decreased transmission line inductance. This inductance is proportional to the distance between the plates. A slight change in the transmission line inductance can explain why the experimental and predicted voltage are not in better agreement.

Shot J1104 probe voltages (both experimental and calculated) are shown in Figure 59. It has been noted the voltage probes are not absolutely calibrated. Current calibrations are relatively reliable. More than 1.3×10^5 Joules (the energy stored in the capacitor bank) are calculated. The voltage is recalibrated so no more than 130 kJ reaches the voltage monitor position. This may also be a cause for the voltage discrepancy. The agreement of the voltage shapes is good (if high frequency components on the experimental voltage are ignored). The probe voltage shows a depression at about 3 μs. This could be the effect of the plasma focus at the gun muzzle communicated to voltage probe position. The voltage must be communicated through tens of nanohenries from the gun muzzle to the position of the voltage probes.

In Figure 60, the positional derivative $\frac{\Delta I}{\Delta z}$ is displayed. A sharp snowplow behavior is only shown for the bottom to mid-bottom region peaking at a time of 2.3 μs. A weak snowplow is seen between the mid-bottom and mid-top region at 2.6 μs, but it shows behavior more characteristic of the deflagration mode. The region from the mid-top to top region shows deflagration characteristics.
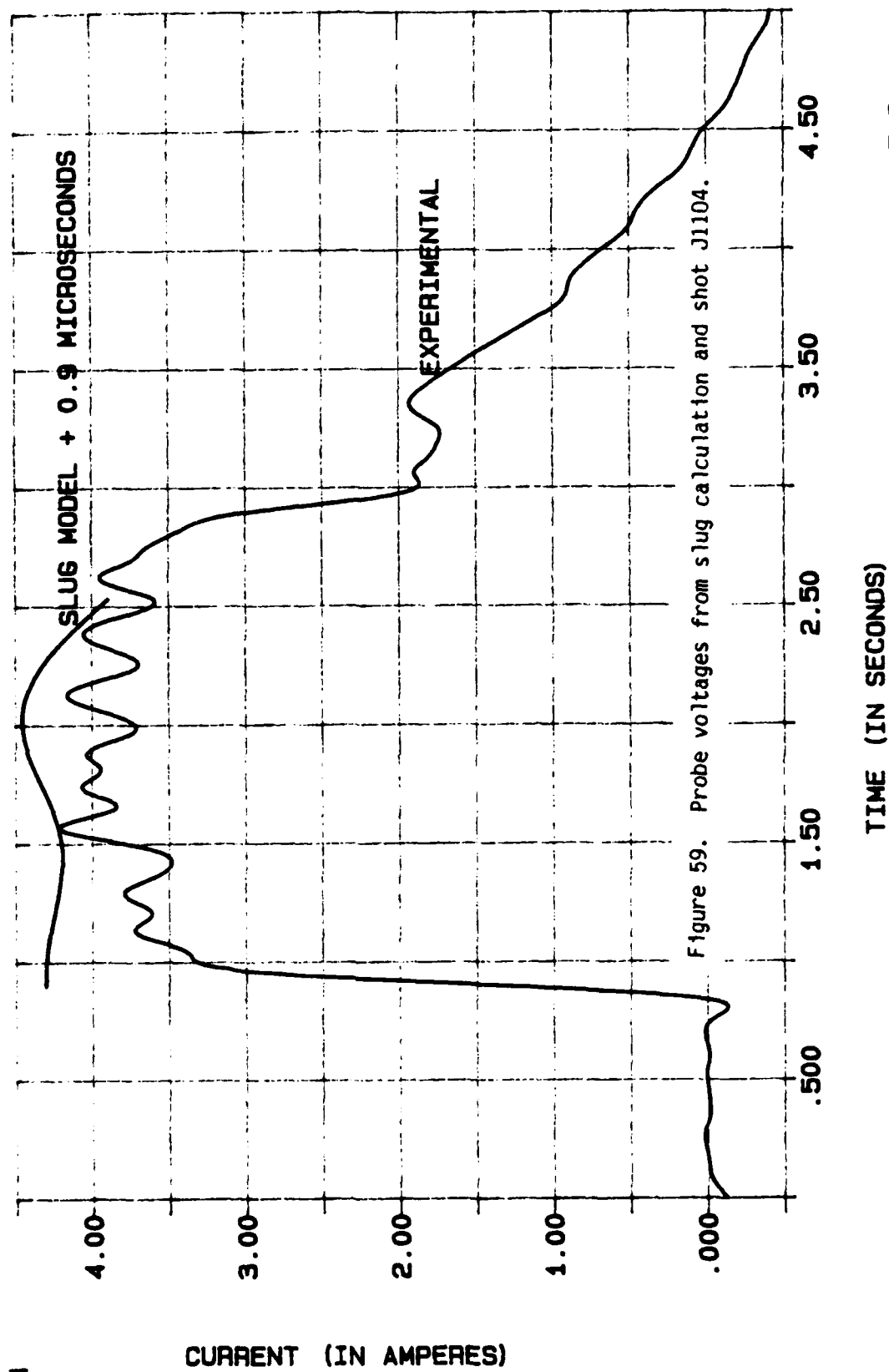
Figure 59.   Probe voltages from slug calculation and shot J1104.

202

Figure 60. Shot J1104 $\frac{\Delta I}{\Delta z}$.

203
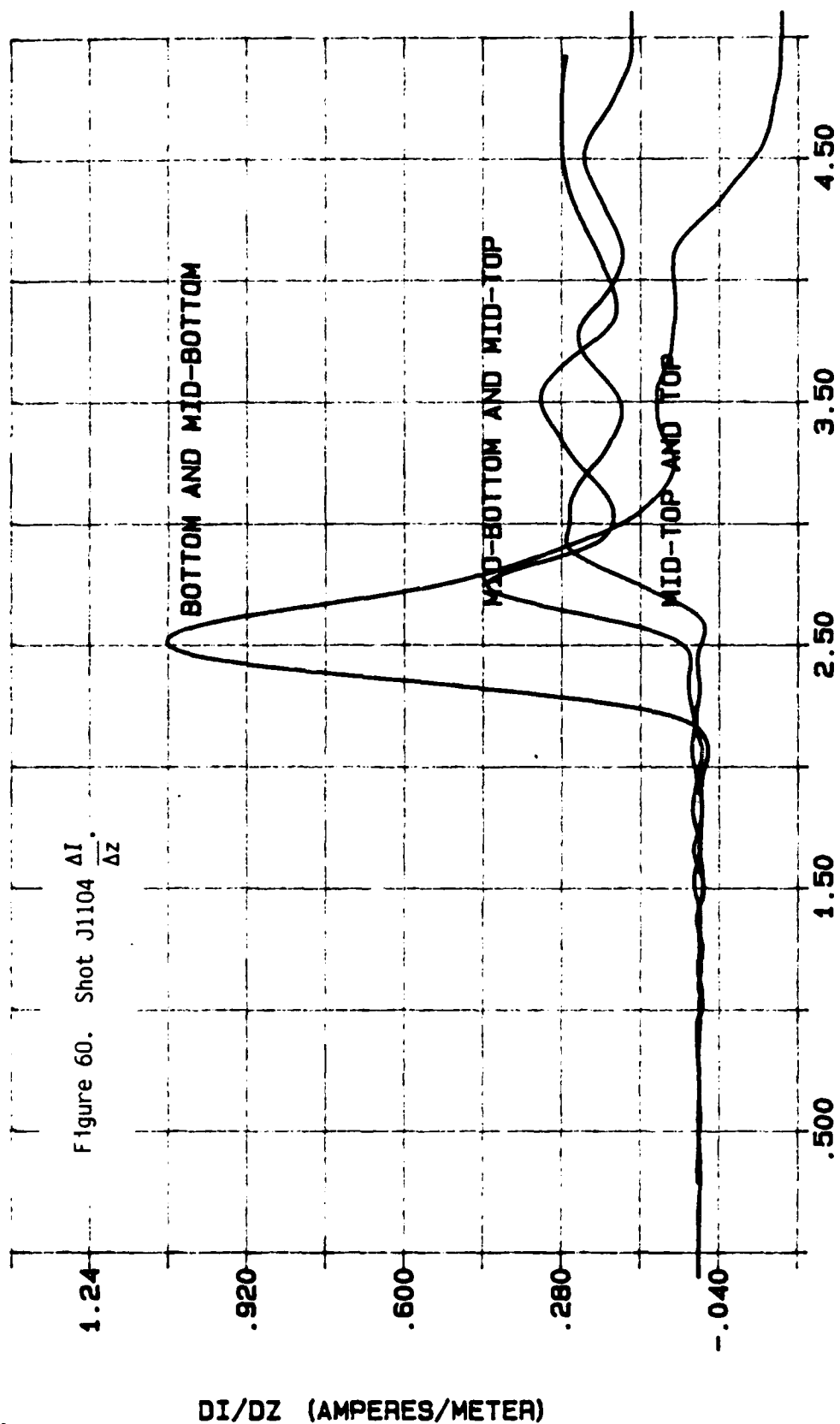
In Figure 61, electrical power is displayed. The uncorrelated and correlated powers are in good agreement, both in timing and in magnitude. They both show a peak power of about 70 GW at 2.1 μs. They also show a depression of the power at approximately 3 μs. The electrical power in Figure 61 represents the adjusted probe voltage.

In Figure 62, the electrical energy delivered past the voltage monitor position is shown. The peak energy has been adjusted to equal the capacitor bank energy.

In Figure 63, the calculated inductances are shown. Except for the early behavior (before 1.8 μs) where the calculated inductance shows the effects of finite computer calculations, the slug model describes the inductance well until about 2.6 μs. At this time, the calculated inductance is reduced. This variation is undoubtedly due to the effects of the extra gas loading. This represents a stagnation of the plasma sheath caused by the neutral gas released from the upper valve.

Calculating the adjusted plasma sheath current rise time and using the time averaged sheath and the position dependent velocities discussed in Section 4.5.1, Table 13 is generated.

Examining the Table 13 data, the plasma sheath is thick. Using the time averaged velocity, the plasma sheath varies from about 0.11 m at the bottom level to 0.15 m at the top. This does not indicate plasma sheath expansion. If position dependent sheath velocities are used, sheath velocities range from 0.13 m at the bottom to 0.41 m at the top level.

Table 13. J1104 Calculated Plasma Sheath Thickness

Level	Time Averaged Plasma Thickness (m)	Axial Level Plasma Thickness (m)
Bottom	$(1.10\pm0.24)\times10^{-1}$	$(1.33\pm0.29)\times10^{-1}$
Mid-bottom	$(1.41\pm0.23)\times10^{-1}$	$(2.62\pm0.43)\times10^{-1}$
Mid-top	$(1.25\pm0.25)\times10^{-1}$	$(2.91\pm0.59)\times10^{-1}$
Top	$(1.53\pm0.22)\times10^{-1}$	$(4.09\pm0.58)\times10^{-1}$

For the time averaged sheath velocity, the plasma sheath cannot be said to expand as a function of position, that is, if the plasma sheath does expand, it is masked by the velocity errors. If the position dependent velocity profiles are used, the sheath appears to be stable (with the errors) in the region from the mid-bottom to mid-top levels. For all locations, the plasma sheath appears to expand.

In summary, shot J1104 operates in Len's transition region. The plasma sheath is at least 0.1 m thick. The slug model represents the plasma sheath behavior well until the neutral gas from the upper valve
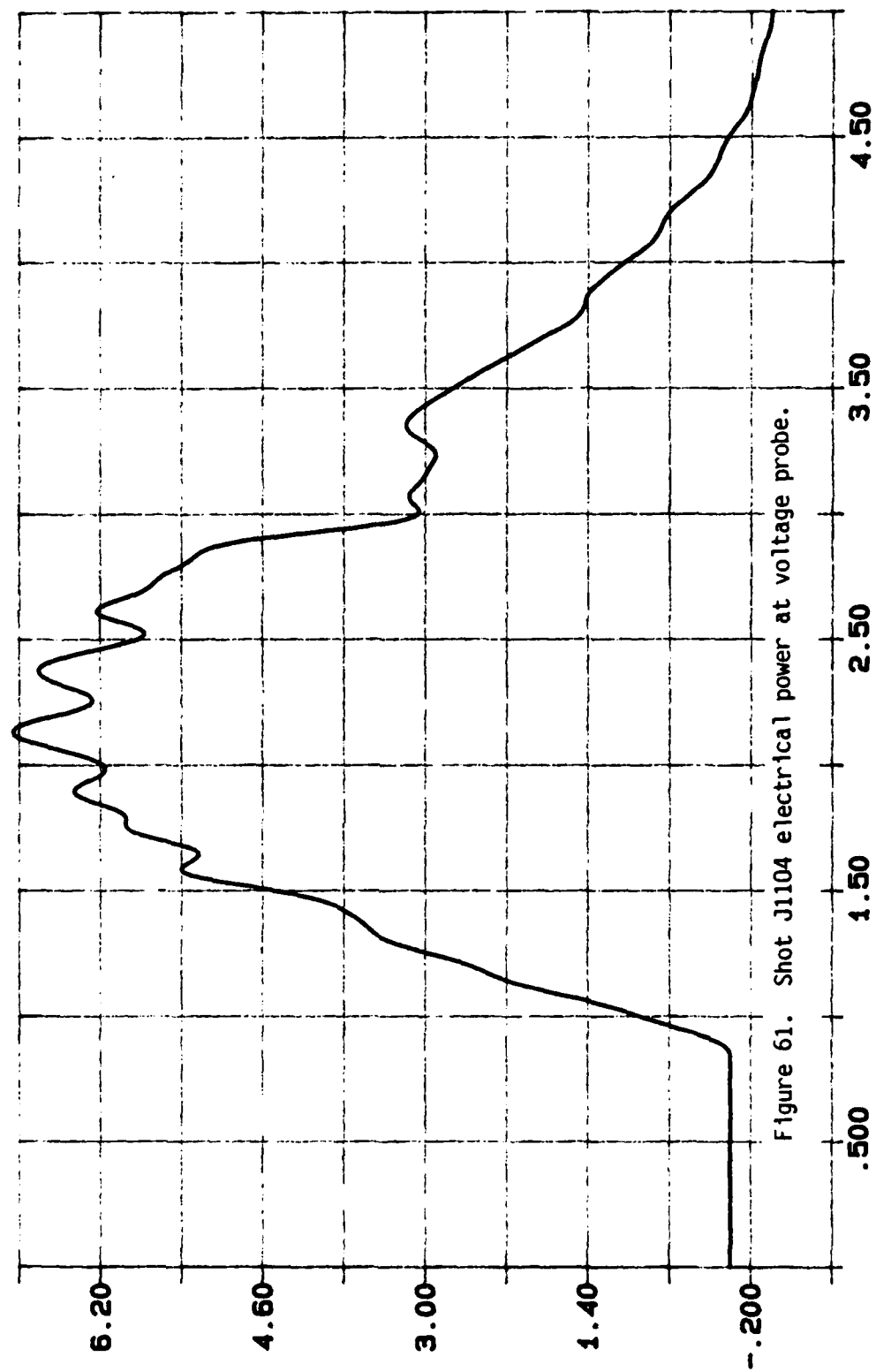
Figure 61. Shot J1104 electrical power at voltage probe.

TIME (IN SECONDS)

E-6

POWER (IN WATTS)

E 10

206
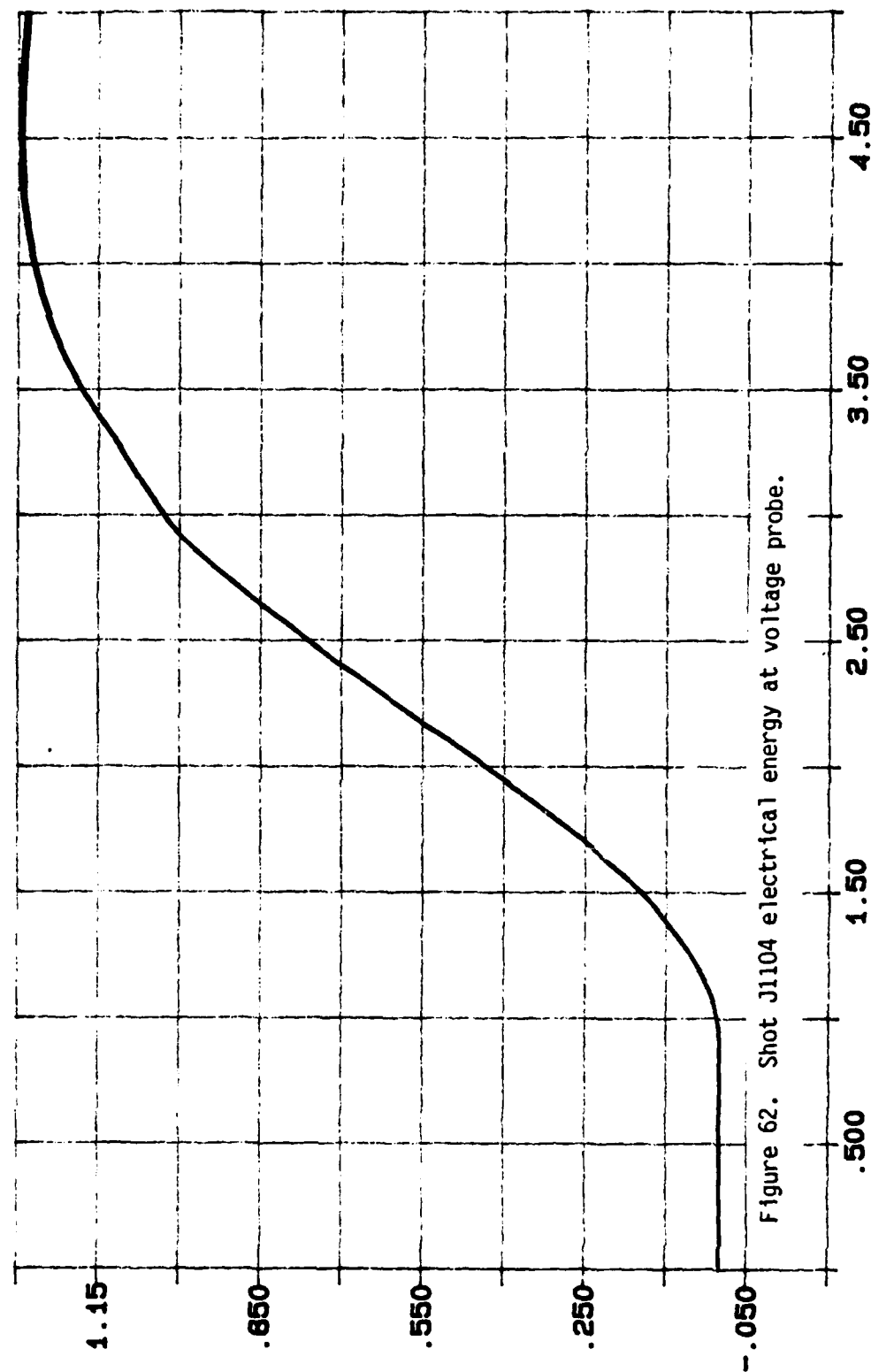
Figure 62. Shot J1104 electrical energy at voltage probe.

ENERGY (IN JOULES)

TIME (IN SECONDS)

E 5

E-6

207

Figure 63. Gun inductances from slug calculation and shot J1104.

208
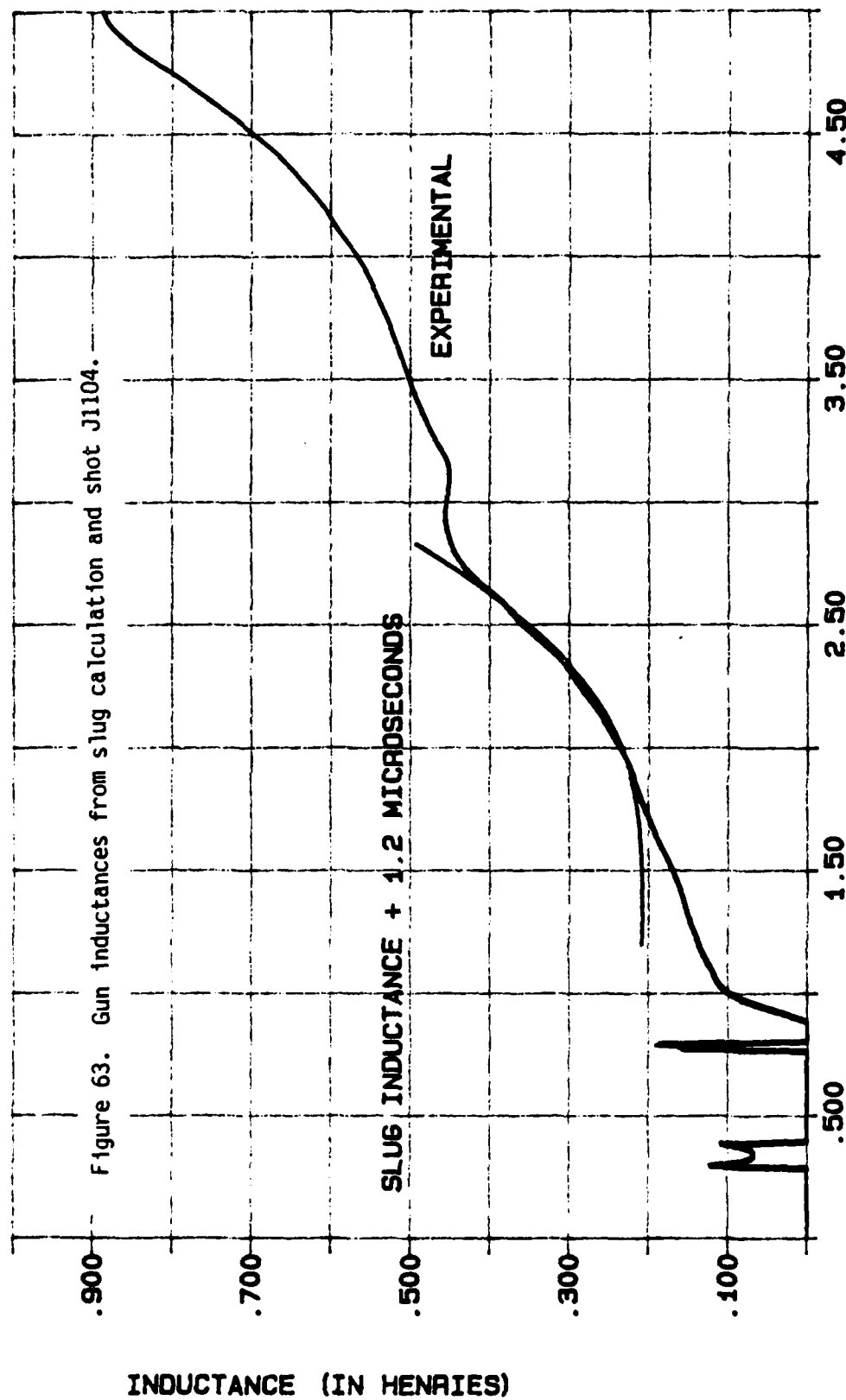
interacts with the charged particles of the plasma sheath. As noted before, only the $\mathbf{E} \times \mathbf{B}$ single particle drift velocity yields velocities of the right order of magnitude.

4.6 DISCUSSIONS OF CURRENT

It is interesting that a large number of shots showed behavior that suggests plasma formation is not limited to the gas injection site. It seems to continue throughout the coaxial plasma gun from the gas injection site to the middle of the gun. This is indicated by increasing current from the bottom to the mid-bottom levels. This suggests a diffuse plasma or a sporadic plasma formation away from the gas injection site. The data only suggests this behavior; it does not positively indicate this behavior, since calibration errors are sufficiently large to be an explanation.

The following shots show this behavior (where mid-bottom current exceeds the bottom current): D3001, D3004, D3005, D3007, D3008, D3009, D3010, J0703, J1003, J1006, J1007, J1009, J1106, J1007, J1110 and J1111. That some, but not all, the shots exhibit this behavior indicates the phenomenon is not necessarily a result of the probe calibrations, but may be a characteristic of the individual shots. In most of these cases, the current increase from the bottom to the mid-bottom levels is 5% or less. (The current increase is determined by the difference between the bottom and mid-bottom currents divided by the average of the bottom and mid-bottom currents.) For shots D3005, J1007, J1009 and J1110, the increase is larger with 8%, 6%, 11% and 11% respectively.

209

Currents are directly determined by Rogowski coil measurements and by the $\dot{B}$ probes (at the bottom, mid-bottom, mid-top and top levels). Gun muzzle current is not directly measured. However, muzzle current can be extrapolated from $\dot{B}$ probe data. A first order extrapolation assumes a current delivery of the form

$$I_1(z) = mz + b$$

where $I_1(z)$ is linearized current as a function of position, m is the current slope and b is current at the position $z = 0$ (the presumed current initiation point at the gas feed port center). Given the shot data, current slope should be negative.

Assuming plasma sheath current decreases by particle interactions, another model can be generated. The current delivery is of the form

$$I_e(z) = I_o e^{\mu z}$$

where $I_e(z)$ is exponential current as a function of position, I_o is current at $z = 0$ and μ is a coefficient representing plasma sheath current loss. Here, μ is also negative since current generally decreases as position increases from $z = 0$ to $z = z_o$ (with z_o the coaxial gun end = 0.4636 m).

Table 14. Summary of Current Delivery

Shot	Neutron Yield	Center Current (MA)	Top Level Current (MA)	Linear Extrap. Current (MA)	Exponential Extrap. Current (MA)
D2901	2.8×10^6	----	0.18	----	0.05
D3001	1.2×10^7	1.43	1.00	0.99	0.99
D3002	1.4×10^7	1.31	0.48	----	----
D3003	7.7×10^6	1.29	1.06	1.02	1.02
D3004	9.2×10^6	1.24	1.06	1.02	1.02
D3005	1.1×10^7	1.44	0.97	0.95	0.95
D3006	2.3×10^7	1.39	0.68	0.52	0.56
D3007	1.2×10^7	1.44	1.07	0.98	0.98
D3008	3.1×10^7	1.57	0.97	0.90	0.91
D3009	4.4×10^7	1.19	0.92	0.85	0.86
D3010	3.0×10^7	1.40	0.89	0.83	0.84
J0701	5.8×10^7	1.54	0.89	1.02	1.02
J0702	2.0×10^7	1.92	1.02	0.57	0.59

Table 14 (continued).

Shot	Neutron Yield	Center Current (MA)	Top Level Current (MA)	Linear Extrap. Current (MA)	Exponential Extrap. Current (MA)
J0703	1.6×10^8	1.57	0.64	0.54	0.59
J0706	4.0×10^7	1.46	0.85	0.80	0.82
J0707	7.4×10^7	1.55	0.75	0.67	0.70
J0708	4.2×10^7	----	0.76	0.71	0.72
J0902	6.9×10^7	1.76	0.66	0.63	0.64
J0903	7.9×10^6	2.09	0.56	0.42	0.48
J0904	5.2×10^7	1.65	0.59	0.48	0.53
J0905	2.7×10^6	2.36	0.40	0.33	0.37
J1001	3.0×10^6	2.12	0.52	0.43	0.47
J1002	1.2×10^8	1.48	0.95	0.92	0.93
J1003	4.0×10^7	1.65	0.86	0.84	0.85
J1005	7.3×10^7	----	0.55	0.50	0.52
J1006	4.4×10^6	1.30	0.62	0.56	0.58

Table 14 (concluded).

Shot	Neutron Yield	Center Current (MA)	Top Level Current (MA)	Linear Extrap. Current (MA)	Exponential Extrap. Current (MA)
J1007	5.0×10^7	1.46	0.78	0.69	0.72
J1008	5.0×10^6	2.22	0.22	0.09	0.19
J1009	1.1×10^8	1.52	0.82	0.78	0.80
J1103	2.3×10^7	1.96	0.51	0.38	0.43
J1104	1.1×10^8	1.70	0.73	0.63	0.67
J1105	3.9×10^8	1.51	0.97	0.88	0.90
J1106	1.9×10^8	1.53	0.89	0.63	0.64
J1107	2.8×10^8	1.61	0.78	----	----
J1108	3.1×10^8	1.61	0.78	0.69	0.73
J1109	1.3×10^8	1.51	0.89	0.83	0.85
J1110	1.1×10^8	1.61	0.84	0.76	0.78
J1111	5.0×10^8	1.47	0.84	0.77	0.79
J1201	3.0×10^8	----	0.79	0.69	0.72

Using reasonable data, current loss model profiles can be derived. This extrapolated data (derived by using a linear least squares fit) is presented in Table 14. Reasonable data assumes physical constraints. As long as the current is driven by $J \times B$ forces, it is never less than zero. This has application in calculating the linearized current $I_1(z)$.

4.7 DISCUSSIONS OF VELOCITY

In Figure 64, the calculated slug velocity as a function of axial position is displayed. Sheath velocity is a monotonic slowly increasing function of the position, similar to a curve generated by a velocity proportional to the square root of axial position.

Average slug model sheath velocity is 2.8×10^5 m/s. The averaged sheath velocity is not the linear average of the slug model velocity since a time average (instead of a spatial average) was used. Sheath velocity and axial position are small until the driving current develops a sufficiently large acceleration.

Sheath velocities are calculated for the shots studied in detail (D3004, J1006 and J1104). This sheath velocity is determined by the use of a reference current. The reference current is a substantial fraction of the peak current at all four axial positions (either 0.4 or 0.5 MA). The time when this reference current is reached is then determined for each axial position. In this way, a time differential Δt is created. Knowing the difference in axial position, 4" (0.1016 m), an averaged velocity is generated. These are shown in Figure 64.
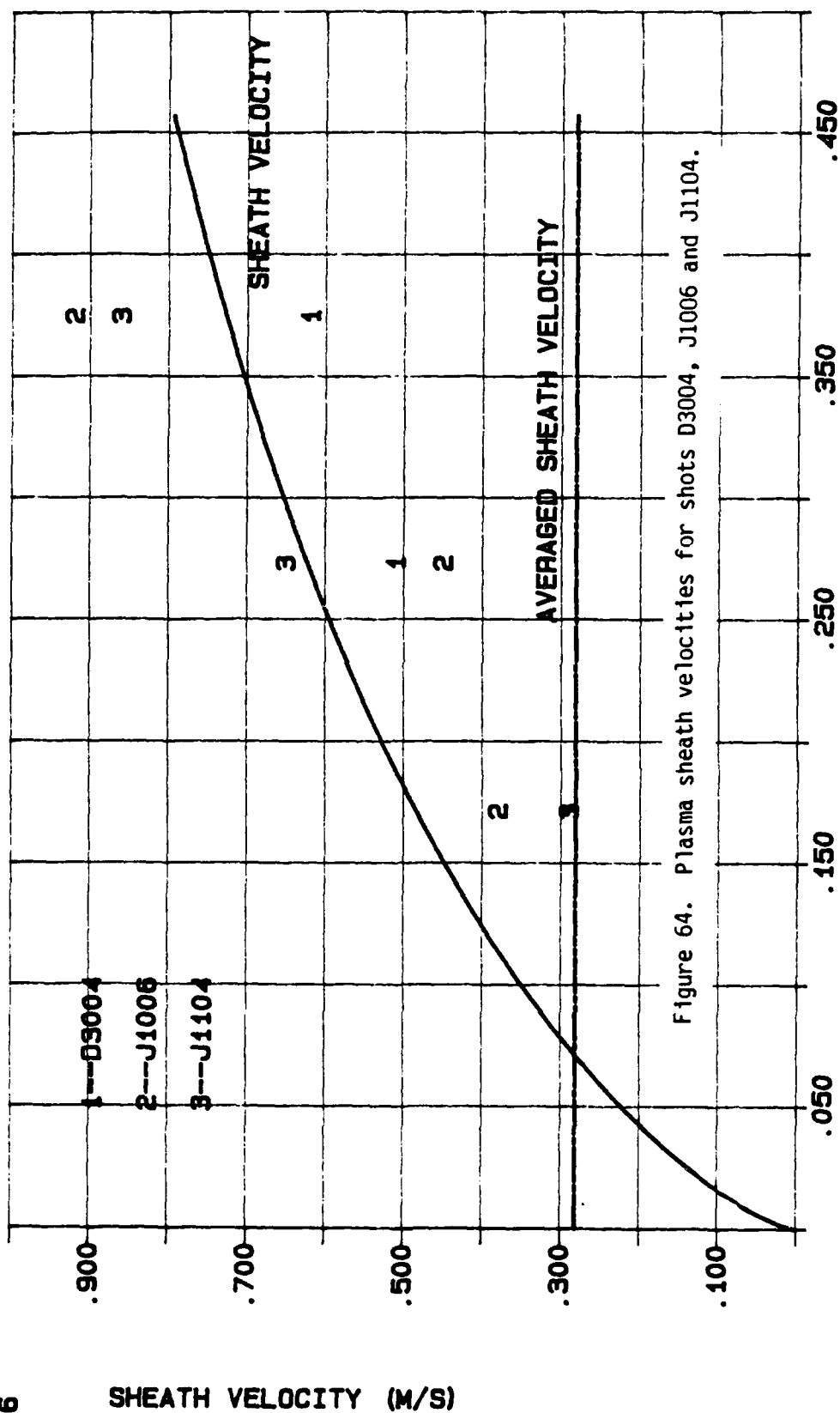
Figure 64. Plasma sheath velocities for shots D3004, J1006 and J1104.

215

Agreement between the position-velocity curve and averaged velocities of the selected shots is relatively good. The averaged velocities are the magnitude of slug model predictions and show increasing sheath velocity as a function of position.

The data covers 5 μs of elapsed time. Behavior after this time cannot be predicted beyond trends already present. Although some errors exist in the velocity calculation and even with the limitations on timing, the data suggests several components with different velocities in the plasma sheath. A first wave travels with a velocity of 8×10^5 m/s. A second wave has a velocity of 2×10^5 m/s. This multivelocity behavior is not predicted by the model. Multiple plasma sheath components with different velocities are suggested by the data in Figures 65 and 66.

Both Figures 65 and 66 present all shots where an averaged sheath velocity could be calculated. Since there were 39 shots yielding current data and there is a great deal of scatter in the data, these Figures are extremely "busy". Even so, the data still highlights several trends in the plasma sheath behavior. In Figure 65, averaged sheath velocities are calculated as a function of position for reference currents of 0.3 MA and less. In Figure 66, averaged sheath velocities are given for reference currents larger than 0.3 MA. Although much data is closely spaced, some individual data points may be distinguished. The legend for the two Figures is given in Table 15.

In Figure 65 (for reference currents of 0.3 MA or less), most plasma sheath velocities are between 2.8 and 5.0×10^5 m/s at 0.14605 m
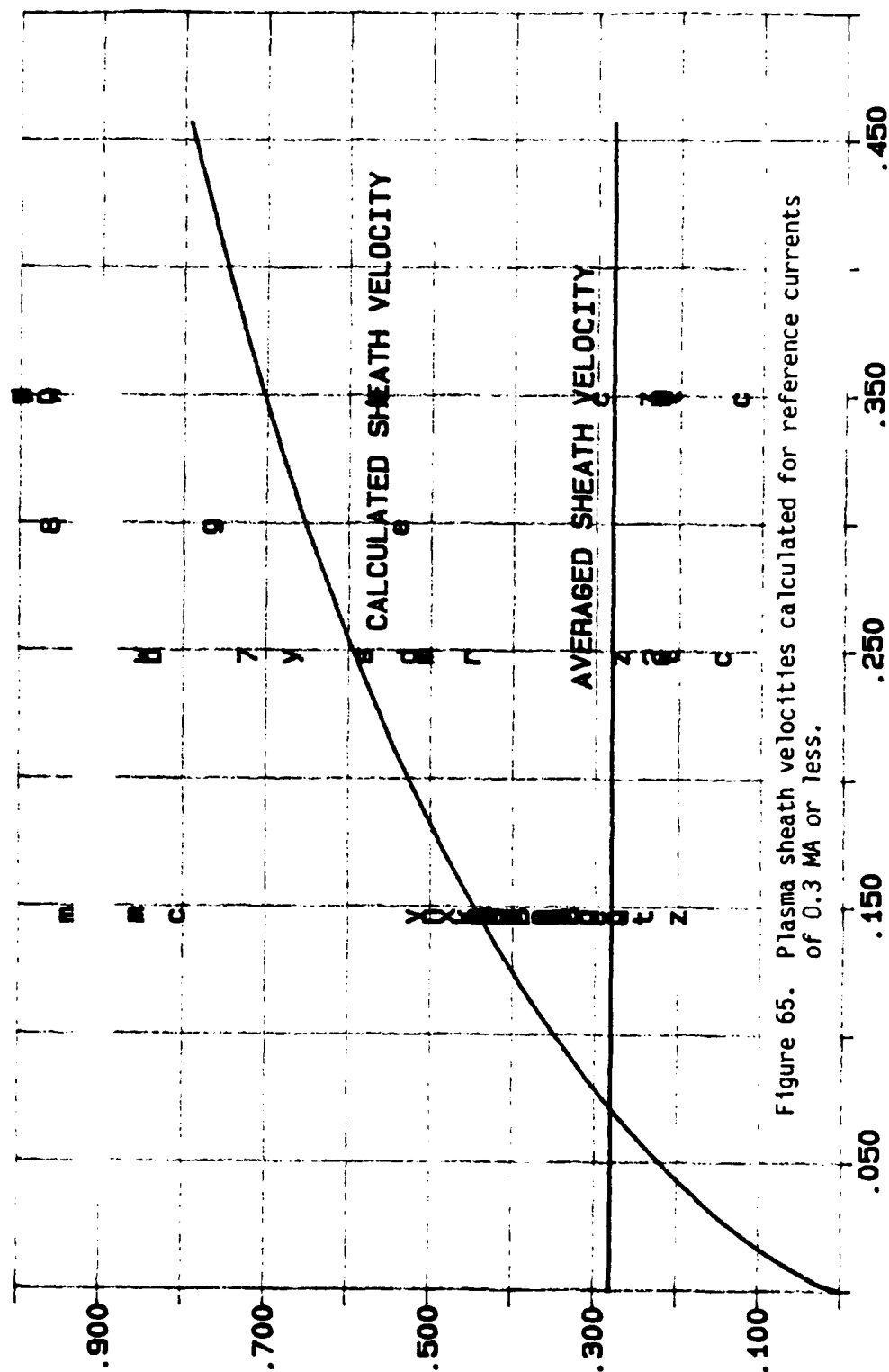
Figure 65. Plasma sheath velocities calculated for reference currents of 0.3 MA or less.

217

Figure 66. Plasma sheath velocities calculated for reference currents greater than 0.3 MA.

218
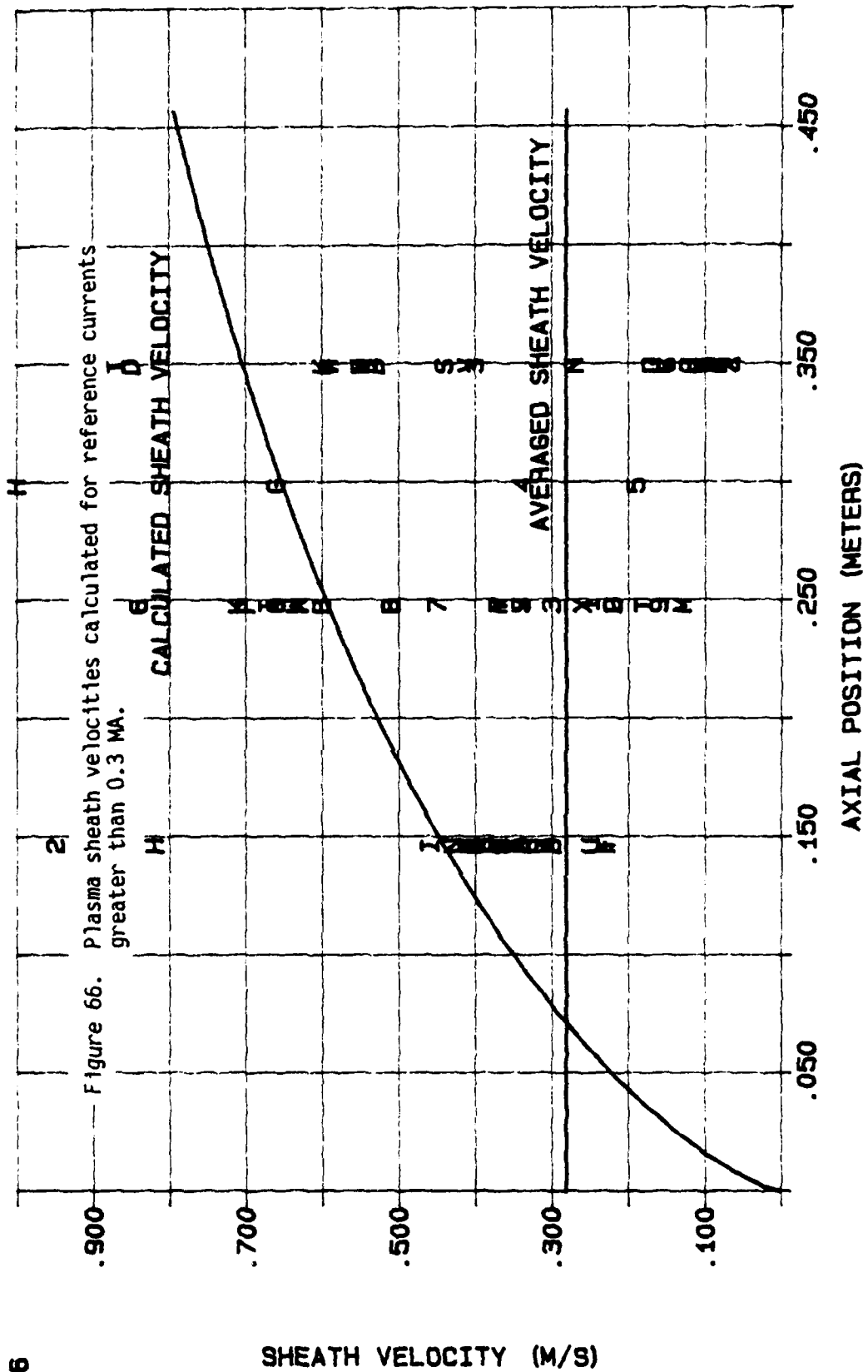
(mid-plane between the bottom and mid-bottom levels). After that position, there is a great deal of scatter of the averaged sheath velocities. At an axial position of 0.24765 m (mid-plane between the mid-bottom and mid-top levels), calculated averaged sheath velocities range from 1.5 to 9.0×10^5 m/s. At an axial position of 0.34925 m (the mid-plane between the mid-top and top levels), two groupings of calculated averaged sheath velocities are identifiable, one clustered at 2×10^5 m/s and the other clustered at 10^6 m/s. Since Figure 65 uses a small reference current, a larger sheath velocity is indicated. (Several calculated averaged sheath velocities greater than 1.0×10^6 m/s are excluded from Figure 65 to allow the rest of the data to be displayed.) Larger averaged sheath velocities are readily indicated in this Figure, since they form the initial plasma sheath front and will be detected first.

In Figure 66 (for reference currents greater than 0.3 MA), the behavior of Figure 6ɔ is generally repeated. At 0.14605 m, most averaged plasma sheath velocities range from 3.0 to 4.5×10^5 m/s. At 0.24765 m, two groups of plasma sheath velocities are indicated, one clustered at 3.0×10^5 m/s and the other at 6.5×10^5 m/s. At 0.34925 m, several plasma sheath velocities are seen, at 1.0×10^5 m/s, 4.0×10^5 m/s and 5.5×10^5 m/s. A slower plasma sheath front is indicated in the cluster of the velocities at 1.0×10^5 m/s at 0.34925 m. For the observed data, this slower plasma sheath appears to be separating from the faster plasma sheath. A slower plasma sheath velocity is indicated for larger reference currents where the slower plasma velocity is necessary to produce the higher reference currents.

219

Table 15. Legend for Figures 65 and 66

Shot	Figure 65 notation	Figure 66 notation
D2901	a	
D3001	b	B
D3002	c	
D3003	d	D
D3005	e	E
D3006		F
D3007	g	G
D3008		H
D3009	i	I
D3010		J
J0701	k	K
J0702	l	
J0703	m	M
J0706	n	N
J0707	o	O
J0708	p	P
J0902	q	Q
J0903	r	R
J0904	s	S
J0905	t	T
J1001	u	U
J1002	v	V
J1003	w	W
J1005	x	X
J1007	y	Y
J1008	z	
J1009	1	1
J1103	2	2
J1105	3	3
J1106	4	4
J1107	5	5
J1108	6	6
J1109	7	7
J1110	8	8
J1111	9	9
J1201	*	

NOTE: In Table 15, the lower case alphabetic character indicates the slower sheath velocities (in Figure 65) and the upper case alphabetic character indicates the faster sheath velocities. Blanks in the Table indicate no appropriate data is generated for that shot. Should this slower velocity sheath component not be present, larger reference currents may not be attained.

The data suggests the single particle $E \times B$ drift velocity of 7×10^5 m/s and the terminal slug model sheath velocity (8×10^5 m/s) are relevant models for fast plasma sheath velocity component. The slower sheath velocities (on the order of 1 to 2×10^5 m/s) suggest either the Rosenbluth or the reported Fishbine sheath velocities may be valid. The slower velocities are evident only at long times (longer than 5 μs). Late time data is required to conclusively indicate the appropriate model for slower plasma sheath velocities.

4.8 DISCUSSION OF NEUTRON YIELDS

Analysis of the neutron data suggests the neutron production is more a function of the delivered current to the D-D pinch than the driving current. The experimental relation between the neutron yield Y_N and the current I is [57, 190]

$$Y_N = 1.2 \times 10^{10} \; I^{3.3}$$

with I in units of MA. (A graphical relation is displayed in Figure 67.) Theoretical analysis predicts I^4 relation for neutron yield. Cowan [191] notes the $I^{3.3}$ behavior is due to insulator limitations. For the experimental neutron yields (from 2.7×10^6 to 5.0×10^8), the relevant currents are from 0.08 to 0.38 MA.

The neutron yield for each shot is displayed as a function of current in Figures 68 to 71. Four different current measurements are used. Relevant currents are gun current (measured by the chamber Rogowski coil

221

Figure 67. Bernard relation, D-D neutron yield as a function of current.

222
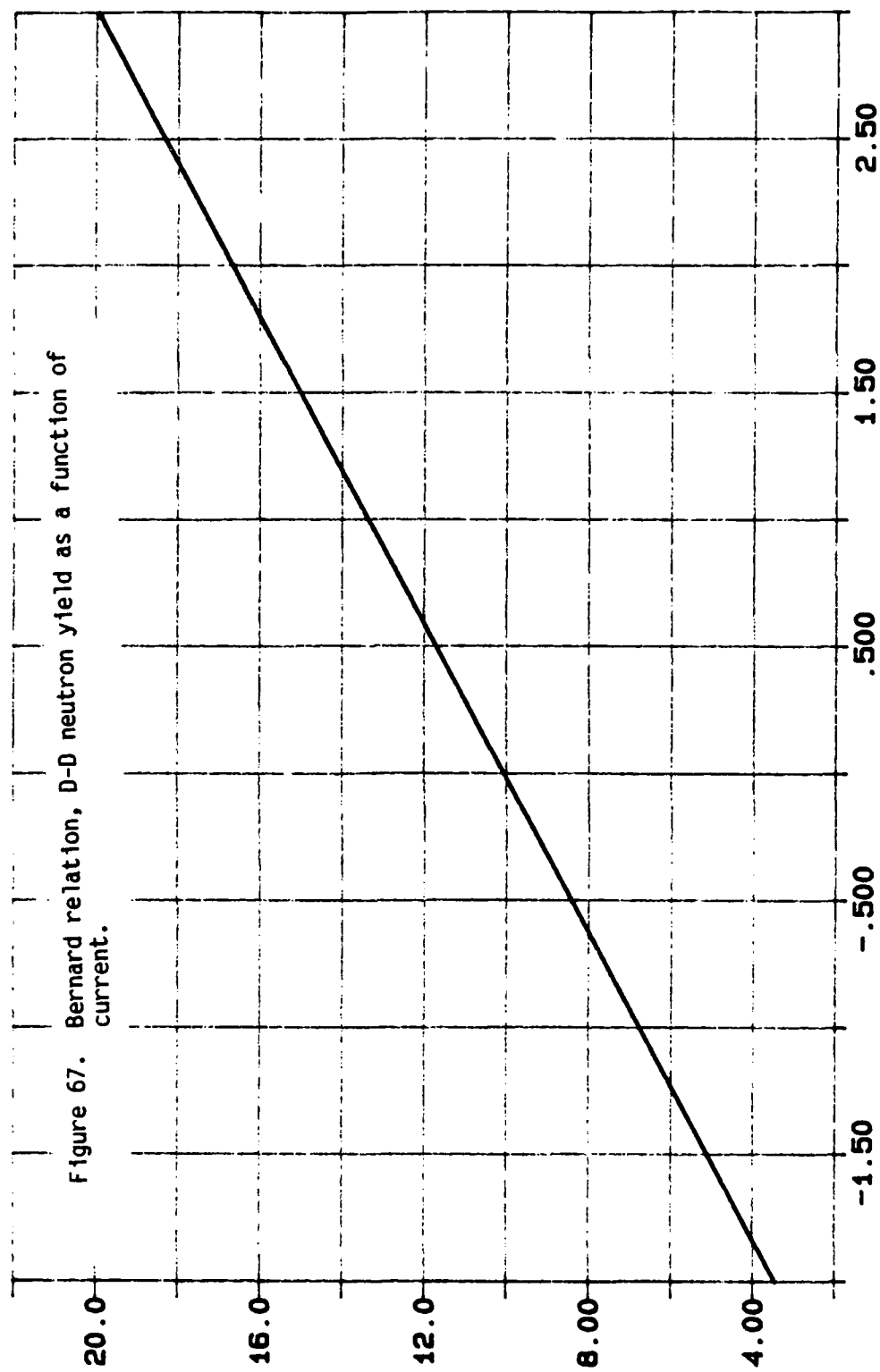
and shown in Figure 68), top current (measured by the top level $\overset{\circ}{B}$ probes and shown in Figure 69) and extrapolated muzzle current. Two models are used to extrapolate the muzzle current, a linear model (shown in Figure 70) and an exponential model (shown in Figure 71). These currents are discussed in Section 4.6. The data is displayed in Table 14.

To examine the behavior of the neutrons as a function of current, a simple power law is presumed. This model assumes

$$Y_N = \kappa \, I^\eta$$

with κ and η constants. A linearized least squares fit is performed and the results displayed in Table 16.

Using the information in Table 16, several observations can be made. The first is neutron yield does not scale with gun current. A second is the coaxial gun with both the upper and lower gas valves yields more neutrons than the gun with only the single lower valve. A third is the experiment does not match the predicted Bernard neutron yield.

Table 16 shows neutron yield does not correlate with the driving gun current. Simple physical arguments state the neutron yield goes as I^m, m a positive number of about 4. Least squares fit of the chamber current yields a negative exponent--an unphysical result. A negative exponent would imply neutron yield goes to infinity as the current

223

Figure 68. Experimental neutron yield as a function of chamber current.

224

Figure 69. Experimental neutron yield as a function of top current.
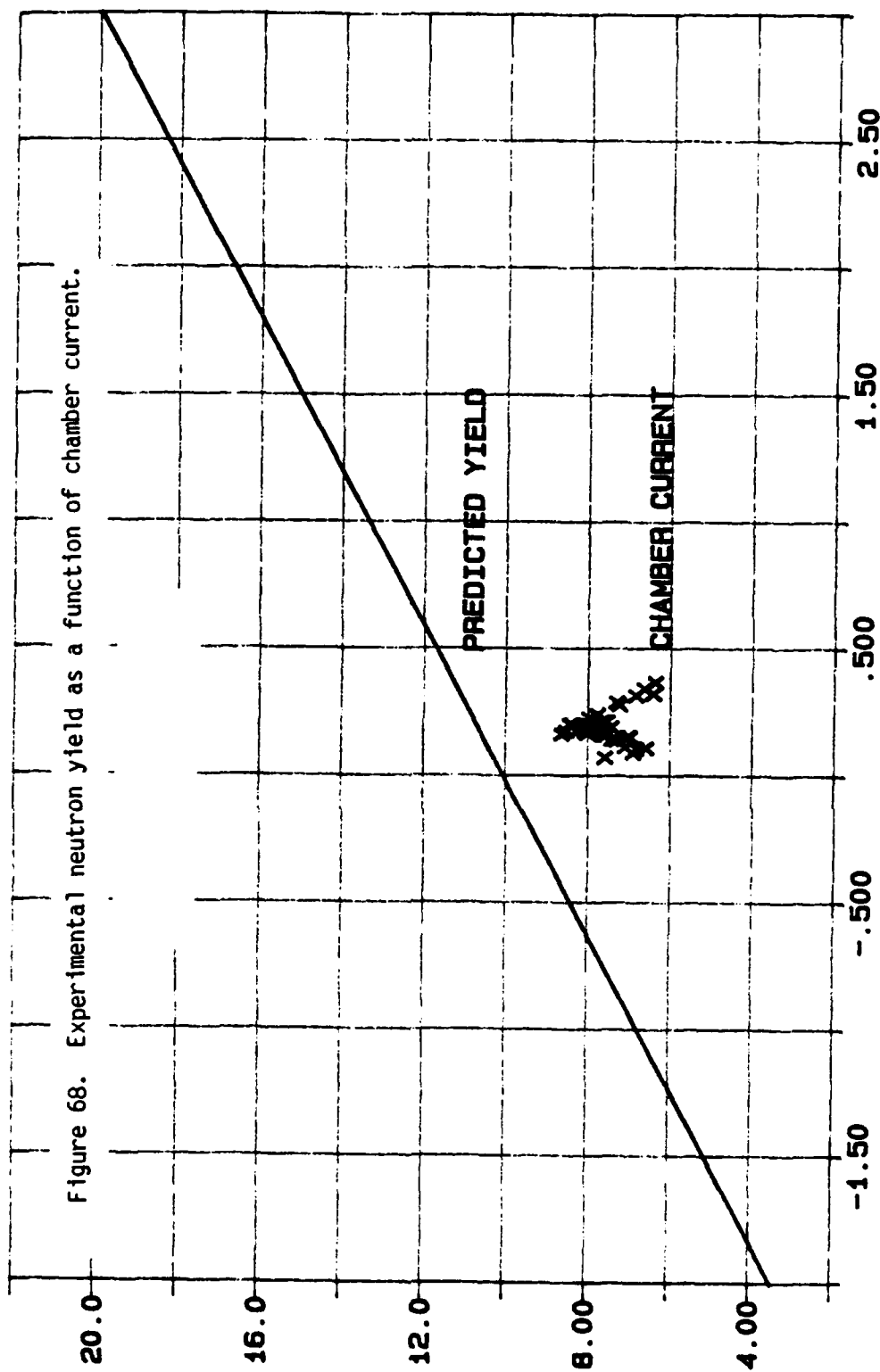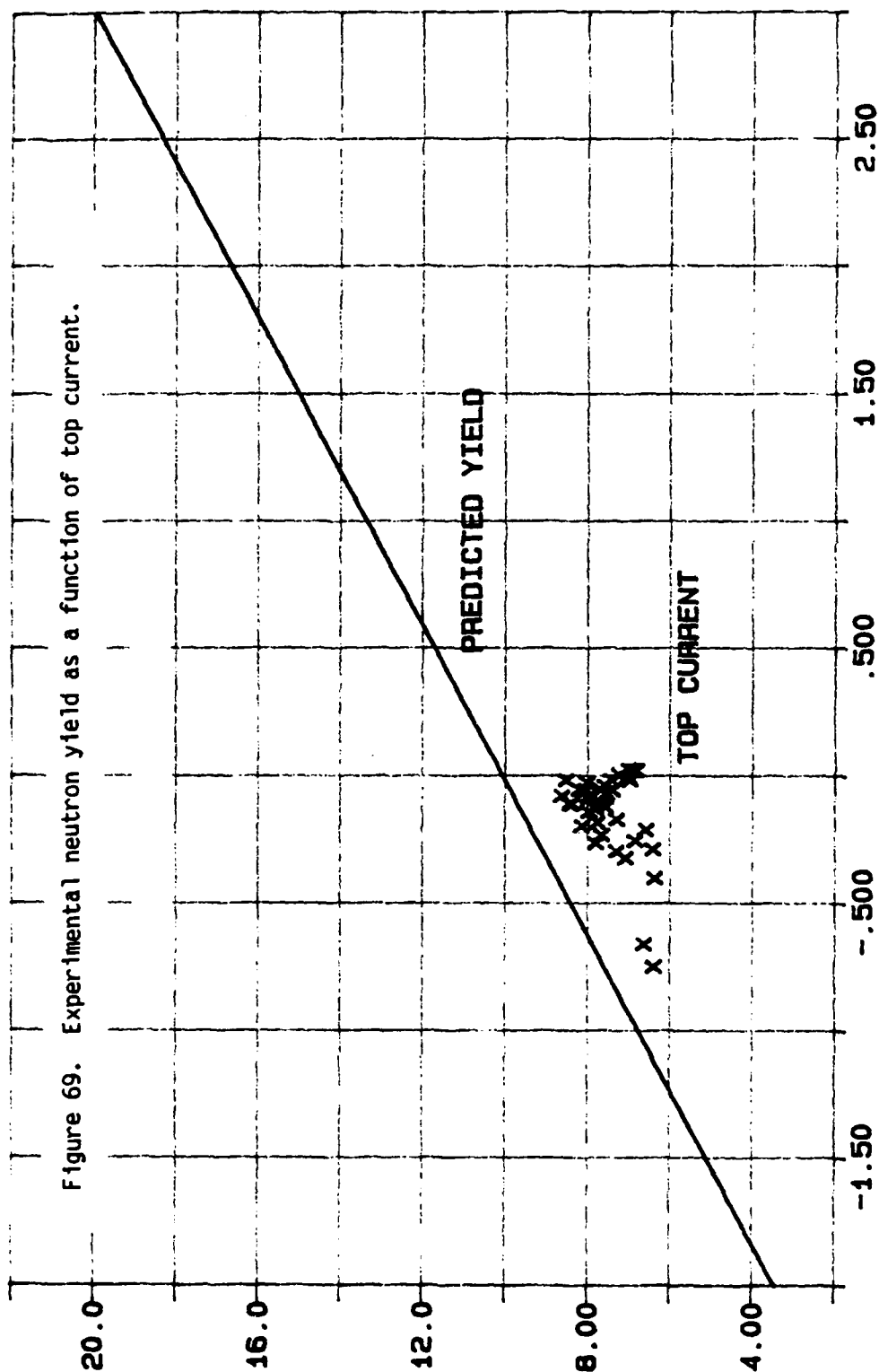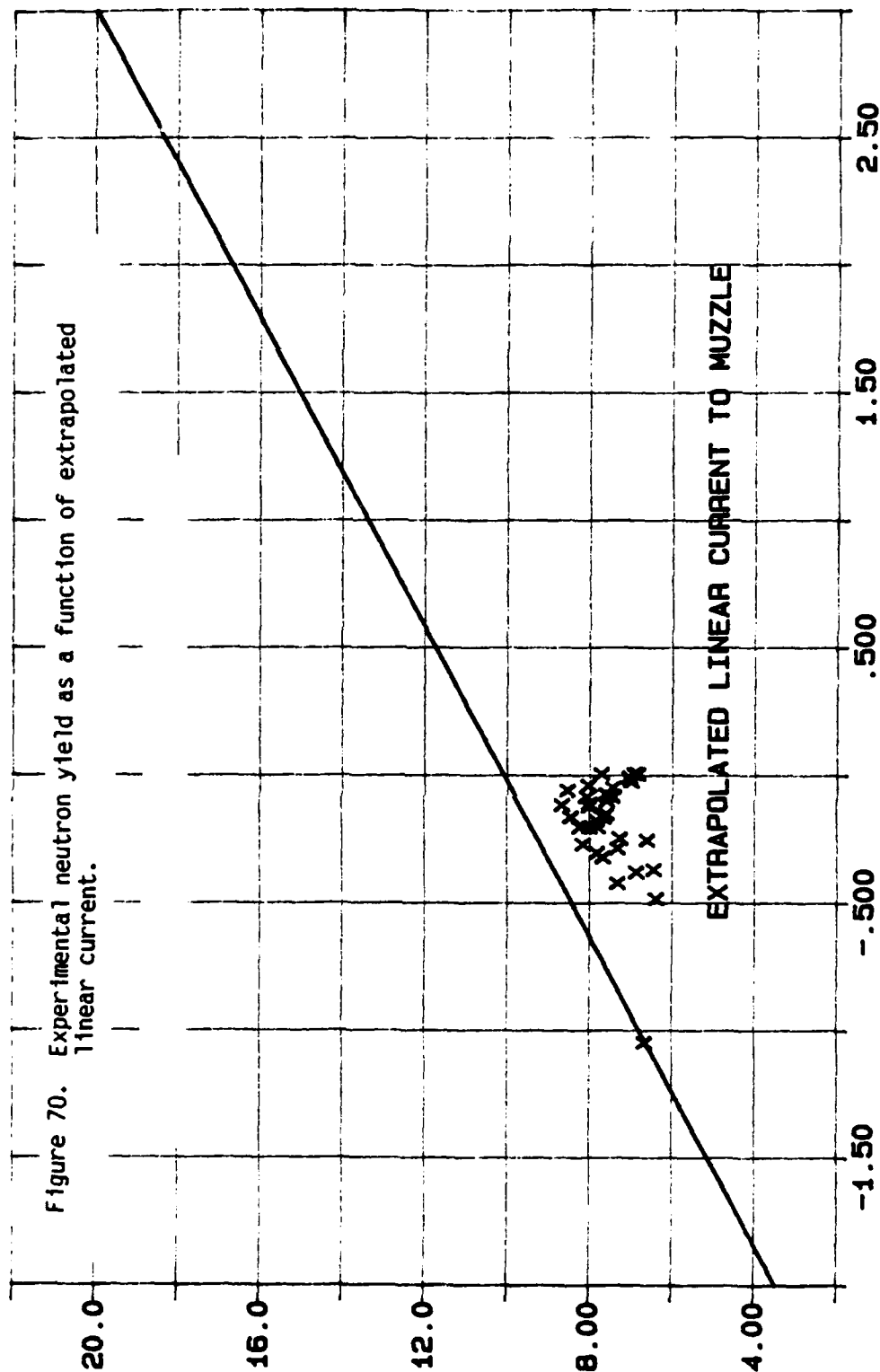
Figure 70. Experimental neutron yield as a function of extrapolated linear current.

Figure 71. Experimental neutron yield as a function of extrapolated exponential current.

227
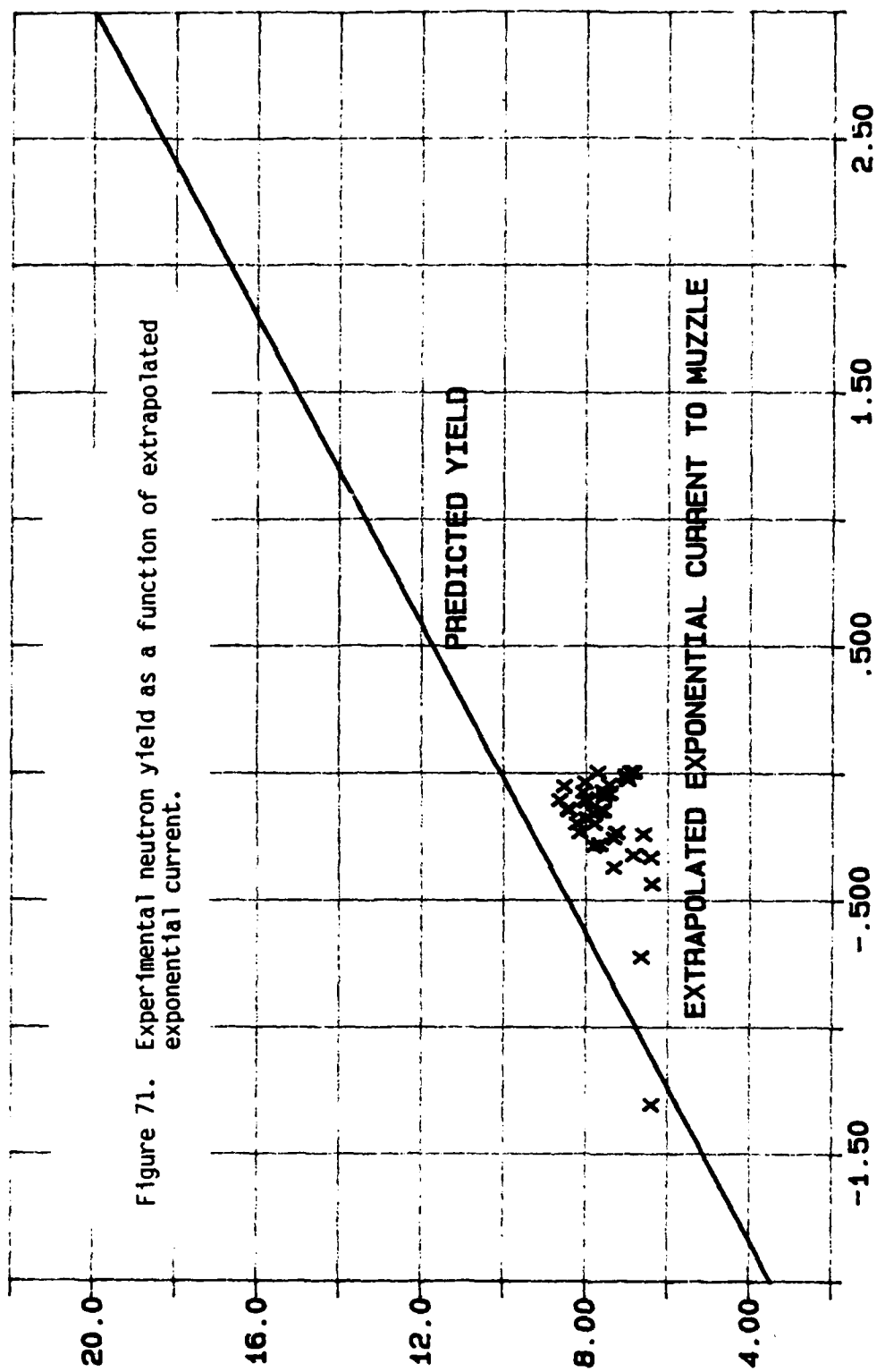
Table 16. Summary of Neutron Yield Data

Relevant Current	Data Set Used	κ	η	Confidence Level
Chamber current	All shot data	9.5×10^7	-2.054	>80%
	One valve data	2.9×10^7	-1.925	>80%
	Two valve data	3.0×10^8	-1.415	>50%
Top current	All shot data	6.6×10^7	1.682	>99.5%
	One valve data	3.2×10^7	1.180	>95%
	Two valve data	4.2×10^8	3.860	>99%
Extrapolated	All shot data	6.2×10^7	1.055	>95%
Linearized	One valve data	3.2×10^7	0.772	>90%
Muzzle Current	Two valve data	4.6×10^8	2.783	>95%
Extrapolated	All shot data	6.1×10^7	1.150	>99%
Exponential	One valve data	3.2×10^7	0.878	>95%
Muzzle Current	Two valve data	4.6×10^8	3.133	>95%

approaches 0. The statistical confidence level for these fits is much poorer than the other models. The neutron yield is not a function of the driving current.

The data shows gas valve conditions affect neutron yield. Using the lower valve system alone consistently produces neutron yields less than

the two valve system. Two gas valve data shows a constant α about an order of magnitude above the single gas valve. The exponent β for the two valve system data is larger than the exponent for the single valve data by about 2.0. Using both single valve and two valve data gives intermediate values. Exponents for the two valve system is from 2.8 to 3.9 (depending on the data set).

Because of the cathode rod structure, plasma may be lost from the gun annulus region by particle collisions, charged-charged, charged-neutral or neutral-neutral. Current is reduced from the plasma initiation site to the plasma gun muzzle. This current attenuation is observed. The plasma sheath is also be diminished and the mass delivered to the gun muzzle is reduced. With the additional gas from the second valve, total deuterium mass and the gas density at the gun muzzle is increased. Increased deuterium density increases the D-D fusion reaction rate and the neutron yield. With a short distance from the upper gas valve to the gun muzzle, a substantial fraction of the upper gas valve gas is delivered to the gun muzzle.

The top current data has a higher confidence level than the extrapolated muzzle currents. The top current data has the advantage of being consistent, since it is derived from actual measurements. Extrapolated muzzle data reflect current variations at each level. The extrapolated data reflects, at most, four axial positions. The position data is not always consistent and extrapolated data variations are to be expected.

Seen in Figures 67 to 71, agreement between the experimental data and the predicted neutron yield is not good. The magnitude of the neutron yield is small by a factor of 100 to 1000. The disagreement between the shot data and the predicted neutron yield can be ascribed to different multivelocity components in the plasma sheath and the transition mode operation of the coaxial plasma gun. The plasma gun does not create a plasma that will focus at the muzzle. The vacuum/insulator interface has an effect on neutron yield, but the magnitude of the effect cannot be extracted from this experimental series.

5.0 SUMMARY AND CONCLUSIONS

I have described a sequence of coaxial plasma gun shots performed on the AFWL PUFF capacitor bank. This experimental series use the 72 μF capacitor bank and a 8 nH flat plate transmission line to deliver voltage and current to a plasma gun. Currents of 1.6 MA are delivered to the coaxial plasma gun. Initial current rise for the plasma gun $\frac{dI}{dt}$ is 2×10^{12} A/s. The capacitor bank voltage ranges from 60 to 70 kV corresponding to stored energies from 130 to 176 kJ.

The coaxial plasma gun has an inner anode of 5.125" (0.1302 m) diameter and a cathode structure of 24 rods of 1/2" diameter (1.27×10^{-2} m). Cathode inner diameter is 7" (0.1778 m). The anode structure is 24.75" (0.6287 m) long; the cathode rods are about 0.5" shorter. Plasma gun inductance is 21 nH. Gas is fed to plasma gun at two places: a series of 96 0.25" diameter through holes in the anode at axial positions from 5.75" (0.1461 m) to 7.25" (0.1842 m) above the plasma gun base. Deuterium is the only fill gas used in this series.

Diagnostic devices described in this dissertation are: capacitive voltage probes, Rogowski coil current monitors, $\dot{B}$ probes and a thermal neutron activated silver Geiger-Müller tubes. Capacitive voltage probes are mounted in the transmission line outside the plasma gun. Rogowski coils are mounted in the transmission line external to the plasma gun and at the base of the plasma gun. $\dot{B}$ probes are mounted at four different axial and four different azimuthal positions in the plasma gun

231

for a total of 16 different positions. The $\dot{B}$ probes measure the magnetic field as the plasma sheath passes them. Of these 16 $\dot{B}$ probes, 13 of them operated throughout the entire sequence of data shots. The neutron detector is mounted external to the coaxial plasma gun. I have examined the physics of the diagnostic devices stressing experimental applications. Passive (RC) integrators are discussed as they have applications to voltage outputs diagnostic devices. Calibration methods for the diagnostic devices are also discussed. Diagnostic hardware limitations are discussed.

In modeling the plasma sheath velocity, I have investigated four sheath velocity models: an Alfven charged-neutral dominated model, the Rosenbluth model, a single particle $E \times B$ drift velocity model and Fishbine's limited or saturated model. Additionally, I have used a simple slug model computer code to predict the position and velocity of an axial sheath. This code is used to predict the voltage seen by the voltage probe, the current driving the plasma sheath and the inductance caused by the plasma sheath moving through the plasma gun.

I have examined the plasma sheath velocity profiles within the plasma gun and the neutron products of the deuterium interactions. I have estimated the plasma sheath thickness in the gun. I have compared velocity profiles to slug model predictions and compared neutron yields as a function of current to predicted neutron yields.

I have used experimental data to generate information about delivered power and energy past the site of the voltage monitor positions.

I have used Len's technique to differentiate between the snowplow and deflagration modes of operation of a coaxial plasma gun. This technique involves an incremental change in current as a function of axial position $\frac{\Delta I(t)}{\Delta z}$. A snowplow mode is indicated if the value of $\frac{\Delta I}{\Delta z}$ is sharp (i.e., a delta-like function in time). A deflagration mode is indicated if $\frac{\Delta I}{\Delta z}$ is relatively flat (with no substantial positive or negative variations).

I have discussed the procedure for converting oscilloscope records into digitized data. I have included discussions of the data format and a program for data conversion and correction. An interactive computer program was written to provide the routines required for data conversion. The program included routines for adding, subtracting, multiplying, dividing and averaging data files. Other program routines allowed data differentiation, integration, functional transformation, baseline correction, angular rotation about the axis, smoothing and correction for "RC droop".

I have analyzed the behavior of the AFWL PUFF coaxial plasma gun using the output of diagnostic Rogowski coils, $\dot{B}$ probes and capacitive voltage probes. For this system, I have observed:

1) The AFWL PUFF coaxial plasma gun does not operate completely in either the snowplow or deflagration mode. It operates in Len's transition region. The plasma gun may begin with snowplow behavior; however, the mode of operation becomes characteristic

233

of deflagration. This was observed in all cases of operation.
Only when the driving current is isolated from the plasma gun
is snowplow behavior sustained. Since the plasma gun operated
in a transition region, it showed characteristics of both the
snowplow and deflagration modes. A high velocity plasma
component (of 80 cm/μs or 8×10^5 m/s) is created in the plasma
gun. Estimates for the plasma sheath appear to be 0.10 m or
more thick. The AFWL PUFF coaxial plasma gun produces neutrons
at the gun muzzle. It appears neither mode is particularly
efficient in terms of ionic conversion of deuterium--only about
0.1 mg (10^{-7} kg) deuterium mass appears in the plasma sheath.

2) The plasma is formed by the gas breakdown of the leading edge
of the fill gas density. Paschen breakdown drives the plasma
formation. Plasma formation may occur over an extended region
in the plasma gun.

3) Coaxial plasma gun behavior is altered by using the upper
plasma valve. The upper gas valve appears to cause stagnation
of the plasma sheath and to decrease the sheath velocity. It
is possible the two valve system increases the magnitude of the
plasma current by concentrating gas and plasma. Using the
upper gas valve increases neutron production.

4) The plasma sheath velocity is not adequately characterized by
the Alfven critical velocity, the Rosenbluth sheath velocity or
Fishbine's saturated plasma sheath velocity model. Only the

234

single particle $E \times B$ drift velocity is of the magnitude for the gun plasma sheath. The plasma sheath appears to be composed of several components. The faster plasma sheath velocity is described by the single particle theory or the slug model computation given here. Slower plasma sheath components may be described by the Rosenbluth or the Fishbine model. Only Alfven's model finds no application in the current studies.

5) The AFWL PUFF coaxial plasma gun is well modeled early in time by a 0-D slug model driven by a lumped element circuit model. The model performs well modeling from the plasma initiation site to the gun muzzle. The simulation terminates the plasma reaches the gun muzzle. Plasma flow past the end of the plasma gun muzzle is not incorporated into the model. Internal plasma behavior is not characterized.

6) The azimuthal variation of the different probes in the coaxial plasma gun indicates the plasma flow is laminar, but does exhibit some turbulence. The plasma sheath seems to have asymmetric characteristics (spoking) away from the plasma initiation site.

7) The lack of optimization of either the snowplow or deflagration modes may be due to the plasma initiation process. In the AFWL PUFF gun, the insulator is isolated from the neutral feed gas. Gas breaks down without the insulator as a breakdown site or as a source for ultraviolet and soft X-rays for pre-ionization.

235

8) The number of neutrons produced by the coaxial plasma gun is a factor of 100 to 1000 smaller than the Bernard relation prediction. Neutron production for the two valve system is higher than the one valve system, likely due to the increased gun muzzle deuterium density delivered. The exponent n (in I^n) for the two valve system is about 3. Neutron yield is a function of the current delivered to the gun muzzle, not current delivered to the coaxial plasma gun.

9) With the present AFWL PUFF coaxial plasma gun, plasma current is not completely delivered to the gun muzzle. Loss mechanisms indicated for this system are collisional particle interactions and loss of gas through the cathode rod structure.

5.1. APPLICATIONS OF THE PRESENT WORK

In several respects, the research in this dissertation is limited. It only describes observed behavior of the AFWL PUFF coaxial plasma gun. It does not describe the use of gases other than deuterium. It does not describe the plasma behavior late in time. Plasma sheath behavior is inferred through the use of current and $\dot{B}$ probe diagnostic devices. The main thrust of the present work is directed towards defining a complete range of operating parameters of the present AFWL PUFF coaxial plasma gun design. In terms of immediate applications, the varied coaxial plasma gun uses cited in Section 1 apply. With high plasma sheath velocities and fusion product neutrons, the deuterium filled plasma gun

236

may be used to stress materials and electrical components and to simulate the nuclear effects on materials and components.

5.2. SUGGESTIONS FOR FUTURE RESEARCH

As would be expected, more experimental research on the AFWL PUFF coaxial plasma gun design is recommended. Questions to be answered are:

1) What additional information can be inferred from a repetition of these experiments using absolute timing references?

2) Does the late time behavior of the AFWL PUFF coaxial plasma gun differ significantly from early time behavior described here?

3) What are the mass and charged particle density profiles of the the gas in the plasma gun annular? What are the mass and charged particle densities of the (supposedly charge neutral) gas ahead of the plasma sheath? What are the mass and charged particle densities of the plasma sheath? What are the mass and charged particle densities of the region behind the plasma sheath?

4) What is the composition of the plasma sheath?

5) What effect does the solid anode structure have on the plasma sheath?

6) What effect does the cathode rod structure have on the plasma sheath? How does this effect differ from using solid outer cathodes? What effects could be expected from changing the number of rods and the spacing of the cathode rods?

7) Would the AFWL PUFF coaxial plasma gun show the same behavior with applied polarities opposite those of the described experiments?

8) What effect do the $\dot{B}$ probes have on the plasma initiation and plasma flow?

9) What process causes the snowplow mode to convert to the deflagration mode? Is it a process that can be triggered or controlled by processes external to the plasma gun annular region?

10) What effect does preionization of the fill gas have on the gun operation?

11) What effect do different fill gases have on the operation of the AFWL PUFF coaxial plasma gun?

12) Is the AFWL PUFF coaxial gun design convertible; can it be triggered to convert from one operating mode to another?

13) What are the causes of the plasma turbulence and spoking behavior in the middle of the plasma gun well away from the plasma initiation site?

14) What are the mechanisms for plasma formation in the AFWL PUFF coaxial plasma gun design? With no accessible vacuum/insulator interface, does the plasma form at a particular site or does it form over an extended volume in the annulus?

15) Can shorting the radial electric field be used as a method to either remove or reduce azimuthal spoking in the coaxial plasma gun?

16) In the AFWL PUFF coaxial plasma gun, what impact does plasma spoking have on plasma sheath initiation?

17) Why does only a small proportion of the fill gas ionize and form the plasma sheath?

18) Why do various velocity components appear in the plasma sheath? Why do these components show a variation ranging from less than 10^5 to 2×10^6 m/s?

19) What are the specific mechanisms for current loss as the plasma travels from the initiation site to the gun muzzle?

Can these plasma losses be controlled, minimized and optimized for specific applications?

20) How can delivered gun muzzle current be optimized for more efficient neutron production? What effect does isolating the insulator/dielectric interface from the feed deuterium gas have on neutron production?

21) The increased neutron yield from the AFWL coaxial plasma gun is related to the use of the second (upper) gas valve. What portion of increased neutron yield is due to the increased gas loading? What portion of the neutron yield increase is due to gas stagnation in the plasma gun allowing more simultaneous current delivery?

REFERENCES

1. L. K. Len, PhD dissertation, Univ. New Mexico, Albuquerque, New Mexico, Aug 1983, pp. 31-38.

2. L. K. Len, _ibid._, pp. 39-41.

3. L. K. Len, _ibid._, pp. 156-158.

4. J. Marshall, _The Physics of Fluids_, vol. 3, no. 1, Jan/Feb 1960, pp. 134-135.

5. A. I. Morozov and L. S. Solov'ev, _Soviet Physics--Technical Physics_, vol. 5, no. 9, Mar 1961, pp. 1033-1038.

6. P. J. Hart, _The Physics of Fluids_, vol. 5, no. 1, Jan 1962, pp. 38-47.

7. L. C. Burkhardt and R. H. Lovberg, _The Physics of Fluids_, vol. 5, no. 3, Mar 1962, pp. 341-347.

8. S. Yu. Luk'yanov, I. M. Podgornyi and S. A. Chuvatin, _Soviet Physics--Technical Physics_, vol. 6, no. 9, Mar 1962, pp. 750-754.

9. J. W. Mather, _The Physics of Fluids_, vol. 7, no. 11, pt. 2, Nov 1964, pp. S28-S34.

10. A. Dattner and J. Eninger, _The Physics of Fluids_, vol. 7, no. 11, pt. 2, Nov 1964, pp. S41-S43.

11. K. Thom, J. Norwood and N. Jalufka, _The Physics of Fluids_, vol. 7, no. 11, pt. 2, Nov 1964, pp. S67-S70.

12. P. J. Hart, _Journal of Applied Physics_, vol. 35, no. 12, Dec 1964, pp. 3425-3431.

13. I. M. Zolototrubov, V. A. Kiselev and Yu. M. Novikov, _Soviet Physics--Technical Physics_, vol. 9, no. 6, Dec 1964, pp. 773-778.

14. I. M. Zolototrubov, V. A. Kiselev and Yu. M. Novikov, _Soviet Physics--Technical Physics_, vol. 10, no. 2, Aug 1965, pp. 204-207.

15. G. J. Pert, PhD thesis, Univ. London, England, Apr 1966.

16. T. D. Butler and J. L. Cook, _The Physics of Fluids_, vol. 11, no. 10, Oct 1968, pp. 2286-2288.

17. G. J. Pert, _British Journal of Applied Physics (Journal of Physics D: Applied Physics)_, series 2, vol. 1, no. 11, Nov 1968, pp. 1487-1493.

18. G. J. Pert, _British Journal of Applied Physics (Journal of Physics D: Applied Physics)_, series 2, vol. 2, no. 3, Mar 1969, pp. 429-434.

19. N. F. Tsagas, G. L. R. Mair and A. E. Prinn, Journal of Physics D: Applied Physics, vol. 11, no. 9, Jun 1978, pp. 1263-1272.

20. G. Herziger, H. Krompholz, W. Schneider and K. Schönbach, Physics Letters, vol. 71A, no. 1, 16 Apr 1979, pp. 54-56.

21. A. Donges, G. Herziger, H. Krompholz et al., Physics Letters, vol. 76A, no. 5/6, 14 Apr 1980, pp. 391-392.

22. D. M. Woodall and L. K. Len, Journal of Applied Physics, vol. 57, no. 3, 1 Feb 1985, pp. 961-964.

23. D. Dietz, Journal of Applied Physics, vol. 62, no. 7, 1 Oct 1987, pp. 2669-2674.

24. C. B. Hilland, PhD dissertation, Ohio State University, Columbus Ohio, 1970.

25. N. V. Filippov and T. I. Filippova, JETP Letters, vol. 25, no. 5, 5 Mar 1977, pp. 241-244.

26. V. S. Komel'kov and V. I. Modzolevskii, Soviet Journal of Plasma Physics, vol. 3, no. 5, Sep/Oct 1977, pp. 533-538.

27. D. Y. Cheng, Nuclear Fusion, vol. 10, no. 3, Sep 1970, pp. 305-317.

28. V. A. Burtsev, V. N. Litunovskii and M. P. Nadgornaya, Soviet Physics--Technical Physics, vol. 17, no. 8, Feb 1973, pp. 1363-1368.

29. V. A. Burtsev, V. N. Litunovskii and M. P. Nadgornaya, Soviet Physics--Technical Physics, vol. 17, no. 10, Apr 1973, pp. 1670-1676.

30. V. A. Burtsev, V. N. Litunovskii and M. P. Nadgornaya, Soviet Physics--Technical Physics, vol. 19, no. 6, Dec 1974, pp. 736-740.

31. C. L. Enloe and R. E. Reinovsky, Digest of Technical Papers, Proc. of 5th IEEE Pulsed Power Conf., Arlington Virginia, 10-12 Jun 1985, P. J. Turchi and M. F. Rose, eds., IEEE, New York, NY, 1985, pp. 724-727.

32. V. I. Aref'ev and L. V. Leskov, Soviet Physics--Technical Physics, vol. 17, no. 11, May 1973, pp. 1822-1828.

33. V. I. Aref'ev and L. V. Leskov, Soviet Physics--Technical Physics, vol. 17, no. 11, May 1973, pp. 1829-1832.

34. N. P. Kozlov, L. V. Leskov, Yu. S. Protasov and V. I. Khvesyuk, Soviet Physics--Technical Physics, vol. 18, no. 4, Oct 1973, pp. 466-470.

35. Yu. M. Grishin, N. P. Kozlov and V. I. Khvesyuk, Soviet Physics--Technical Physics, vol. 18, no. 4, Oct 1973, p. 542.

36. Yu. M. Grishin, N. P. Kozlov, Yu. S. Protasov and V. I. Khvesyuk, Soviet Physics--Technical Physics, vol. 18, no. 7, Jan 1974, pp. 948-950.

37. A. A. Kalmykov, A. D. Timofeev and B. A. Shevchuk, Soviet Physics--Technical Physics, vol. 18, no. 12, Jun 1974, pp. 1601-1603.

38. Yu. M. Grishin, N. P. Kozlov, L. V. Leskov and V. I. Khvesyuk, Soviet Physics--Technical Physics, vol. 20, no. 9, Sep 1975, pp. 1183-1187.

39. I. F. Kvartskhava, N. G. Reshetnyak, N. N. Zhukov et al., Soviet Physics--Technical Physics, vol. 21, no. 5, May 1976, pp. 570-574.

40. I. S. Gushchin, Yu. P. Popov and V. V. Savichev, Soviet Journal of Plasma Physics, vol. 2, no. 5, Sep/Oct 1976, pp. 413-417.

41. A. S. Kamrukov, A. P. Kozlov and Yu. S. Protasov, Soviet Journal of Plasma Physics, vol. 5, no. 2, Mar/Apr 1979, pp. 206-210.

42. Yu. A. Alekseev and M. N. Kazeev, Soviet Journal of Plasma Physics, vol. 7, no. 5, Sep/Oct 1981, pp. 596-603.

43. J. W. Mather, The Physics of Fluids, vol. 8, no. 2, Feb 1965, pp. 366-377.

44. E. H. Beckner, Journal of Applied Physics, vol. 37, no. 13, Dec 1966, pp. 4944-4952.

45. J. W. Mather and P. J. Bottoms, The Physics of Fluids, vol. 11, no. 3, Mar 1968, pp. 611-618.

46. A. Bernard, A. Coudeville and J. P. Watteau, Physics Letters, vol. 33A, no. 8, 28 Dec 1970, pp. 477-478.

47. D. E. Potter, The Physics of Fluids, vol. 14, no. 9, Sep 1971, pp. 1911-1924.

48. W. H. Bostick, V. Nardi and W. Prior, Journal of Plasma Physics, vol. 8, part 1, Aug 1972, pp. 7-20.

49. N. W. Jalufka and J. H. Lee, The Physics of Fluids, vol. 15, no. 11, Nov 1972, pp. 1954-1958.

50. H. Rapp, Physics Letters, vol. 43A, no. 5, 9 Apr 1973, pp. 420-422.

51. L. Michel, K. H. Schönbach and H. Fischer, Applied Physics Letters, vol. 24, no. 2, 15 Jan 1974, pp. 57-59.

52. A. Bernard, A. Coudeville, A. Jolas et al., The Physics of Fluids, vol. 18, no. 2, Feb 1975, pp. 180-194.

53. M. Trunk, Plasma Physics, vol. 17, no. 4, Apr 1975, pp. 237-248.

54. G. V. Karpov, E. N. Smirnov and V. N. Suvorov, Soviet Physics--Technical Physics, vol. 21, no. 3, Mar 1976, pp. 293-296.

55. V. V. Vikhrev, Soviet Journal of Plasma Physics, vol. 3, no. 5, Sep/Oct 1977, pp. 539-542.

56. T. Oppenländer, G. Pross, G. Decker and M. Trunk, Plasma Physics, vol. 19, no. 11, Nov 1977, pp. 1075-1083.

57. A. Bernard, P. Cloth, H. Conrads et al., Nuclear Instruments and Methods, vol. 145, 1977, pp. 191-218.

58. S. Maxon and J. Eddleman, The Physics of Fluids, vol. 21, no. 10, Oct 1978, pp. 1856-1865.

59. H. Fischer and K. H. Haering, Applied Optics, vol. 18, no. 13, 1 Jul 1979, pp. 2258-2261.

60. H. Fischer and K. H. Haering, Applied Optics, vol. 18, no. 22, 15 Nov 1979, pp. 3733-3734.

61. H. Krompholz, W. Neff, F. Rühl et al., Physics Letters, vol. 77A, no. 4, 26 May 1980, pp. 246-248.

62. H. Krompholz, F. Rühl, W. Schneider et al., Physics Letters, vol. 82A, no. 2, 9 Mar 1981, pp. 82-84.

63. S. I. Ananin and V. V. Vikhrev, Soviet Journal of Plasma Physics, vol. 7, no. 3, May/Jun 1981, pp. 266-271.

64. G. Decker, W. Kies and G. Pross, Physics Letters, vol. 89A, no. 8, 7 Jun 1982, pp. 393-396.

65. W. Stygar, G. Gerdin, F. Venneri and J. Mandrekas, Nuclear Fusion, vol. 22, no. 9, Sep 1982, pp. 1161-1172.

66. P. G. Eltgroth, The Physics of Fluids, vol. 25, no. 12, Dec 1982, pp. 2408-2414.

67. N. V. Filippov, Soviet Journal of Plasma Physics, vol. 9, no. 1, Jan/Feb 1983, pp. 14-25.

68. G. Decker, W. Kies and G. Pross, The Physics of Fluids, vol. 26, no. 2, Feb 1983, pp. 571-578.

69. C. R. Haas, R. Noll, F. Rühl and G. Herziger, Nuclear Fusion, vol. 24, no. 9, Sep 1984, pp. 1216-1220.

70. L. Bilbao, H. A. Bruzzone, and H. J. Kelly, Plasma Physics and Controlled Fusion, vol. 27, no. 11, Nov 1985, pp. 1207-1215.

71. V. K. Chernyshev, V. A. Tsukerman, V. M. Gerasimov et al., Soviet Physics--Technical Physics, vol. 31, no. 5, May 1986, pp. 558-559.

72. W. Kies, _Plasma Physics and Controlled Fusion_, vol. 28, no. 11, Nov 1986, pp. 1645-1657.

73. P. J. Hart, _Journal of Applied Physics_, vol. 31, no. 2, Feb 1960, pp. 436-437.

74. C. T. Chang, _The Physics of Fluids_, vol. 4, no. 9, Sep 1961, pp. 1085-1096.

75. J. C. Keck, _The Physics of Fluids_, vol. 5, no. 5, May 1962, pp. 630-632.

76. F. J. Fishman and H. Petschek, _The Physics of Fluids_, vol. 5, no. 5, May 1962, pp. 632-633.

77. F. J. Fishman and H. E. Petschek, _The Physics of Fluids_, vol. 5, no. 10, Oct 1962, pp. 1188-1195.

78. G. D. Cormack, _Canadian Journal of Physics_, vol. 41, no. 10, Oct 1963, pp. 1591-1603.

79. W. H. Heiser, _The Physics of Fluids_, vol. 7, no. 1, Jan 1964, pp. 143-145.

80. J. A. Bakken, _The Physics of Fluids_, vol. 7, no. 8, Aug 1964, pp. 1381-1383.

81. D. W. Koopman, _The Physics of Fluids_, vol. 7, no. 10, Oct 1964, pp. 1651-1657.

82. J. Keck, _The Physics of Fluids_, vol. 7, no. 11, pt. 2, Nov 1964, pp. S16-S27.

83. J. B. Workman, _The Physics of Fluids_, vol. 8, no. 11, Dec 1965, pp. 2162-2168.

84. H. Muntenbruch, _The Physics of Fluids_, supplement I, vol. 12, no. 5, pt. 2, May 1969, pp. I-11-I-21.

85. T. K. Allen, A. J. Cox and I. J. Spaulding, _Proc. of 2nd Int. Conf. on Plasma Physics and Controlled Nuclear Fusion Research, Culham, England, 6-10 Sep 1965_, IAEA, Vienna, Austria, Apr 1966, pp. 427-448.

86. J. Marshall, _Proc. of High Beta Workshop, Los Alamos, New Mexico, 28 Jul--1 Aug 1975_, report no. ERDA-76/108, E. Oktay, ed., ERDA, Washington DC, 1976, pp. 470-480.

87. K. F. McKenna and R. E. Siemon, _Nuclear Fusion_, vol. 25, no. 9, Sep 1985, pp. 1267-1270.

88. L. C. Burkhardt, R. E. Dunaway, J. W. Mather et al., _Journal of Applied Physics_, vol. 28, no. 5, May 1957, pp. 519-521.

89. I. F. Kvartskhava and Yu. V. Matveev, <u>Nuclear Fusion</u>, vol. 11, no. 4, Aug 1971, pp. 385-387.

90. C. S. Maclatchy and A. J. Barnard, <u>Canadian Journal of Physics</u>, vol. 50, no. 20, 15 Oct 1972, pp. 2475-2481.

91. J. Bailey, Y. Ettinger, A. Fisher and N. Rostoker, <u>Applied Physics Letters</u>, vol. 40, no. 6, 15 Mar 1982, pp. 460-462.

92. T. Miyamoto, <u>Nuclear Fusion</u>, vol. 24, no. 3, Mar 1984, pp. 337-348.

93. V. V. Vikhrev, V. V. Ivanov and V. V. Prut, <u>Soviet Journal of Plasma Physics</u>, vol. 12, no. 3, Mar 1986, pp. 190-196.

94. M. A. Liberman and A. L. Velikovich, <u>Nuclear Fusion</u>, vol. 26, no. 6, Jun 1986, pp. 709-728.

95. A. E. Dangor, <u>Plasma Physics and Controlled Fusion</u>, vol. 28, no. 12B, Dec 1986, pp. 1931-1942.

96. N. A. Bobrova and T. L. Razinka, <u>Soviet Journal of Plasma Physics</u>, vol. 13, no. 1, Jan 1987, pp. 53-57.

97. B. F. Fishbine, PhD dissertation, Univ. New Mexico, Albuquerque, New Mexico, December 1984, pages 21-24.

98. J. H. Degnan, S. W. R. Warren, D. W. Price, M. P. Snell and R. J. Richter-Sand, <u>Bull. of American Physical Society</u>, vol. 29, no. 8, Oct 1984, p. 1232.

99. D. W. Price, J. H. Degnan, M. P. Snell and S. W. R. Warren, <u>Bull. of American Physical Society</u>, vol. 29, no. 8, Oct 1984, p. 1232.

100. M. P. Snell, J. H. Degnan, S. W. R. Warren and D. W. Price, <u>Bull. of American Physical Society</u>, vol. 29, no. 8, Oct 1984, p. 1232.

101. S. W. R. Warren, J. H. Degnan, C. W. Beason, D. W. Price, M. P. Snell and S. S. Payne, <u>Bull. of American Physical Society</u>, vol. 29, no. 8, Oct 1984, p. 1232.

102. J. H. Degnan, W. L. Baker, S. W. R. Warren, D. W. Price, M. P. Snell, R. J. Richter-Sand and P. J. Turchi, <u>Journal of Applied Physics</u>, vol. 61, no. 8, 15 Apr 1987, pp. 2763-2770.

103. C. W. Beason, Master's thesis, Air Force Institute of Technology, Wright-Patterson AFB, Ohio, Mar 1984.

104. S. W. R. Warren, J. H. Degnan, C. W. Beason, D. W. Price and M. P. Snell, <u>Journal of Applied Physics</u>, vol. 61, no. 8, 15 Apr 1987, pp. 2771-2777.

105. I. F. Kvartskhava, R. D. Meladze and K. V. Suladze, <u>Soviet Physics--Technical Physics</u>, vol. 5, no. 3, Sep 1960, pp. 266-273.

106. S. W. Kash, _Plasma Acceleration_, S. W. Kash, ed., Stanford University Press, Stanford, California, 1960, pp. 79-93.

107. C. J. Michels and P. Ramins, _The Physics of Fluids_, vol. 7, no. 11, pt. 2, Nov 1964, pp. S71-S74.

108. R. G. Jahn, _Physics of Electric Propulsion_, McGraw-Hill Book Company, New York, NY, 1968, pp. 257-316.

109. S. D. Grishin, A. K. Litvak, S. N. Ogorodnikov et al., _Soviet Physics--Technical Physics_, vol. 22, no. 2, Feb 1977, pp. 280-283.

110. D. Y. Cheng and C. N. Chang, _Orbit-Raising and Maneuvering Propulsion: Research Status and Needs_, L. H. Caveny, ed., American Institute of Aeronautics and Astronautics, Inc., New York, NY, 1984, pp. 371-384.

111. N. T. Kozlov and Yu. S. Protasov, _Soviet Physics--Doklady_, vol. 20, no. 7, Jul 1975, pp. 500-501.

112. F. Hohl, J. H. Lee and D. R. McFarland, _IEEE Journal of Quantum Electronics_, vol. QE15, no. 9, Sep 1979, pp. 90D.

113. J. H. Lee, D. R. McFarland and F. Hohl, _Applied Optics_, vol. 19, no. 19, 1 Oct 1980, pp. 3343-3348.

114. H. Rieger and K. Kim, _Journal of Applied Physics_, vol. 54, no. 11, Nov 1983, pp. 6199-6212.

115. K. S. Han, S. H. Nam and J. H. Lee, _Journal of Applied Physics_, vol. 55, no. 11, 1 Jun 1984, pp. 4113-4115.

116. K. S. Han, C. H. Oh and J. H. Lee, _Journal of Applied Physics_, vol. 60, no. 10, 15 Nov 1986, pp. 3414-3416.

117. J. L. Tuck, _Physical Review Letters_, vol. 3, no. 7, 1 Oct 1959, pp. 313-315.

118. D. C. Hagerman and J. E. Osher, _The Physics of Fluids_, vol. 4, no. 7, Jul 1961, pp. 905-911.

119. J. E. Osher, _Physical Review Letters_, vol. 8, no. 8, 15 Apr 1962, pp. 305-309.

120. I. M. Zolototrubov, V. A. Kiselev, Yu. M. Novikov et al., _Soviet Physics--Technical Physics_, vol. 11, no. 6, Dec 1966, pp. 766-771.

121. P. Gloersen, _The Physics of Fluids_, vol. 12, no. 4, Apr 1969, pp. 945-947.

122. A. A. Kalmykov and S. A. Trubchaninov, _Soviet Physics--Technical Physics_, vol. 14, no. 10, Apr 1970, pp. 1379-1386.

123. H. de la Fuente, PhD dissertation, Univ. Wisconsin, Madison, Wisconsin, Aug 1970.

124. A. Ya. Kislov and A. I. Morozov, Soviet Physics--Technical Physics, vol. 15, no. 4, Oct 1970, pp. 595-598.

125. H. de la Fuente and H. K. Forsen, The Review of Scientific Instruments, vol. 42, no. 10, Oct 1971, pp. 1453-1455.

126. N. N. Glotova, V. I. Kazanskii, K. P. Kirdyashev et al., Soviet Physics--Technical Physics, vol. 23, no. 7, Jul 1978, pp. 779-783.

127. V. S. Komel'kov, V. V. Perebeinos and M. T. Solomonov, Soviet Journal of Plasma Physics, vol. 7, no. 1, Jan/Feb 1981, pp. 46-48.

128. H. L. Berk, J. H. Hammer and J. W. Shearer, The Physics of Fluids, vol. 25, no. 1, Jan 1982, pp. 102-106.

129. V. N. Lyashenko, Yu. V. Skvortsov, V. M. Strunnikov and S. S. Tserevitinov, Soviet Physics--JETP, vol. 57, no. 1, Jan 1983, pp. 41-46.

130. W. C. Turner, G. C. Goldenbaum, E. H. A. Granneman et al., The Physics of Fluids, vol. 26, no. 7, Jul 1983, pp. 1965-1986.

131. G. A. Askar'yan and A. A. Lerman, Soviet Physics--Technical Physics, vol. 10, no. 1, Jan 1984, pp. 21-22.

132. V. V. Sidnev, Yu. V. Skvortsov, V. G. Solov'eva and N. M. Umrikhin, Soviet Journal of Plasma Physics, vol. 10, no. 2, Mar/Apr 1984, pp. 230-234.

133. H. Bruhns, Plasma Physics and Controlled Fusion, vol. 28, no. 9A, Sep 1986, pp. 1389-1400.

134. A. A. Kalmykov, A. D. Timofeev and B. A. Shevchuk, Soviet Physics--Technical Physics, vol. 15, no. 12, Jun 1971, pp. 2002-2009.

135. A. G. Belikov, V. P. Goncharenko, D. K. Goncharenko et al., Soviet Physics--Technical Physics, vol. 16, no. 9, Mar 1972, pp. 1488-1491.

136. E. J. Strait and J. C. Sprott, Nuclear Fusion, vol. 18, no. 11, Nov 1978, pp. 1595-1598.

137. T. L. Buller, R. J. Turnbull and K. Kim, Applied Physics Letters, vol. 34, no. 12, 15 Jun 1979, pp. 826-828.

138. H. P. Furth, Journal of Vacuum Science and Technology, vol. 18, no. 3, Apr 1981, pp. 1073-1080.

139. A. A. Harms and M. Heindler, Nuclear Science and Engineering, vol. 66, no. 1, Apr 1978, pp. 1-8.

140. J. H. Lee, Atomkernenergie, vol. 32, no. 1, 1978, pp. 76-84.

141.   A. V. Donskoi, V. S. Klubnikin and R. I. Kenkhi, <u>Welding Production</u>, vol. 25, no. 2, Feb 1978, pp. 8-10.

142.   I. S. Shapiro et al., <u>Welding Production</u>, vol. 26, no. 1, Jan 1979, pp. 39-42.

143.   I. M. Shapiro and Z. M. Barkan, <u>Welding Production</u>, vol. 29, no. 11, Nov 1982, pp. 28-30.

144.   S. P. Chow, S. Lee and B. C. Tan, <u>Journal of Plasma Physics</u>, vol. 8, pt. 1, Aug 1972, pp. 21-31.

145.   P. J. Turchi, G. Bird, C. B. Boyer et al., <u>Ultrahigh Magnetic Fields: Physics, Techniques, Applications</u>, V. M. Titov and G. A. Shvetsov, eds., Nauka, Moscow, USSR, 1984, pp. 145-159.

146.   O. Milton, <u>IEEE Transactions on Electrical Insulation</u>, vol. EI-7, no. 1, 1972, pp. 9-15.

147.   Maxwell Laboratories, Inc., San Diego, California, 1982, Maxwell Bulletin no. MLB-2038A.

148.   Maxwell Laboratories, Inc., San Diego, California, Mar 1983, Engineering Bulletin.

149.   J. H. Degnan and R. E. Reinovsky, report no. AFWL-TR-75-265, Air Force Weapons Laboratory, Kirtland AFB, New Mexico, Mar 1976.

150.   J. H. Degnan, R. E. Reinovsky, D. L. Honea and R. D. Bengtson, <u>Journal of Applied Physics</u>, vol. 52, no. 11, Nov 1981, pp. 6550-6561.

151.   I. Henins and J. Marshall, <u>Status Report of the LASL Controlled Thermonuclear Research Program for the 12-Month Period Ending Oct 31, 1968</u>, report no. LA-4075-MS, Los Alamos Scientific Laboratory, Los Alamos, New Mexico, 15 Jan 1969, pp. 48-52.

152.   I. Henins and J. Marshall, <u>Review of Scientific Instruments</u>, vol. 40, no. 7, Jul 1969, pp. 875-878.

153.   D. H. Birdsall and P. E. Ping, <u>Review of Scientific Instruments</u>, vol. 36, no. 7, Dec 1965, pp. 1777-1778.

154.   L. K. Len, <u>op cit</u>, pp. 20-23.

155.   S. L. Leonard, <u>Plasma Diagnostic Techniques</u>, R. H. Huddlestone and S. L. Leonard, eds., Academic Press, New York, NY, 1965, pp. 8-13.

156.   V. Nassisi and A. Luches, <u>Review of Scientific Instruments</u>, vol. 50, no. 7, Jul 1979, pp. 900-902.

157.   D. G. Pellinen, M. S. DiCapua, S. E. Sampayan et al., <u>Review of Scientific Instruments</u>, vol. 51, no. 11, Nov 1980, pp. 1535-1540.

158.   L. K. Len, <u>op cit</u>, p. 29.

159. F. W. Grover, Inductance Calculations: Working Formulas and Tables, Dover Publications, Inc., New York, NY, 1962, pp. 151-155.

160. C. R. McClenahan, report no. AFWL-TR-80-113, Air Force Weapons Laboratory, Kirtland AFB, New Mexico, Jan 1981, pp. 3-5.

161. Maxwell Laboratories, Inc., report no. MLR-1669, San Diego, California, Feb 1984, pp. 3-159-3-161.

162. J. H. Degnan, R. J. Sand, G. F. Kiuttu and D. M. Woodall, Low Energy X-Ray Diagnostics--1981, Monterey, AIP Conf. Proc., no. 75, D. T. Attwood and B. L. Henke, eds., pp. 264-269.

163. R. J. Lanter and D. E. Bannerman, report no. LA-3498-MS, Los Alamos Scientific Laboratory, Los Alamos, New Mexico, 14 Jul 1966.

164. T. Mukaiyama and J. Geiger, report no. 73, Laboratory for Laser Energetics, Univ. Rochester, Rochester, NY, Mar 1978.

165. J. K. Tuli, "Nuclear Wallet Cards," Brookhaven National Laboratory, Upton NY, Jan 1985.

166. R. C. Weast, ed., Handbook of Chemistry and Physics, 68th edition, CRC Press, Inc., Boca Raton, Florida, 1987, pp. B-274-B-275.

167. W. J. Price, Nuclear Radiation Detection, 2nd Edition, McGraw-Hill Book Company, New York, NY, 1964, pp. 17-20.

168. J. W. Mather, private communication.

169. D. L. Book, NRL Plasma Formulary, 1987 revision, NRL Publication 0084-4040, Naval Research Laboratory, Washington, D.C., 1987, p. 28.

170. R. A. Alpher and D. R. White, Plasma Diagnostic Techniques, R. H. Huddlestone and S. L. Leonard, eds., Academic Press, New York, NY, 1965, pp. 442-446.

171. S. L. Leonard, op cit, pp. 45-53.

172. S. L. Leonard, ibid., pp. 28-29.

173. H. Alfven, On the Origin of the Solar System, Oxford University Press, Oxford, England, 1954.

174. I. Axnäs, report no. TRITA-EPP-72-31, Department of Plasma Physics, Royal Institute of Technology, Stockholm, Sweden, Dec 1972.

175. I. Axnäs, report no. TRITA-EPP-76-02, Department of Plasma Physics, Royal Institute of Technology, Stockholm, Sweden, Apr 1976.

176. I. Axnäs, Astrophysics and Space Science, vol. 55, no. 1, May 1978, pp. 139-146.

177. I. Axnäs, report no. TRITA-EPP-81-07, Department of Plasma Physics, Royal Institute of Technology, Stockholm Sweden, Dec 1981.

178. M. A. Raadu, report no. TRITA-EPP-77-02, Department of Plasma Physics, Royal Institute of Technology, Stockholm Sweden, Jan 1977.

179. M. A. Raadu, Journal of Physics D: Applied Physics, vol. 11, no. 3, 21 Feb 1978, pp. 363-378.

180. M. Rosenbluth, report no. LA-1850, Los Alamos Scientific Laboratory, Los Alamos, New Mexico, 14 Sep 1954.

181. B. H. Fishbine, op cit, pp. 68-77.

182. C. Gourlan, H. Kroegler, C. Maisonnier et al., Energy Storage, Compression, and Switching, vol. 2, V. Nardi, H. Sahlin and W. H. Bostick, eds., Plenum Press, New York, NY, 1983, pp. 221-245.

183. J. W. Mather, Methods of Experimental Physics, vol. 9, pt. B. R. H. Lovberg and H. R. Griem, eds., Academic Press, New York, NY, 1971, pp. 187-249.

184. B. H. Fishbine, op cit, pp. 44-46.

185. L. Spitzer, Jr., Physics of Fully Ionized, 2nd Edition, Interscience Publishers, New York, NY, 1962.

186. F. F. Chen, Introduction to Plasma Physics and Controlled Fusion 2nd edition, vol. 1, Plenum Press, New York, NY, 1984, p. 183.

187. D. L. Book, op cit, p. 34.

188. D. L. Book, ibid., p. 37.

189. F. F. Chen, op cit, p. 181.

190. B. F. Fishbine, op cit, p. 12.

191. M. Cowan, private communication.

APPENDIX A

PUFF CAPACITOR BANK OPERATING PROCEDURES

1. Check that diagnostics and cabling is in place and connected.

2. Check that screen room power and air conditioning are on.

3. Check that oscilloscopes, oscilloscopes triggers, delays and cameras are ready.

4. Check that pre-fire feedback connections are correct.

5. Check that the switch gas is correct in pressurized switches.
   Bank switch gas--15% SF_6 in Ar. For operation at ± 30, 40, 50 kV, set gas at 41, 53, 65 psig pressure.
   Master trigger generator--synthetic air. 90 psig pressure.
   Planar triode--synthetic air. 50 psig pressure.
Prior to setting switch gas:
   Set gas flow on.
   Set synthetic air regulator at 100 psig pressure.
   Set SF_6/Ar gas mixture input at 70 psig pressure.
   Set master trigger generator planar input to 100 psig pressure.
   Set master trigger generator triode synthetic air flow to 200 cc/min.
   Purge SF_6/Ar in bank switches for 1 minute, then set pressure.

6. Check and record bank switch pressures in the north and south switches.

7. Lock and secure outer door to PUFF area.

8. Clear bank area of unnecessary personnel.

9. Visually inspect transmission line. Clear all tools and unneccessary items from PUFF bank.

10. Remove overhead crane from PUFF area. Turn off crane power.

11. Check that D_2 gas lines are properly connected.

12. Check primary gas valve plug. Set the plug pressure at 2000 psig.

13. Check primary gas valve plug for electrical continuity.

14. Turn on console power to the PUFF bank.

15. Set the master trigger generator high voltage to 0.0.

16. Turn on master trigger generator and planar triode. (5 minute warm-up required.)

17. Set master trigger generator and planar triode gas flow to 0.

18. Check deadsticks for proper resistance (330 Ω).

19. Wipe down trigger surfaces to remove excess dust.

20. Perform pre-fire response test. Apply a 3.0 V signal into the master trigger generator mixer. Verify planar triode fires.

21. Set primary valve trigger high voltage to +2000 V.

22. Check krytron and ignitron switch operation.

23. Set planar triode high voltage to 25 kV.

24. Set master trigger generator high voltage to 58 kV.

25. Perform planar triode and master trigger generator trigger checks.

26. Flush the planar triode and the master trigger generator. Perform a 15 second flush and then set the gas flow to 200 cc/min.

27. Verify a minimum of 200 psig pressure of SF_6/Ar and synthetic air at gas bottle.

28. Announce 5 minute warning. Turn off lights in PUFF area.

29. Verify plug pressure is 2000 psig.

30. Fill D_2 gas valve plenum to the correct pressure (generally 900 psig for the lower valve and 45 psig for the upper valve).

31. Verify vacuum pressure is acceptable ($\lesssim 10^{-4}$ Torr).

32. Turn off vacuum gauges and gauge controllers. Remove gauge fuses. Disconnect ion gauge.

33. Prepare cameras to view PUFF bank. Open film for exposure.

34. Clear PUFF area.

35. Remove deadsticks.

36. Close door to PUFF area. Engage interlocks.

37. Charge gas valve banks. (Bottom gas valve set to -6 kV.)

38. Prepare the screen room.
    Turn on silver detector high voltage (+900 V).
    Reset oscilloscopes, delays and triggers.
    Turn on scintillator neutron detector high voltage (-2600 V).
    Open camera shutters.

39. Set valve delay to lower valve.

40. If used, set valve delay to upper valve.

41. Turn on warning light and siren power (28 V).

42. Turn on bank charging power supply.

43. Push the bank charge reset button.

44. Charge PUFF capacitor bank.

45. Close D_2 fill valve.

46. Fire bank trigger and close high vacuum valve.

47. Close camera shutters. Pull film from oscilloscope cameras.

48. Verify capacitor bank was discharged.

49. Dump all capacitor banks.

50. Turn off bank charging supply.

51. Turn off all high voltages except silver detector power supply.
    Turn off master trigger generator and planar triode high voltage.

52. Open interlocked door to PUFF area.

53. Deadstick all banks.·

54. Pull film from cameras viewing PUFF bank.

55. Turn off warning light and siren power.

56. Turn on PUFF area lights.

57. Pump up hydraulic jack (to seal lower gas valve).

58. Open roughing valve.

59. Install new plug in lower gas valve.

60. Mark backs of film (oscillograms).

61. Purge gas switches.
    Purge bank switches for 1 minute.
    Purge master trigger generator for 15 seconds.
    Purge planar triode for 15 seconds.

62. If more shots are desired, return to step 11. If no more shots are
    desired:
    Close all gas bottle valves and set gas flow to 0.
    Turn off silver detector high voltage.
    Turn off console and screen room power.

63. Before departing, verify all power is off and all gas bottles
    secured.

APPENDIX B

LISTING OF SLUG MODEL PROGRAM

This FORTRAN program listing is provided to document the slug model
modeling plasma behavior in a coaxial plasma gun. The program was
written by Dr. James H. Degnan (AFWL/AWPP) and subsequently modified by
David W. Price (AFWL/AWPP). The model assumes lumped elements and
performs a simple integration to predict plasma slug behavior.

The model assumes fixed capacitance C (the driving capacitance),
two fixed inductances LO1 and LO2 and a fixed resistance R. LO1 is the
inductance up to the physical location of the voltage monitor. LO2 is
the inductance from the voltage monitor to the load inductance. Both
LO1 and LO2 are system inductances; the sum of LO1 and LO2 equals the
total system inductance. The system resistance is fixed at R. Strictly
speaking, this is not accurate, but for the O-D analysis this
calculation provides, the accuracy is sufficient. The LLOAD inductance
is the time varying load resistance. It varies linearly with the axial
position of the slug in plasma gun channel.

The program is heavily commented. The user should read through
these comments before proceeding to program use.

Attached to the end of the program listing is a sample input file.
The user will need to modify the input to suit the modeled circuit.

The program is currently hosted on the AFWL/AWPP VAX 11/750. The
source code may have to be modified for different computer systems.

```
      PROGRAM CLIN
C
C     This program calculates the inductance, voltages and current delivery
C     for a coaxial plasma gun with a plasma acting as a plasma armature.
C
C     The model assumes three inductances -- two system inductances
C     and a time varying load inductance.  All other circuit parameters are
C     lumped constants.
C
C     The lumped circuit model looks like the schematic below:
C
C        ------------/L01/------/L02/---------/Lload/-------- .
C        |           |   __   |   __           ____       |
C        |           |        |                           |
C        |           VP       |                          ___
C        |           |        |                         | R |
C        ---------    C       |                         |___|
C        |           |        |                           |
C        |           |        |                           |
C        |_____|_____|_____|
C
C
C     where in this model,
C           C is the total capacitance of the system (assumed system driver),
C           L01 is the inductance of the system at the voltage probe VP,
C           L02 is the system inductance after the voltage probe VP,
C           Lload is the time-varying load inductance and
C           R is the total lumped system resistance.
C
C     The current drives a plasma along the axis of the coaxial plasma gun.
C     It then acts as an armature to carry current along the length of the gun.
C     This changes the inductance of the gun and the performance of the system.
C
C     The plasma slug motion is calculated by a 0-D slug model using fixed time
C     steps and coupled finite difference equations.
C
C     The plasma slug is assumed infinitesimally thin and azimuthally and
C     radially uniform.  It is driven by J x B forces along the length of the
C     coaxial plasma gun.
C
C     All units are rationalized MKSA (meters/kilograms/seconds/amperes).
C
C     Identified parameters are:
C
C     A1 -- acceleration of the plasma slug before iteration
C     A2 -- acceleration of the plasma slug after iteration
C     C -- the system capacitance; input
C     CURRENT(I) = the calculated system current
C     DT -- the time step for system calculation
C     EO -- the total system energy
C     EC -- the time-varying energy stored in the capacitance C
C     EK -- the kinetic energy of the plasma slug
C     EL -- the magnetic energy stored in the total inductance
```

```
C    ER1 -- the dissipated ohmic energy before iteration
C    ER2 -- the dissipated ohmic energy after iteration
C    ET -- total system energy
C    I1 -- the system current before iteration
C    I2 -- the system current after iteration
C    IDOT1 -- the calculated dI/dt before iteration
C    IDOT2 -- the calculated dI/dt after iteration
C    IMAX -- the calculated maximum current = VZERO/Z
C    LO1 -- the time-invariant system inductance before the voltage probe VP;
C           input
C    LO2 -- the time-invariant system inductance after the voltage probe VP;
C           input
C    L1 -- the total calculated system inductance before iteration
C    L2 -- the total calculated system inductance after iteration
C    LDOT1 -- the calculated dL/dt before iteration
C    LDOT2 -- the calculated dL/dt after iteration
C    LLOAD(I) -- the calculated time-varying load inductance array
C    LZERO -- the total time-invariant system inductance = LO1 + LO2
C    M -- the mass of the plasma slug
C    MU -- the permeability of free space = 4.0E-7 * pi H/m
C    PI -- the fundamental mathematical constant
C    PK -- LDOT2 * I1 * I1/2.0E0
C    Q1 -- the total charge on the capacitance before iteration
C    Q2 -- the total charge on the capacitance after iteration
C    RATIO -- the calculated system energy over the initial system energy
C            = ET/EO
C    RES -- the total system resistance; input
C    RI -- the coaxial inner radius; input
C    RO -- the coaxial outer radius; input
C    T1 -- the time step before iteration
C    T2 -- the time step after iteration
C    TAU -- the quarter cycle rise time of the system
C           = (pi/2.0E0)  * SQRT(LZERO*C)
C    TIME(I) -- the calculated time array
C    V1 -- the plasma velocity before iteration
C    V2 -- the plasma velocity after iteration
C    VC -- the capacitor voltage
C    VLOAD(I) -- the calculated load voltage array
C    VP(I) -- the calculated probe voltage array for a single step
C    VZERO -- the system voltage at time t = 0.0E0; input
C    XK -- a parameter used to vary the amount of data printed out.  As
C          currently given, the number of time steps printed out to hard copy
C          is the integer value of 3000/XK.
C    XL -- the power of 10 calculated for the time step.  The time step is
C          roughly 10.0E0 * XL (where XL is approximately ALOG10(TAU)).
C    Z -- the effective impedance of the circuit
C         = SQRT(LZERO/C)
C    Z1 -- the axial position of the plasma before iteration
C    Z2 -- the axial position of the plasma after iteration
C    ZX(I) -- the calculated (axial) position array of the plasma slug
C
C
C    The value of I presently varies from 1 to 3001.
C
```

257

```
C
C          The system equations are given below:
C
C                    Q = C * V  (for the capacitance)
C
C                    V = dL/dt * I + L * dI/dt (for the inductors)
C
C                    Q/C = VC = (L01 + L02 + Lload) * dI/dt +
C                               (dL/dt + R) * I
C
C                    Lload = MU * z * ALOG(RO/RI)/(2 * pi)
C
C                    d(Lload)/dt = MU * v * ALOG(RO/RI)/(2 * pi)
C
C                    F = M * a
C
C                    a = MU * ALOG(RO/RI) * I * I/(2.0E0 * pi * M)
C
C                    a = dv/dt
C
C                    v = dz/dt
C
C                    VP = (L02 + Lload) * dI/dt + (d(Lload)dt + R) * I
C
C                    Vload = Lload * dI/dt + (d(Lload)/dt + R) * I
C
C
C          This code was originally written by Dr. James H. Degnan and was
C          subsequently modified by David W. Price.
C
C          The following Tektronix plot compatible files are output under this code:
C
C                 LLOAD.DAT -- the load inductance
C                 SLUGI.DAT -- the slug current
C                 V.DAT -- the slug velocity
C                 VLOAD.DAT -- the load voltage
C                 VPROBE.DAT -- the probe voltage
C                 Z.DAT -- the plasma axial distance
C
C          The data file -- CLIN.DAT -- outputs the total code results.
C
C
C
          REAL A1, A2, C, DT, EO, EC, EK, EL, ER1, ER2, ET, I1, I2, IDOT1,
         1 IDOT2, IMAX, L01, L02, L1, L2, LDOT1, LDOT2, LZERO, M, MU, PI,
         2 PK, Q1, Q2, RATIO, RES, RI, RO, T1, T2, TAU, V1, V2, VC, VZERO,
         3 XK, XL, Z, Z1, Z2, ZL
          REAL TIME(3001), CURRENT(3001), VEL (3001), VP(3001), ZX(3001),
         1 VLOAD(3001), LLOAD(3001)
          PI = 4.0E0 * ATAN(1.0E0)
          MU = 4.0E-7 * PI
C
C***  OPEN FILES FOR DATA.  NOTE: ALL UNITS ARE MKS
C
          OPEN(UNIT=1,NAME='CLIN.INP',TYPE='OLD',READONLY)
```

```fortran
      OPEN(UNIT=2,NAME='CLIN.DAT',TYPE='NEW')
      OPEN(UNIT=3,NAME='SLUGI.DAT',TYPE='NEW')
      OPEN(UNIT=4,NAME='VPROBE.DAT',TYPE='NEW')
      OPEN(UNIT=5,NAME='Z.DAT',TYPE='NEW')
      OPEN(UNIT=6,NAME='VLOAD.DAT',TYPE='NEW')
      OPEN(UNIT=7,NAME='LLOAD.DAT',TYPE='NEW')
      OPEN(UNIT=8,NAME='V.DAT',TYPE='NEW')
C
C***  INPUT DATA
C
  101 CONTINUE
      READ (1,*) C, VZERO, LO1, LO2, RES
      LZERO = LO1 + LO2
    9 FORMAT(A)
      IF (C.LE.0.0E0) GO TO 999
  102 CONTINUE
      READ (1,*) RI, RO, M, Z1
      IF (RI.LE.0.0E0) GO TO 101
      TAU = (PI/2.0E0) * (SQRT(LZERO*C))
      XL = ALOG10(TAU) + 5.0E-1
      IF ((XL-JNINT(XL)).LE.5.0E-1) XL = FLOAT(JNINT(XL)) - 1.0E0
      IF ((XL-JNINT(XL)).GT.5.0E-1) XL = FLOAT(JNINT(XL))
      Z = SQRT(LZERO/C)
      IMAX = VZERO/Z
      WRITE (2,*)
      WRITE (2,*) ' L1 = ', LO1, ' L2 = ', LO2, ' LZERO = ', LZERO
      WRITE (2,*)
      WRITE (2,20)
   20 FORMAT(1H1,///,1X,'    C           VZERO        LZERO       RES
     1        TAU          Z         IMAX         RI         RO         Z1'
     2,'           M',/)
      WRITE (2,21) C, VZERO, LZERO, RES, TAU, Z, IMAX, RI, RO, Z1, M
   21 FORMAT (1X,11(1PE10.3,1X))
      WRITE (2,*)
      WRITE (2,23)
C
C***  OUTPUT TABLE HEADING
C
   23 FORMAT(1X,'    T           I           Z           V           A
     1           VC          EC          KE          PK          VPROBE      ',
     2' RATIO',//)
C
C***  DEFINE INITIAL VALUES
C
      T1 = 0.0E0
      TIME(1) = 0.0E0
      I1 = 0.0E0
      CURRENT(1) = 0.0E0
      Z1 = 0.0E0
      ZX(1) = 0.0E0
      V1 = 0.0E0
      VEL(1) = 0.0E0
      VP(1) = VZERO * (LO2/LZERO)
      VLOAD(1) = 0.0E0
```

259

```
              A1 = 0.0E0
              EO = 0.5E0 * C * VZERO * VZERO
              IDOT1 = VZERO/LZERO
              DT = 1.0E-3 * 10**XL
              L1 = LZERO
              Q1 = C * VZERO
              ER1 = 0.0E0
              RATIO = 1.0E0
              EC = Q1 * Q1/(2.0E0 * C)
              EK = M * V1 * V1/2.0E0
              PK = I1 * I1 * LDOT1/2.0E0
              LLOAD(1) = 0.0E0
              WRITE (2,21) T1, I1, Z1, V1, A1, VZERO, EC, EK, PK, VP(1), RATIO
C
C***   ITERATION LOOP
C
              DO 103 K = 1,3000
              ICOUNT = k + 1
              T2 = T1 + DT
              TIME(K+1) = T2
              I2 = I1 + IDOT1 * DT
              CURRENT(K+1) = I2
              IDOT2 = (1.0E0/L1) * ((Q1/C)-(I1*(LDOT1+RES)))
              Q2 = Q1 - I1 * DT
              V2 = V1 + A1 * DT
              VEL(K+1) = V2
              Z2 = Z1 + 0.5E0 * (V1+V2) * DT
              ZX(K+1) = Z2
              A2 = (MU/(4.0E0*PI)) * (ALOG(RO/RI)) * (I2*I2/M)
              L2 = L1 + LDOT1 * DT
              LLOAD(K+1) = MU * Z2 * ALOG(RO/RI)/(2.0E0*PI)
              LDOT2 = MU * V2 * ALOG(RO/RI)/(2.0E0*PI)
              VLOAD(K+1) = (LLOAD(K+1)) * IDOT2 + (LDOT2 + RES) * I2
              VP(K+1) = (LO2 + LLOAD(K+1)) * IDOT2 + (LDOT2 + RES) * I2
              ER2 = ER1 + I1 * I1 * RES * DT
              EK = 0.5E0 * M * V2 * V2
              EL = 0.5E0 * L2 * I2 * I2
              EC = Q2*Q2/(2.0E0*C)
              VC = Q2/C
              ET = EC + EK + EL + ER2
              RATIO = ET/EO
              PK = 0.5E0 * I2 * I2 * LDOT2
              IF (V2.GE.0.0E0) GO TO 105
                  WRITE(2,21) T2, I2, Z2, V2, A2, VC, EC, EK, PK, VP(K+1), RATIO
              GO TO 999
          105 CONTINUE
              Z1 = Z2
              T1 = T2
              I1 = I2
              Q1 = Q2
              L1 = L2
              IDOT1 = IDOT2
              LDOT1 = LDOT2
              ER1 = ER2
```

```fortran
      V1 = V2
      A1 = A2
      XK = FLOAT(K)/1.OE1
      IF((XK-INT(XK)).LE.1.0E-5*XK)
     1 WRITE(2,21) T1,I1,Z1,V1,A1,VC,EC,EK,PK,VP(K+1),RATIO
C
C*** AT THIS POINT THE CALCULATION IS LIMITED.  IF THE AXIAL DISTANCE IS
C*** IS LONGER THAN THE INPUT VALUE OF THE LENGTH OF THE GUN, THE CALCULATION
C*** IS ENDED.  IF THE COAXIAL GUNS USED ARE OF DIFFERENT LENGTHS, THE USER
C*** WILL HAVE TO CHANGE THIS LIMITING VALUE.
C
      ZL = 4.6335E-1
      IF (Z2.GT.ZL) GO TO 106
C
C*** TEST FOR ENERGY RATIO.  IF THE ENERGY RATIO IS OFF BY MORE THAN 3%, END
C*** THE CALCULATION.
C
      IF (ABS(1.0EO-RATIO).GE.3.OE-2) THEN
         WRITE (2,*)
         WRITE (2,*) ' Count at termination = ', K
         WRITE (2,*) '          Energy ratio = ', RATIO
         WRITE (2,*)
         GO TO 106
      ENDIF
  103 CONTINUE
C
C***  OUTPUT DATA
C
  106 CONTINUE
      KOUNT = 0
      DO I = 2, ICOUNT/10 + 1
         IF (ZX(10*I-9).EQ.0.0EO) KOUNT = KOUNT + 1
      ENDDO
      WRITE (3,9) ' Slug current '
      WRITE (3,*) ICOUNT/10 + 1 - KOUNT
      WRITE (4,9) ' Probe voltage '
      WRITE (4,*) ICOUNT/10 + 1 - KOUNT
      WRITE (5,9) ' Axial distance '
      WRITE (5,*) ICOUNT/10 + 1 - KOUNT
      WRITE (6,9) ' Load voltage '
      WRITE (6,*) ICOUNT/10 + 1 - KOUNT
      WRITE (7,9) ' Load inductance '
      WRITE (7,-) ICOUNT/10 + 1 - KOUNT
      WRITE (8,9) ' Slug velocity '
      WRITE (8,*) ICOUNT/10 + 1 - KOUNT
      DO J = 1, ICOUNT/10 + 1 - KOUNT
         WRITE (3,*) TIME(10*J-9)
         WRITE (4,*) TIME(10*J-9)
         WRITE (5,*) TIME(10*J-9)
         WRITE (6,*) TIME(10*J-9)
         WRITE (7,*) TIME(10*J-9)
         WRITE (8,*) TIME(10*J-9)
      ENDDO
      DO J = 1, ICOUNT/10 + 1 - KOUNT
```

```
      WRITE (3,*) CURRENT(10*J-9)
      WRITE (4,*) VP(10*J-9)
      WRITE (5,*) ZX(10*J-9)
      WRITE (6,*) VLOAD(10*J-9)
      WRITE (7,*) LLOAD(10*J-9)
      WRITE (8,*) VEL(10*J-9)
   ENDDO
   GO TO 999
999 CONTINUE
   DO I = 1, 8
   CLOSE(UNIT=I)
   ENDDO
   STOP
   END
```

A typical input file (the input used to generate in this dissertation) is provided for the CLIN program. All data is in SI metric units. The data is input in two lines of free format. The input file format is as follows:

First line --
   first entry   C, system capacitance (in Farads)
   second entry   VZERO, initial system voltage (in Volts)
   third entry   LO1, fixed inductance prior to voltage probe (in Henries)
   fourth entry   LO2, fixed inductance after voltage probe (in Henries)
   fifth entry   RES, fixed system resistance (in Ohms)

Second line --
   first entry   RI, coaxial gun inner radius (in meters)
   second entry   RO, coaxial gun outer radius (in meters)
   third entry   M, mass of the plasma sheath (in kilograms)
   fourth entry   Z1, the initial position of the plasma sheath (in meters)

   72.0E-6   6.00E+4   8.20E-9   20.8E-9   1.00E-3
   0.0651   0.0889   1.00E-7   0.0

262

APPENDIX C

LISTING OF DATA MANIPULATION PROGRAM

In this appendix, a listing of the FORTRAN source code for the data manipulation program is given. This program is written especially for the manipulation of digitized data traces in a specific format. Although there are certainly other, probably better, computer programs available for manipulating and revising raw data, the author did not have access to these codes when he needed them. Because he needed data manipulation and data analysis tools, the author wrote and assembled the FORTRAN program which source code follows.

This code is interactive and menu-driven (asking for specific keyboard responses). It is designed to be "user friendly" both at the interactive user and at the programmer level. The interactive user will find many of the program and subprogram concepts explained through the use of user prompts. The programmer will find embedded program comments to show the logic of subroutines and of the program as a whole. The code is modular so that sections can be extracted, revised, deleted and inserted with a minimum of impact on the rest of the program. Through the use of modular code segmentation, the program has the potential for further expansion. The program is not in a state of perfection, however. All portions of the program have been run and examined for correct responses; not all portions of the code have been extensively tested and could contain "bugs" or other unidentified problems. Any comments and corrections would be greatly appreciated.

The data manipulation program outputs data in terms of calculated data to the screen and program generated output files. Program generated output files (with the exception of output from the MAXMIN and MEANY SUBROUTINEs) are in the same format as the input files.

The data input and output files are in ASCII text. The user should know the data input files _must_ have the following format:

(one line) TITLE OF DATA FILE

(one line; a single integer N--1.LE.N.LE.1000) N

(many lines) N ordinate (X) data points; X_1, X_2, ..., X_N

(many lines) N abscissa (Y) data points; Y_1, Y_2, ..., Y_N

(many lines) The user may wish to comment the input data file following all the other input data. These comments are optional for input data files. However, these comments will not be transferred from the input to the output file. Except for the SUBROUTINEs FUNCTION and CURRENT, comments are not appended to any output files by the data manipulation program.

The integer limit N in the second input data line may be changed, but it must be changed uniformly throughout the program. If this is not done, the program may not manipulate the data properly.

263

The program is currently hosted on the AFWL/AWPP VAX 11/780 computer. It is written in FORTRAN 77, so it should be able to be hosted on any computer having interactive and FORTRAN 77 capabilities.

It should be noted parts of this program are very CPU intensive and are very slow. (SUBROUTINEs INTEGRATE and REVISE that invoke SUBROUTINE SIMP are especially bad in this regard.) The program can use a great deal of CPU (core) time. The user should be aware of this to avoid problems with other users and computer operators.

The data manipulation program is internally titled ANALYZE. In its present state, the following SUBROUTINEs are called:

TRANSFORM -- linearly transforms X- and Y-axes of data traces

FUNCTION -- functionally transforms X- and Y-axes of data traces

ROTATE -- rotates X- and Y-axes through a calculated angle

BASELINE -- corrects X- and Y-axes for baseline slope

FILEC -- performs spline fit of the Y-axis data, allowing an increase/decrease in the number of data points

DIFFER -- performs a numerical differentiation on the Y-axis

INTEGRATE -- performs a Runge-Kutta 4th order integration on a spline fit of the Y-axis data

SUM -- adds the Y-axes of up to 10 data traces and outputs to another file

SUBTRACT -- subtracts the Y-axis of one data file from the Y-axis of another data file and outputs to a third file

MULTIPLY -- multiplies the Y-axes of up to 10 data traces and outputs to another file

DIVIDE -- divides the Y-axis of one data file by the Y-axis of another and outputs to a third file

AVERAGE -- averages the Y-axes of up to 10 data traces and outputs to another data file

INTCOR -- performs RC "droop correction" on the Y-axis

REVISE -- given input voltage and current traces, calculates inductances and associated data traces

CURRENT -- calculates a current trace from an input data file

MEANY -- calculates the arithmetic average of a portion of the Y-axis of a data trace

MAXMIN -- calculates the maxima and minima from a data trace, both from the X- and Y-axes

SMOOTH -- performs a running 7-point smoothing on the Y-axis of a data trace

EXCHANGE -- exchanges the X- and Y-axes of a data trace

FOURIER -- performs a Fourier smoothing of the Y-axis of a data trace

Additional importance SUBROUTINEs not directly called from the ANALYZE main program are:

DDIFFER -- performs a numerical differentiation for the INTCOR SUBROUTINE

SIMP -- performs an adaptive integration. It is called by SUBROUTINEs INTEGRATE and REVISE.

SPCOEF -- calculates cubic splines for data files. It is called by the SUBROUTINEs FILEC, INTEGRATE, SUM, SUBTRACT, MULTIPLY, DIVIDE, AVERAGE, REVISE, SMOOTH and FOURIER.

```
      PROGRAM ANALYZE
      CHARACTER*1 ANS, FILE
C
C     The ANALYZE program is a driver to allow the analysis of data from
C     oscilloscope pictures digitized to a Tektronix plot compatible
C     format.
C
C     Version current to 15 July 1987
C
    1 CONTINUE
      WRITE (*,11)
   11 FORMAT (1X,'This is the main menu.',//,
     1 6X,'A -- X- and Y-axes contraction/expansion and transformation'
     2  ,/,6X,'B -- X- and Y-axes functional transformation',/,6X,
     3 'C -- rotation of the X- and Y-axes through the origin',/,
     4  6X,'D -- baseline correction',
     5 /,6X,'E -- spline fit of file data',
     6 /,6X,'F -- differentiate',/,6X,'G -- ',
     7 'integrate',/,6X,'H -- add up to 10 traces',/,6X,'I -- ',
     8 'subtract one data trace from another',/,6X,
     9 'J -- multiply up to 10 traces',/,6X,'K -- divide one trace by'
     A  ,' another',/,6X,'L -- average up to 10 traces',/,6X,
     B 'M -- correction of trace data for passive RC integration ',
     C '"voltage droop"',/,6X,
     D 'N -- calculate an inductance trace, given voltage and current'
     E  ' trace',/,6X,'O -- calculate current traces',/,6X,
     F 'P -- calculate arithmetic average of a portion of y-axes of',
```

```
G   ' data trace',/,6X,'Q -- find the maximum and minimum of a ',
H   'trace',/,6X,'R -- 7 point smoothing',/,6X,'S -- exchange X- ',
I   'and Y-axes',/,6X,'T -- Fourier smoothing',/,6X,
J   'U (or any other character not previously cited)',
K   ' -- exit program',//,1X,'$ Which option do you'
L   ' want?  (Input a single letter for the option you want.)')
    READ (*,9) FILE
9 FORMAT (A)
    IF ((FILE.EQ.'A').OR.(FILE.EQ.'a')) THEN
        CALL TRANSFORM
        GO TO 1
        ENDIF
    IF ((FILE.EQ.'B').OR.(FILE.EQ.'b')) THEN
        CALL FUNCTION
        GO TO 1
    ENDIF
    IF ((FILE.EQ.'C').OR.(FILE.EQ.'c')) THEN
        CALL ROTATE
        GO TO 1
    ENDIF
    IF ((FILE.EQ.'D').OR.(FILE.EQ.'d')) THEN
        CALL BASELINE
        GO TO 1
    ENDIF
    IF ((FILE.EQ.'E').OR.(FILE.EQ.'e')) THEN
        CALL FILEC
        GO TO 1
    ENDIF
    IF ((FILE.EQ.'F').OR.(FILE.EQ.'f')) THEN
        CALL DIFFER
        GO TO 1
    ENDIF
    IF ((FILE.EQ.'G').OR.(FILE.EQ.'g')) THEN
        CALL INTEGRATE
        GO TO 1
    ENDIF
    IF ((FILE.EQ.'H').OR.(FILE.EQ.'h')) THEN
        CALL SUM
        GO TO 1
    ENDIF
    IF ((FILE.EQ.'I').OR.(FILE.EQ.'i')) THEN
        CALL SUBTRACT
        GO TO 1
    ENDIF
    IF ((FILE.EQ.'J').OR.(FILE.EQ.'j')) THEN
        CALL MULTIPLY
        GO TO 1
    ENDIF
    IF ((FILE.EQ.'K').OR.(FILE.EQ.'k')) THEN
        CALL DIVIDE
        GO TO 1
    ENDIF
    IF ((FILE.EQ.'L').OR.(FILE.EQ.'l')) THEN
        CALL AVERAGE
```

266

```
          GO TO 1
      ENDIF
      IF ((FILE.EQ.'M').OR.(FILE.EQ.'m')) THEN
          CALL INTCOR
          GO TO 1
      ENDIF
      IF ((FILE.EQ.'N').OR.(FILE.EQ.'n')) THEN
          CALL REVISE
          GO TO 1
      ENDIF
      IF ((FILE.EQ.'O').OR.(FILE.EQ.'o')) THEN
          CALL CURRENT
          GO TO 1
      ENDIF
      IF ((FILE.EQ.'P').OR.(FILE.EQ.'p')) THEN
          CALL MEANY
          GO TO 1
      ENDIF
      IF ((FILE.EQ.'Q').OR.(FILE.EQ.'q')) THEN
          CALL MAXMIN
          GO TO 1
      ENDIF
      IF ((FILE.EQ.'R').OR.(FILE.EQ.'r')) THEN
          CALL SMOOTH
          GO TO 1
      ENDIF
      IF ((FILE.EQ.'S').OR.(FILE.EQ.'s')) THEN
          CALL EXCHANGE
          GO TO 1
      ENDIF
      IF ((FILE.EQ.'T').OR.(FILE.EQ.'t')) THEN
          CALL FOURIER
          GO TO 1
      ENDIF
      IF ((FILE.EQ.'T').OR.(FILE.EQ.'t')) GO TO 999
 999  WRITE (*,50)
  50  FORMAT(1X,'$ Do you want to end the program? (Y o: N)')
      READ (*,9) ANS
      IF ((ANS.EQ.'Y').OR.(ANS.EQ.'y')) THEN
      WRITE (*,51)
  51  FORMAT (1X,'$ The program will terminate now!')
      STOP
      ENDIF
      GO TO 1
      END
```

```
      SUBROUTINE TRANSFORM
      DIMENSION XOLD(1000), XNEW(1000), YOLD(1000), YNEW(1000)
      REAL AX, AY, BX, BY, XTEMP1, XTEMP2, YTEMP1, YTEMP2
      INTEGER MX, MY, N
      CHARACTER*132 TITLE, INFILE, OUTFILE
```

```
          CHARACTER*1 ANS
C
C      This program calculates a linear transformation and expansion
C      and/or contraction of data according to the relations:
C
C          XNEW(I) = AX * XOLD(I) + BX - XTEMP1 - XTEMP2
C
C          YNEW(I) = AY * YOLD(I) + BY - YTEMP1 - YTEMP2
C
C           where AX, AY, BX and BY are input constants.
C
C           XTEMP1 = XOLD(MX) if 1.LE.MX.LE.N or
C                  = 0.0E0     if MX.LT.1 or MX.GT.N
C
C           XTEMP2 = XOLD(MY) if 1.LE.MY.LE.N or
C                  = 0.0E0     if MY.LT.1 or MY.GT.N
C
C           YTEMP1 = YOLD(MX) if 1.LE.MX.LE.N or
C                  = 0.0E0     if MX.LT.1 or MX.GT.N
C
C           YTEMP2 = YOLD(MY) if 1.LE.MY.LE.N or
C                  = 0.0E0     if MY.LT.1 or MY.GT.N
C
C      MX and MY are input offsets.  N is the number of data points.
C
 1        CONTINUE
          AX = 1.0E0
          AY = 1.0E0
          BX = 0.0E0
          BY = 0.0E0
          XTEMP1 = 0.0E0
          XTEMP2 = 0.0E0
          YTEMP1 = 0.0E0
          YTEMP2 = 0.0E0
          MX = 0
          MY = 0
 700      WRITE (*,5)
 5        FORMAT (1X,'$ Enter file name to be linearly transformed.')
          READ (*,9,ERR=700) INFILE
 701      WRITE (*,10)
 10       FORMAT (1X,'$ Enter output file name.')
          READ (*,9,ERR=701) OUTFILE
          OPEN (UNIT=5,STATUS='OLD',FILE=INFILE,READONLY)
          REWIND (UNIT=5)
          OPEN (UNIT=10,STATUS='NEW',FILE=OUTFILE)
          READ (5,9) TITLE
 9        FORMAT (A)
          READ (5, *) N
          READ (5, *) (XOLD(I), I = 1, N)
          READ (5, *) (YOLD(I), I = 1, N)
C
C      Prompt for input values of AX, AY, BX, BY, MX and MY.
C      If any of these values are not input explicitly, the default
C          values are used.
```

268

```fortran
C     The default values are:
C
C                      AX = AY = 1.0E0
C
C         BX = BY = XTEMP1 = XTEMP2 = YTEMP1 = YTEMP2 = 0.0E0.
C
   20 FORMAT(1X,'The transformation of the x- and y-axes are according',
     1   'to the relations',//,11X,
     2   'XNEW(I) = AX * XOLD(I) + BX - XTEMP1 - XTEMP2',/,11X,
     3   'YNEW(I) = AY * YOLD(I) + BY - YTEMP1 - YTEMP2',//,6X,
     4   'where AX, AY, BX and BY are input constants and XTEMP1, ',
     5   'XTEMP2,',/,6X,' YTEMP1 and YTEMP2 are functions of MX and ',
     6   'MY.',//,6X,'If 1.LE.MX.LE.N, XTEMP1 = XOLD(MX) and YTEMP1 = ',
     7   'YOLD(MX). ',/,6X,'Otherwise, XTEMP1 = YTEMP1 = 0.0E0.',/,6X,
     8   'If 1.LE.MY.LE.N, XTEMP2 = XOLD(MY) and YTEMP2 = YOLD(MY).',/,
     9    6X,'Otherwise, XTEMP2 = YTEMP2 = 0.0E0.',/)
        WRITE (*,20)
  702   WRITE (*,21)
   21 FORMAT (1X,'$ Do you want to input AX? (Y or N)')
        READ (*,9,ERR=702) ANS
        IF ((ANS.EQ.'Y').OR.(ANS.EQ.'y')) THEN
  703      WRITE (*,22)
   22 FORMAT (1X,'$ What is AX?')
           READ (*,*,ERR=703) AX
        ENDIF
  704   WRITE (*,23)
   23 FORMAT (1X,'$ Do you want to input AY? (Y or N)')
        READ (*,9,ERR=704) ANS
        IF ((ANS.EQ.'Y').OR.(ANS.EQ.'y')) THEN
  705      WRITE (*,24)
   24 FORMAT (1X,'$ What is AY?')
           READ (*,*,ERR=705) AY
        ENDIF
  706   WRITE (*,25)
   25 FORMAT (1X,'$ Do you want to input BX? (Y or N)')
        READ (*,9,ERR=706) ANS
        IF ((ANS.EQ.'Y').OR.(ANS.EQ.'y')) THEN
  707      WRITE (*,26)
   26 FORMAT (1X,'$ What is BX?')
           READ (*,*,ERR=707) BX
        ENDIF
  708   WRITE (*,27)
   27 FORMAT (1X,'$ Do you want to input BY? (Y or N)')
        READ (*,9,ERR=708) ANS
        IF ((ANS.EQ.'Y').OR.(ANS.EQ.'y')) THEN
  709      WRITE (*,28)
   28 FORMAT (1X,'$ What is BY?')
           READ (*,*,ERR=709) BY
        ENDIF
  710   WRITE (*,29)
   29 FORMAT (1X,'$ Do you want to input MX? (Y or N)')
        READ (*,9,ERR=710) ANS
        IF ((ANS.EQ.'Y').OR.(ANS.EQ.'y')) THEN
  711      WRITE (*,30)
```

```
   30 FORMAT (1X,'$ What is MX?')
          READ (*,*,ERR=711) MX
        ENDIF
  712    WRITE (*,31)
   31 FORMAT (1X,'$ Do you want to input MY? (Y or N)')
        READ (*,9,ERR=712) ANS
        IF ((ANS.EQ.'Y').OR.(ANS.EQ.'y')) THEN
  713      WRITE (*,32)
   32 FORMAT (1X,'$ What is MY?')
          READ (*,*,ERR=713) MY
        ENDIF
C
C
C
      IF ((MX.LT.1).OR.(MX.GT.N)) THEN
         XTEMP1 = 0.0E0
         YTEMP1 = 0.0E0
      ENDIF
      IF ((1.LE.MX).AND.(MX.LE.N)) THEN
         XTEMP1 = XOLD(MX)
         YTEMP1 = YOLD(MX)
      ENDIF
      IF ((MY.LT.1).OR.(MY.GT.N)) THEN
         XTEMP2 = 0.0E0
         YTEMP2 = 0.0E0
      ENDIF
      IF ((1.LE.MY).AND.(MY.LE.N)) THEN
         XTEMP2 = XOLD(MY)
         YTEMP2 = YOLD(MY)
      ENDIF
C
C     Output values of AX, AY, BX, BY, MX, MY, XTEMP1, XTEMP2, YTEMP1
C     and YTEMP2.
C
      WRITE (*,*)
      WRITE (*,*) ' AX = ', AX, ' AY = ', AY
      WRITE (*,*) ' BX = ', BX, ' BY = ', BY
      WRITE (*,*) ' MX = ', MX, ' MY = ', MY
      WRITE (*,*) ' XTEMP1 = ', XTEMP1, ' XTEMP2 = ', XTEMP2
      WRITE (*,*) ' YTEMP1 = ', YTEMP1, ' YTEMP2 = ', YTEMP2
      WRITE (*,*)
         DO 250 I = 1, N
         XNEW(I) = AX * XOLD(I) + BX - XTEMP1 - XTEMP2
  250    YNEW(I) = AY * YOLD(I) + BY - YTEMP1 - YTEMP2
         WRITE (10,9) TITLE(1:42)//'TRANSFORM/'//TITLE(58:132)
         WRITE (10, *) N
         WRITE (10, *) (XNEW(I), I = 1, N)
         WRITE (10, *) (YNEW(I), I = 1, N)
         CLOSE (UNIT=5)
         CLOSE (UNIT=10)
C
C     Query to see if more linear transformations are needed
C
  714    WRITE (*,35)
```

270

```
   35 FORMAT (1X,'$ Do you want to linearly transform any more data? ',
    1           '(Y or N)')
         READ (*,9,ERR=714) ANS
         IF ((ANS.EQ.'Y').OR.(ANS.EQ.'y')) GO TO 1
         WRITE (*,36)
   36 FORMAT (1X,'$ Subroutine TRANSFORM is ending now.')
         RETURN
         END
```

```
      SUBROUTINE FUNCTION
C
C     This subroutine will functionally transform a set of data.  In this
C     transformation, the X- and Y-arrays are transformed independently
C     of each other.
C
C     PLEASE NOTE:  In this routine, the number of data points is
C     limited to 1000.  If more data points are wanted, the subroutine
C     and the driver program must be appropriately modified.
C     Additionally, no more than 80 transformations should be run on a
C     single data file.  If more are run, the listing of transformations
C     (TRANSACT) will run out of space and the subroutine might bomb off.
C
      REAL XOLD(1000), XNEW(1000), YOLD(1000), YNEW(1000), YHIGH,
    1      YLOW, C
      INTEGER N, K
      CHARACTER*800 TRANSACT
      CHARACTER*132 INPUT, OUTPUT, TITLE
      CHARACTER*3 ANS3
      CHARACTER*1 ANS
    1 CONTINUE
      DO L = 1, 800
      TRANSACT(L:L) = ' '
      ENDDO
      K = 0
C
C     Input file data
C
  700 WRITE (*,11)
   11 FORMAT (1X,'$ Enter file name to be functionally transformed.')
    9 FORMAT (A)
      READ (*,9,ERR=700) INPUT
      OPEN (UNIT=1,NAME=INPUT,TYPE='OLD',READONLY)
      REWIND (UNIT=1)
  701 WRITE (*,12)
   12 FORMAT (1X,'$ Enter output file name.')
      READ (*,9,ERR=701) OUTPUT
      OPEN (UNIT=2,NAME=OUTPUT,TYPE='NEW')
      REWIND (UNIT=1)
      READ (1,9) TITLE
      READ (1,*) N
      READ (1,*) (XOLD(I), I = 1, N)
```

```
          READ (1,*) (YOLD(I), I = 1, N)
          DO I = 1, N
          XNEW(I) = XOLD(I)
          YNEW(I) = YOLD(I)
          ENDDO
          CLOSE (UNIT=1)
      2 CONTINUE
C
C      Query for which axes to be transformed
C
  702 WRITE (*,13)
   13 FORMAT (1X,'$ Do you want to transform the X-axis (X), transform',
     1    ' the Y-axis (Y)',/,2X,'or end the subroutine (E)?')
          READ (*,9,ERR=702) ANS
          IF ((ANS.EQ.'X').OR.(ANS.EQ.'x')) GO TO 200
          IF ((ANS.EQ.'Y').OR.(ANS.EQ.'y')) GO TO 500
          IF ((ANS.EQ.'E').OR.(ANS.EQ.'e')) GO TO 900
          GO TO 2
  200 CONTINUE
C
C      Query for kinds of X-axis transformation
C
  703 WRITE (*,201)
  201 FORMAT (1X,'X Functional Transform Menu:',/,
     1    6X,'X01 -- add a constant, X + C',/,
     2    6X,'X02 -- multiply by a constant, C * X (C.GT.0.0E0)',/,
     3    6X,'X03 -- square root, SQRT(X) (X.GE.0.0E0)',/,
     4    6X,'X04 -- natural logarithm, ALOG(X) (X.GT.0.0E0)',/,
     5    6X,'X05 -- common logarithm, ALOG10(X) (X.GT.0.0E0)',/,
     6    6X,'X06 -- exponential, EXP(X)',/,
     7    6X,'X07 -- arctangent, ATAN(X)',/,
     8    6X,'X08 -- hyperbolic sine, SINH(X)',/,
     9    6X,'X09 -- hyperbolic tangent, TANH(X)',/,
     1    6X,'X10 -- take X to a power, X**C (X.GE.0.0E0, C.GT.0.0E0)',/,
     2    6X,'X11 -- take a number to a power of X, C**X (C.GT.0.0E0)',/,
     3    6X,'X12 -- end X transform and go to function main menu.',//,
     4    1X,'$ Which transform do you want? (X##)')
  206 FORMAT (1X,'The X value has been limited at I = ',I6,' to X = ',
     1    1PE16.8)
          READ (*,9,ERR=703) ANS3
          IF ((ANS3.EQ.'X01').OR.(ANS3.EQ.'x01')) THEN
             C = 0.0E0
  704        WRITE (*,202)
  202        FORMAT (1X,'$ What is the constant C?')
             READ (*,*,ERR=704) C
             DO I = 1, N
             XNEW(I) = XNEW(I) + C
             ENDDO
             TRANSACT(10*K+1:10*K+10) = '    X + C    '
             K = K + 1
             GO TO 200
          ENDIF
          IF ((ANS3.EQ.'X02').OR.(ANS3.EQ.'x02')) THEN
             C = 1.0E0
```

272

```fortran
705       WRITE (*,202)
          READ (*,*,ERR=705) C
          IF (C.LE.0.0E0) THEN
              WRITE (*,203)
203           FORMAT (1X,'The constant C must be greater than 0.0E0.')
              GO TO 200
          ENDIF
          DO I = 1, N
          XNEW(I) = C * XNEW(I)
          ENDDO
          TRANSACT(10*K+1:10*K+10) = '    C * X    '
          K = K + 1
          GO TO 200
      ENDIF
      IF ((ANS3.EQ.'X03').OR.(ANS3.EQ.'x03')) THEN
          DO I = 1, N
          IF (XNEW(I).LT.0.0E0) THEN
              WRITE (*,204) I, XNEW(I)
204           FORMAT (1X,'X must be greater than or equal to 0.0E0.',
     1                 /,2X,'At I = ',I6,' XNEW(I) = ',1PE16.8)
              GO TO 200
          ENDIF
          ENDDO
          DO I = 1, N
          XNEW(I) = SQRT(XNEW(I))
          ENDDO
          TRANSACT(10*K+1:10*K+10) = '   SQRT(X)   '
          K = K + 1
          GO TO 200
      ENDIF
      IF ((ANS3.EQ.'X04').OR.(ANS3.EQ.'x04')) THEN
          DO I = 1, N
          IF (XNEW(I).LE.0.0E0) THEN
              WRITE (*,205) I, XNEW(I)
205           FORMAT (6X,'X must be greater than 0.0E0.',/,2X,
     1                   'At I = ',I6,' XNEW(I) = ',1PE16.8)
              GO TO 200
          ENDIF
          ENDDO
          DO I = 1, N
          XNEW(I) = ALOG(XNEW(I))
          ENDDO
          TRANSACT(10*K+1:10*K+10) = ' ALOG(X)    '
          K = K + 1
          GO TO 200
      ENDIF
      IF ((ANS3.EQ.'X05').OR.(ANS3.EQ.'x05')) THEN
          DO I = 1, N
          IF (XNEW(I).LE.0.0E0) THEN
              WRITE (*,205) I, XNEW(I)
              GO TO 200
          ENDIF
          ENDDO
          DO I = 1, N
```

273

```fortran
      XNEW(I) = ALOG10(XNEW(I))
      ENDDO
      TRANSACT(10*K+1:10*K+10) = ' ALOG10(X) '
      K = K + 1
      GO TO 200
   ENDIF
   IF ((ANS3.EQ.'X06').OR.(ANS3.EQ.'x06')) THEN
      DO I = 1, N
      IF (XNEW(I).GE.8.289E1) THEN
         XNEW(I) = 8.289E1
         WRITE (*,206) I, XNEW(I)
      ENDIF
      IF (XNEW(I).LE.-8.289E1) THEN
         XNEW(I) = -8.289E1
         WRITE (*,206) I, XNEW(I)
      ENDIF
      XNEW(I) = EXP(XNEW(I))
      ENDDO
      TRANSACT(10*K+1:10*K+10) = '   EXP(X)   '
      K = K + 1
      GO TO 200
   ENDIF
   IF ((ANS3.EQ.'X07').OR.(ANS3.EQ.'x07')) THEN
      DO I = 1, N
      XNEW(I) = ATAN(XNEW(I))
      ENDDO
      TRANSACT(10*K+1:10*K+10) = '   ATAN(X)   '
      K = K + 1
      GO TO 200
   ENDIF
   IF ((ANS3.EQ.'X08').OR.(ANS3.EQ.'x08')) THEN
      DO I = 1, N
      IF (XNEW(I).GE.8.289E1) THEN
         XNEW(I) = 8.289E1
         WRITE (*,206) I, XNEW(I)
      ENDIF
      IF (XNEW(I).LE.-8.289E1) THEN
         XNEW(I) = -8.289E1
         WRITE (*,206) I, XNEW(I)
      ENDIF
      XNEW(I) = SINH(XNEW(I))
      ENDDO
      TRANSACT(10*K+1:10*K+10) = '   SINH(X)   '
      K = K + 1
      GO TO 200
   ENDIF
   IF ((ANS3.EQ.'X09').OR.(ANS3.EQ.'x09')) THEN
      DO I = 1, N
      IF (XNEW(I).GE.8.289E1) THEN
         XNEW(I) = 8.289E1
         WRITE (*,206) I, XNEW(I)
      ENDIF
      IF (XNEW(I).LE.-3.289E1) THEN
         XNEW(I) = -8.289E1
```

274

```fortran
            WRITE (*,206) I, XNEW(I)
         ENDIF
         XNEW(I) = TANH(XNEW(I))
         ENDDO
         TRANSACT(10*K+1:10*K+10) = '   TANH(X)   '
         K = K + 1
         GO TO 200
      ENDIF
      IF ((ANS3.EQ.'X10').OR.(ANS3.EQ.'x10')) THEN
         C = 1.0E0
         WRITE (*,202)
         READ (*,*) C
         IF (C.LE.0.0E0) THEN
            WRITE (*,203)
            GO TO 200
         ENDIF
         DO I = 1, N
         IF (XNEW(I).LT.0.0E0) THEN
            WRITE (*,204) I, XNEW(I)
            GO TO 200
         ENDIF
         ENDDO
         DO I = 1, N
         IF (C*ALOG(XNEW(I)).GE.8.289E1) THEN
            XNEW(I) = EXP(AMIN1(8.289E1,8.289E1/C))
        .    WRITE (*,206) I, XNEW(I)
         ENDIF
         IF (C*ALOG(XNEW(I)).LE.-8.289E1) THEN
            XNEW(I) = EXP(AMAX1(-8.289E1,-8.289E1/C))
            WRITE (*,206) I, XNEW(I)
         ENDIF
         XNEW(I) = XNEW(I)**C
         ENDDO
         TRANSACT(10*K+1:10*K+10) = '    X**C     '
         K = K + 1
         GO TO 200
      ENDIF
      IF ((ANS3.EQ.'X11').OR.(ANS3.EQ.'x11')) THEN
  707    WRITE (*,202)
         READ (*,*,ERR=707) C
         IF (C.LE.0.0E0) THEN
            WRITE (*,203)
            GO TO 200
         ENDIF
         DO I = 1, N
         IF (C.EQ.1.0E0) THEN
            WRITE (*,207)
  207    FORMAT (1X,'The constant C cannot equal 1.0E0;',
     1              ' the functional relation would be violated.')
            GO TO 200
         ENDIF
         IF (XNEW(I).GE.8.289E1/ABS(ALOG(C))) THEN
            XNEW(I) = AMIN1(8.289E1,8.289E1/ABS(ALOG(C)))
            WRITE (*,206) I, XNEW(I)
```

275

```
          ENDIF
          IF (XNEW(I).LE.-8.289E1/ABS(ALOG(C))) THEN
             XNEW(I) = AMAX1(-8.289E1,-8.289E1/ABS(ALOG(C)))
             WRITE (*,206) I, XNEW(I)
          ENDIF
 250      XNEW(I) = C**XNEW(I)
          ENDDO
          TRANSACT(10*K+1:10*K+10) = '    C**X     '
          K = K + 1
          GO TO 200
       ENDIF
       IF ((ANS3.EQ.'X12').OR.(ANS3.EQ.'x12')) GO TO 2
       GO TO 200
  500 CONTINUE
C
C     Query for kinds of Y-axis transformation
C
  708 WRITE (*,501)
  501 FORMAT (1X,'Y Functional Transform Menu:',/,
     1    6X,'Y01 -- add a constant, Y + C',/,
     2    6X,'Y02 -- multiply by a constant, C * Y',/,
     3    6X,'Y03 -- square root, SQRT(Y) (Y.GE.0.0E0)',/,
     4    6X,'Y04 -- natural logarithm, ALOG(Y) (Y.GT.0.0E0)',/,
     5    6X,'Y05 -- common logarithm, ALOG10(Y) (Y.GT.0.0E0)',/,
     6    6X,'Y06 -- exponential, EXP(Y)',
     7    T50,'Y07 -- sine, SIN(Y)',/,
     8    6X,'Y08 -- cosine, COS(Y)',
     9    T50,'Y09 -- tangent, TAN(Y)',/,
     1    6X,'Y10 -- arcsine, ASIN(Y) (ABS(Y).LE.1.0E0)',/,
     2    6X,'Y11 -- arccosine, ACOS(Y) (ABS(Y).LE.1.0E0)',/,
     3    6X,'Y12 -- arctangent, ATAN(Y)',/,
     4    6X,'Y13 -- hyperbolic sine, SINH(Y)',/,
     5    6X,'Y14 -- hyperbolic cosine, COSH(Y)',/,
     6    6X,'Y15 -- hyperbolic tangent, TANH(Y)',/,
     7    6X,'Y16 -- take Y to a power, Y**C (Y.GE.0.0E0, C.GT.0.0E0)',/,
     8    6X,'Y17 -- take a number to a power of Y, C**Y (C.GT.0.0E0)',/,
     9    6X,'Y18 -- take the absolute value of Y, ABS(Y)',/,
     1    6X,'Y19 -- cutoff Y values to input upper and lower limits',/,
     2    6X,'Y20 -- go to subdirectory for further Y function ',
     3                                        'transforms',/,
     4    6X,'Y21 -- end Y transform and go to function main menu',/,
     5    1X,'$ Which transform do you want? (Y##)')
  509 FORMAT (1X,'The Y value has been limited at I = ',I6,' to Y = ',
     1            1PE16.8)
      READ (*,9,ERR=708) ANS3
      IF ((ANS3.EQ.'Y01').OR.(ANS3.EQ.'y01')) THEN
         C = 0.0E0
  709    WRITE (*,502)
  502    FORMAT (1X,'$ What is the constant C?')
         READ (*,*,ERR=709) C
         DO I = 1, N
         YNEW(I) = YNEW(I) + C
         ENDDO
         TRANSACT(10*K+1:10*K+10) = '    Y + C    '
```

276

```
              K = K + 1
              GO TO 500
           ENDIF
           IF ((ANS3.EQ.'Y02').OR.(ANS.EQ.'y02')) THEN
              C = 1.0E0
710           WRITE (*,502)
              READ (*,*,ERR=710) C
              IF (C.LE.0.0E0) THEN
                 WRITE (*,503)
503           FORMAT (1X,'The constant C must be greater than 0.0E0.')
                 GO TO 500
              ENDIF
              DO I = 1, N
              YNEW(I) = C * YNEW(I)
              ENDDO
              TRANSACT(10*K+1:10*K+10) = '   C * Y   '
              K = K + 1
              GO TO 500
           ENDIF
           IF ((ANS3.EQ.'Y03').OR.(ANS3.EQ.'y03')) THEN
              DO I = 1, N
              IF (YNEW(I).LT.0.E0) THEN
                 WRITE (*,504) I, YNEW(I)
504           FORMAT (1X,'Y must be greater than or equal to 0.0E0.',/,
     1                 /,2X,'At I = ',I6,' YNEW(I) = ',1PE16.8)
                 GO TO 500
              ENDIF
              ENDDO
              DO I = 1, N
              YNEW(I) = SQRT(YNEW(I))
              ENDDO
              TRANSACT(10*K+1:10*K+10) = '  SQRT(Y)  '
              K = K + 1
              GO TO 500
           ENDIF
           IF ((ANS3.EQ.'Y04').OR.(ANS3.EQ.'y04')) THEN
              DO I = 1, N
              IF (YNEW(I).LE.0.0E0) THEN
                 WRITE (*,505) I, YNEW(I)
505           FORMAT (/,1X,'Y must be greater than 0.0E0.',/,2X,
     1                    'At I = ',I6,' YNEW(I) = ',1PE16.8)
                 GO TO 500
              ENDIF
              ENDDO
              DO I = 1, N
              YNEW(I) = ALOG(YNEW(I))
              ENDDO
              TRANSACT(10*K+1:10*K+10) = '  ALOG(Y)  '
              K = K + 1
              GO TO 500
           ENDIF
           IF ((ANS3.EQ.'Y05').OR.(ANS3.EQ.'y05')) THEN
              DO I = 1, N
              IF (YNEW(I).LE.0.0E0) THEN
```

```
            WRITE (*,505) I, YNEW(I)
            GO TO 500
       ENDIF
       ENDDO
       DO I = 1, N
       YNEW(I) = ALOG10(YNEW(I))
       ENDDO
       TRANSACT(10*K+1:10*K+10) = ' ALOG10(Y) '
       K = K + 1
       GO TO 500
    ENDIF
    IF ((ANS3.EQ.'Y06').OR.(ANS3.EQ.'y06')) THEN
       DO I = 1, N
       IF (YNEW(I).GE.8.289E1) THEN
            YNEW(I) = 8.289E1
            WRITE (*,509) I, YNEW(I)
       ENDIF
       IF (YNEW(I).LE.-8.289E1) THEN
            YNEW(I) = -8.289E1
            WRITE (*,509) I, YNEW(I)
       ENDIF
       YNEW(I) = EXP(YNEW(I))
       ENDDO
       TRANSACT(10*K+1:10*K+10) = '   EXP(Y)  '
       K = K + 1
       GO TO 500
    ENDIF
    IF ((ANS3.EQ.'Y07').OR.(ANS3.EQ.'y07')) THEN
       DO I = 1, N
       YNEW(I) = SIN(YNEW(I))
       ENDDO
       TRANSACT(10*K+1:10*K+10) = '   SIN(Y)  '
       K = K + 1
       GO TO 500
    ENDIF
    IF ((ANS3.EQ.'Y08').OR.(ANS3.EQ.'y08')) THEN
       DO I = 1, N
       YNEW(I) = COS(YNEW(I))
       ENDDO
       TRANSACT(10*K+1:10*K+10) = '   COS(Y)  '
       K = K + 1
       GO TO 500
    ENDIF
    IF ((ANS3.EQ.'Y09').OR.(ANS3.EQ.'y09')) THEN
       DO I = 1, N
       YNEW(I) = TAN(YNEW(I))
       ENDDO
       TRANSACT(10*K+1:10*K+10) = '   TAN(Y)  '
       K = K + 1
       GO TO 500
    ENDIF
    IF ((ANS3.EQ.'Y10').OR.(ANS3.EQ.'y10')) THEN
       DO I = 1, N
       IF (ABS(YNEW(I)).GT.1.0E0) THEN
```

```fortran
                 WRITE (*,506) I, YNEW(I)
506              FORMAT (1X,'ABS(Y) must be less than or equal to 1.0E0.',/,
     1               2X,'At I = ',I6,' YNEW(I) = ',1PE16.8)
                 GO TO 500
           ENDIF
           ENDDO
           DO I = 1, N
           YNEW(I) = ASIN(YNEW(I))
           ENDDO
           TRANSACT(10*K+1:10*K+10) = '  ASIN(Y)  '
           K = K + 1
           GO TO 500
        ENDIF
        IF ((ANS3.EQ.'Y11').OR.(ANS3.EQ.'y11')) THEN
           DO I = 1, N
           IF (ABS(YNEW(I)).GT.1.0E0) THEN
              WRITE (*,506) I, YNEW(I)
              GO TO 500
           ENDIF
           ENDDO
           DO I = 1, N
           YNEW(I) = ACOS(YNEW(I))
           ENDDO
           TRANSACT(10*K+1:10*K+10) = '  ACOS(Y)  '
           K = K + 1
           GO TO 500
        ENDIF
        IF ((ANS3.EQ.'Y12').OR.(ANS3.EQ.'y12')) THEN
           DO I = 1, N
           IF (YNEW(I).GE.1.0E36) THEN
              YNEW(I) = 1.0E36
              WRITE (*,509) I, YNEW(I)
           ENDIF
           IF (YNEW(I).LE.-1.0E36) THEN
              YNEW(I) = -1.0E36
              WRITE (*,509) I, YNEW(I)
           ENDIF
           YNEW(I) = ATAN(YNEW(I))
           ENDDO
           TRANSACT(10*K+1:10*K+10) = '  ATAN(Y)  '
           K = K + 1
           GO TO 500
        ENDIF
        IF ((ANS3.EQ.'Y13').OR.(ANS3.EQ.'y13')) THEN
           DO I = 1, N
           IF (YNEW(I).GE.8.289E1) THEN
              YNEW(I) = 8.289E1
              WRITE (*,509) I, YNEW(I)
           ENDIF
           IF (YNEW(I).LE.-8.289E1) THEN
              YNEW(I) = -8.289E1
              WRITE (*,509) I, YNEW(I)
           ENDIF
           YNEW(I) = SINH(YNEW(I))
```

279

```
         ENDDO
         TRANSACT(10*K+1:10*K+10) = '   SINH(Y)   '
         K = K + 1
         GO TO 500
      ENDIF
      IF ((ANS3.EQ.'Y14').OR.(ANS3.EQ.'y14')) THEN
         DO I = 1, N
         IF (YNEW(I).GT.8.289E1) THEN
            YNEW(I) = 8.289E1
            WRITE (*,509) I, YNEW(I)
         ENDIF
         IF (YNEW(I).LT.-8.289E1) THEN
            YNEW(I) = -8.289E1
            WRITE (*,509) I, YNEW(I)
         ENDIF
         YNEW(I) = COSH(YNEW(I))
         ENDDO
         TRANSACT(10*K+1:10*K+10) = '   COSH(Y)   '
         K = K + 1
         GO TO 500
      ENDIF
      IF ((ANS3.EQ.'Y15').OR.(ANS3.EQ.'y15')) THEN
         DO I = 1, N
         IF (YNEW(I).GE.8.289E1) THEN
            YNEW(I) = 8.289E1
            WRITE (*,509) I, YNEW(I)
         ENDIF
         IF (YNEW(I).LE.-8.289E1) THEN
            YNEW(I) = -8.289E1
            WRITE (*,509) I, YNEW(I)
         ENDIF
         YNEW(I) = TANH(YNEW(I))
         ENDDO
         TRANSACT(10*K+1:10*K+10) = '   TANH(Y)   '
         K = K + 1
         GO TO 500
      ENDIF
      IF ((ANS3.EQ.'Y16').OR.(ANS3.EQ.'y16')) THEN
         C = 1.0E0
711      WRITE (*,502)
         READ (*,*,ERR=711) C
         IF (C.LE.0.0E0) THEN
            WRITE (*,503)
            GO TO 500
         ENDIF
         DO I = 1, N
         IF (YNEW(I).LT.0.0E0) THEN
            WRITE (*,504) I, YNEW(I)
            GO TO 500
         ENDIF
         ENDDO
         DO I = 1, N
         IF (C*ALOG(YNEW(I)).GE.8.289E1) THEN
            YNEW(I) = EXP(AMIN1(8.289E1,8.289E1/C))
```

```fortran
            WRITE (*,509) I, YNEW(I)
        ENDIF
        IF (C*ALOG(YNEW(I)).LE.-8.289E1) THEN
            YNEW(I) = EXP(AMAX1(-8.289E1,-8.289E1/C))
            WRITE (*,509) I, YNEW(I)
        ENDIF
        YNEW(I) = YNEW(I)**C
        ENDDO
        TRANSACT(10*K+1:10*K+10) = '    Y**C     '
        K = K + 1
        GO TO 500
      ENDIF
      IF ((ANS3.EQ.'Y17').OR.(ANS3.EQ.'y17')) THEN
712     WRITE (*,502)
        READ (*,*,ERR=712) C
        IF (C.LE.0.0E0) THEN
            WRITE (*,503)
            GO TO 500
        ENDIF
        DO I = 1, N
        IF (C.EQ.1.0E0) YNEW(I) = 1.0E0
        IF (YNEW(I).GE.8.289E1/ABS(ALOG(C))) THEN
            YNEW(I) = AMIN1(8.289E1,8.289E1/ABS(ALOG(C)))
            WRITE (*,509) I, YNEW(I)
        ENDIF
        IF (YNEW(I).LE.-8.289E1/ABS(ALOG(C))) THEN
            YNEW(I) = AMAX1(-8.289E1,-8.289E1/ABS(ALOG(C)))
            WRITE (*,509) I, YNEW(I)
        ENDIF
550     YNEW(I) = C**YNEW(I)
        ENDDO
        TRANSACT(10*K+1:10*K+10) = '    C**Y     '
        K = K + 1
        GO TO 500
      ENDIF
      IF ((ANS3.EQ.'Y18').OR.(ANS3.EQ.'y18')) THEN
        DO I = 1, N
        YNEW(I) = ABS(YNEW(I))
        ENDDO
        TRANSACT(10*K+1:10*K+10) = '   ABS(Y)    '
        K = K + 1
        GO TO 500
      ENDIF
      IF ((ANS3.EQ.'Y19').OR.(ANS3.EQ.'y19')) THEN
        YHIGH = 1.0E36
        YLOW = -1.0E36
        WRITE (*,507)
507     FORMAT (1X,'What is the upper limit of the Y values?')
        READ (*,*) YHIGH
        WRITE (*,508)
508     FORMAT (1X,'What is the lower limit of the Y values?')
        READ (*,*) YLOW
        DO I = 1, N
        IF (YNEW(I).GT.YHIGH) YNEW(I) = YHIGH
```

281

```
          IF (YNEW(I).LT.YLOW) YNEW(I) = YLOW
          ENDDO
          TRANSACT(10*K+1:10*K+10) = ' limited Y '
          K = K + 1
          GO TO 500
      ENDIF
      IF ((ANS3.EQ.'Y21').OR.(ANS3.EQ.'y21')) GO TO 2
      IF ((ANS3.EQ.'Y20').OR.(ANS3.EQ.'y20')) THEN
713     WRITE (*,519)
        READ (*,9,ERR=713) ANS3
        GO TO 570
      ENDIF
560 CONTINUE
    WRITE (*,519)
    READ (*,9) ANS3
570 CONTINUE
519 FORMAT (1X,'Y Functional Transform Subdirectory Menu:',/,
   1    6X,'Y22 -- logarithm of Y to the base C, LOG-sub C-(Y)',/,
   2    6X,'Y23 -- secant of Y, SEC(Y)',/,
   3    6X,'Y24 -- cosecant of Y, CSC(Y)',/,
   4    6X,'Y25 -- cotangent of Y, CTN(Y)',/,
   5    6X,'Y26 -- arcsecant of Y, ARCSEC(Y)',/,
   6    6X,'Y27 -- arccosecant of Y, ARCCSC(Y)',/,
   7    6X,'Y28 -- arccotangent of Y, ARCCTN(Y)',/,
   8    6X,'Y29 -- hyperbolic secant of Y, SECH(Y)',/,
   9    6X,'Y30 -- hyperbolic cosecant of Y, CSCH(Y)',/,
   1    6X,'Y31 -- hyperbolic cotangent of Y, CTNH(Y)',/,
   2    6X,'Y32 -- hyperbolic arcsine of Y',/,
   3    6X,'Y33 -- hyperbolic arccosine of Y',/,
   4    6X,'Y34 -- hyperbolic arctangent of Y',/,
   5    6X,'Y35 -- hyperbolic arcsecant of Y',/,
   6    6X,'Y36 -- hyperbolic arccosecant of Y',/,
   7    6X,'Y37 -- hyperbolic arccotangent of Y',/,
   8    6X,'Y38 -- return to main Y transform menu',/,
   9    1X,'$ Which transform do you want? (Y##)')
    IF ((ANS3.EQ.'Y22').OR.(ANS3.EQ.'y22')) THEN
714     WRITE (*,510)
510 FORMAT (1X,'$ What is the base of the logarithm you wish to ',
   1                    'transform Y with?')
        READ (*,*,ERR=714) C
        IF (C.LE.0.0E0) THEN
           WRITE (*,203)
           GO TO 560
        ENDIF
        IF (C.EQ.1.0E0) THEN
           WRITE (*,512)
512 FORMAT (1X,'C.EQ.1.0E0; C has been set to EXP(1.0E0)')
           C = EXP(1.0E0)
        ENDIF
        DO I = 1, N
        IF (YNEW(I).LE.0.0E0) THEN
           WRITE (*,505) I, YNEW(I)
           GO TO 560
        ENDIF
```

282

```fortran
            ENDDO
            DO I = 1, N
            YNEW(I) = ALOG(YNEW(I))/ALOG(C)
            ENDDO
            TRANSACT(10*K+1:10*K+10) = 'LOG-C-(Y) '
            K = K + 1
            GO TO 560
         ENDIF
         IF ((ANS3.EQ.'Y23').OR.(ANS3.EQ.'y23')) THEN
            DO I = 1, N
            IF (ABS(COS(YNEW(I))).LE.1.0E-36) THEN
               YNEW(I) = SIGN(1.0E36,COS(YNEW(I)))
               IF (COS(YNEW(I)).EQ.0.0E0) YNEW(I) = 1.0E36
               GO TO 571
            ENDIF
            YNEW(I) = 1.0E0/COS(YNEW(I))
571         CONTINUE
            ENDDO
            TRANSACT(10*K+1:10*K+10) = '  SEC(Y)  '
            K = K + 1
            GO TO 560
         ENDIF
         IF ((ANS3.EQ.'Y24').OR.(ANS3.EQ.'y24')) THEN
            DO I = 1, N
            IF (ABS(SIN(YNEW(I))).LE.1.0E-36) THEN
               YNEW(I) = SIGN(1.0E36,SIN(YNEW(I)))
               IF (SIN(YNEW(I)).EQ.0.0E0) YNEW(I) = 1.0E36
               GO TO 572
            ENDIF
            YNEW(I) = 1.0E0/SIN(YNEW(I))
572         CONTINUE
            ENDDO
            TRANSACT(10*K+1:10*K+10) = '  CSC(Y)  '
            K = K + 1
            GO TO 560
         ENDIF
         IF ((ANS3.EQ.'Y25').OR.(ANS3.EQ.'y25')) THEN
            DO I = 1, N
            IF (ABS(TAN(YNEW(I))).LE.1.0E-36) THEN
               YNEW(I) = SIGN(1.0E36,TAN(YNEW(I)))
               IF (TAN(YNEW(I)).EQ.0.0E0) YNEW(I) = 1.0E36
               GO TO 573
            ENDIF
            YNEW(I) = 1.0E0/TAN(YNEW(I))
573         CONTINUE
            ENDDO
            TRANSACT(10*K+1:10*K+10) = '  CTN(Y)  '
            K = K + 1
            GO TO 560
         ENDIF
         IF ((ANS3.EQ.'Y26').OR.(ANS3.EQ.'y26')) THEN
            DO I = 1, N
            IF (ABS(YNEW(I)).LT.1.0E0) THEN
               WRITE (*,511) I, YNEW(I)
```

283

```fortran
          GO TO 560
      ENDIF
      ENDDO
      DO I = 1, N
      IF (YNEW(I).GE.0.0E0) TEMP = 1.0E0
      IF (YNEW(I).LT.0.0E0) TEMP = -1.0E0
      YNEW(I) = ACOS(1.0E0/YNEW(I)) * TEMP
      ENDDO
      TRANSACT(10*K+1:10*K+10) = 'ARCSEC(Y) '
      K = K + 1
      GO TO 560
ENDIF
IF ((ANS3.EQ.'Y27').OR.(ANS3.EQ.'y27')) THEN
      DO I = 1, N
      IF (ABS(YNEW(I)).LT.1.0E0) THEN
         WRITE (*,511) I, YNEW(I)
      GO TO 560
      ENDIF
      ENDDO
      DO I = 1, N
      IF (YNEW(I).GE.0.0E0) YNEW(I) = ASIN(1.0E0/YNEW(I))
      IF (YNEW(I).LT.0.0E0) THEN
         YNEW(I) = -4.0E0 * ATAN(1.0E0) - ASIN(1.0E0/YNEW(I))
      ENDIF
      ENDDO
      TRANSACT(10*K+1:10*K+10) = 'ARCCSC(Y) '
      K = K + 1
      GO TO 560
ENDIF
IF ((ANS3.EQ.'Y28').OR.(ANS3.EQ.'y28')) THEN
      DO I = 1, N
      YNEW(I) = 2.0E0 * ATAN(1.0E0) - ATAN(YNEW(I))
      ENDDO
      TRANSACT(10*K+1:10*K+10) = 'ARCCTN(Y) '
      K = K + 1
      GO TO 560
ENDIF
IF ((ANS3.EQ.'Y29').OR.(ANS3.EQ.'y29')) THEN
      DO I = 1, N
      IF (YNEW(I).GE.8.289E1) THEN
         YNEW(I) = 8.289E1
         WRITE (*,509) I, YNEW(I)
      ENDIF
      IF (YNEW(I).LE.-8.289E1) THEN
         YNEW(I) = -8.289E1
         WRITE (*,509) I, YNEW(I)
      ENDIF
      YNEW(I) = 1.0E0/COSH(YNEW(I))
      ENDDO
      TRANSACT(10*K+1:10*K+10) = ' SECH(Y)  '
      K = K + 1
      GO TO 560
ENDIF
IF ((ANS3.EQ.'Y30').OR.(ANS3.EQ.'y30')) THEN
```

284

```fortran
         DO I = 1, N
         IF (YNEW(I).GE.8.289E1) THEN
            YNEW(I) = 8.289E1
            WRITE (*,509) I, YNEW(I)
         ENDIF
         IF (YNEW(I).LE.-8.289E1) THEN
            YNEW(I) = -8.289E1
            WRITE (*,509) I, YNEW(I)
         ENDIF
         IF (ABS(SINH(YNEW(I))).LE.1.0E-36) THEN
            YNEW(I) = SIGN(1.0E-36,SINH(YNEW(I)))
            IF (SINH(YNEW(I)).EQ.0.0E0) YNEW(I) = 1.0E-36
            GO TO 574
         ENDIF
         YNEW(I) = 1.0E0/SINH(YNEW(I))
574      CONTINUE
         ENDDO
         TRANSACT(10*K+1:10*K+10) = 'CSCH(Y)   '
         K = K + 1
         GO TO 560
      ENDIF
      IF ((ANS3.EQ.'Y31').OR.(ANS3.EQ.'y31')) THEN
         DO I = 1, N
         IF (YNEW(I).GE.8.289E1) THEN
            YNEW(I) = 8.289E1
            WRITE (*,509) I, YNEW(I)
         ENDIF
         IF (YNEW(I).LE.-8.289E1) THEN
            YNEW(I) = -8.289E1
            WRITE (*,509) I, YNEW(I)
         ENDIF
         IF (ABS(TANH(YNEW(I))).LE.1.0E-36) THEN
            YNEW(I) = SIGN(1.0E-36,TANH(YNEW(I)))
            IF (TANH(YNEW(I)).EQ.0.0E0) YNEW(I) = 1.0E-36
            GO TO 575
         ENDIF
         YNEW(I) = 1.0E0/TANH(YNEW(I))
575      CONTINUE
         ENDDO
         TRANSACT(10*K+1:10*K+10) = ' COTH(Y)  '
         K = K + 1
         GO TO 560
      ENDIF
      IF ((ANS3.EQ.'Y32').OR.(ANS3.EQ.'y32')) THEN
         DO I = 1, N
         IF (ABS(YNEW(I)).GE.1.0E18) YNEW(I) = SIGN(1.0E18,YNEW(I))
         IF (ABS(YNEW(I)).LE.1.0E-18) YNEW(I) = SIGN(1.0E-18,YNEW(I))
         YNEW(I) = ALOG(YNEW(I) + SQRT(YNEW(I)**2 + 1.0E0))
         ENDDO
         TRANSACT(10*K+1:10*K+10) = 'ARCSINH(Y)'
         K = K + 1
         GO TO 560
      ENDIF
      IF ((ANS3.EQ.'Y33').OR.(ANS3.EQ.'y33')) THEN
```

285

```fortran
      DO I = 1, N
          IF (YNEW(I).LT.1.0EO) THEN
          WRITE (*,511) I, YNEW(I)
511 FORMAT (1X,'Y must be greater than or equal to 1.0EO.',/,2X,
     1          'At I = ',I6,' YNEW(I) = ',1PE16.8)
          GO TO 560
      ENDIF
      ENDDO
      DO I = 1, N
      IF (ABS(YNEW(I)).GE.1.0E18) YNEW(I) = SIGN(1.0E18,YNEW(I))
      YNEW(I) = ALOG(YNEW(I) + SQRT(YNEW(I)**2 - 1.0EO))
      ENDDO
      TRANSACT(10*K+1:10*K+10) = 'ARCCOSH(Y)'
      K = K + 1
      GO TO 560
    ENDIF
    IF ((ANS3.EQ.'Y34').OR.(ANS3.EQ.'y34')) THEN
      DO I = 1, N
      IF (ABS(YNEW(I)).GE.1.0EO) THEN
          WRITE (*,515) I, YNEW(I)
515 FORMAT (1X,'ABS(Y) must be less than 1.0EO.',/,
     1          2X,'At I = ',I6,' YNEW(I) = ',1PE16.8)
          GO TO 560
      ENDIF
      YNEW(I) = 0.5EO * (ALOG(1.0EO+YNEW(I))-ALOG(1.0EO-YNEW(I)))
      ENDDO
      TRANSACT(10*K+1:10*K+10) = 'ARCTANH(Y)'
      K = K + 1
      GO TO 560
    ENDIF
    IF ((ANS3.EQ.'Y35').OR.(ANS3.EQ.'y35')) THEN
      DO I = 1, N
      IF (YNEW(I).LE.0.0EO) THEN
          WRITE (*,505) I, YNEW(I)
          GO TO 560
      ENDIF
      IF (YNEW(I).GT.1.0EO) THEN
          WRITE (*,516) I, YNEW(I)
516 FORMAT (1X,'Y must be less than or equal to 1.0EO.',/,2X,
     1          'At I = ',I6,' YNEW(I) = ',1PE16.8)
          GO TO 560
      ENDIF
      ENDDO
      DO I = 1, N
      IF (ABS(YNEW(I)).LE.1.0E-18) YNEW(I) = SIGN(1.0E-18,YNEW(I))
      IF (ABS(YNEW(I)).LE.1.0E18) YNEW(I) = SIGN(1.0E18,YNEW(I))
      YNEW(I) = ALOG(1.0EO/YNEW(I)+SQRT((1.0EO/YNEW(I)**2)-1.0EO))
      ENDDO
      TRANSACT(10*K+1:10*K+10) = 'ARCSECH(Y)'
      K = K + 1
      GO TO 560
    ENDIF
    IF ((ANS3.EQ.'Y36').OR.(ANS3.EQ.'y36')) THEN
      DO I = 1, N
```

286

```fortran
              IF (ABS(YNEW(I)).LT.1.0E-18) THEN
                  YNEW(I) = SIGN(1.0E-18,YNEW(I))
                  IF (YNEW(I).EQ.0.0E0) YNEW(I) = 1.0E-18
              ENDIF
              IF (ABS(YNEW(I)).GE.1.0E18) YNEW(I) = SIGN(1.0E18,YNEW(I))
              YNEW(I) = ALOG(1.0E0/YNEW(I)
     1              +SIGN(1.0E0,YNEW(I))*SQRT((1.0E0/YNEW(I)**2 + 1.0E0)))
              ENDDO
              TRANSACT(10*K+1:10*K+10) = 'ARCCSCH(Y)'
              K = K + 1
              GO TO 560
          ENDIF
          IF ((ANS3.EQ.'Y37').OR.(ANS3.EQ.'y37')) THEN
              DO I = 1, N
              IF (ABS(YNEW(I)).LE.1.0E0) THEN
                  WRITE (*,511) I, YNEW(I)
                  GO TO 560
              ENDIF
              ENDDO
              DO I = 1, N
              IF (YNEW(I).GT.0.0E0) THEN
                  YNEW(I) = ALOG(1.0E0+SQRT(YNEW(I)**2+1.0E0))-ALOG(YNEW(I))
              ENDIF
              IF (YNEW(I).LT.0.0E0) THEN
                  YNEW(I)=
     1              (1.0E0/YNEW(I)-SQRT(YNEW(I)**2+1.0E0)/YNEW(I))
              ENDIF
              ENDDO
              TRANSACT(10*K+1:10*K+10) = 'ARCCTNH(Y)'
              K = K + 1
              GO TO 560
          ENDIF
          IF ((ANS3.EQ.'Y38').OR.(ANS3.EQ.'y38')) GO TO 500
          GO TO 560
C
C     Query for more transformations
C
  900 CONTINUE
  715 WRITE (*,901)
  901 FORMAT (1X,'$ Do you want to transform any more of this file?',
     1          ' (Y or N)')
      READ (*,9,ERR=715) ANS
      IF ((ANS.EQ.'Y').OR.(ANS.EQ.'y')) GO TO 2
C
C     Output the transformed data
C
      WRITE (2,9) TITLE(1:52)//'FUNCTION/'//TITLE(62:132)
      WRITE (2,*) N
      WRITE (2,*) (XNEW(I), I = 1, N)
      WRITE (2,*) (YNEW(I), I = 1, N)
      DO J = 1, 10
      WRITE (2,9) TRANSACT(80*J-79:80*J)
      ENDDO
      CLOSE (UNIT=2)
```

287

```
C
C      Query for transformations of other files
C
  716 WRITE (*,902)
  902 FORMAT (1X,'$ Do you want to transform any other files? (Y or N)')
      READ (*,9,ERR=716) ANS
      IF ((ANS.EQ.'Y').OR.(ANS.EQ.'y')) GO TO 1
      WRITE (*,903)
  903 FORMAT (1X,'$ Subroutine FUNCTION is ending now.')
      RETURN
      END
```

```
      SUBROUTINE ROTATE
C
C      This subroutine rotates a data array (in plot compatible format)
C      through the origin and places this data into another data array.
C      The format for these arrays is given below:
C
C         line 1 -- title of data file
C         line 2 -- number of data points N    (free * format)
C         line 3 - J -- data arrays              (free * format)
C                   First, x data arrays X(1), X(2), . . . , X(N), then
C                       y data arrays Y(1), Y(2), . . . , Y(N).
C
C      NOTE: The condition X(1)<X(2)< . . . <X(N) must hold and should
C            NOT be changed!
C
C      The rotation correction becomes
C
C            M = least squares fit of the slope of the input linear
C                 portion of the data trace
C
C            THETA = angle of rotation through origin = DATAN(M)
C
C            XNEW(I) = XOLD(I) * COS(THETA) + YOLD(I) * SIN(THETA)
C
C            YNEW(I) = -XOLD(I) * SIN(THETA) + YOLD(I) * COS (THETA)
C
C
C      The subroutine will be halted in the case of invalid data,
C      i.e. when any of the following conditions exists:
C
C      for invalid input data--
C
C            XLO .GE. XHI or
C            XLO .LE. XOLD(1) or
C            XHI .GE. XOLD(N)
C
C      for invalid derived data--
C
C            (IHI - ILO) .LT. 1
```

288

```fortran
C
C
C        As the subroutine is now configured, the subroutine is limited to
C        a maximum of 1000 data points.  If a larger number of data points
C        is required, this subroutine must be appropriately modified.
C
         DIMENSION XOLD(1000), XNEW(1000), YOLD(1000), YNEW(1000)
         DOUBLE PRECISION M, NUMBER, SUMX, SUMX2, SUMXY, SUMY, THETA
         DOUBLE PRECISION PI, XSCALE, YSCALE, XMIN, XMAX, YMIN, YMAX
         REAL XHI, XLO
         INTEGER IDEL, IHI, ILO
         CHARACTER*132  INNAME, OUTNAME, TITLE, TITLENEW
         CHARACTER*1 ANS
       1 CONTINUE
     700 WRITE (*, 15)
      15 FORMAT (1X,'$ Enter file name to be rotated.')
         READ (*,9,ERR=700) INNAME
     701 WRITE (*,25)
      25 FORMAT (1X,'$ Enter rotated output file name.')
         READ (*,9,ERR=701) OUTNAME
         OPEN (UNIT=5, STATUS='OLD',FILE=INNAME,READONLY)
         REWIND (UNIT=5)
         OPEN (UNIT=10, STATUS='NEW',FILE=OUTNAME)
         READ (5,9) TITLE
       9 FORMAT (A)
         TITLENEW = TITLE(1:60)//'ROTATED/'//TITLE(69:132)
         READ (5,*) N
C
C     Check for an appropriate number of data points.
C
         IF (N.GT.1000) THEN
            N = 1000
            WRITE (*,10)
      10    FORMAT (5X,'Number of data points has been limited to 1000.')
         ENDIF
         IF (N.LE.3) THEN
            WRITE (*,20)
      20    FORMAT (5X,'Number of data points is too small.',/,5X,
       1              'The subroutine is now being halted.')
            GO TO 1
         ENDIF
     702 WRITE (*,35)
      35 FORMAT (1X,'$ Input lower value of baseline x-value.',/,
       1         1X,'This value corresponds to first x-value of baseline.')
         READ (*,*,ERR=702) XLO
     703 WRITE (*,45)
      45 FORMAT (1X,'$ Input upper value of baseline x-value.',/,
       1         1X,'This value corresponds to last x-value of baseline.')
         READ (*,*,ERR=703) XHI
         READ (5,*) (XOLD(I), I = 1, N)
         READ (5,*) (YOLD(I), I = 1, N)
C
C     Check for valid limits on the subroutine values.
C
```

```fortran
      IF ((XLO.GT.XHI).OR.(XLO.LT.XOLD(1)).OR.(XHI.GT.XOLD(N))) THEN
         WRITE (*,30)
30       FORMAT (5X,'The limits on the baseline are invalid.',/,5X,
     1            'The subroutine is now being halted.')
         WRITE (*,40) XLO, XHI
40       FORMAT (5X,'XLO = ',1PE15.8,5X,'XHI = ',1PE15.8)
         WRITE (*,50) XOLD(1), XOLD(N)
50       FORMAT (5X,'X(1) = ',1PE15.8,5X,'X(N) = ',1PE15.8)
         GO TO 999
      ENDIF
C
C     Sort throughout the XOLD array to find the values of ILO and IHI
C
      DO I = 2, N
      XXL1 = XLO - XOLD(I - 1)
      XXLO = XOLD(I) - XLO
      IF (XXL1.EQ.0.0E0) ILO = MAX0(1,I-1)
      IF (XXLO.EQ.0.0E0) ILO = I
      IF (XXL1*XXLO.GT.0.0E0) THEN
         IF (ABS(XXL1).LE.ABS(XXLO)) ILO = I - 1
         IF (ABS(XXL1).GT.ABS(XXLO)) ILO = I
      ENDIF
      ENDDO
      DO I = 2, N
      XXL1 = XHI - XOLD(I - 1)
      XXHI = XOLD(I) - XHI
      IF (XXL1.EQ.0.0E0) IHI = I - 1
      IF (XXHI.EQ.0.0E0) IHI = I
      IF (XXL1*XXHI.GT.0.0E0) THEN
         IF (ABS(XXL1).LT.ABS(XXHI)) IHI = I - 1
         IF (ABS(XXL1).GE.ABS(XXHI)) IHI = I
      ENDIF
      ENDDO
      IF ((IHI-ILO).LT.1) THEN
         WRITE (*,30)
         WRITE (*,60) ILO, IHI
60       FORMAT (5X,'ILO = ',I8,10X,'IHI = ',I8)
         GO TO 999
      ENDIF
C
C     Scale and transform axes for calculation
C
      XMIN = DBLE(XOLD(1))
      XMAX = DBLE(XOLD(1))
      YMIN = DBLE(XOLD(1))
      YMAX = DBLE(XOLD(1))
      DO I = 1, N
      XMIN = DMIN1(DBLE(XOLD(I)),XMIN)
      XMAX = DMAX1(DBLE(XOLD(I)),XMAX)
      YMIN = DMIN1(DBLE(YOLD(I)),YMIN)
      YMAX = DMAX1(DBLE(YOLD(I)),YMAX)
      ENDDO
      XSCALE = XMAX - XMIN
      YSCALE = YMAX - YMIN
```

```fortran
      DO I = 1, N
      XOLD(I) = XOLD(I)/XSCALE
      YOLD(I) = YOLD(I)/YSCALE
      ENDDO
C
C     Calculate the slope and angle of rotation
C
      IDEL = IHI - ILO + 1
      NUMBER = DBLE(IDEL)
      SUMX = 0.0D0
      SUMX2 = 0.0D0
      SUMXY = 0.0D0
      SUMY = 0.0D0
      DO 550 I = ILO, IHI
      SUMX = SUMX + DBLE(XOLD(I))
      SUMX2 = SUMX2 + DBLE(XOLD(I))**2
      SUMXY = SUMXY + DBLE(XOLD(I)) * DBLE(YOLD(I))
  550 SUMY = SUMY + DBLE(YOLD(I))
      M = ((NUMBER * SUMXY) - (SUMX * SUMY))/
     1        ((NUMBER * SUMX2) - (SUMX**2))
      THETA = DATAN(-M)
      PI = 4.0D0*DATAN(1.0D0)
      DO I = 1, 4
      IF (THETA.GE.PI/2.0D0) THETA = THETA - PI
      IF (THETA.LT.-PI/2.0D0) THETA = THETA + PI
      IF ((THETA.GE.-PI/2.0D0).AND.(THETA.LT.PI/2.0D0)) GO TO 551
      ENDDO
  551 CONTINUE
C
C     Calculate the rotated X- and Y-values
C
      DO  I = 1, N
      TEMP = DBLE(XOLD(I))*DCOS(THETA) + DBLE(YOLD(I))*DSIN(THETA)
      XNEW(I) = SNGL(TEMP)
      ENDDO
      DO  I = 1, N
      TEMP = -DBLE(XOLD(I))*DSIN(THETA) + DBLE(YOLD(I))*DCOS(THETA)
      YNEW(I) = SNGL(TEMP)
      ENDDO
C
C     Rescale axes for output
C
      DO I = 1, N
      XNEW(I) = SNGL(DBLE(XOLD(I)) * XSCALE)
      YNEW(I) = SNGL(DBLE(YOLD(I)) * YSCALE)
      ENDDO
C
C     Output the rotation corrected data file.
C
      WRITE (*,*)
      WRITE (*,*) ' SLOPE = ', M
      WRITE (*,*) ' ANGLE (in radians) = ', -THETA
      WRITE (*,*)
      WRITE (10,9) TITLENEW
```

291

```
      WRITE (10,*) N
      WRITE (10,*) (XNEW(I), I = 1, N)
      WRITE (10,*) (YNEW(I), I = 1, N)
  999 CONTINUE
      CLOSE (UNIT = 5)
      CLOSE (UNIT = 10)
  704 WRITE (*,105)
  105 FORMAT (1X,'$ Do you want to perform any more rotation ',
     1          'corrections? (Y or N)')
      READ (*,9,ERR=704) ANS
      IF ((ANS.EQ.'Y').OR.(ANS.EQ.'y')) GO TO 1
      WRITE (*,115)
  115 FORMAT (1X,'Subroutine ROTATE is ending now.')
      RETURN
      END
```

```
      SUBROUTINE BASELINE
C
C     This subroutine subtracts a linear baseline from a data array
C     (in plot compatible format) and places this data into another
C     data array.  The format for these arrays are given below:
C
C         line 1 -- title of data file
C         line 2 -- number of data points N    (free * format)
C         line 3 - J -- data arrays             (free * format)
C                 First, x data arrays X(1), X(2), . . . , X(N), then
C                         y data arrays Y(1), Y(2), . . . , Y(N).
C
C     NOTE: The condition X(1)<X(2)< . . . <X(N) must hold and should
C           NOT be changed!
C
C     This subroutine has been revised to allow for two options in
C     subtracting baseline corrections from digitized data signals.
C
C        The first option will determine the baseline when the data
C     trace has a segment that is continous and unaffected by the signal
C     voltage driver.  If these conditions can be fulfilled, the
C     subroutine will apply a first order linear fit of the line segment
C     data to generate a baseline from the data array.  Whenever
C     possible, this option should be used as it is likely to be more
C     accurate in all cases.
C
C        The second option takes a lower and upper x-value from the
C     original user and corresponding y-values taken from the data
C     array.  The baseline is determined from the x-data points closest
C     to XLO and XHI.  The XOLD(I) data point closest to XLO yield ILO.
C     The XOLD(I) data point closest to XHI yields IHI.  From these
C     current values, the baseline correction becomes
C
C     YNEW(I) = YOLD(I) - YOLD(ILO)
C       - (YOLD(IHI)-YOLD(ILO))/(XOLD(IHI)-XOLD(ILO))*(XOLD(I)-XOLD(ILO))
```

292

```
C
C
C        The subroutine will be halted in the case of invalid data,
C        i.e. when the following conditions exist:
C
C        for invalid input data--
C
C                XLO .GE. XHI or
C                XLO .LE. XOLD(1) or
C                XHI .GE. XOLD(N)
C
C        for invalid derived data--
C
C                (IHI - ILO) .LT. 1
C
C
C        As the subroutine is now configured, the subroutine is limited to
C        a maximum of 1000 data points.  If a larger number of data points
C        is required, this subroutine must be appropriately modified.
C
        DIMENSION XOLD(1000), YOLD(1000), YNEW(1000)
        DOUBLE PRECISION B, M, NUMBER, SUMX, SUMX2, SUMXY, SUMY, TEMP
        REAL XHI, XLO
        INTEGER IDEL, IHI, ILO, KOUNT, N
        CHARACTER*132  INNAME, OUTNAME, TITLE, TITLENEW
        CHARACTER*1 ANS
      1 CONTINUE
    750 WRITE (*, 15)
     15 FORMAT (1X,'$ Enter file name to be baseline corrected.')
        READ (*,9,ERR=750) INNAME
    751 WRITE (*,25)
     25 FORMAT (1X,'$ Enter output file name.')
        READ (*,9,ERR=751) OUTNAME
        OPEN (UNIT=5, STATUS='OLD',FILE=INNAME,READONLY)
        REWIND (UNIT=5)
        OPEN (UNIT=10, STATUS='NEW',FILE=OUTNAME)
        READ (5,9) TITLE
      9 FORMAT (A)
        TITLENEW = TITLE(1:68)//'BASELINE/'//TITLE(78:132)
        READ (5,*) N
C
C       Check for an appropriate number of data points.
C
        IF (N.GT.1000) THEN
            N = 1000
            WRITE (10,10)
            WRITE (*,10)
     10     FORMAT (5X,'Number of data points has been limited to 1000.')
        ENDIF
        IF (N.LE.3) THEN
            WRITE (10,20)
            WRITE (*,20)
     20     FORMAT (5X,'Number of data points is too small.')
            GO TO 1
```

293

```fortran
      ENDIF
C
C     Determine the option to be used.
C
      WRITE (*, 22)
   22 FORMAT (/,1X,'Two options may be used to determine the baseline ',
     1    'correction.',/,1X,'The first option used assumes that there',
     2    ' is a line segment that is',/,1X,'continuous and relatively ',
     3    'unaffected by the driver signal.  The line',/,1X,'segment is'
     4    ' then least-square-fitted to a first order (linear) baseline.',
     5    /,1X,'The second method uses a lower and an upper x-value ',
     6    'supplied by the user',/,1X,'and corresponding y-values taken '
     7    ,'from the data array.  A straight line',/,1X,'is then fitted',
     8    ' between the lower and the upper y-value.',
     9    /,1X,'The first method is preferable.',/)
      KOUNT = 0
  752 WRITE (*,24)
   24 FORMAT (1X,'$ Is there a continuous line segment on the data ',/
     1         ,1X,'trace suitable for use in the least squares fitting',
     2         /,1X,'under the first option?')
      READ (*,9,ERR=752) ANS
      IF ((ANS.EQ.'Y').OR.(ANS.EQ.'y')) THEN
         KOUNT = 1
         GO TO 27
      ENDIF
   27 CONTINUE
      IF (KOUNT.EQ.1) WRITE (*,32)
   32 FORMAT (1X,'The baseline is determined by least-squares-fitting ',
     1         'data between',/,1X,'the lower and upper x-values of the ',
     2         'input file data.',//)
  753 WRITE (*,35)
   35 FORMAT (1X,'$ Input lower value of baseline x-value.',/,
     1         1X,'This value corresponds to first x-value of baseline.')
      READ (*,*,ERR=753) XLO
  754 WRITE (*,45)
   45 FORMAT (1X,'$ Input upper value of baseline x-value.',/,
     1         1X,'This value corresponds to last x-value of baseline.')
      READ (*,*,ERR=754) XHI
      READ (5,*) (XOLD(I), I = 1, N)
      READ (5,*) (YOLD(I), I = 1, N)
C
C     Check for valid limits on the subroutine values.
C
      IF ((XLO.GT.XHI).OR.(XLO.LT.XOLD(1)).OR.(XHI.GT.XOLD(N))) THEN
         WRITE (*,30)
   30    FORMAT (5X,'The limits on the baseline are invalid.')
         WRITE (*,40) XLO, XHI
   40    FORMAT (5X,'XLO = ',1PE15.8,5X,'XHI = ',1PE15.8)
         WRITE (*,50) XOLD(1), XOLD(N)
   50    FORMAT (5X,'X(1) = ',1PE15.8,5X,'X(N) = ',1PE15.8)
         GO TO 999
      ENDIF
C
C     Sort throughout the XOLD array to find the values of ILO and IHI
```

```
C
      DO 150 I = 2, N
      XXL1 = XLO - XOLD(I - 1)
      XXLO = XOLD(I) - XLO
      IF (XXL1.EQ.0.0E0) ILO = MAXO(1,I-1)
      IF (XXL1.EQ.0.0E0) ILO = I
      IF (XXL1*XXLO.GT.0.0E0) THEN
         IF (ABS(XXL1).LE.ABS(XXLO)) ILO = I - 1
         IF (ABS(XXL1).GT.ABS(XXLO)) ILO = I
      ENDIF
  150 CONTINUE
      DO 200 I = 2, N
      XXL1 = XHI - XOLD(I - 1)
      XXHI = XOLD(I) - XHI
      IF (XXL1.EQ.0.0E0) IHI = I - 1
      IF (XXL1.EQ.0.0E0) IHI = I
      IF (XXL1*XXHI.GT.0.0E0) THEN
         IF (ABS(XXL1).LT.ABS(XXHI)) IHI = I - 1
         IF (ABS(XXL1).GE.ABS(XXHI)) IHI = I
      ENDIF
  200 CONTINUE
      IF ((IHI-ILO).LT.1) THEN
         WRITE (*,30)
         WRITE (*,60) ILO, IHI
   60    FORMAT (5X,'ILO = ',I8,10X,'IHI = ',I8)
         GO TO 999
      ENDIF
C
C     Calculate the slope and intercept for the second option.
C
      IF (KOUNT.GE.1) GO TO 500
      M = (DBLE(YOLD(IHI)) - DBLE(YOLD(ILO)))/
     1       (DBLE(XOLD(IHI)) - DBLE(XOLD(ILO)))
      B = DBLE(YOLD(ILO)) - M * DBLE(XOLD(ILO))
      GO TO 600
C
C     Calculate the slope and intercept for the first option.
C
  500 CONTINUE
      IDEL = IHI - ILO + 1
      NUMBER = DBLE(IDEL)
      SUMX = 0.0D0
      SUMX2 = 0.0D0
      SUMXY = 0.0D0
      SUMY = 0.0D0
      DO 550 I = ILO, IHI
      SUMX = SUMX + DBLE(XOLD(I))
      SUMX2 = SUMX2 + DBLE(XOLD(I))**2
      SUMXY = SUMXY + DBLE(XOLD(I)) * DBLE(YOLD(I))
  550 SUMY = SUMY + DBLE(YOLD(I))
      M = ((NUMBER * SUMXY) - (SUMX * SUMY))/
     1       ((NUMBER * SUMX2) - (SUMX**2))
      B = (SUMY/NUMBER) - M * (SUMX/NUMBER)
C
```

```
C     Calculate the corrected y-values.
C
  600 CONTINUE
      DO 700 I = 1, N
      TEMP = DBLE(YOLD(I)) - M * DBLE(XOLD(I)) - B
  700 YNEW(I) = SNGL(TEMP)
C
C     Calculate the baseline-corrected data file.
C
      WRITE (10,9) TITLENEW
      WRITE (10,*) N
      WRITE (10,*) (XOLD(I), I = 1, N)
      WRITE (10,*) (YNEW(I), I = 1, N)
  999 CONTINUE
      CLOSE (UNIT = 5)
      CLOSE (UNIT = 10)
C
C     Query for completion
C
  755 WRITE (*,105)
  105 FORMAT(1X,'$ Do you want to perform any more baseline ',
     1             'corrections? (Y or N)')
      READ (*,9,ERR=755) ANS
      IF ((ANS.EQ.'Y').OR.(ANS.EQ.'y')) GO TO 1
      WRITE (*,115)
  115 FORMAT (1X,'$ Subroutine BASELINE is ending now.')
      RETURN
      END


      SUBROUTINE FILEC
      REAL XIN(1000), YIN(1000), SIN(1000), XOUT(1000),
     1     YOUT(1000)
      INTEGER INDEXIN(1000), NIN, NOUT
      CHARACTER*132 INPUT, OUTPUT, TITLE
      CHARACTER*1 ANS
    1     CONTINUE
    9     FORMAT (A)
  700     WRITE (*,12)
   12     FORMAT (1X,'$ Enter the file name to be spline fit.')
          READ (*,9,ERR=700) INPUT
  701     WRITE (*,13)
   13     FORMAT (1X,'$ Enter the output file name.')
          READ (*,9,ERR=701) OUTPUT
  702     WRITE (*,14)
   14     FORMAT (1X,'$ Write the number of data points in the final ',
     1             'spline fit.',/,1X,'This number must be .LE. 1000.')
          READ (*,*,ERR=702) NOUT
          OPEN (UNIT=5,STATUS='OLD',FILE=INPUT,READONLY)
          REWIND (UNIT=5)
          OPEN (UNIT=10,STATUS='NEW',FILE=OUTPUT)
          READ (5,9) TITLE
```

```
            READ (5,*) NIN
            READ (5,*) (XIN(I), I = 1, NIN)
            READ (5,*) (YIN(I), I = 1, NIN)
            CLOSE (UNIT=5)
C
C       Check for compatibility of the numbers of points.
C
            IF (NIN.EQ.NOUT) THEN
               WRITE (*,*)
               WRITE (*,*)  ' NIN = NOUT; No modified file will be created'
               WRITE (*,*)
               WRITE (10,9) TITLE
               WRITE (10,*) NOUT
               WRITE (10,*) (XIN(I), I = 1, NOUT)
               WRITE (10,*) (YIN(I), I = 1, NOUT)
               CLOSE (UNIT = 10)
               GO TO 999
            ENDIF
            IF (NIN.GT.1000) THEN
               WRITE (*,21) NIN
    21 FORMAT (1X,'Number of input points = ',I4,' This is too large.')
               GO TO 1
            ENDIF
            IF (NOUT.LE.1) THEN
               WRITE (*,16)
    16      FORMAT (1X,'The number of output points is too small.')
               GO TO 1
            ENDIF
            IF (NOUT.GT.1000) THEN
               NOUT = 1000
               WRITE (*,17)
    17      FORMAT (1X,'The number of output points has been limited to',
      1              ' 1000 points.')
            ENDIF
            WRITE (*,*)
            WRITE (*,*) ' Number of input points = ', NIN
            WRITE (*,*) ' Number of output points = ', NOUT
            WRITE (*,*)
C
C       Calculate the spline fit parameters
C
            CALL SPCOEF(NIN,XIN,YIN,SIN,INDEXIN)
C
C       Calculate the new spline fit data
C
C       XOUT(1) = XIN(1)
C       YOUT(1) = YIN(1)
C       XOUT(NOUT) = XIN(NIN)
C       YOUT(NOUT) = YIN(NIN)
C
            DO I = 1, NOUT
            XOUT(I) = (XIN(NIN) - XIN(1)) * FLOAT(I-1)/FLOAT(NOUT-1)
      1                        + XIN(1)
            YOUT(I) = SPLINE(NIN,XIN,YIN,SIN,INDEXIN,XOUT(I))
```

297

```
        ENDDO
        WRITE (10,9) TITLE(1:124)//'SPLINE/'
        WRITE (10,*) NOUT
        WRITE (10,*) (XOUT(I), I = 1, NOUT)
        WRITE (10,*) (YOUT(I), I = 1, NOUT)
  999   CONTINUE
        CLOSE (UNIT=10)
C
C     Query for completion
C
  703   WRITE (*,18)
   18 FORMAT (1X,'$ Do you wish to calculate any more spline fits?')
        READ (*,9,ERR=703) ANS
        IF ((ANS.EQ.'Y').OR.(ANS.EQ.'y')) GO TO 1
        WRITE (*,19)
   19   FORMAT (1X,'$ Subroutine FILEC is ending now.')
        RETURN
        END


_____
_____


        SUBROUTINE INTCOR
C
C     This subroutine will correct for voltage droop of the passive RC
C     integrator according to the relation
C
C                 VCOR = RC * VDIFF + V
C
C        where VCOR is the corrected output voltage,
C              RCINT is the integrator RC time constant,
C              VDIFF is the time differential of voltage and
C              V is the original voltage from the traces.
C
C     VCOR is then integrated to yield a smoothed value.
C
C     All the arrays (VCOR, VDIFF and V) are in plot compatible format.
C
C     This subroutine assumes that the x-arrays of all the voltage data
C     are identical.  If this is not the case, another subroutine must
C     be used.
C
C     This subroutine does perform simple integration and
C     differentiation.
C
        DOUBLE PRECISION T, V, VDIFF, VCOR, XLO, XHI
        DIMENSION V(1000), VDIFF(1000), T(1000), VCOR(1000)
        CHARACTER*132 TITLE, TITLENEW, INNAME, OUTNAME
        CHARACTER*1 ANS
        INTEGER N
    1 CONTINUE
  700 WRITE (*, 15)
        READ (*, 9,ERR=700) INNAME
  701 WRITE (*, 35)
```

298

```fortran
          READ (*, 9,ERR=702) OUTNAME
       15 FORMAT (1X,'$ Enter input file to be RC corrected.')
       35 FORMAT (1X,'$ Enter output file name.')
          OPEN (UNIT=10,STATUS='NEW',FILE=OUTNAME)
          OPEN (UNIT=15,STATUS='OLD',FILE=INNAME,READONLY)
          REWIND (UNIT=15)
C
C      Enter input voltage values
C
          READ (15, 9) TITLE
        9 FORMAT (A)
          TITLENEW = TITLE(1:77)//'RC cor/'//TITLE(85:132)
          READ (15, *) N
          READ (15, *) (T(I), I = 1, N)
          READ (15, *) (V(I), I = 1, N)
C
C      Calculate differentiated voltage values
C
          CALL DDIFFER (N, T, V, VDIFF)
C
C      Enter integrator value
C
      702 WRITE (*,70)
       70 FORMAT (1X,'$ Enter integrator value (in seconds).')
          READ (*,*,ERR=702) RC
C
C      Calculate "corrected" voltage values by integration of VDIFF
C
          DO 300 I = 1, N
      300 VCOR(I) = RC * VDIFF(I) + V(I)
          SUM = 0.0D0
          Y1 = VCOR(1)
          DO 500 I = 2, N
          XLO = T(I - 1)
          XHI = T(I)
          Y2 = VCOR(I)
          SUM = SUM + 0.5D0 * (Y2 + Y1) * (XHI - XLO)
          Y1 = Y2
      500 VCOR(I) = SUM/RC
          VCOR(1) = 2.0D0 * VCOR(2) - VCOR(3)
C
C      Output corrected values
C
          WRITE (10,9) TITLENEW
          WRITE (10, *) N
          WRITE (10, *) (SNGL(T(I)), I = 1, N)
          WRITE (10, *) (SNGL(VCOR(I)), I = 1, N)
          CLOSE (UNIT = 10)
          CLOSE (UNIT = 15)
C
C      Query for more RC integration corrections
C
      703 WRITE (*,45)
       45 FORMAT (1X,'$ Do you want to RC correct any more data files?',
```

```
      1              ' (Y or N)')
      READ (*,9,ERR=703) ANS
      IF ((ANS.EQ.'Y').OR.(ANS.EQ.'y')) GO TO 1
      WRITE (*,55)
   55 FORMAT (1X,'$ The subroutine INTCOR is ending now.')
      RETURN
      END
```

```
      SUBROUTINE DDIFFER(N,X,Y,YDIFF)
C
C     NOTE: The condition X(1)<X(2)< . . . <X(N) must hold and should
C           NOT be changed!
C
C     Three different formulae are used to differentiate the given data.
C     These formulae are :
C
C           5 point differential --
C
C     Y'(I) = (Y(I-2)-8*Y(I-1)+8*Y(I+1)-Y(I+2))/(3*(X(I+2)-X(I-2)))
C
C           3 point differential --
C
C           Y'(I) = (Y(I+1) - Y(I-1))/(X(I+1) - X(I-1))
C
C           2 point differential (Standard slope intercept form; used on
C                     end points only)
C
C           Y'(1) = (Y(2) - Y(1))/(X(2) - X(1)) and
C
C           Y'(N) = (Y(N) - Y(N-1))/((X(N) - X(N-1))
C
C     As the subroutine is now configured, the subroutine is limited to
C     a maximum of 1000 data points.  If a larger number of data points
C     is required, this subroutine must be appropriately modified.
C
      DIMENSION X(1000), Y(1000), YDIFF(1000)
      DOUBLE PRECISION X, Y, YDIFF
      INTEGER N
C
C     Check for an appropriate number of data points.
C
      IF (N.GT.1000) THEN
         N = 1000
         WRITE (*,10)
   10    FORMAT (5X,'Number of data points has been limited to 1000.')
      ENDIF
      IF (N.LE.1) THEN
         WRITE (*,20)
   20    FORMAT (5X,'Number of data points is too small.',/,5X,
      1             'The subroutine is now being halted.')
         RETURN
```

300

```
      ENDIF
C
C     Test for more than five data points.  If there are more than
C     five data points, use a 5 pt. differential.
C
      IF (N.LE.5) GO TO 250
      DO 200 I = 3, N-2
  200 YDIFF(I) =
     1    (Y(I-2)+8.0E0*(Y(I+1)-Y(I-1))-Y(I+2))/(3.0E0*(X(I+2)-X(I-2)))
C
C     Test for (3.LE.N.LT.5).  If true, use 3 pt. differential.
C
  250 CONTINUE
      IF (N.LE.3) GO TO 350
      YDIFF(2) = (Y(3) - Y(1))/(X(3) - X(1))
      YDIFF(N-1) = (Y(N) - Y(N-2))/(X(N) - X(N-2))
C
C     Test for valid number of data points.  If there is a valid number
C     of data points, finish processing end points.  If the number is
C     invalid, end the subroutine and flag the error.
C
  350 CONTINUE
      IF (N.LT.2) THEN
         WRITE (5,500)
  500    FORMAT (5X,'The number of data points is invalid.',/,5X,
     1                'The subroutine is being halted now.')
         RETURN
         ENDIF
      YDIFF(1) = (Y(2) - Y(1))/(X(2) - X(1))
      YDIFF(N) = (Y(N) - Y(N-1))/(X(N) - X(N-1))
      RETURN
      END
```

```
      SUBROUTINE DIFFER
C
C     This subroutine differentiates one data array (in plot compatible
C     format) into another plot compatible data array.  The format of
C     these data arrays are given below:
C
C         line 1 -- title of data file
C         line 2 -- number of data points N    (I12)
C         line 3 - J -- data arrays            (free * format)
C                   First, x data arrays X(1), X(2), . . . . , X(N), then
C                          y data arrays Y(1), Y(2), . . . . , Y(N).
C
C     NOTE: The condition X(1)<X(2)< . . . . <X(N) must hold and should
C           NOT be changed!
C
C     Three different formulae are used to differentiate the given data.
C     These formulae are :
C
```

301

```
C          5 point differential --
C
C     Y'(I) = (Y(I-2)-8*Y(I-1)+8*Y(I+1)-Y(I+2))/(3*(X(I+2)-X(I-2)))
C
C          3 point differential --
C
C     Y'(I) = (Y(I+1) - Y(I-1))/(X(I+1) - X(I-1))
C
C          2 point differential (Standard slope intercept form; used on
C                    end points only)
C
C     Y'(1) = (Y(2) - Y(1))/(X(2) - X(1)) and
C
C     Y'(N) = (Y(N) - Y(N-1))/((X(N) - X(N-1))
C
C     As the subroutine is now configured, the subroutine is limited to
C     a maximum of 1000 data points.  If a larger number of data points
C     is required, this subroutine must be appropriately modified.
C
      DIMENSION X(1000), YOLD(1000), YDIFF(1000)
      INTEGER N
      CHARACTER*132  TITLE, TITLENEW, INNAME, OUTNAME
      CHARACTER*1 ANS
    1 CONTINUE
  700 WRITE (*,15)
   15 FORMAT (1X,'$ Enter file name to be differentiated.')
      READ (*,9,ERR=700) INNAME
  701 WRITE (*,25)
   25 FORMAT (1X,'$ Enter differentiated output file name.')
      READ (*,9,ERR=701) OUTNAME
      OPEN (UNIT=5, STATUS='OLD',FILE=INNAME,READONLY)
      REWIND (UNIT=5)
      OPEN (UNIT=10, STATUS='NEW',FILE=OUTNAME)
      READ (5,9) TITLE
    9 FORMAT (A)
      TITLENEW = TITLE(1:84)//'dY/dX/'//TITLE(91:132)
      READ (5,*) N
C
C     Check for an appropriate number of data points.
C
      IF (N.GT.1000) THEN
         N = 1000
         WRITE (*,10)
   10    FORMAT (5X,'Number of data points has been limited to 1000.')
      ENDIF
      IF (N.LE.1) THEN
         WRITE (*,20)
   20    FORMAT (5X,'Number of data points is too small.',/,5X,
      1             'The subroutine is now being halted.')
         GO TO 999
      ENDIF
      READ (5,*) (X(I), I = 1, N)
      READ (5,*) (YOLD(I), I = 1, N)
C
```

```fortran
C     Test for more than five data points.  If there are more than
C     five data points, use a 5 pt. differential.
C
      IF (N.LE.5) GO TO 250
      DO 200 I = 3, N-2
  200 YDIFF(I) = (YOLD(I-2)-8.0*YOLD(I-1)+8.0*YOLD(I+1)-YOLD(I+2))/
     1                   (3.0*(X(I+2)-X(I-2)))
C
C     Test for (3.LE.N.LT.5).  If true, use 3 pt. differential.
C
  250 CONTINUE
      IF (N.LE.3) GO TO 350
      YDIFF(2) = (YOLD(3) - YOLD(1))/(X(3) - X(1))
      YDIFF(N-1) = (YOLD(N) - YOLD(N-2))/(X(N) - X(N-2))
C
C     Test for valid number of data points.  If true, finish processing
C     end points.  If false, end subroutine and flag error.
C
  350 CONTINUE
      IF (N.LT.2) THEN
         WRITE (5,500)
  500    FORMAT (5X,'The number of data points is invalid.',/,5X,
     1                 'The subroutine is being halted now.')
         GO TO 999
         ENDIF
      YDIFF(1) = (YOLD(2) - YOLD(1))/(X(2) - X(1))
      YDIFF(N) = (YOLD(N) - YOLD(N-1))/(X(N) - X(N-1))
      WRITE (10,9) TITLENEW
      WRITE (10,*) N
      WRITE (10,*) (X(I), I = 1, N)
      WRITE (10,*) (YDIFF(I), I = 1, N)
      CLOSE (UNIT = 5)
      CLOSE (UNIT = 10)
C
C     Continue for more differentiation
C
  702 WRITE (*,35)
   35 FORMAT (1X,'$ Do you want to differentiate any more files? (Y or',
     1                   ' N)')
      READ (*,9,ERR=702) ANS
      IF ((ANS.EQ.'Y').OR.(ANS.EQ.'y')) GO TO 1
      WRITE (*,45)
   45 FORMAT (1X,'$ The subroutine DIFFER is ending now.')
  999 CONTINUE
      RETURN
      END
```

SUBROUTINE INTEGRATE
```fortran
C
C     This subroutine will integrate a plot compatible file into another
C     plot compatible file.  The subroutine uses an adaptive Simpson's
```

```
C      rule to integrate the data.
C
       EXTERNAL F
       DOUBLE PRECISION SUM
       DIMENSION YINT(1000)
       CHARACTER*132 TITLE, TITLENEW, INNAME, OUTNAME
       CHARACTER*1 ANSER
       COMMON N, XR(1000), YR(1000), S(1000), INDEX(1000)
     1 CONTINUE
   700 WRITE (*,10)
    10 FORMAT (1X,'$ Enter file name to be integrated.')
       READ (*,9,ERR=700) INNAME
   701 WRITE (*,20)
    20 FORMAT (1X,'$ Enter output file name.')
       READ (*,9,ERR=701) OUTNAME
       OPEN (UNIT=10,STATUS='NEW',FILE=OUTNAME)
       OPEN (UNIT=15,STATUS='OLD',FILE=INNAME,READONLY)
       REWIND (UNIT=15)
       READ (15, 9) TITLE
     9 FORMAT (A)
       TITLENEW = TITLE(1:90)//'INT(YdX)/'//TITLE(100:132)
       READ (15, *) N
       READ (15, *) (XR(I), I = 1, N)
       READ (15, *) (YR(I), I = 1, N)
       CALL SPCOEF(N, XR, YR, S, INDEX)
       ACC = 5.0E-7
       SUM = 0.0D0
       DO 500 I = 2, N
       WRITE (*, 300) I
   300 FORMAT (5X,'Working on subroutine INTEGRATE; I = ',2X,I4)
       XLO = XR(I - 1)
       XHI = XR(I)
       CALL SIMP(F, XLO, XHI, ACC, ANS, ERROR, AREA, IFLAG)
       SUM = SUM + DBLE(ANS)
   500 YINT(I) = SNGL(SUM)
       WRITE (10, 9) TITLENEW
       WRITE (10, *) N
       WRITE (10, *) (XR(I), I = 1, N)
       WRITE (10, *) (YINT(I), I = 1, N)
       CLOSE (UNIT = 10)
       CLOSE (UNIT = 15)
C
C      Query to determine if more integrations are needed
C
   702 WRITE (*,55)
    55 FORMAT (1X,'$ Do you want to perform any more integrations? ',
     1          ' (Y or N)')
       READ (*,9,ERR=702) ANSER
       IF ((ANSER.EQ.'Y').OR.(ANSER.EQ.'y')) GO TO 1
       WRITE (*,65)
    65 FORMAT (1X,'$ The subroutine INTEGRATE is ending now.')
       RETURN
       END
```

```fortran
      FUNCTION F(X)
      COMMON N, XR(1000), YR(1000), S(1000), INDEX(1000)
      F = SPLINE (N, XR, YR, S, INDEX, X)
      RETURN
      END
```

```fortran
      SUBROUTINE SUM
C
C     This subroutine will input up to 10 data files and output the file
C     that is the arithmetic sum of the input files.  The subroutine can
C     perform a correlation dependent on the calculated x-intercept of
C     the initial slope of the trace.  With proper modification, the
C     subroutine can be used to find the arithmetic sum of more than
C     10 files.
C
      PARAMETER NUPTS=1000
      CHARACTER*132 FILENAME(11), TXT(11)
      CHARACTER*1 ANS
      INTEGER INDEX(10,NUPTS), II(NUPTS), IMAX(10), IMIN(10), KC(10)
      INTEGER KN, NUM(10)
      REAL ASIGN(10), B(10), CMAX(10), CQ(10), CT(10), DELQI(10)
      REAL DELQIP1(10), DELTI(10), DELTIP1(10), FMAX(10), FMIN(10)
      REAL S(10,NUPTS), SLOPE(10), SS(NUPTS), TEMP, TEST, TMAX
      REAL TMIN, TZERO(10), X(11,NUPTS), XX(NUPTS), XMAX(10)
      REAL XMIN(10), Y(11,NUPTS), YY(NUPTS)
      DOUBLE PRECISION DK(10), DSUMX(10), DSUMX2(10), DSUMXY(10)
      DOUBLE PRECISION DSUMY(10)
      LL = 1
   99 CONTINUE
      LL = LL + 1
C
C     Enter the number of files to be added
C
  700 WRITE (*,555)
  555 FORMAT (1X,'$ Enter the number of files to be added.')
      READ (*,*,ERR=700) KN
      IF ((KN.LE.0).OR.(KN.GT.10)) THEN
         WRITE (*,556)
  556 FORMAT (1X,'The number of files is in error -- either it is too '
     1               ,'large or too small.')
         GO TO 905
      ENDIF
      DO I = 1, 11
         DO J = 1, 132
         FILENAME(I)(J:J) = ' '
         ENDDO
      ENDDO
C
```

```
C      Enter file names
C
      DO L = 1, KN
  701 WRITE (*,1) L
    1 FORMAT (1X,'$ Enter the name for input file for file # ',I2)
      READ (*,2,ERR=701) FILENAME(L)
      ENDDO
    2 FORMAT (A)
  702 WRITE (*,3)
    3 FORMAT (1X,'$ Enter the name of the output file.')
      READ (*,2,ERR=702) FILENAME(11)
C
C      Enter the input files
C
      DO L = 1, KN
      IF(LL.GE.2) REWIND (UNIT=L)
      OPEN (UNIT=L,NAME=FILENAME(L),TYPE='OLD',READONLY)
      READ (L,2) TXT(L)
      READ (L,*) NUM(L)
      READ (L,*) (X(L,J),J=1,NUM(L))
      READ (L,*) (Y(L,J),J=1,NUM(L))
      CLOSE (UNIT=L)
      ENDDO
      OPEN (UNIT=11,NAME=FILENAME(11),TYPE='NEW')
C
C      Find the maximum of the absolute value of each of the input files
C
      DO L = 1, KN
      CMAX(L) = 0.0E0
      DO J = 1, NUM(L)
      TEMP = CMAX(L)
      CMAX(L) = AMAX1(CMAX(L),ABS(Y(L,J)))
      IF (CMAX(L).GT.TEMP) ASIGN(L)=SIGN(1.0E0,Y(L,J))
      ENDDO
      WRITE (*,*) ' L = ',L,' ASIGN * CMAX(L) = ',ASIGN(L)*CMAX(L)
      ENDDO
C
C      Query if a time correlation is required.  If the answer is yes,
C      continue as given.  If the answer is no, jump directly to the
C      summation step.
C
  703 WRITE (*,7)
    7 FORMAT (1X,'$ Do you want to perform a time correlation on the',
    1          ' data traces? (Y or N)')
      READ (*,2,ERR=703) ANS
      IF ((ANS.EQ.'Y').OR.(ANS.EQ.'y')) GO TO 200
      GO TO 500
  200 CONTINUE
C
C      Query if user wishes to adjust the limits for time correlation
C
          WRITE (*,201)
  201     FORMAT (//,1X,'For the purposes of adjusting the timing ',
    1       '(ordinate) of the digitized data,',/,1X,'the user ',
```

306

```fortran
     2     'can select limits on the digitized trace rise/fall',
     3     ' based on fractions',/,1X,'of trace maximum.',//,1X,
     4     'Implicit in this correlation are the assumptions',
     5     ' that the trace rise/fall is',/,1X,'monotonic ',
     6     'and that an extrapolated zero can be calculated by',
     7     ' linear fitting',/,1X,'the portion of trace ',
     8     'rise/fall determined from fractional limits of ',
     9     'maximum.',//,1X,
     1     'The curve will extrapolate a zero point from the trace',
     2     ' between FMIN * CMAX',/,1X,'and FMAX * CMAX.  Here,',
     3     ' FMIN is the lower fraction, FMAX is the upper fraction',
     4     /,1X,'and CMAX is the trace maximum.  ',//,1X,
     5     'Unless set by user, FMIN = 0.1 and FMAX = 0.9.',/)
202   FORMAT (//,1X,'$ Do you want to set the limits for time',
     1     ' correlation? (Y or N)')
      WRITE (*,202)
      READ (*,2) ANS
      IF ((ANS.EQ.'Y').OR.(ANS.EQ.'y')) THEN
         WRITE (*,203)
203   FORMAT (1X,'$ Do you want the same fractional limits on all ',
     1     'traces? (Y or N)')
         READ (*,2) ANS
         IF ((ANS.NE.'Y').AND.(ANS.NE.'y')) THEN
            DO L = 1, KN
204            CONTINUE
               WRITE (*,205) L
205   FORMAT (1X,'$ What is FMIN(',I2,')?')
               READ (*,*,ERR=204) FMIN(L)
               FMIN(L) = AMIN1(0.9E0,AMAX1(0.10E0,FMIN(L)))
206            CONTINUE
               WRITE (*,207) L
207   FORMAT (1X,'$ What is FMAX(',I2,')?')
               READ (*,*,ERR=206) FMAX(L)
               FMAX(L) = AMAX1(0.1E0,AMIN1(0.90E0,FMAX(L)))
            ENDDO
            DO L = 1, KN
            IF (FMIN(L).GT.FMAX(L)) THEN
               TEMP = FMAX(L)
               FMAX(L) = FMIN(L)
               FMIN(L) = TEMP
            ENDIF
            IF (FMIN(L).EQ.FMAX(L)) THEN
               FMIN(L) = 0.1E0
               FMAX(L) = 0.9E0
            ENDIF
            ENDDO
            WRITE (*,210) (L,FMIN(L),FMAX(L),L=1,KN)
210   FORMAT (1X,' L = ',I6,' FMIN(L) = ',1PE10.3,' FMAX(L) =',
     1     1PE10.3)
         ELSE
211         CONTINUE
            WRITE (*,205) 1
            READ (*,*,ERR=211) FMIN(1)
            FMIN(1) = AMIN1(0.9E0,AMAX1(0.10E0,FMIN(1)))
```

307

```
212          CONTINUE
             WRITE (*,207) 1
             READ (*,*,ERR=212) FMAX(1)
             FMAX(1) = AMAX1(0.1E0,AMIN1(0.90E0,FMAX(1)))
             IF (FMIN(1).GT.FMAX(1)) THEN
                TEMP = FMAX(1)
                FMAX(1) = FMIN(1)
                FMIN(1) = TEMP
             ENDIF
             IF (FMIN(1).EQ.FMAX(1)) THEN
                FMIN(1) = 0.10E0
                FMAX(1) = 0.90E0
             ENDIF
             DO L = 2, KN
             FMIN(L) = FMIN(1)
             FMAX(L) = FMAX(1)
             ENDDO
             WRITE (*,210) (L,FMIN(L),FMAX(L),L=1,KN)
             ENDIF
             ELSE
             DO L = 1, KN
             FMIN(L) = 0.1E0
             FMAX(L) = 0.9E0
             ENDDO
             WRITE (*,210) (L,FMIN(L),FMAX(L),L=1,KN)
             ENDIF
         DO L = 1, KN
         CT(L) = FMIN(L) * CMAX(L)
         CQ(L) = FMAX(L) * CMAX(L)
         ENDDO
         DO L = 1, KN
         WRITE (*,*)
         WRITE (*,*) ' L = ',L,' CMAX(L) = ',CMAX(L)
         WRITE (*,*) ' L = ',L,' CT(L) = ',CT(L),' CQ(L) = ',CQ(L)
         WRITE (*,*)
         ENDDO
C
C     Find the corresponding times of the quarter and tenth values of
C     digitized data traces
C
      DO L = 1, KN
      IMIN(L) = -1
      IMAX(L) = -1
      DO I = 1, NUM(L)
          DELQI(L) = CQ(L) - Y(L,I)
          DELQIP1(L) = Y(L,I+1) - CQ(L)
          DELTI(L) = CT(L) - Y(L,I)
          DELTIP1(L) = Y(L,I+1) - CT(L)
          IF ((IMAX(L).GT.0).AND.(IMIN(L).GT.0)) GO TO 110
          IF (DELQI(L).EQ.0.0E0) THEN
             IMAX(L) = MAX0(I-1,1)
             GO TO 101
          ENDIF
          IF ((IMAX(L).GT.0).AND.(IMIN(L).GT.0)) GO TO 110
```

308

```fortran
      IF (DELQIP1(L).EQ.0.0E0) THEN
         IMAX(L) = MINO(I+1,NUM(L))
         GO TO 101
      ENDIF
101   CONTINUE
      IF ((IMAX(L).GT.0).AND.(IMIN(L).GT.0)) GO TO 110
      IF (DELTI(L).EQ.0.0E0) THEN
         IMIN(L) = MAXO(I-1,1)
         GO TO 102
      ENDIF
      IF ((IMAX(L).GT.0).AND.(IMIN(L).GT.0)) GO TO 110
      IF (DELTIP1(L).EQ.0.0E0) THEN
         IMIN(L) = MINO(I+1,NUM(L))
         GO TO 102
      ENDIF
102   CONTINUE
      IF ((IMAX(L).GT.0).AND.(IMIN(L).GT.0)) GO TO 110
      IF (DELTI(L)*DELTIP1(L).GT.0.0E0) THEN
         IMIN(L) = I + JNINT((CT(L) - Y(L,I))/(Y(L,I+1) - Y(L,I)))
         IMIN(L) = MAXO(IMIN(L)-1,1)
      ENDIF
      IF ((IMAX(L).GT.0).AND.(IMIN(L).GT.0)) GO TO 110
      IF (DELQI(L)*DELQIP1(L).GT.0.0E0) THEN
         IMAX(L) = I + JNINT((CQ(L) - Y(L,I))/(Y(L,I+1) - Y(L,I)))
         IMAX(L) = MINO(IMAX(L)+1,NUM(L))
      ENDIF
110   CONTINUE
      ENDDO
      IF ((IMIN(L).LE.1).OR.(IMIN(L).GE.NUM(L))) THEN
         WRITE (*,9)
         WRITE (*,*) ' L = ',L,' NUM(L) = ',NUM(L),' IMIN(L) = ',IMIN(L)
9        FORMAT (1X,'The calculated limits on 10% of the value of the'
     1             ' current are invalid.')
         GO TO 905
      ENDIF
      IF ((IMAX(L).LE.1).OR.(IMAX(L).GE.NUM(L))) THEN
         WRITE (*,11)
         WRITE (*,*) ' L = ',L,' NUM(L) = ',NUM(L),' IMAX(L) = ',IMAX(L)
11       FORMAT (1X,'The calculated limits on 25% of the value of the',
     1             ' current are invalid.')
         GO TO 905
      ENDIF
      IF (IMIN(L).GE.IMAX(L)) THEN
         WRITE (*,12)
      WRITE (*,*)' L = ',L,' IMIN(L) = ',IMIN(L),' IMAX(L) = ',IMAX(L)
12       FORMAT (1X,'The lower limit on current is greater than or ',
     1             'equal to upper limit.')
         GO TO 905
      ENDIF
      XMIN(L) = X(L,IMIN(L))
      XMAX(L) = X(L,IMAX(L))
      WRITE (*,*) ' L = ',L,' IMIN(L) = ',IMIN(L),' IMAX(L) = ',IMAX(L)
      WRITE (*,*) ' L = ',L,' XMIN(L) = ',XMIN(L),' XMAX(L) = ',XMAX(L)
C
```

309

```fortran
C        Calculate the "zero" point of the data by least-squares-fitting
C        of the data between X = XMIN(L) AND X = XMAX(L)
C
         KC(L) = IMAX(L) - IMIN(L) + 1
         DSUMXY(L) = 0.0D0
         DSUMX(L) = 0.0D0
         DSUMY(L) = 0.0D0
         DSUMX2(L) = 0.0D0
         DO I = IMIN(L), IMAX(L)
         DSUMXY(L) = DSUMXY(L) + X(L,I) * Y(L,I)
         DSUMX(L) = DSUMX(L) + X(L,I)
         DSUMY(L) = DSUMY(L) + Y(L,I)
         DSUMX2(L) = DSUMX2(L) + X(L,I)**2
         ENDDO
         DK(L) = DBLE(KC(L))
         SLOPE(L) = (DK(L)*DSUMXY(L)-DSUMX(L)*DSUMY(L))/
      1           (DK(L)*DSUMX2(L)-DSUMX(L)**2)
         B(L) = (DSUMY(L)/DK(L)) - SLOPE(L)*(DSUMX(L)/DK(L))
         TZERO(L) = - B(L)/SLOPE(L)
         WRITE (*,*) ' L = ',L,' TZERO(L) = ', TZERO(L)
C
C        Calculate the new time base for the data files
C
         DO I = 1, NUM(L)
         X(L,I) = X(L,I) - TZERO(L)
         ENDDO
         ENDDO
C
C        After subtracting off the zero offset from each of the KN number
C        of traces, find the average of the offsets and add the averaged
C        offset to each of the traces to gain a common time reference with
C        respect to all all of the other traces.
C
         TEMP = 0.0E0
         DO L = 1, KN
         TEMP = TEMP + TZERO(L)
         ENDDO
         TEMP = TEMP/FLOAT(KN)
         DO L = 1, KN
         DO I = 1, NUM(L)
         X(L,I) = X(L,I) + TEMP
         ENDDO
         ENDDO
  500 CONTINUE
C
C        Calculate the minimum and the maximum times for all the averaging
C        calculations
C
         TMIN = X(1,1)
         TMAX = X(1,NUM(1))
         DO L = 1, KN
         TMIN = AMAX1(TMIN,X(L,1))
         TMAX = AMIN1(TMAX,X(L,NUM(L)))
         ENDDO
```

```fortran
        WRITE (*,*) ' TMIN = ', TMIN, ' TMAX = ', TMAX
C
C       Spline fit the input data files
C
        DO L = 1, KN
           N = NUM(L)
           DO K = 1, N
           XX(K) = X(L,K)
           YY(K) = Y(L,K)
           SS(K) = S(L,K)
           II(K) = INDEX(L,K)
        ENDDO
        CALL SPCOEF (N,XX,YY,SS,II)
        DO K = 1, N
           S(L,K) = SS(K)
           INDEX(L,K) = II(K)
           ENDDO
        ENDDO
C
C       Add the input data
C
        DO I = 1, 501
        Y(11,I) = 0.0E0
        ENDDO
        DO I = 1, 501
        X(11,I) = TMIN + (TMAX - TMIN)*FLOAT(I - 1)/5.0E2
        DO L = 1, KN
        N = NUM(L)
        DO K = 1, N
           XX(K) = X(L,K)
           YY(K) = Y(L,K)
           SS(K) = S(L,K)
           II(K) = INDEX(L,K)
        ENDDO
        Y(11,I) = SPLINE(N,XX,YY,SS,II,X(11,I)) + Y(11,I)
        ENDDO
        ENDDO
C
C       Output the sum file
C
        TXT(11) =  ' Sum of files '//FILENAME(1)(1:10)//', '//
     1      FILENAME(2)(1:10)//', '//FILENAME(3)(1:10)//', '//
     2      FILENAME(4)(1:10)//', '//FILENAME(5)(1:10)//', '//
     3      FILENAME(6)(1:10)//', '//FILENAME(7)(1:10)//', '//
     4      FILENAME(8)(1:10)//', '//FILENAME(9)(1:10)//', '//
     5      FILENAME(10)(1:10)
      WRITE (11,2) TXT(11)
      WRITE (11,*) 501
      WRITE (11,*) (X(11,I),I=1,501)
      WRITE (11,*) (Y(11,I),I=1,501)
      CLOSE (UNIT=11)
  704 WRITE (*,850)
  850 FORMAT (1X,'$ Do you want to add any more data files? (Y or N)')
      READ (*,2,ERR=704) ANS
```

311

```
          IF ((ANS.EQ.'Y').OR.(ANS.EQ.'y')) GO TO 99
      905 CONTINUE
          WRITE (*,901)
      901 FORMAT (1X,'$ The subroutine SUM is terminating now.')
          RETURN
          END



          SUBROUTINE SUBTRACT
C
C     This subroutine compares the results of two files and yields a
C     third file as a difference of the two files.  Both files must be
C     in plot compatible form.
C
          REAL X1(1000), X2(1000), XDIFF(1000), Y1(1000), Y2(1000),
         1     YDIFF(1000), S1(1000), S2(1000), XLO, XHI, X
          INTEGER INDEX1(1000), INDEX2(1000), N1, N2, NDIFF, NUM1
          CHARACTER*132 NAME1, NAME2, DIFFNAME
          CHARACTER*1 ANS
        1 CONTINUE
C
C     Prompt for first input file
C
      700 WRITE (*,10)
        9 FORMAT (A)
       10 FORMAT (1X,'$ Enter data file name to be subtracted.')
          READ (*,9,ERR=700) NAME1
C
C     Prompt for second input file name
C
      701 WRITE (*,20)
       20 FORMAT (1X,'$ Enter data file name to subtract.')
          READ (*,9,ERR=701) NAME2
C
C     Prompt for difference file name
C
      702 WRITE (*,30)
       30 FORMAT (1X,'$ Enter file name of the new (differenced) file.')
          READ (*,9,ERR=702) DIFFNAME
          OPEN (UNIT=10,STATUS='OLD',FILE=NAME1,READONLY)
          OPEN (UNIT=20,STATUS='OLD',FILE=NAME2,READONLY)
          REWIND (UNIT=10)
          REWIND (UNIT=20)
          OPEN (UNIT=30,STATUS='NEW',FILE=DIFFNAME)
C
C     Enter first file characteristics
C
          READ (10,*)
          READ (10,*) N1
          READ (10,*) (X1(I), I = 1, N1)
          READ (10,*) (Y1(I), I = 1, N1)
C
```

```
C      Enter second file characteristics
C
       READ (20,*)
       READ (20,*) N2
       READ (20,*) (X2(I), I = 1, N2)
       READ (20,*) (Y2(I), I = 1, N2)
C
C
C
       NDIFF = MAX0(2,MIN0(1000,MAX0(IABS(N1),IABS(N2),501)))
C
C      Spline fit the data of FILE1 and FILE2
C
       CALL SPCOEF(N1,X1,Y1,S1,INDEX1)
       CALL SPCOEF(N2,X2,Y2,S2,INDEX2)
C
C      Define the limits of the X-values
C
       XLO = AMAX1(X1(1),X2(1))
       XHI = AMIN1(X1(N1),X2(N2))
       NUM1 = NDIFF - 1
C
C      Calculate the difference file
C
       DO I = 1, NDIFF
       XDIFF(I) = XLO + (XHI - XLO) * FLOAT(I - 1)/FLOAT(NUM1)
       X = XDIFF(I)
       YDIFF(I) = SPLINE(N1,X1,Y1,S1,INDEX1,X)
      1                 - SPLINE(N2,X2,Y2,S2,INDEX2,X)
       ENDDO
C
C      Output the difference file
C
       WRITE (30,9) '  Difference file between '//NAME1(1:20)//
      1    ' and '//NAME2(1:20)
       WRITE (30,*) NDIFF
       WRITE (30,*) (XDIFF(I), I = 1, NDIFF)
       WRITE (30,*) (YDIFF(I), I = 1, NDIFF)
       CLOSE (UNIT=10)
       CLOSE (UNIT=20)
       CLOSE (UNIT=30)
C
C      Query for completion
C
  703 WRITE (*,15)
   15 FORMAT (1X,'$ Do you want to create any more difference files?',
      1              ' (Y or N)')
       READ (*,9,ERR=703) ANS
       IF ((ANS.EQ.'Y').OR.(ANS.EQ.'y')) GO TO 1
       WRITE (*,25)
   25 FORMAT (1X,'$ Subroutine SUBTRACT is ending now.')
       RETURN
       END
```

313

```
      SUBROUTINE MULTIPLY
C
C     This subroutine will input up to 10 data files and output the file
C     that is the product of the input files.  The subroutine can
C     perform a correlation dependent on the calculated x-intercept of
C     the initial slope of the trace.  With proper modification, the
C     subroutine can be used to find the product of more than 10 files.
C
      PARAMETER NUPTS=1000
      CHARACTER*132 FILENAME(11), TXT(11)
      CHARACTER*1 ANS
      INTEGER INDEX(10,NUPTS), II(NUPTS), IMAX(10), IMIN(10), KC(10)
      INTEGER KN, NUM(10)
      REAL ASIGN(10), B(10), CMAX(10), CQ(10), CT(10), DELQI(10)
      REAL DELQIP1(10), DELTI(10), DELTIP1(10), FMAX(10), FMIN(10)
      REAL S(10,NUPTS), SIGNE, SLOPE(10), SS(NUPTS), TEMP, TEST, TMAX
      REAL TMIN , TZERO(10), X(11,NUPTS), XX(NUPTS), XMAX(10), XMIN(10)
      REAL Y(11,NUPTS), YY(NUPTS)
      DOUBLE PRECISION DK(10), DSUMX(10), DSUMX2(10), DSUMXY(10)
      DOUBLE PRECISION DSUMY(10)
      LL = 1
   99 CONTINUE
      LL = LL + 1
C
C     Enter the number of files to be multiplied
C
  700 WRITE (*,555)
  555 FORMAT (1X,'$ Enter the number of files to be multiplied.')
      READ (*,*,ERR=700) KN
      IF ((KN.LE.0).OR.(KN.GT.10)) THEN
         WRITE (*,556) KN
  556 FORMAT (1X,'The number of files is in error -- either it is too '
     1            ,'large or too small.',/,6X,'Input number of files = '
     2            , I5)
         GO TO 905
      ENDIF
      DO I = 1, 11
         DO J = 1, 132
         FILENAME(I)(J:J) = ' '
         ENDDO
      ENDDO
C
C     Enter file names
C
      DO L = 1, KN
  701    WRITE (*,1) L
    1 FORMAT (1X,'$ Enter the name for input file for file # ',I2)
         READ (*,2,ERR=701) FILENAME(L)
      ENDDO
    2 FORMAT (A)
  702 WRITE (*,3)
```

314

```fortran
    3 FORMAT (1X,'$ Enter the name of the output file.')
      READ (*,2,ERR=702) FILENAME(11)
C
C     Enter the input files
C
      DO L = 1, KN
         IF(LL.GE.2) REWIND (UNIT=L)
         OPEN (UNIT=L,NAME=FILENAME(L),TYPE='OLD',READONLY)
         READ (L,2) TXT(L)
         READ (L,*) NUM(L)
         READ (L,*) (X(L,J),J=1,NUM(L))
         READ (L,*) (Y(L,J),J=1,NUM(L))
         CLOSE (UNIT=L)
      ENDDO
      OPEN (UNIT=11,NAME=FILENAME(11),TYPE='NEW')
C
C     Find the maximum of the absolute value of each of the input files
C
      DO L = 1, KN
      CMAX(L) = 0.0E0
      DO J = 1, NUM(L)
         TEMP = CMAX(L)
         CMAX(L) = AMAX1(CMAX(L),ABS(Y(L,J)))
         IF (CMAX(L).GT.TEMP) ASIGN(L)=SIGN(1.0E0,Y(L,J))
      ENDDO
      WRITE (*,*) ' L = ',L,' ASIGN * CMAX(L) = ',ASIGN(L)*CMAX(L)
      ENDDO
C
C     If ASIGN(I) is negative, multiply the current data from the input
C     files so that all the data files will all have the same polarity.
C     Retain the final SIGNE = ASIGN(1) * ... * ASIGN(KN) for final
C     polarity.
C
      SIGNE = 1.0E0
      DO L = 1, KN
      SIGNE = SIGNE * ASIGN(L)
      IF (ASIGN(L).LT.0.0E0) THEN
         DO J = 1, NUM(L)
         Y(L,J) = -1.0E0 * Y(L,J)
         ENDDO
      ENDIF
      ENDDO
C
C     Query if a time correlation is required.  If the answer is yes,
C     continue as given.  If the answer is no, jump directly to the
C     multiplying step.
C
  703 WRITE (*,7)
    7 FORMAT (1X,'$ Do you want to perform a time correlation on the',
     1          ' data traces? (Y or N)')
      READ (*,2,ERR=703) ANS
      IF ((ANS.EQ.'Y').OR.(ANS.EQ.'y')) GO TO 200
      GO TO 500
  200 CONTINUE
```

315

```fortran
C
C      Query if user wishes to adjust the limits for time correlation
C
          WRITE (*,201)
201       FORMAT (//,1X,'For the purposes of adjusting the timing ',
     1         '(ordinate) of the digitized data,',/,1X,'the user ',
     2         'can select limits on the digitized trace rise/fall',
     3         ' based on fractions',/,1X,'of trace maximum.',//,1X,
     4         'Implicit in this correlation are the assumptions',
     5         ' that the trace rise/fall is',/,1X,'monotonic ',
     6         'and that an extrapolated zero can be calculated by',
     7         ' linear fitting',/,1X,'the portion of trace ',
     8         'rise/fall determined from fractional limits of ',
     9         'maximum.',//,1X,
     1         'The curve will extrapolate a zero point from the trace',
     2         ' between FMIN * CMAX',/,1X,'and FMAX * CMAX.  Here,',
     3         ' FMIN is the lower fraction, FMAX is the upper fraction',
     4         /,1X,'and CMAX is the trace maximum.  ',//,1X,
     5         'Unless set by user, FMIN = 0.1 and FMAX = 0.9.',/)
202       FORMAT (//,1X,'$ Do you want to set the limits for time',
     1         ' correlation? (Y or N)')
          WRITE (*,202)
          READ (*,2) ANS
          IF ((ANS.EQ.'Y').OR.(ANS.EQ.'y')) THEN
             WRITE (*,203)
203       FORMAT (1X,'$ Do you want the same fractional limits on all ',
     1         'traces? (Y or N)')
             READ (*,2) ANS
             IF ((ANS.NE.'Y').AND.(ANS.NE.'y')) THEN
                DO L = 1, KN
204                CONTINUE
                   WRITE (*,205) L
205       FORMAT (1X,'$ What is FMIN(',I2,')?')
                   READ (*,*,ERR=204) FMIN(L)
                   FMIN(L) = AMIN1(0.9E0,AMAX1(0.10E0,FMIN(L)))
206                CONTINUE
                   WRITE (*,207) L
207       FORMAT (1X,'$ What is FMAX(',I2,')?')
                   READ (*,*,ERR=206) FMAX(L)
                   FMAX(L) = AMAX1(0.1E0,AMIN1(0.90E0,FMAX(L)))
                ENDDO
                DO L = 1, KN
                IF (FMIN(L).GT.FMAX(L)) THEN
                   TEMP = FMAX(L)
                   FMAX(L) = FMIN(L)
                   FMIN(L) = TEMP
                ENDIF
                IF (FMIN(L).EQ.FMAX(L)) THEN
                   FMIN(L) = 0.1E0
                   FMAX(L) = 0.9E0
                ENDIF
                ENDDO
                WRITE (*,210) (L,FMIN(L),FMAX(L),L=1,KN)
210       FORMAT (1X,' L = ',I6,' FMIN(L) = ',1PE10.3,' FMAX(L) =',
```

```fortran
      1         1PE10.3)
                ELSE
211             CONTINUE
                WRITE (*,205) 1
                READ (*,*,ERR=211) FMIN(1)
                FMIN(1) = AMIN1(0.9E0,AMAX1(0.10E0,FMIN(1)))
212             CONTINUE
                WRITE (*,207) 1
                READ (*,*,ERR=212) FMAX(1)
                FMAX(1) = AMAX1(0.1E0,AMIN1(0.90E0,FMAX(1)))
                IF (FMIN(1).GT.FMAX(1)) THEN
                    TEMP = FMAX(1)
                    FMAX(1) = FMIN(1)
                    FMIN(1) = TEMP
                ENDIF
                IF (FMIN(1).EQ.FMAX(1)) THEN
                    FMIN(1) = 0.10E0
                    FMAX(1) = 0.90E0
                ENDIF
                DO L = 2, KN
                FMIN(L) = FMIN(1)
                FMAX(L) = FMAX(1)
                ENDDO
                WRITE (*,210) (L,FMIN(L),FMAX(L),L=1,KN)
                ENDIF
                ELSE
                DO L = 1, KN
                FMIN(L) = 0.1E0
                FMAX(L) = 0.9E0
                ENDDO
                WRITE (*,210) (L,FMIN(L),FMAX(L),L=1,KN)
                ENDIF
            DO L = 1, KN
            CT(L) = FMIN(L) * CMAX(L)
            CQ(L) = FMAX(L) * CMAX(L)
            ENDDO
            DO L = 1, KN
            WRITE (*,*)
            WRITE (*,*) ' L = ',L,' CMAX(L) = ',CMAX(L)
            WRITE (*,*) ' L = ',L,' CT(L) = ',CT(L),' CQ(L) = ',CQ(L)
            WRITE (*,*)
            ENDDO
C
C     Find the corresponding times of the high and low values of
C     digitized data traces
C
      DO L = 1, KN
      IMIN(L) = -1
      IMAX(L) = -1
      DO I = 1, NUM(L)
          DELQI(L) = CQ(L) - Y(L,I)
          DELQIP1(L) = Y(L,I+1) - CQ(L)
          DELTI(L) = CT(L) - Y(L,I)
          DELTIP1(L) = Y(L,I+1) - CT(L)
```

317

```
            IF ((IMAX(L).GT.O).AND.(IMIN(L).GT.O)) GO TO 110
            IF (DELQI(L).EQ.O.OEO) THEN
               IMAX(L) = MAXO(I-1,1)
               GO TO 101
            ENDIF
            IF ((IMAX(L).GT.O).AND.(IMIN(L).GT.O)) GO TO 110
            IF (DELQIP1(L).EQ.O.OEO) THEN
               IMAX(L) = MINO(I+1,NUM(L))
               GO TO 101
            ENDIF
101         CONTINUE
            IF ((IMAX(L).GT.O).AND.(IMIN(L).GT.O)) GO TO 110
            IF (DELTI(L).EQ.O.OEO) THEN
               IMIN(L) = MAXO(I-1,1)
               GO TO 102
            ENDIF
            IF ((IMAX(L).GT.O).AND.(IMIN(L).GT.O)) GO TO 110
            IF (DELTIP1(L).EQ.O.OEO) THEN
               IMIN(L) = MINO(I+1,NUM(L))
               GO TO 102
            ENDIF
102         CONTINUE
            IF ((IMAX(L).GT.O).AND.(IMIN(L).GT.O)) GO TO 110
            IF (DELTI(L)*DELTIP1(L).GT.O.OEO) THEN
               IMIN(L) = I + JNINT((CT(L) - Y(L,I))/(Y(L,I+1) - Y(L,I)))
               IMIN(L) = MAXO(IMIN(L)-1,1)
            ENDIF
            IF ((IMAX(L).GT.O).AND.(IMIN(L).GT.O)) GO TO 110
            IF (DELQI(L)*DELQIP1(L).GT.O.OEO) THEN
               IMAX(L) = I + JNINT((CQ(L) - Y(L,I))/(Y(L,I+1) - Y(L,I)))
               IMAX(L) = MINO(IMAX(L)+1,NUM(L))
            ENDIF
110         CONTINUE
      ENDDO
      IF ((IMIN(L).LE.1).OR.(IMIN(L).GE.NUM(L))) THEN
         WRITE (*,9)
         WRITE (*,*) ' L = ',L,' NUM(L) = ',NUM(L),' IMIN(L) = ',IMIN(L)
  9      FORMAT (1X,'The calculated limits on 10% of the value of the'
     1                ' current are invalid.')
         GO TO 905
      ENDIF
      IF ((IMAX(L).LE.1).OR.(IMAX(L).GE.NUM(L))) THEN
         WRITE (*,11)
         WRITE (*,*) ' L = ',L,' NUM(L) = ',NUM(L),' IMAX(L) = ',IMAX(L)
  11     FORMAT (1X,'The calculated limits on 25% of the value of the',
     1                ' current are invalid.')
         GO TO 905
      ENDIF
      IF (IMIN(L).GE.IMAX(L)) THEN
         WRITE (*,12)
      WRITE (*,*)' L = ',L,' IMIN(L) = ',IMIN(L),' IMAX(L) = ',IMAX(L)
  12     FORMAT (1X,'The lower limit on current is greater than or ',
     1                'equal to upper limit.')
         GO TO 905
```

318

```fortran
      ENDIF
      XMIN(L) = X(L,IMIN(L))
      XMAX(L) = X(L,IMAX(L))
      WRITE (*,*) ' L = ',L,' IMIN(L) = ',IMIN(L),' IMAX(L) = ',IMAX(L)
      WRITE (*,*) ' L = ',L,' XMIN(L) = ',XMIN(L),' XMAX(L) = ',XMAX(L)
C
C     Calculate the "zero" point of the data by least-squares-fitting
C     of the data between X = XMIN(L) AND X = XMAX(L)
C
      KC(L) = IMAX(L) - IMIN(L) + 1
      DSUMXY(L) = 0.0D0
      DSUMX(L) = 0.0D0
      DSUMY(L) = 0.0D0
      DSUMX2(L) = 0.0D0
      DO I = IMIN(L), IMAX(L)
         DSUMXY(L) = DSUMXY(L) + X(L,I) * Y(L,I)
         DSUMX(L) = DSUMX(L) + X(L,I)
         DSUMY(L) = DSUMY(L) + Y(L,I)
         DSUMX2(L) = DSUMX2(L) + X(L,I)**2
      ENDDO
      DK(L) = DBLE(KC(L))
      SLOPE(L) = (DK(L)*DSUMXY(L)-DSUMX(L)*DSUMY(L))/
     1           (DK(L)*DSUMX2(L)-DSUMX(L)**2)
      B(L) = (DSUMY(L)/DK(L)) - SLOPE(L)*(DSUMX(L)/DK(L))
      TZERO(L) = - B(L)/SLOPE(L)
      WRITE (*,*) ' L = ',L,' TZERO(L) = ', TZERO(L)
C
C     Calculate the new time base for the data files
C
      DO I = 1, NUM(L)
         X(L,I) = X(L,I) - TZERO(L)
      ENDDO
      ENDDO
C
C     After subtracting off the zero offset from each of the KN number
C     of traces, find the average of the offsets and add the averaged
C     offset to each of the traces to gain a common time reference with
C     respect to all of the other traces.
C
      TEMP = 0.0E0
      DO L = 1, KN
         TEMP = TEMP + TZERO(L)
      ENDDO
      TEMP = TEMP/FLOAT(KN)
      DO L = 1, KN
      DO I = 1, NUM(L)
         X(L,I) = X(L,I) + TEMP
      ENDDO
      ENDDO
  500 CONTINUE
C
C     Calculate the minimum and the maximum times for all the averaging
C     calculations
C
```

```fortran
      TMIN = X(1,1)
      TMAX = X(1,NUM(1))
      DO L = 1, KN
         TMIN = AMAX1(TMIN,X(L,1))
         TMAX = AMIN1(TMAX,X(L,NUM(L)))
      ENDDO
      WRITE (*,*) ' TMIN = ', TMIN, ' TMAX = ', TMAX
C
C     Spline fit the input data files
C
      DO L = 1, KN
      N = NUM(L)
      DO K = 1, N
         XX(K) = X(L,K)
         YY(K) = Y(L,K)
         SS(K) = S(L,K)
         II(K) = INDEX(L,K)
      ENDDO
      CALL SPCOEF (N,XX,YY,SS,II)
         DO K = 1, N
         S(L,K) = SS(K)
         INDEX(L,K) = II(K)
         ENDDO
      ENDDO
C
C     Multiply the input data
C
      DO I = 1, 501
         Y(11,I) = 1.0E0
      ENDDO
      DO I = 1, 501
      X(11,I) = TMIN + (TMAX - TMIN)*FLOAT(I - 1)/5.0E2
      DO L = 1, KN
      N = NUM(L)
         DO K = 1, N
         XX(K) = X(L,K)
         YY(K) = Y(L,K)
         SS(K) = S(L,K)
         II(K) = INDEX(L,K)
         ENDDO
      TEMP = FLOAT(KN-1)/FLOAT(KN)
      IF (KN.EQ.1) TEMP = 1.0E0
      IF (ALOG10(ABS(Y(11,I))).GE.38.0E0*TEMP) THEN
         Y(11,I) = SIGN(1.0E36,Y(11,I))
         WRITE (*,33)
   33 FORMAT (1X,'The product is too large.  It has been limited out.')
         GO TO 44
      ENDIF
      Y(11,I) = SPLINE(N,XX,YY,SS,II,X(11,I)) * Y(11,I)
   44    CONTINUE
      ENDDO
      ENDDO
      DO I = 1, 500
      Y(11,I) = SIGNE * Y(11,I)
```

```fortran
      ENDDO
C
C     Output the product file
C
      TXT(11) =  ' Prod. of files '//FILENAME(1)(1:10)//', '//
     1       FILENAME(2)(1:10)//', '//FILENAME(3)(1:10)//', '//
     2       FILENAME(4)(1:10)//', '//FILENAME(5)(1:10)//', '//
     3       FILENAME(6)(1:10)//', '//FILENAME(7)(1:10)//', '//
     4       FILENAME(8)(1:10)//', '//FILENAME(9)(1:10)//', '//
     5       FILENAME(10)(1:10)
      WRITE (11,2) TXT(11)
      WRITE (11,*) 501
      WRITE (11,*) (X(11,I),I=1,501)
      WRITE (11,*) (Y(11,I),I=1,501)
      CLOSE (UNIT=11)
  704 WRITE (*,850)
  850 FORMAT (1X,'$ Do you want to multiply any more data? (Y or N)')
      READ (*,2,ERR=704) ANS
      IF ((ANS.EQ.'Y').OR.(ANS.EQ.'y')) GO TO 99
  905 CONTINUE
      WRITE (*,901)
  901 FORMAT (1X,'$ The subroutine MULTIPLY is terminating now.')
      RETURN
      END
```

```fortran
      SUBROUTINE DIVIDE
C
C     This subroutine divides one file by another (i.e. Y1/Y2) and
C     yields a third file as a quotient of the two files.  Both files
C     must be in plot compatible form.
C
      REAL X1(1000), X2(1000), XDIV(1000), Y1(1000), Y2(1000),
     1     YDIV(1000), S1(1000), S2(1000), X, XHI, XLO, XLOG, XSUM,
     2     YAVG1, YAVG2, YNEW(1000), YMAX1, YMAX2, YMIN1, YMIN2
      INTEGER INDEX1(1000), INDEX2(1000), LOG1, LOG2, N1, N2, NDIV,
     1    NUM1
      CHARACTER*132 NAME1, NAME2, DIVNAME
      CHARACTER*1 ANS
    1 CONTINUE
C
C     Prompt for first input file
C
  700 WRITE (*,10)
    9 FORMAT (A)
   10 FORMAT (1X,'$ Enter file name to be divided.')
      READ (*,9,ERR=700) NAME1
C
C     Prompt for second input file name
C
  701 WRITE (*,20)
   20 FORMAT (1X,'$ Enter file name to divide.')
```

321

```
        READ (*,9,ERR=701) NAME2
C
C       Prompt for difference file name
C
  702 WRITE (*,30)
   30 FORMAT (1X,'$ Enter file name of the new (quotient) file.')
        READ (*,9,ERR=702) DIVNAME
        OPEN (UNIT=10,STATUS='OLD',FILE=NAME1,READONLY)
        OPEN (UNIT=20,STATUS='OLD',FILE=NAME2,READONLY)
        OPEN (UNIT=30,STATUS='NEW',FILE=DIVNAME)
        REWIND (UNIT=10)
        REWIND (UNIT=20)
C
C       Enter first file characteristics
C
        READ (10,*)
        READ (10,*) N1
        READ (10,*) (X1(I), I = 1, N1)
        READ (10,*) (Y1(I), I = 1, N1)
C
C       Enter second file characteristics
C
        READ (20,*)
        READ (20,*) N2
        READ (20,*) (X2(I), I = 1, N2)
        READ (20,*) (Y2(I), I = 1, N2)
C
C       Create a new Y-array from the second file so that division by the
C       new Y-value will not cause the quotient to "blow up", i.e. go to a
C       large value.
C
        YMIN1 = Y1(1)
        YMAX1 = Y1(1)
        DO I = 1, N1
        YMIN1 = AMIN1(Y1(I),YMIN1)
        YMAX1 = AMAX1(Y1(I),YMAX1)
        ENDDO
        YMAX1 = AMAX1(ABS(YMIN1),ABS(YMAX1))
        XSUM = 0.0E0
        DO I = 1, N1
        XSUM = XSUM + ABS(Y1(I))
        ENDDO
        YAVG1 = XSUM/FLOAT(N1)
        LOG1 = JNINT(ALOG10(YAVG1/YMAX1))
C
C       First find the maximum and minimum of the second file Y-value
C
        YMIN2 = Y2(1)
        YMAX2 = Y2(1)
        DO I = 2, N2
        YMIN2 = AMIN1(Y2(I),YMIN2)
        YMAX2 = AMAX1(Y2(I),YMAX2)
        ENDDO
        YMAX2 = AMAX1(ABS(YMIN2),ABS(YMAX2))
```

322

```fortran
      XSUM = 0.0E0
      DO I = 1, N2
      XSUM = XSUM + ABS(Y2(I))
      ENDDO
      YAVG2 = XSUM/FLOAT(N2)
      LOG2 = JNINT(ALOG10(YAVG2/YMAX2))
      XLOG = AMIN1(-2.0E0,-3.0E0 - FLOAT(MINO(35,IABS(LOG2-LOG1))))
C
C     If a ABS(Y) is within a lower limit
C     (in this case, 10**(-3.0+LOG1-LOG2)),
C     set this value to a maximum of
C         10.0**(3.0+LOG2-LOG1) * YMAX * sign(Y(I)).
C
C     This will reduce the chance of having the quotient blow up.
C
      DO I = 1, N2
      YNEW(I) = Y2(I)
      IF (ABS(Y2(I)).LE.(1.0E1**XLOG)*YMAX) THEN
         YNEW(I) = SIGN(YMAX,Y2(I)) * (1.0E1**(-1.0E0*XLOG))
      ENDIF
      ENDDO
C
C
C
      NDIV = MAXO(2,MINO(1000,MAXO(IABS(N1),IABS(N2),501)))
C
C     Spline fit the data of FILE1 and the modified FILE2
C
      CALL SPCOEF(N1,X1,Y1,S1,INDEX1)
      CALL SPCOEF(N2,X2,YNEW,S2,INDEX2)
C
C     Define the limits of the X-values
C
      XLO = AMAX1(X1(1),X2(1))
      XHI = AMIN1(X1(N1),X2(N2))
      NUM1 = NDIV - 1
C
C     Calculate the difference file
C
      DO I = 1, NDIV
      XDIV(I) = XLO + (XHI - XLO) * FLOAT(I - 1)/FLOAT(NUM1)
      X = XDIV(I)
      YDIV(I) = SPLINE(N1,X1,Y1,S1,INDEX1,X)/
     1           SPLINE(N2,X2,YNEW,S2,INDEX2,X)
      ENDDO
C
C     Output the difference file
C
      WRITE (30,9) ' Quotient file of '//NAME1(1:30)//
     1   ' divided by '//NAME2(1:30)
      WRITE (30,*) NDIV
      WRITE (30,*) (XDIV(I), I = 1, NDIV)
      WRITE (30,*) (YDIV(I), I = 1, NDIV)
      CLOSE (UNIT=10)
```

323

```
      CLOSE (UNIT=20)
      CLOSE (UNIT=30)
C
C     Query for completion
C
  703 WRITE (*,15)
   15 FORMAT (1X,'$ Do you want to create any more quotient files?',
     1        ' (Y or N)')
      READ (*,9,ERR=703) ANS
      IF ((ANS.EQ.'Y').OR.(ANS.EQ.'y')) GO TO 1
         WRITE (*,25)
   25 FORMAT (1X,'$ Subroutine DIVIDE is ending now.')
      RETURN
      END
```

```
      SUBROUTINE AVERAGE
C
C     This subroutine will input up to 10 data files and output the file
C     that is the arithmetic mean of the input files.  The subroutine
C     can perform a correlation dependent on the calculated x-intercept
C     of the initial slope of the trace.  With proper modification, the
C     subroutine can be used to find the arithmetic mean of more than
C     10 files.
C
      PARAMETER NUPTS=1000
      CHARACTER*132 FILENAME(11), TXT(11)
      CHARACTER*1 ANS
      INTEGER INDEX(10,NUPTS), II(NUPTS), IMAX(10), IMIN(10), KC(10)
      INTEGER KN, NUM(10)
      REAL ASIGN(10), B(10), CMAX(10), CQ(10), CT(10), DELQI(10)
      REAL DELQIP1(10), DELTI(10), DELTIP1(10), FMAX(10), FMIN(10)
      REAL S(10,NUPTS), SLOPE(10), SS(NUPTS), TEMP, TMAX, TMIN
      REAL TZERO(10), X(11,NUPTS), XX(NUPTS), XMAX(10), XMIN(10)
      REAL Y(11,NUPTS), YY(NUPTS)
      DOUBLE PRECISION DK(10), DSUMX(10), DSUMX2(10), DSUMXY(10)
      DOUBLE PRECISION DSUMY(10)
      LL = 1
   99 CONTINUE
      LL = LL + 1
C
C     Enter the number of files to be averaged
C
  700 WRITE (*,555)
  555 FORMAT (1X,'$ Enter the number of files to be averaged.')
      READ (*,*,ERR=700) KN
      IF ((KN.LE.0).OR.(KN.GT.10)) THEN
         WRITE (*,556)
  556 FORMAT (1X,'The number of files is in error -- either it is too '
     1            ,'large or too small.')
         GO TO 905
      ENDIF
```

```
          DO I = 1, 11
          DO J = 1, 132
             FILENAME(I)(J:J) = ' '
          ENDDO
          ENDDO
C
C       Enter file names
C
          DO L = 1, KN
    701 WRITE (*,1) L
      1 FORMAT (1X,'$ Enter the name for input file for file # ',I2)
          READ (*,2,ERR=701) FILENAME(L)
          ENDDO
      2 FORMAT (A)
    702 WRITE (*,3)
      3 FORMAT (1X,'$ Enter the name of the output file.')
          READ (*,2,ERR=702) FILENAME(11)
C
C       Enter the input files
C
          DO L = 1, KN
          IF(LL.GE.2) REWIND (UNIT=L)
          OPEN (UNIT=L,NAME=FILENAME(L),TYPE='OLD',READONLY)
          READ (L,2) TXT(L)
          READ (L,*) NUM(L)
          READ (L,*) (X(L,J),J=1,NUM(L))
          READ (L,*) (Y(L,J),J=1,NUM(L))
          CLOSE (UNIT=L)
          ENDDO
          OPEN (UNIT=11,NAME=FILENAME(11),TYPE='NEW')
C
C       Find the maximum of the absolute value of each of the input files
C
          DO L = 1, KN
          CMAX(L) = 0.0E0
          DO J = 1, NUM(L)
             TEMP = CMAX(L)
             CMAX(L) = AMAX1(CMAX(L),ABS(Y(L,J)))
             IF (CMAX(L).GT.TEMP) ASIGN(L)=SIGN(1.0E0,Y(L,J))
          ENDDO
          WRITE (*,*) ' L = ',L,' ASIGN * CMAX(L) = ',ASIGN(L)*CMAX(L)
          ENDDO
C
C       Query if a time correlation is required.  If the answer is yes,
C       continue as given.  If the answer is no, jump directly to the
C       averaging step.
C
    703 WRITE (*,7)
      7 FORMAT (1X,'$ Do you want to perform a time correlation on the',
      1          ' data traces? (Y or N)')
          READ (*,2,ERR=703) ANS
          IF ((ANS.EQ.'Y').OR.(ANS.EQ.'y')) GO TO 200
          GO TO 500
    200 CONTINUE
```

```fortran
C
C      Query if user wishes to adjust the limits for time correlation
C
            WRITE (*,201)
201      FORMAT (//,1X,'For the purposes of adjusting the timing ',
     1      '(ordinate) of the digitized data,',/,1X,'the user ',
     2      'can select limits on the digitized trace rise/fall',
     3      ' based on fractions',/,1X,'of trace maximum.',//,1X,
     4      'Implicit in this correlation are the assumptions',
     5      ' that the trace rise/fall is',/,1X,'monotonic ',
     6      'and that an extrapolated zero can be calculated by',
     7      ' linear fitting',/,1X,'the portion of trace ',
     8      'rise/fall determined from fractional limits of ',
     9      'maximum.',//,1X,
     1      'The curve will extrapolate a zero point from the trace',
     2      ' between FMIN * CMAX',/,1X,'and FMAX * CMAX.  Here,',
     3      ' FMIN is the lower fraction, FMAX is the upper fraction',
     4      /,1X,'and CMAX is the trace maximum.  ',//,1X,
     5      'Unless set by user, FMIN = 0.1 and FMAX = 0.9.',/)
202      FORMAT (//,1X,'$ Do you want to set the limits for time',
     1      ' correlation? (Y or N)')
            WRITE (*,202)
            READ (*,2) ANS
            IF ((ANS.EQ.'Y').OR.(ANS.EQ.'y')) THEN
               WRITE (*,203)
203      FORMAT (1X,'$ Do you want the same fractional limits on all ',
     1      'traces? (Y or N)')
               READ (*,2) ANS
               IF ((ANS.NE.'Y').AND.(ANS.NE.'y')) THEN
                  DO L = 1, KN
204                  CONTINUE
                     WRITE (*,205) L
205      FORMAT (1X,'$ What is FMIN(',I2,')?')
                     READ (*,*,ERR=204) FMIN(L)
                     FMIN(L) = AMIN1(0.9E0,AMAX1(0.10E0,FMIN(L)))
206                  CONTINUE
                     WRITE (*,207) L
207      FORMAT (1X,'$ What is FMAX(',I2,')?')
                     READ (*,*,ERR=206) FMAX(L)
                     FMAX(L) = AMAX1(0.1E0,AMIN1(0.90E0,FMAX(L)))
                  ENDDO
                  DO L = 1, KN
                  IF (FMIN(L).GT.FMAX(L)) THEN
                     TEMP = FMAX(L)
                     FMAX(L) = FMIN(L)
                     FMIN(L) = TEMP
                  ENDIF
                  IF (FMIN(L).EQ.FMAX(L)) THEN
                     FMIN(L) = 0.1E0
                     FMAX(L) = 0.9E0
                  ENDIF
                  ENDDO
                  WRITE (*,210) (L,FMIN(L),FMAX(L),L=1,KN)
210      FORMAT (1X,' L = ',I6,' FMIN(L) = ',1PE10.3,' FMAX(L) =',
```

326

```
      1           1PE10.3)
                  ELSE
    211           CONTINUE
                  WRITE (*,205) 1
                  READ (*,*,ERR=211) FMIN(1)
                  FMIN(1) = AMIN1(0.9E0,AMAX1(0.10E0,FMIN(1)))
    212           CONTINUE
                  WRITE (*,207) 1
                  READ (*,*,ERR=212) FMAX(1)
                  FMAX(1) = AMAX1(0.1E0,AMIN1(0.90E0,FMAX(1)))
                  IF (FMIN(1).GT.FMAX(1)) THEN
                     TEMP = FMAX(1)
                     FMAX(1) = FMIN(1)
                     FMIN(1) = TEMP
                  ENDIF
                  IF (FMIN(1).EQ.FMAX(1)) THEN
                     FMIN(1) = 0.10E0
                     FMAX(1) = 0.90E0
                  ENDIF
                  DO L = 2, KN
                  FMIN(L) = FMIN(1)
                  FMAX(L) = FMAX(1)
                  ENDDO
                  WRITE (*,210) (L,FMIN(L),FMAX(L),L=1,KN)
                  ENDIF
                  ELSE
                  DO L = 1, KN
                  FMIN(L) = 0.1E0
                  FMAX(L) = 0.9E0
                  ENDDO
                  WRITE (*,210) (L,FMIN(L),FMAX(L),L=1,KN)
                  ENDIF
               DO L = 1, KN
               CT(L) = FMIN(L) * CMAX(L)
               CQ(L) = FMAX(L) * CMAX(L)
               ENDDO
               DO L = 1, KN
               WRITE (*,*)
               WRITE (*,*) ' L = ',L,' CMAX(L) = ',CMAX(L)
               WRITE (*,*) ' L = ',L,' CT(L) = ',CT(L),' CQ(L) = ',CQ(L)
               WRITE (*,*)
               ENDDO
C
C      Find the corresponding times of the high and low values of
C      digitized data trace
C
       DO L = 1, KN
       IMIN(L) = -1
       IMAX(L) = -1
       DO I = 1, NUM(L)
          DELQI(L) = CQ(L) - Y(L,I)
          DELQIP1(L) = Y(L,I+1) - CQ(L)
          DELTI(L) = CT(L) - Y(L,I)
          DELTIP1(L) = Y(L,I+1) - CT(L)
```

327

```fortran
      IF ((IMAX(L).GT.O).AND.(IMIN(L).GT.O)) GO TO 110
      IF (DELQI(L).EQ.O.OEO) THEN
         IMAX(L) = MAXO(I-1,1)
         GO TO 101
      ENDIF
      IF ((IMAX(L).GT.O).AND.(IMIN(L).GT.O)) GO TO 110
      IF (DELQIP1(L).EQ.O.OEO) THEN
         IMAX(L) = MINO(I+1,NUM(L))
         GO TO 101
      ENDIF
101   CONTINUE
      IF ((IMAX(L).GT.O).AND.(IMIN(L).GT.O)) GO TO 110
      IF (DELTI(L).EQ.O.OEO) THEN
         IMIN(L) = MAXO(I-1,1)
         GO TO 102
      ENDIF
      IF ((IMAX(L).GT.O).AND.(IMIN(L).GT.O)) GO TO 110
      IF (DELTIP1(L).EQ.O.OEO) THEN
         IMIN(L) = MINO(I+1,NUM(L))
         GO TO 102
      ENDIF
102   CONTINUE
      IF ((IMAX(L).GT.O).AND.(IMIN(L).GT.O)) GO TO 110
      IF (DELTI(L)*DELTIP1(L).GT.O.OEO) THEN
         IMIN(L) = I + JNINT((CT(L) - Y(L,I))/(Y(L,I+1) - Y(L,I)))
         IMIN(L) = MAXO(IMIN(L)-1,1)
      ENDIF
      IF ((IMAX(L).GT.O).AND.(IMIN(L).GT.O)) GO TO 110
      IF (DELQI(L)*DELQIP1(L).GT.O.OEO) THEN
         IMAX(L) = I + JNINT((CQ(L) - Y(L,I))/(Y(L,I+1) - Y(L,I)))
         IMAX(L) = MINO(IMAX(L)+1,NUM(L))
      ENDIF
110   CONTINUE
      ENDDO
      IF ((IMIN(L).LE.1).OR.(IMIN(L).GE.NUM(L))) THEN
         WRITE (*,9)
      WRITE (*,*)' L = ',L,' NUM(L) = ',NUM(L),' IMIN(L) = ',IMIN(L)
 9    FORMAT (1X,'The calculated limits on 10% of the value of the'
     1             ' current are invalid.')
         GO TO 905
      ENDIF
      IF ((IMAX(L).LE.1).OR.(IMAX(L).GE.NUM(L))) THEN
         WRITE (*,11)
      WRITE (*,*)' L = ',L,' NUM(L) = ',NUM(L),' IMAX(L) = ',IMAX(L)
 11   FORMAT (1X,'The calculated limits on 25% of the value of the',
     1             ' current are invalid.')
      GO TO 905
      ENDIF
      IF (IMIN(L).GE.IMAX(L)) THEN
         WRITE (*,12)
      WRITE (*,*)' L = ',L,' IMIN(L) = ',IMIN(L),' IMAX(L) = ',IMAX(L)
 12   FORMAT (1X,'The lower limit on current is greater than or ',
     1             'equal to upper limit.')
         GO TO 905
```

328

```fortran
      ENDIF
      XMIN(L) = X(L,IMIN(L))
      XMAX(L) = X(L,IMAX(L))
      WRITE (*,*) ' L = ',L,' IMIN(L) = ',IMIN(L),' IMAX(L) = ',IMAX(L)
      WRITE (*,*) ' L = ',L,' XMIN(L) = ',XMIN(L),' XMAX(L) = ',XMAX(L)
C
C     Calculate the "zero" point of the data by least-squares-fitting
C     of the data between X = XMIN(L) AND X = XMAX(L)
C
      KC(L) = IMAX(L) - IMIN(L) + 1
      DSUMXY(L) = 0.0D0
      DSUMX(L) = 0.0D0
      DSUMY(L) = 0.0D0
      DSUMX2(L) = 0.0D0
      DO I = IMIN(L), IMAX(L)
      DSUMXY(L) = DSUMXY(L) + X(L,I) * Y(L,I)
      DSUMX(L) = DSUMX(L) + X(L,I)
      DSUMY(L) = DSUMY(L) + Y(L,I)
      DSUMX2(L) = DSUMX2(L) + X(L,I)**2
      ENDDO
      DK(L) = DBLE(KC(L))
      SLOPE(L) = (DK(L)*DSUMXY(L)-DSUMX(L)*DSUMY(L))/
     1           (DK(L)*DSUMX2(L)-DSUMX(L)**2)
      B(L) = (DSUMY(L)/DK(L)) - SLOPE(L)*(DSUMX(L)/DK(L))
      TZERO(L) = - B(L)/SLOPE(L)
      WRITE (*,*) ' L = ',L,' TZERO(L) = ', TZERO(L)
C
C     Calculate the new time base for the data files
C
      DO I = 1, NUM(L)
      X(L,I) = X(L,I) - TZERO(L)
      ENDDO
      ENDDO
C
C     After subtracting off the zero offset from each of the KN number
C     of traces, find the average of the offsets and add the averaged
C     offset to each of the traces to gain a common time reference with
C     respect to all of the other traces.
C
      TEMP = 0.0E0
      DO L = 1, KN
      TEMP = TEMP + TZERO(L)
      ENDDO
      TEMP = TEMP/FLOAT(KN)
      DO L = 1, KN
      DO I = 1, NUM(L)
      X(L,I) = X(L,I) + TEMP
      ENDDO
      ENDDO
  500 CONTINUE
C
C     Calculate the minimum and the maximum times for all the averaging
C     calculations
C
```

```fortran
      TMIN = X(1,1)
      TMAX = X(1,NUM(1))
      DO L = 1, KN
      TMIN = AMAX1(TMIN,X(L,1))
      TMAX = AMIN1(TMAX,X(L,NUM(L)))
      ENDDO
      WRITE (*,*) ' TMIN = ', TMIN, ' TMAX = ', TMAX
C
C     Spline fit the input data files
C
      DO L = 1, KN
      N = NUM(L)
      DO K = 1, N
         XX(K) = X(L,K)
         YY(K) = Y(L,K)
         SS(K) = S(L,K)
         II(K) = INDEX(L,K)
      ENDDO
      CALL SPCOEF (N,XX,YY,SS,II)
      DO K = 1, N
         S(L,K) = SS(K)
         INDEX(L,K) = II(K)
         ENDDO
      ENDDO
C
C     Average the input data
C
      DO I = 1, 501
      Y(11,I) = 0.0E0
      ENDDO
      DO I = 1, 501
      X(11,I) = TMIN + (TMAX - TMIN)*FLOAT(I - 1)/5.0E2
      DO L = 1, KN
      N = NUM(L)
      DO K = 1, N
         XX(K) = X(L,K)
         YY(K) = Y(L,K)
         SS(K) = S(L,K)
         II(K) = INDEX(L,K)
      ENDDO
      Y(11,I) = SPLINE(N,XX,YY,SS,II,X(11,I)) + Y(11,I)
      ENDDO
      Y(11,I) = Y(11,I)/FLOAT(KN)
      ENDDO
C
C     Output the averaged file
C
      TXT(11) =  ' Avg. of files '//FILENAME(1)(1:10)//', '//
     1       FILENAME(2)(1:10)//', '//FILENAME(3)(1:10)//', '//
     2       FILENAME(4)(1:10)//', '//FILENAME(5)(1:10)//', '//
     3       FILENAME(6)(1:10)//', '//FILENAME(7)(1:10)//', '//
     4       FILENAME(8)(1:10)//', '//FILENAME(9)(1:10)//', '//
     5       FILENAME(10)(1:10)
      WRITE (11,2) TXT(11)
```

```
      WRITE (11,*) 501
      WRITE (11,*) (X(11,I),I=1,501)
      WRITE (11,*) (Y(11,I),I=1,501)
      CLOSE (UNIT=11)
  704 WRITE (*,850)
  850 FORMAT (1X,'$ Do you want to average any more data? (Y or N)')
      READ (*,2,ERR=704) ANS
      IF ((ANS.EQ.'Y').OR.(ANS.EQ.'y')) GO TO 99
  905 CONTINUE
      WRITE (*,901)
  901 FORMAT (1X,'$ The subroutine AVERAGE is terminating now.')
      RETURN
      END
```

```
      SUBROUTINE REVISE
C     adapted from PROGRAM INDUCTOR version 2.1
C
C
C     This subroutine is a revised version of an inductance calculation
C     subroutine where input data is the voltage trace, the current
C     trace and a time shift between the two traces.
C
C     Additionally, the subroutine has been modified to allow the
C     calculation of energy, power and impedance as a function of time.
C
C     The output data are all calculated from the current and voltage
C     traces.
C
C     Important variables describing the current and voltage are:
C
C         NPTSC -- number of current (electrical) data points
C
C         TXTI -- title of current data (on first line of data file)
C
C         TIMEC -- time array corresponding to the current array; NPTSC
C                   time points
C
C         CMAX -- absolute value of maximum current value
C
C         CUR -- current array; NPTSC current data points
C
C         CURC -- modified current array; NPTSC current data points
C
C         NPTSV -- number of voltage data points
C
C         TXTV -- title of voltage data (on first line of data file)
C
C         TIMEV -- time array corresponding to voltage array; NPTSV time
C                   points
C
C         VOLT -- voltage array; NPTSV voltage points
C
```

331

```
C          VMAX -- absolute value of maximum voltage value
C
C          TMIN -- the minimum time used in calculation; given by
C                     AMAX1(TIMEC(1),TIMEV(1)-TEMP)
C
C          TMAX -- the maximum time used in calculation; given by
C                     AMIN1(TIMEC(NPTSC),TIMEV(NPTSV)-TEMP)
C
C          TEMP -- the time shift used in calculating inductance,
C                     impedance, power and energy
C
C    The modified current CURC(I) is essentially the current trace
C    (CUR(I)) with small current (where CUR(I) is less than 0.25% CMAX),
C    CURC(I) values are set to 4.0E2 * SIGN(CMAX,CUR(I)).  This allows
C    the calculated inductance trace to be within some given limits.
C
C    The inductance L(t) is calculated from the relation
C
C          L(t) = INT[V(t)dt - R * I(t)dt]/IM(t)
C
C       where INT is the time integral;
C          V(t) is the input voltage (VOLT);
C          I(t) is the input voltage (CUR);
C          R is the assumed constant plasma resistance
C            = 0 to 10 milliohms;
C        and IM(t) is the modified current (CURC).
C
C    The power P(t) (PT(I)) is calculated from the relation
C
C          P(t) = V(t) * I(t)
C
C    The energy E(t) (ET(I)) is calculated from the relation
C
C          E(t) = INT[P(t)dt]
C
C    The impedance Z(t) (IMPEDE(I)) is calculated from the relation
C
C          Z(t) = INT[V(t)dt]/INT[I(t)dt]
C
C    This version of the code is the version dated 15 July 1987 written
C    by David W. Price, AFWL/AWPPE.  It supersedes the version (1.1)
C    dated 7 September 1984 written by David W. Price, AFWL/NTYPH.  The
C    initial version (INDUCTOR) was written by Lt. Michael P. Snell and
C    David W. Price, AFWL/NTYPH.
C
C
      PARAMETER NPTS=1000
      EXTERNAL FC, FV
      CHARACTER*132 CNAME, ENERGY, IMPNAME, INTCNAM, INTVNAM, LNAME
      CHARACTER*132 POWER, TITLE, TXTI, TXTV, VNAME
      CHARACTER*4 CR(5)
      CHARACTER*1 ANSER
      INTEGER ICMAX, ICMIN, IFLAG, INDEXC(NPTS), INDEXV(NPTS), IVMAX
      INTEGER IVMIN, K, KC, KV, NPTSC, NPTSV
```

```
        REAL ACC, ANS, AREA, BC, BV, CMAX, CQ, CSIGN, CT, CUR(NPTS)
        REAL CURC(NPTS), DELCQI, DELCQIP1, DELCTI, DELCTIP1, DELVQI
        REAL DELVQIP1, DELVTI, DELVTIP1, ET(501), ERROR, IC(NPTS)
        REAL IMPEDE(501), IV(NPTS), L(NPTS), PT(501), SC(NPTS), SLOPEC
        REAL SLOPEV, SV(NPTS), TEMP, TIME(501), TIMEC(NPTS), TIMEV(NPTS)
        REAL TMAX, TMIN, R(5), TZEROC, TZEROV, VMAX, VOLT(NPTS), VQ, VSIGN
        REAL VT, XCMAX, XCMIN, XHI, XLO, XVMAX, XVMIN
        DOUBLE PRECISION DKC, DKV, DSUM, DSUMC, DSUMV, SUMXC, SUMXV
        DOUBLE PRECISION SUMX2C, SUMX2V, SUMXYC, SUMXYV, SUMYC, SUMYV
        DATA CR/' 0.0',' 1.0',' 3.0',' 6.0','10.0'/
        DATA R/0.0E0,1.0E-3,3.0E-3,6.0E-3,10.0E-3/
        COMMON /I/NPTSC,TIMEC,CUR,SC,INDEXC
        COMMON /V/NPTSV,TIMEV,VOLT,SV,INDEXV
     99 CONTINUE
C
C       Enter file names
C
    600 WRITE (*,1)
      1 FORMAT (1X,'$ Enter integrated current filename.')
        READ (*,2,ERR=600) INTCNAM
      2 FORMAT (A)
    601 WRITE (*,3)
      3 FORMAT (1X,'$ Enter integrated voltage filename.')
        READ (*,2,ERR=601) INTVNAM
    602 WRITE (*,4)
      4 FORMAT (1X,'$ Enter input current filename.')
        READ (*,2,ERR=602) CNAME
    603 WRITE (*,5)
      5 FORMAT (1X,'$ Enter input voltage filename.')
        READ (*,2,ERR=603) VNAME
    604 WRITE (*,6)
      6 FORMAT (1X,'$ Enter inductance output filename.')
        READ (*,2,ERR=604) LNAME
    605 WRITE (*,7)
      7 FORMAT (1X,'$ Enter power output filename.')
        READ (*,2,ERR=605) POWER
    606 WRITE (*,8)
      8 FORMAT (1X,'$ Enter energy output filename.')
        READ (*,2,ERR=606) ENERGY
    607 WRITE (*,9)
      9 FORMAT (1X,'$ Enter impedance output filename.')
        READ (*,2,ERR=607) IMPNAME
        OPEN (UNIT=3,NAME=CNAME,TYPE='OLD',READONLY)
        OPEN (UNIT=4,NAME=VNAME,TYPE='OLD',READONLY)
        REWIND (UNIT=3)
        REWIND (UNIT=4)
C
C       Enter current data
C
        READ (3,2) TXTI
        READ (3,*) NPTSC
        READ (3,*) (TIMEC(I), I = 1, NPTSC)
        READ (3,*) (CUR(I), I = 1, NPTSC)
C
```

333

```fortran
C       Enter voltage data
C
        READ (4,2) TXTV
        READ (4,*) NPTSV
        READ (4,*) (TIMEV(I), I = 1, NPTSV)
        READ (4,*) (VOLT(I), I = 1, NPTSV)
C
C       Find the maximum of the absolute value of the current
C
        CMAX = 0.0E0
        DO I = 1, NPTSC
        TEMP = CMAX
        CMAX = AMAX1(CMAX,ABS(CUR(I)))
        IF (CMAX.GT.TEMP) CSIGN = SIGN(1.0E0,CUR(I))
        ENDDO
C
C       Find the maximum of the absolute value of the voltage
C
        VMAX = 0.0E0
        DO I = 1, NPTSV
        TEMP = VMAX
        VMAX = AMAX1(VMAX,ABS(VOLT(I)))
        IF (VMAX.GT.TEMP) VSIGN = SIGN(1.0E0,VOLT(I))
        ENDDO
        WRITE (*,*) ' VMAX = ', VSIGN * VMAX, ' CMAX = ', CSIGN * CMAX
C
C       If VSIGN and CSIGN are of different signs, multiply current
C       data by -1 to reduce the possibility of a negative calculated
C       inductance.
C
        IF (CSIGN*VSIGN.LT.0.0E0) THEN
           DO I = 1, NPTSC
           CUR(I) = -1.0E0 * CUR(I)
           ENDDO
           CSIGN = -1.0E0 * CSIGN
        ENDIF
C
C       Calculate quarter and tenth of the maximum current and voltage
C       values
C
        CQ = CSIGN * CMAX/4.0E0
        CT = CSIGN * CMAX/10.0E0
        VQ = VSIGN * VMAX/4.0E0
        VT = VSIGN * VMAX/10.0E0
        WRITE (*,*) ' CT = ', CT, ' CQ = ', CQ
        WRITE (*,*) ' VT = ', VT, ' VQ = ', VQ
C
C
C
        DO 900 K = 1, 5
        OPEN (UNIT=5,NAME=LNAME,TYPE='NEW')
        IF (K.GT.1) GO TO 800
C
C       Query if a time correlation is required.  If the answer is yes,
```

```fortran
C     continue as given.  If the answer is no, jump directly to the
C     integration step.
C
  608 WRITE (*,11)
   11 FORMAT (1X,'$ Do you want to perform a time correlation on the',
     1        ' data traces? (Y or N)')
      READ (*,2,ERR=608) ANSER
      IF ((ANSER.EQ.'Y').OR.(ANSER.EQ.'y')) GO TO 200
      GO TO 500
  200 CONTINUE
  609 WRITE (*,12)
   12 FORMAT (1X,'$ Do you wish to input your own time correlation ',
     1   'factor instead of calculating',/,1X,'a correlation factor',
     2   ' (Y or N)')
      READ (*,2,ERR=609) ANSER
      IF ((ANSER.EQ.'Y').OR.(ANSER.EQ.'y')) GO TO 210
      GO TO 220
  210 CONTINUE
      WRITE (*,230)
  230 FORMAT (1X,'$ Enter the input correlation factor.',/,1X,
     1   ' (- time indicates sliding voltage to the right with respect',
     2   /,1X,' to the current trace; + time indicates sliding voltage',
     3   /,1X,' to the left with respect to the current trace.)')
      READ (*,*) TEMP
      GO TO 400
  220 CONTINUE
C
C     Find the corresponding times of the quarter and tenth values of
C     current.
C
      DO I = 1, NPTSC
      IF ((ICMAX.GT.0).AND.(ICMIN.GT.0)) GO TO 300
      DELCQI = CQ - CUR(I)
      DELCQIP1 = CUR(I+1) - CQ
      DELCTI = CT - CUR(I)
      DELCTIP1 = CUR(I+1) - CT
      IF (DELCQI.EQ.0.0E0) ICMAX = I
      IF (DELCQIP1.EQ.0.0E0) ICMAX = I + 1
      IF (DELCTI.EQ.0.0E0) ICMIN = I
      IF (DELCTIP1.EQ.0.0E0) ICMIN = I + 1
      IF (DELCTI*DELCTIP1.GT.0.0E0) THEN
          ICMIN = I + JNINT((CT - CUR(I))/(CUR(I+1) - CUR(I)))
          ICMIN = MAXO(1,ICMIN-1)
      ENDIF
      IF (DELCQI*DELCQIP1.GT.0.0E0) THEN
          ICMAX = I + JNINT((CQ - CUR(I))/(CUR(I+1) - CUR(I)))
          ICMAX = MINO(NPTSC,ICMAX+1)
      ENDIF
      ENDDO
  300 CONTINUE
      IF ((ICMIN.LE.1).OR.(ICMIN.GE.NPTSC)) THEN
          WRITE (*,13)
          WRITE (*,*) ' NPTSC = ', NPTSC, ' ICMIN = ', ICMIN
   13     FORMAT (1X,'The calculated limits on 10% of the value of the'
```

```fortran
     1                    ' current are invalid.')
           GO TO 950
        ENDIF
        IF ((ICMAX.LE.1).OR.(ICMAX.GE.NPTSC)) THEN
           WRITE (*,15)
           WRITE (*,*) ' NPTSC = ', NPTSC, ' ICMAX = ', ICMAX
  15       FORMAT (1X,'The calculated limits on 25% of the value of the',
     1                    ' current are invalid.')
           GO TO 950
        ENDIF
        IF (ICMIN.GE.ICMAX) THEN
           WRITE (*,16)
           WRITE (*,*) ' ICMIN = ', ICMIN, ' ICMAX = ', ICMAX
  16       FORMAT (1X,'The lower limit on current is greater than or ',
     1                    'equal to upper limit.')
           GO TO 950
        ENDIF
        XCMIN = TIMEC(ICMIN)
        XCMAX = TIMEC(ICMAX)
        WRITE (*,*) ' ICMIN = ', ICMIN, ' ICMAX = ', ICMAX
        WRITE (*,*) ' XCMIN = ', XCMIN, ' XCMAX = ', XCMAX
C
C     Find the corresponding times of the quarter and tenth values of
C         the voltage
C
        DO I = 1, NPTSV
        IF ((IVMAX.GT.O).AND.(IVMIN.GT.O)) GO TO 350
        DELVQI = VQ - VOLT(I)
        DELVQIP1 = VOLT(I+1) - VQ
        DELVTI = VT - VOLT(I)
        DELVTIP1 = VOLT(I+1) - VT
        IF (DELVQI.EQ.0.OEO) IVMAX = I
        IF (DELVQIP1.EQ.0.OEO) IVMAX = I + 1
        IF (DELVTI.EQ.0.OEO) IVMIN = I
        IF (DELVTIP1.EQ.0.OEO) IVMIN = I + 1
        IF (DELVTI*DELVTIP1.GT.0.OEO) THEN
           IVMIN = I + JNINT((VT-VOLT(I))/(VOLT(I+1)-VOLT(I)))
           IVMIN = MAXO(1,IVMIN-1)
        ENDIF
        IF (DELVQI*DELVQIP1.GT.0.OEO) THEN
           IVMAX = I + JNINT((VQ-VOLT(I))/(VOLT(I+1)-VOLT(I)))
           IVMAX = MINO(NPTSV,IVMAX+1)
        ENDIF
        ENDDO
  350 CONTINUE
        IF ((IVMIN.LE.1).OR.(IVMIN.GE.NPTSV)) THEN
           WRITE (*,17)
           WRITE (*,*) 'NPTSV = ', NPTSV, ' IVMIN = ', IVMIN
  17       FORMAT (1X,'The calculated limits on 10% of the value of the ',
     1                    'voltage are invalid.')
           GO TO 950
        ENDIF
        IF ((IVMAX.LE.1).OR.(IVMAX.GE.NPTSV)) THEN
           WRITE (*,18)
```

336

```fortran
18      FORMAT (1X,'The calculated limits on 25% of the value of the ',
     1          'voltage are invalid.')
        WRITE (*,*) 'NPTSV = ', NPTSV, ' IVMAX = ', IVMAX
        GO TO 950
      ENDIF
      IF (IVMIN.GE.IVMAX) THEN
        WRITE (*,19)
19      FORMAT (1X,'The lower limit on voltage is greater than or ',
     1      'equal to the upper limit.')
        WRITE (*,*) ' IVMIN = ', IVMIN, ' IVMAX = ', IVMAX
        GO TO 950
      ENDIF
      XVMIN = TIMEV(IVMIN)
      XVMAX = TIMEV(IVMAX)
      WRITE (*,*) ' IVMIN = ', IVMIN, ' IVMAX = ', IVMAX
      WRITE (*,*) ' XVMIN = ', XVMIN, ' XVMAX = ', XVMAX
C
C     Calculate the "zero" point of the voltage by least-squares-fitting
C     the voltage data between X = XVMIN and X = XVMAX
C
      KV = IVMAX - IVMIN + 1
      SUMXYV = 0.0E0
      SUMXV = 0.0E0
      SUMYV = 0.0E0
      SUMX2V = 0.0E0
      DO I = IVMIN, IVMAX
      SUMXYV = SUMXYV + TIMEV(I) * VOLT(I)
      SUMXV = SUMXV + TIMEV(I)
      SUMYV = SUMYV + VOLT(I)
      SUMX2V = SUMX2V + TIMEV(I)**2
      ENDDO
      DKV = DBLE(KV)
      SLOPEV = (DKV*SUMXYV-SUMXV*SUMYV)/(DKV*SUMX2V-SUMXV**2)
      BV = (SUMYV/DKV) - SLOPEV*(SUMXV/DKV)
      TZEROV = - BV/SLOPEV
      WRITE (*,*) ' TZEROV = ', TZEROV
C
C     Calculate the "zero" point of the current by least-squares-fitting
C     of the data between X = XCMIN AND X = XCMAX
C
      KC = ICMAX - ICMIN + 1
      SUMXYC = 0.0E0
      SUMXC = 0.0E0
      SUMYC = 0.0E0
      SUMX2C = 0.0E0
      DO I = ICMIN, ICMAX
      SUMXYC = SUMXYC + TIMEC(I) * CUR(I)
      SUMXC = SUMXC + TIMEC(I)
      SUMYC = SUMYC + CUR(I)
      SUMX2C = SUMX2C + TIMEC(I)**2
      ENDDO
      DKC = DBLE(KC)
      SLOPEC = (DKC*SUMXYC-SUMXC*SUMYC)/(DKC*SUMX2C-SUMXC**2)
      BC = (SUMYC/DKC) - SLOPEC*(SUMXC/DKC)
```

337

```
           TZEROC = - BC/SLOPEC
           WRITE (*,*) ' TZEROC = ', TZEROC
           TEMP = TZEROV - TZEROC
           WRITE (*,*)
           WRITE (*,*) ' TZEROV - TZEROC = ', TEMP
           WRITE (*,*)
       400 CONTINUE
   C
   C       Calculate the new time base for the voltage
   C
           DO I = 1, NPTSV
           TIMEV(I) = TIMEV(I) - TEMP
           ENDDO
       500 CONTINUE
   C
   C       Calculate the minimum and the maximum time for the inductance
   C       calculations
   C
           TMIN = AMAX1(TIMEC(1),TIMEV(1))
           TMAX = AMIN1(TIMEC(NPTSC),TIMEV(NPTSV))
           WRITE (*,*) ' TMIN = ', TMIN, ' TMAX = ', TMAX
           DO I = 1, 501
           TIME(I) = TMIN + (TMAX - TMIN) * FLOAT(I-1)/5.0E2
           ENDDO
   C
   C       Spline fit the current and the voltage
   C
           CALL SPCOEF (NPTSC,TIMEC,CUR,SC,INDEXC)
           CALL SPCOEF (NPTSV,TIMEV,VOLT,SV,INDEXV)
   C
   C       Integrate the current
   C
           ACC = 3.0E-7
           DSUMC = 0.0D0
           IC(1) = SNGL(DSUMC)
           WRITE (*,150) 1
           DO I = 1, 500
           WRITE (*,150) I + 1
       150 FORMAT (5X,'Subroutine REVISE is working; I = ',2X,I4)
           XLO = TIME(I)
           XHI = TIME(I+1)
           CALL SIMP(FC,XLO,XHI,ACC,ANS,ERROR,AREA,IFLAG)
           DSUMC = DSUMC + DBLE(ANS)
           IC(I+1) = SNGL(DSUMC)
           ENDDO
   C
   C       Integrate the voltage
   C
           DSUMV = 0.0D0
           IV(1) = SNGL(DSUMV)
           WRITE (*,150) 1
           DO I = 1, 500
           WRITE (*,150) I + 1
           XLO = TIME(I)
```

```fortran
      XHI = TIME(I+1)
      CALL SIMP(FV,XLO,XHI,ACC,ANS,ERROR,AREA,IFLAG)
      DSUMV = DSUMV + DBLE(ANS)
      IV(I+1) = SNGL(DSUMV)
      ENDDO
  610 WRITE (*,701)
  701 FORMAT (1X,'$ Do you want output the integrated current data',
     1        ' to a separate file? (Y or N)')
      READ (*,2,ERR=610) ANSER
      IF ((ANSER.NE.'Y').AND.(ANSER.NE.'y')) GO TO 710
C
C     Write integrated current data to output
C
      OPEN (UNIT=1,NAME=INTCNAM,TYPE='NEW')
      TITLE = TXTI(1:90)//'INT(YdX)/'//TXTI(100:132)
      WRITE (1,2) TITLE
      WRITE (1,*) 501
      WRITE (1,*) (TIME(I),I = 1, 501)
      WRITE (1,*) (IC(I),I = 1, 501)
  710 CONTINUE
      CLOSE (UNIT=1)
  611 WRITE (*,711)
  711 FORMAT (1X,'$ Do you want to output the integrated voltage file ',
     1        'to a separate file? (Y or N)')
      READ (*,2,ERR=611) ANSER
      IF ((ANSER.NE.'Y').AND.(ANSER.NE.'y')) GO TO 720
C
C     Write integrated voltage to output
C
      OPEN (UNIT=2,NAME=INTVNAM,TYPE='NEW')
      TITLE = TXTV(1:90)//'INT(YdX)/'//TXTV(100:132)
      WRITE (2,2) TITLE
      WRITE (2,*) 501
      WRITE (2,*) (TIME(I), I = 1, 501)
      WRITE (2,*) (IV(I), I = 1, 501)
  720 CONTINUE
      CLOSE (UNIT=2)
  800 CONTINUE
  612 WRITE (*,730) R(K)
  730 FORMAT (1X,'$ Do you want to calculate the inductance with R = ',
     1        1PE8.2,' ohms? (Y or N)')
      READ (*,2,ERR=612) ANSER
      IF ((ANSER.NE.'Y').AND.(ANSER.NE.'y')) GO TO 740
C
C     Calculate the inductance according to the relation
C
C         L(t) = [INT(V(t)) - R*INT(I(t))]/[I(t)]
C
      DO I = 1, 501
      IF (ABS(CUR(I)).LE.2.5E-3*CMAX) THEN
          CURC(I) = 4.0E2 * SIGN(CMAX,CUR(I))
      ENDIF
      IF (CURC(I).EQ.0.0E0) CURC(I) = 4.0E2 * CMAX
      IF (ABS(CUR(I)).GT.2.5E-3*CMAX) CURC(I) = CUR(I)
```

```fortran
      L(I) = (IV(I) - R(K)*IC(I))/CURC(I)
      L(I) = AMAX1(L(I),0.0E0)
      ENDDO
C
C     Write the inductance to an output file
C
      WRITE (5,2) ' L(T) vs T w/ V = '//VNAME(1:12)//' w/ I = '//
     1                 CNAME(1:12)//' and R = '//CR(K)//' mohms'
      WRITE (5,*) 501
      WRITE (5,*) (TIME(I), I = 1, 501)
      WRITE (5,*) (L(I), I = 1, 501)
  740 CONTINUE
      CLOSE (UNIT=5)
      IF (K.GT.1) GO TO 900
  613 WRITE (*,751)
  751 FORMAT (1X,'$ Do you want to calculate the power? (Y or N)')
      READ (*,2,ERR=613) ANSER
      IF ((ANSER.NE.'Y').AND.(ANSER.NE.'y')) GO TO 760
C
C     Calculate and output the power
C
      DO I = 1, 501
      PT(I) = P(TIME(I))
      IF (PT(I).LE.-1.05E0*VMAX*CMAX) PT(I) = -1.05E0*VMAX*CMAX
      IF (PT(I).GE.1.05E0*VMAX*CMAX) PT(I) = 1.05E0*VMAX*CMAX
      ENDDO
      OPEN (UNIT=6,NAME=POWER,TYPE='NEW')
      WRITE (6,2) ' Power vs time with V = '//VNAME(1:12)//' with I = '
     1                 //CNAME(1:12)
      WRITE (6,*) 501
      WRITE (6,*) (TIME(I), I = 1, 501)
      WRITE (6,*) (PT(I), I = 1, 501)
  760 CONTINUE
      CLOSE (UNIT=6)
  614 WRITE (*,761)
  761 FORMAT (1X,'$ Do you want to calculate the energy? (Y or N)')
      READ (*,2,ERR=614) ANSER
      IF ((ANSER.NE.'Y').AND.(ANSER.NE.'y')) GO TO 770
C
C     Calculate the energy
C
      DSUM = 0.0D0
      ET(1) = SNGL(DSUM)
      WRITE (*,150) 1
      DO I = 1, 500
      WRITE (*,150) I + 1
      XLO = TIME(I)
      XHI = TIME(I+1)
      CALL SIMP(P,XLO,XHI,ACC,ANS,ERROR,AREA,IFLAG)
      DSUM = DSUM + DBLE(ANS)
      ET(I+1) = SNGL(DSUM)
      ENDDO
C
C     Output energy
```

340

```fortran
C
      OPEN (UNIT=7,NAME=ENERGY,TYPE='NEW')
      WRITE (7,2) ' Energy vs time with V = '//VNAME(1:12)//' with I = '
     1            //CNAME(1:12)
      WRITE (7,*) 501
      WRITE (7,*) (TIME(I), I = 1, 501)
      WRITE (7,*) (ET(I), I = 1, 501)
  770 CONTINUE
      CLOSE (UNIT = 7)
  615 WRITE (*,771)
  771 FORMAT (1X,'$ Do you want to calculate the impedance? (Y or N)?')
      READ (*,2,ERR=615) ANSER
      IF ((ANSER.NE.'Y').AND.(ANSER.NE.'y')) GO TO 780
C
C     Calculate the impedance
C
      DO I = 1, 501
      IF (IC(I).EQ.0.0E0) IMPEDE(I) = 0.0E0
      IF (IC(I).NE.0.0E0) IMPEDE(I) = IV(I)/IC(I)
      ENDDO
C
C     Output the calculated impedance
C
      OPEN (UNIT=8,NAME=IMPNAME,TYPE='NEW')
      WRITE (8,2) ' Impedance vs time with V = '//VNAME(1:12)//
     1            ' with I = '//CNAME(1:12)
      WRITE (8,*) 501
      WRITE (8,*) (TIME(I), I = 1, 501)
      WRITE (8,*) (IMPEDE(I), I = 1, 501)
  780 CONTINUE
      CLOSE (UNIT = 8)
  900 CONTINUE
  616 WRITE (*,930)
  930 FORMAT (1X,'$ Do you want to calculate any more? (Y or N) ')
      READ (*,2,ERR=616) ANSER
      IF ((ANSER.EQ.'Y').OR.(ANSER.EQ.'y')) GO TO 99
  950 CONTINUE
      WRITE (*,999)
      CLOSE (UNIT=3)
      CLOSE (UNIT=4)
  999 FORMAT (1X,'The subroutine REVISE is terminating now.')
      RETURN
      END
```

```fortran
      FUNCTION FC(X)
      COMMON /I/NPTSC,TIMEC,CUR,SC,INDEXC
      DIMENSION TIMEC(1000), CUR(1000), SC(1000), INDEXC(1000)
      FC = SPLINE(NPTSC,TIMEC,CUR,SC,INDEXC,X)
      RETURN
      END
```

341

```
FUNCTION FV(X)
DIMENSION TIMEV(1000), VOLT(1000), SV(1000), INDEXV(1000)
COMMON /V/NPTSV,TIMEV,VOLT,SV,INDEXV
FV = SPLINE(NPTSV,TIMEV,VOLT,SV,INDEXV,X)
RETURN
END
```

```
FUNCTION P(X)
DIMENSION CUR(1000), INDEXC(1000), INDEXV(1000), TIMEC(1000)
DIMENSION TIMEV(1000), SC(1000), SV(1000), VOLT(1000)
COMMON /I/NPTSC, TIMEC, CUR, SC, INDEXC
COMMON /V/NPTSV, TIMEV, VOLT, SV, INDEXV
P = FC(X) * FV(X)
RETURN
END
```

```
      SUBROUTINE CURRENT
C
C     This subroutine will calculate the current response of a B-dot
C     probe or a Rogowski coil given the output response voltage and
C     given detector parameters.  If the Rogowski coil or the B-dot
C     probes are not passively (RC) integrated, the response calculated
C     will be that of dI/dt (time differential of current).
C     Additionally, if the errors are also input, the expected total
C     error is output.
C
C     This program will not integrate or correct for "voltage droop".
C
C
C     The equation to be used is
C
C              I(t) = (2.0E0 * PI * RC * RAD * V(t))/
C                              (MUNOT * XN * A)
C
C     for RC time integrated traces.
C
C     The equation to be used is
C
C              dI(t)/dt = (2.0E0 * PI * RAD * V(t))/(MUNOT * XN * A)
C
C     for traces not passively (RC) integrated.
C
C     It should be noted that the response C becomes
C
C                    = (2.0E0 * PI * RC * RAD)/(MUNOT * XN * A)
```

342

```
C                                              (for RC integrated traces)
C            C
C                       = (2.0EO * PI * RAD)/(MUNOT * XN * A)
C                                              (for no RC integration)
C
      REAL X(1000), YOLD(1000), YNEW(1000), A, C, RAD, RC, XN
C
C              X(I) is the I'th time point;
C              YOLD(I) is the input I'th voltage response;
C              YNEW(I) is the calculate I'th current response;
C              A is the area of the probe in square meters;
C              C is an input overall response
C                 (in Amp/Volts or Amp/Volt-secs);
C              RAD is the radial distance from the center of the current
C                 flow to the center of the coil in meters; and
C              XN is the number of turns of the coil.
C
      REAL AERR, CERR, RADERR, RCERR, YERR, XNERR
C
C              AERR is the total (absolute) error in A;
C              CERR is the total (absolute) error in C;
C              RADERR is the total (absolute) error in RAD;
C              RCERR is the total (absolute) error in RC;
C              YERR is the averaged percent error in the Y array; and
C              XNERR is the total (absolute) error in XN.
C
      REAL ERROR, MUNOT
C
C     ERROR is the total output percent error of the data file; and
C     MUNOT is the permeablility of free space=4.0E-7*PI Henries/meter.
C
      INTEGER N, NT, NERR
      CHARACTER INPUT*132, OUTPUT*132, TITLE*132, ANS*1
      PI = 4.0EO * ATAN(1.0EO)
      MUNOT = 4.0E-7 * PI
    1 CONTINUE
      A = 1.0EO
      AERR = 0.0EO
      RAD = 1.0EO
      RADERR = 0.0EO
      RC = 1.0EO
      RCERR = 0.0EO
      YERR = 0.0EO
      C = 1.0EO
      CERR = 0.0EO
      ERROR = 0.0EO
    9 FORMAT (A)
C
C     Read input file name
C
  600 WRITE (*,100)
  100 FORMAT (1X,'$ What is the input file name to be converted ',
     1          'to current?')
      READ (*,9,ERR=600) INPUT
```

```
         OPEN (UNIT=1,STATUS='OLD',FILE=INPUT,READONLY)
         REWIND (UNIT=1)
     601 WRITE (*,101)
     101 FORMAT (1X,'$ What is the output file name?')
         READ (*,9,ERR=601) OUTPUT
         OPEN (UNIT=2,STATUS='NEW',FILE=OUTPUT)
C
C    Enter input file data
C
         READ (1,9) TITLE
         READ (1,*) N
         READ (1,*) (X(I), I = 1, N)
         READ (1,*) (YOLD(I), I = 1, N)
         CLOSE (UNIT=1)
C
C    Query for the use of passive (RC) integration
C
     602 WRITE (*,102)
     102 FORMAT (1X,'$ Was the probe passively (RC) integrated? (Y or N)')
         READ (*,9,ERR=602) ANS
         IF ((ANS.EQ.'Y').OR.(ANS.EQ.'y')) GO TO 700
     603 WRITE (*,300)
     300 FORMAT (1X,'$ Is there a single lumped response constant? ',
        1      '(Y or N)')
         READ (*,9,ERR=603) ANS
         IF ((ANS.EQ.'Y').OR.(ANS.EQ.'y')) GO TO 500
C
C    Enter values for discrete (non-lumped) system parameters
C
     604 WRITE (*,301)
     301 FORMAT (1X,'$ What is the radial distance (from the center of ',
        1    'the axial current to',/,2X,' the center of the loop)',
        2    ' in meters?')
         READ (*,*,ERR=604) RAD
     605 WRITE (*,302)
     302 FORMAT (1X,'$ What is the absolute error in the radius (in ',
        1    'meters)')
         READ (*,*,ERR=605) RADERR
     606 WRITE (*,303)
     303 FORMAT (1X,'$ What is the number of the turns?')
         READ (*,*,ERR=606) NT
         XN = FLOAT(NT)
     607 WRITE (*,304)
     304 FORMAT (1X,'$ What is the error in the total number of turns?')
         READ (*,*,ERR=607) NERR
         XNERR = FLOAT(NERR)
     608 WRITE (*,305)
     305 FORMAT (1X,'$ What is the total area of one turn (in square ',
        1    'meters)?')
         READ (*,*,ERR=608) A
     609 WRITE (*,306)
     306 FORMAT (1X,'$ What is the error in total area of one turn (in '
        1    'square meters)?')
         READ (*,*,ERR=609) AERR
```

344

```
    610 WRITE (*,307)
    307 FORMAT(1X,'$ What is the averaged relative error in the voltage ',
       1    'trace?')
        READ (*,*,ERR=610) YERR
        AERR = AERR/A
        RADERR = RADERR/RAD
        XNERR = XNERR/XN
        CERR = AERR**2 + RADERR**2 + XNERR**2 + YERR**2
        ERROR = SQRT(CERR)
        C = (2.0E0 * PI * RAD)/(MUNOT * XN * A)
        TITLE = ' dI/dt vs time '//TITLE(1:117)
        GO TO 900
C
C     Enter lumped conversion factor
C
    500 CONTINUE
    611 WRITE (*,501)
    501 FORMAT (1X,'$ What is the conversion factor between the voltage ',
       1        'and dI/dt (in Amp/Volt-secs)?')
        READ (*,*,ERR=611) C
    612 WRITE (*,502)
    502 FORMAT (1X,'$ What is the total error in the conversion factor ',
       1        '(in Amp/Volt-secs)?')
        READ (*,*,ERR=612) CERR
        CERR = CERR/C
        TITLE = ' dI/dt vs time '//TITLE(1:117)
    613 WRITE (*,307)
        READ (*,*,ERR=613) YERR
        ERROR = SQRT(CERR**2 + YERR**2)
        GO TO 900
C
C     Enter RC integrator time constant values
C
    700 CONTINUE
    614 WRITE (*,701)
    701 FORMAT (1X,'$ What is the RC time constant (in seconds)?')
        READ (*,*,ERR=614) RC
    615 WRITE (*,702)
    702 FORMAT (1X,'$ What is the absolute error in the RC time constant',
       1            ' (in seconds)?')
        READ (*,*,ERR=615) RCERR
        TITLE = ' I(t) '//TITLE(1:126)
C
C     Query for lumped parameters
C
    616 WRITE (*,703)
    703 FORMAT (1X,'$ Do you have a conversion factor between input',
       1    ' signal and calculated ',/,2X,'response',
       2    ' (in Amp/Volts)? (Y or N)')
        READ (*,9,ERR=616) ANS
        IF ((ANS.EQ.'Y').OR.(ANS.EQ.'y')) GO TO 800
    617 WRITE (*,301)
        READ (*,*,ERR=617) RAD
    618 WRITE (*,302)
```

345

```fortran
      READ (*,*,ERR=618) RADERR
  619 WRITE (*,303)
      READ (*,*,ERR=619) NT
      XN = FLOAT(NT)
  620 WRITE (*,304)
      READ (*,*,ERR=620) NERR
      XNERR = FLOAT(NERR)
  621 WRITE (*,305)
      READ (*,*,ERR=621) A
  622 WRITE (*,306)
      READ (*,*,ERR=622) AERR
  623 WRITE (*,307)
      READ (*,*,ERR=623) YERR
      AERR = AERR/A
      RADERR = RADERR/RAD
      RCERR = RCERR/RC
      XNERR = XNERR/XN
      CERR = AERR**2 + RADERR**2 + RCERR**2 + XNERR**2 + YERR**2
      ERROR = SQRT(CERR)
      C = (2.0E0 * PI * RAD * RC)/(MUNOT * XN * A)
      GO TO 900
C
C     Enter the lumped parameters
C
  800 CONTINUE
  624 WRITE (*,801)
      READ (*,*,ERR=624) C
  625 WRITE (*,802)
      READ (*,*,ERR=625) CERR
      CERR = CERR/C
  801 FORMAT (1X,'$ What is the conversion factor between the voltage',
     1       ' and current (in Amp/Volts)?')
  802 FORMAT (1X,'$ What is the total error in the conversion factor',
     1       ' (in Amp/Volts)?')
  626 WRITE (*,307)
      READ (*,*,ERR=626) YERR
      ERROR = SQRT(CERR**2 + YERR**2)
C
C     Output the calculated current response
C
  900 CONTINUE
      DO I = 1, N
      YNEW(I) = C * YOLD(I)
      ENDDO
      WRITE (2,9) TITLE
      WRITE (2,*) N
      WRITE (2,*) (X(I), I = 1, N)
      WRITE (2,*) (YNEW(I), I = 1, N)
      WRITE (2,*) ' Area = ', A,' sq. meters; rel.  error in area = ',
     1                AERR
      WRITE (2,*)' Radius = ', RAD, ' meters; rel.  error in radius = ',
     1                     RADERR
      WRITE (2,*) ' RC = ', RC, ' seconds; rel.  error in RC = ', RCERR
      WRITE (2,*) ' number of turns = ', INT(XN),'; error in turns = ',
```

346

```
       1                          INT(XN*XNERR),' turns'
        WRITE (2,*) ' averaged rel. error in voltage = ', YERR
        WRITE (2,*) ' constant C = ', C, '; rel. error in constant',
       1                CERR
        WRITE (2,*) ' total current rel. error = ', ERROR
        CLOSE (UNIT = 2)
C
C      Query for more calculations
C
   627 WRITE (*,950)
   950 FORMAT (1X,'$ Do you want to calculate any more current',
       1              ' responses?  (Y or N)')
        READ (*,9,ERR=627) ANS
        IF ((ANS.EQ.'Y').OR.(ANS.EQ.'y')) GO TO 1
        WRITE (*,951)
   951 FORMAT (1X,'$ The subroutine CURRENT will stop now!')
        RETURN
        END



          SUBROUTINE MEANY
C
C      This program calculates the average y-value value on the discrete
C      y-value trace within given limits using a least squares fit
C      technique.  A lower and an upper x-value are input by the user.
C
        DIMENSION X(1000), Y(1000)
        DOUBLE PRECISION STDDEV, SUMY, SUMY2, XMEAN, XN, XNL1
        REAL XHI, XLO
        INTEGER IDEL, IERR, IHI, ILO
        CHARACTER ANS*1, INFILE*132, OUTFILE*132
C
C      Input initial information
C
   700    WRITE (*,25)
          READ (*,9,ERR=700) OUTFILE
          OPEN (UNIT=10,STATUS='NEW',FILE=OUTFILE)
     1    CONTINUE
   701    WRITE (*,15)
    15    FORMAT(1X,'$ Enter file name of trace to be portion ',
       1              'averaged.')
     9    FORMAT (A)
          READ (*,9,ERR=701) INFILE
          OPEN (UNIT=5,STATUS='OLD',FILE=INFILE,READONLY)
    25    FORMAT (1X,'$ Enter the output file name.')
     2    CONTINUE
          REWIND (UNIT=5)
          WRITE (*,30)
    30    FORMAT (1X,'The averaged y-value is determined from input',
       1              ' x-values.')
   702    WRITE (*,35)
    35    FORMAT (1X,'$ Input lower x-value of the trace to be ',
```

```
      1                         'averaged.')
          READ (*,*,ERR=702) XLO
  703     WRITE (*,40)
   40     FORMAT (1X,'$ Input upper x-value of the trace.')
          READ (*,*,ERR=703) XHI
          READ (5,*)
          READ (5,*) N
          READ (5,*) (X(I), I = 1, N)
          READ (5,*) (Y(I), I = 1, N)
C
C     Check and see if errors have occured on input x-values
C
          IERR = 0
          IF (XLO.LT.X(1)) IERR = 1
          IF (XLO.GT.X(N)) IERR = 1
          IF (XLO.GE.XHI) IERR = 1
          IF (XHI.LT.X(1)) IERR = 1
          IF (XHI.GT.X(N)) IERR = 1
          IF (IERR.EQ.1) THEN
             WRITE (*,51)
             WRITE (*,52) XLO, XHI
             WRITE (*,53) X(1), X(N)
  704        WRITE (*,54)
             READ (*,9,ERR=704) ANS
   51        FORMAT (1X,'There is an error in the x-array limits.')
   52        FORMAT (1X,' XLO = ',1PE20.8,T50,' XHI = ',1PE20.8)
   53        FORMAT (1X,' X(1) = ',1PE20.8,T50,' X(N) = ',1PE20.8)
   54 FORMAT(1X,'$ Do you wish to stop the subroutine now? (Y or N)')
             IF ((ANS.EQ.'Y').OR.(ANS.EQ.'y')) GO TO 998
             GO TO 2
          ENDIF
C
C     Sort through the x-array and find the values for ILO and IHI
C
          DO 100 I = 2, N
          XXL1 = XLO - X(I-1)
          XXLO = X(I) - XLO
          IF (XXL1.EQ.0.0E0) ILO = MAXO(1,I-1)
          IF (XXLO.EQ.0.0E0) ILO = I
          IF (XXL1*XXLO.GT.0.0E0) THEN
          IF (ABS(XXL1).LE.ABS(XXLO)) ILO = I - 1
             IF (ABS(XXL1).GT.ABS(XXLO)) ILO = I
          ENDIF
  100     CONTINUE
          DO 200 I = JMAXO(ILO-1,2), N
          XXL1 = XHI - X(I-1)
          XXHI = X(I) - XHI
          IF (XXL1.EQ.0.0E0) IHI = I - 1
          IF (XXHI.EQ.0.0E0) IHI = I
          IF (XXL1*XXHI.GT.0.0E0) THEN
             IF (ABS(XXL1).LE.ABS(XXHI)) IHI = I - 1
             IF (ABS(XXL1).GT.ABS(XXHI)) IHI = I
          ENDIF
  200     CONTINUE
```

348

```
C
C       Calculate average (XMEAN) and standard deviation from the average
C       (STDDEV)
C
        IDEL = IHI - ILO + 1
        XN = DBLE(IDEL)
        XNL1 = DBLE(IDEL - 1)
        SUMY = 0.0D0
        SUMY2 = 0.0D0
        DO 500 I = ILO, IHI
        SUMY = SUMY + DBLE(Y(I))
500     SUMY2 = SUMY2 + DBLE(Y(I))**2
        STDDEV = SQRT((XN*SUMY2-SUMY**2)/(XN*XNL1))
        XMEAN = SUMY/XN
C
C    Write out results
C
600     FORMAT (/,1X,'Y(average) = ',1PE20.8,5X,'Std. dev. = ',1PE20.8)
        WRITE (10,*)
        WRITE (10,*) ' For input file '
        WRITE (10,9) '        '//INFILE(1:72)
        WRITE (10,600) SNGL(XMEAN), SNGL(STDDEV)
        WRITE (10,*)
        WRITE (*,*)
        WRITE (*,*) ' For input file '
        WRITE (*,9) '        '//INFILE(1:72)
        WRITE (*,600) SNGL(XMEAN), SNGL(STDDEV)
        WRITE (*,*)
C
C    Query for more averaging
C
705     WRITE (*,900)
900     FORMAT (1X,'$ Do you want any more averages? (Y or N)')
        READ (*,9,ERR=705) ANS
        IF ((ANS.EQ.'Y').OR.(ANS.EQ.'y')) GO TO 1
C
C       End subroutine MEANY
C
998     CONTINUE
        CLOSE (UNIT=5)
        CLOSE (UNIT=10)
        WRITE (*,999)
999     FORMAT (1X,'$ Subroutine MEANY is ending now.')
        RETURN
        END




        SUBROUTINE MAXMIN
        DIMENSION X(1000), Y(1000)
        CHARACTER*132 TITLE, INFILE
        CHARACTER*1 ANS
C
```

349

```
C      This subroutine finds the maxima and minima of x-values and
C      y-values and their corresponding y- and x-values in a plot
C      compatible file.
   1      CONTINUE
 700      WRITE (*,5)
   5      FORMAT (1X,'$ Enter input file name to find maximum and'
   1             ' minimum.')
          READ (*,9,ERR=700) INFILE
          OPEN (UNIT=5,STATUS='OLD',FILE=INFILE,READONLY)
          REWIND (UNIT=5)
          READ (5,9) TITLE
   9      FORMAT (A)
          READ (5, *) N
          READ (5, *) (X(I), I = 1, N)
          READ (5, *) (Y(I), I = 1, N)
          IXMIN = 1
          IXMAX = 1
          IYMIN = 1
          IYMAX = 1
          XMIN = X(1)
          XMAX = X(1)
          YMIN = Y(1)
          YMAX = Y(1)
          DO I = 1, N
          IF (X(I).LT.XMIN) IXMIN = I
          XMIN = AMIN1(XMIN,X(I))
          IF (X(I).GT.XMAX) IXMAX = I
          XMAX = AMAX1(XMAX,X(I))
          IF (Y(I).LT.YMIN) IYMIN = I
          YMIN = AMIN1(YMIN,Y(I))
          IF (Y(I).GT.YMAX) IYMAX = I
          YMAX = AMAX1(YMAX,Y(I))
          ENDDO
          WRITE (*,*)
          WRITE (*,*) ' For filename -- '
          WRITE (*,9) '          '//INFILE(1:60)
          WRITE (*,*) ' Minimum x = ', XMIN, ' Y(XMIN) = ', Y(IXMIN)
          WRITE (*,*) ' Maximum x = ', XMAX, ' Y(XMAX) = ', Y(IXMAX)
          WRITE (*,*) ' X(YMIN) = ', X(IYMIN), ' YMIN = ', YMIN
          WRITE (*,*) ' X(YMAX) = ', X(IYMAX), ' YMAX = ', YMAX
          WRITE (*,*)
          CLOSE (UNIT=5)
C
C      Query for more maxima/minima calculations
 701      WRITE (*,21)
  21      FORMAT (1X,'$ Do you want to perform any more maxima/minima',
   1             ' calculations (Y or N)')
          READ (*,9,ERR=701) ANS
          IF ((ANS.EQ.'Y').OR.(ANS.EQ.'y')) GO TO 1
          WRITE (*,22)
  22      FORMAT (1X,'$ Subroutine MAXMIN is ending now.')
          RETURN
          END
```

```
          SUBROUTINE SMOOTH
          DIMENSION X1(1000), X2(1000), Y1(1000), Y2(1000), YNEW(1000)
          DIMENSION S(1000)
          DIMENSION INDEX(1000)
          REAL S, X1, X2, XMIN, XMAX, Y1, Y2, YNEW
          CHARACTER*132 TITLE, INFILE, OUTFILE
          CHARACTER*1 ANS
C
C     This program performs a seven point smoothing on the y-values of
C     the trace.  The x-values are not affected.
C
     1    CONTINUE
   700    WRITE (*,5)
     5    FORMAT (1X,'$ Enter input file name to be smooched.')
     9    FORMAT (A)
          READ (*,9,ERR=700) INFILE
   701    WRITE (*,10)
    10    FORMAT (1X,'$ Enter output file name.')
          READ (*,9,ERR=701) OUTFILE
          OPEN (UNIT=5,STATUS='OLD',FILE=INFILE,READONLY)
          REWIND (UNIT=5)
          OPEN (UNIT=10,STATUS='NEW',FILE=OUTFILE)
          READ (5,9) TITLE
          READ (5,*) N
          IF (N.LT.7) THEN
             WRITE (*, 11) N
    11       FORMAT (1X,'For smoothing, there must be at least 7 data',
     1               ' points; N = ', I6)
             WRITE (10,9) TITLE
             WRITE (10,*) N
             WRITE (10,*) (X1(I), I = 1, N)
             WRITE (10,*) (Y1(I), I = 1, N)
             GO TO 99
          ENDIF
          READ (5,*) (X1(I), I = 1, N)
          READ (5,*) (Y1(I), I = 1, N)
C
C     Perform a spline fit of the data.
C
C     The old x-array is X1; the old y-array is Y1.  The new x-array is
C     X2; the new y-array is Y2.  The new x-array is equally spaced.
C
          CALL SPCOEF(N, X1, Y1, S, INDEX)
          XMIN = X1(1)
          XMAX = X1(1)
          DO I = 2, N
          XMIN = AMIN1(XMIN, X1(I))
          XMAX = AMAX1(XMAX, X1(I))
          ENDDO
          DO I = 1, N
          X2(I) = XMIN + (XMAX - XMIN) * FLOAT(I-1)/FLOAT(N-1)
```

351

```fortran
      ENDDO
      DO I = 1, N
      Y2(I) = SPLINE(N, X1, Y1, S, INDEX, X2(I))
      ENDDO
C
C     Smooth the data.  For data points where 4.LE.I.LE.N-3, a seven
C     point running average is performed, i.e.
C
C        YNEW(I) = Y2(I-3) + Y2(I-2) + Y2(I-1) + Y2(I)
C                      + Y2(I+1) + Y2(I+2) + Y2(I+3)
C
         DO I = 4, N-3
         YNEW(I) = Y2(I-3) + Y2(I-2) + Y2(I-1) + Y2(I) + Y2(I+1)
     1                    + Y2(I+2) + Y2(I+3)
         ENDDO
         YNEW(1) = 4.0E0 * Y2(1) + Y2(2) + Y2(3) + Y2(4)
         YNEW(2) = Y2(1) + 3.0E0 * Y2(2) + Y2(3) + Y2(4) + Y2(5)
         YNEW(3) = Y2(1) + Y2(2) + 2.0E0 * Y2(3) + Y2(4) + Y2(5) + Y2(6)
         YNEW(N-2) = Y2(N-5) + Y2(N-4) + Y2(N-3) + 2.0E0 * Y2(N-2)
     1                    + Y2(N-1) + Y2(N)
         YNEW(N-1) = Y2(N-4) + Y2(N-3) + Y2(N-2) + 3.0E0 * Y2(N-1)
     1                    + Y2(N)
         YNEW(N) = Y2(N-3) + Y2(N-2) + Y2(N-1) + 4.0E0 * Y2(N)
         DO I = 1, N
         YNEW(I) = YNEW(I)/7.0E0
         ENDDO
         WRITE (10,9) TITLE(1:99)//'SMOOTH/'//TITLE(107:132)
         WRITE (10,*) N
         WRITE (10,*) (X2(I), I = 1, N)
         WRITE (10,*) (YNEW(I), I = 1, N)
         CLOSE (UNIT = 5)
         CLOSE (UNIT = 10)
C
C     Query for more smoothing
C
  702    WRITE (*,21)
   21    FORMAT (1X,'$ Do you want to perform any more smoothing? ',
     1          '(Y or N)')
         READ (*,9,ERR=702) ANS
         IF ((ANS.EQ.'Y').OR.(ANS.EQ.'y')) GO TO 1
   99    CONTINUE
         WRITE (*,22)
   22    FORMAT (1X,'$ Subroutine SMOOTH is ending now.')
         CLOSE (UNIT=10)
         RETURN
         END



      SUBROUTINE EXCHANGE
      DIMENSION X(1000), Y(1000)
      CHARACTER*132 TITLE, INFILE, OUTFILE
      CHARACTER*1 ANS
```

352

```
C
C       This subroutine exchanges the x- and y-values in a plot compatible
C       data file.
C
    1       CONTINUE
  700       WRITE (*,5)
    5       FORMAT (1X,'$ Enter input file name to exchange axes values.')
            READ (*,9,ERR=700) INFILE
  701       WRITE (*,10)
   10       FORMAT (1X,'$ Enter output file name.')
            READ (*,9,ERR=701) OUTFILE
            OPEN (UNIT=5,STATUS='OLD',FILE=INFILE,READONLY)
            REWIND (UNIT=5)
            OPEN (UNIT=10,STATUS='NEW',FILE=OUTFILE)
            READ (5,9) TITLE
    9       FORMAT (A)
            READ (5, *) N
            READ (5, *) (X(I), I = 1, N)
            READ (5, *) (Y(I), I = 1, N)
            WRITE (10,9) TITLE(1:106)//'EXCHANGE/'//TITLE(116:132)
            WRITE (10,*) N
            WRITE (10, *) (Y(I), I = 1, N)
            WRITE (10, *) (X(I), I = 1, N)
            CLOSE (UNIT=5)
            CLOSE (UNIT=10)
C
C       Query for more transformations
C
  702       WRITE (*,21)
   21       FORMAT (1X,'$ Do you want to perform any more data exchanges?',
     1          ' (Y or N)')
            READ (*,9,ERR=702) ANS
            IF ((ANS.EQ.'Y').OR.(ANS.EQ.'y')) GO TO 1
            WRITE (*,22)
   22       FORMAT (1X,'$ Subroutine EXCHANGE is ending now.')
            RETURN
            END
```

```
        SUBROUTINE FOURIER
C
C       This subroutine performs a Fourier smoothing of a plot compatible
C       file.
C
C
C       This subroutine was adapted from a program written by Lt. Stephen
C       W. R. Warren and Brian Woolweber of AFWL/AWPPE.  Their program was
C       adapted from the article "Fourier Smoothing Without the Fourier
C       Transform" published in BYTE magazine, February 1985, pp. 207-218.
C
        REAL FK(1000), III(1000), R(1000), SND(1000), X1(1000)
        REAL X2(1000), Y1(1000), Y2(1000), YT(1000)
        REAL BINT, C, PI, RO, S, SLOPE, SUMFR, SUMFRC, SUMI, SUMR,
```

```fortran
      1                   SUMY, TEMP, XMIN, XMAX, YO, YTO
         INTEGER INDEX(1000)
         INTEGER E
         CHARACTER*132 INFILE, OUTFILE, TITLE
         CHARACTER*1 ANS
      1     WRITE (*,10)
     10     FORMAT (1X,'$ Enter the file name to be Fourier smoothed.')
            READ (*,9,ERR=1) INFILE
      2     WRITE (*,15)
     15     FORMAT (1X,'$ Enter the output file name.')
            READ (*,9,ERR=2) OUTFILE
      9     FORMAT (A)
            OPEN (UNIT=10,NAME=INFILE,TYPE='OLD',READONLY)
            REWIND (UNIT=10)
            READ (10,9) TITLE
            READ (10,*) N
            READ (10,*) (X1(I),I=1,N)
            READ (10,*) (Y1(I),I=1,N)
C
C     Perform a spline fit of the data.
C
C     The old x-array is X1; the old y-array is Y1.  The new x-array is
C     X2; the new y-array is Y2.  The X2 array is equally spaced.
C
         CALL SPCOEF(N, X1, Y1, SND, INDEX)
         XMIN = X1(1)
         XMAX = X1(1)
         DO I = 2, N
         XMIN = AMIN1(XMIN, X1(I))
         XMAX = AMAX1(XMAX, X1(I))
         ENDDO
         DO I = 1, N
         X2(I) = XMIN + (XMAX - XMIN) * FLOAT(I-1)/FLOAT(N-1)
         ENDDO
         DO I = 1, N
         Y2(I) = SPLINE(N, X1, Y1, SND, INDEX, X2(I))
         ENDDO
            CLOSE (UNIT=10)
C
C     Begin the Fourier smoothing process
C
         SLOPE = (Y2(N) - Y2(1))/(X2(N) - X2(1))
         BINT = Y2(1) - SLOPE * X2(1)
         DO I = 1, N
         Y2(I) = Y2(I) - SLOPE * X2(I) - BINT
         ENDDO
      3     WRITE(*,11)
     11     FORMAT (1X,'$ Enter the value of E: 0 < E < (N/2)')
            READ (*,*,ERR=3) E
            IF (E.LT.1) THEN
               WRITE (*,21) E
     21         FORMAT (1X,' E must be greater than or equal to 1; E =',I6)
               GO TO 3
            ENDIF
```

```fortran
        IF (E.GE.(N/2)) THEN
           WRITE (*,22) (N/2)
22         FORMAT (1X,' E has been limited to ',I6)
           E = N/2
        ENDIF
        WRITE (*,12)
12      FORMAT (/,1X,'Performing R(k) calculations',/)
        PI = 4.0E0 * ATAN(1.0E0)
        YO = Y2(1)
        SUMY = 0.0E0
        DO I = 1, N
           SUMY = Y2(I) + SUMY
           IF (I.GE.E) FK(I) = 0.0E0
           IF (I.LT.E) FK(I) = 1.0E0 - (FLOAT(I)/FLOAT(E))**2
        ENDDO
        RO = SUMY/FLOAT(N)
        WRITE (*,12)
        DO K = 1, (E-1)
           SUMR = 0.0E0
           DO J = 1, (N-1)
              TEMP = FLOAT(J) * FLOAT(K)/FLOAT(N)
              C = COS(2.0E0 * PI * TEMP)
              SUMR = Y2(J) * C + SUMR
           ENDDO
           R(K) = (YO + SUMR)/FLOAT(N)
        ENDDO
        WRITE(*,13)
13      FORMAT (/, 1X, 'Performing I(k) calculations', /)
        DO K = 1, (E-1)
           SUMI = 0.0E0
           DO J = 1, (N-1)
              TEMP = FLOAT(J) * FLOAT(K)/FLOAT(N)
              S = SIN(2.0E0 * PI * TEMP)
              SUMI = Y2(J) * S + SUMI
           ENDDO
           III(K) = -SUMI/FLOAT(N)
        ENDDO
        SUMFR = 0.0E0
        DO K = 1, (E-1)
           SUMFR = FK(K) * R(K) + SUMFR
        ENDDO
        YTO = RO + 2.0E0 * SUMFR
        DO J = 1, (N-1)
           SUMFRC = 0.0E0
           DO K = 1, (E-1)
              TEMP = FLOAT(J) * FLOAT(K)/FLOAT(N)
              S = SIN(2.0E0 * PI * TEMP)
              C = COS(2.0E0 * PI * TEMP)
              SUMFRC = FK(K) * R(K) * C - FK(K) * III(K) * S + SUMFRC
           ENDDO
           YT(J) = RO + 2.0E0 * SUMFRC
        ENDDO
        Y2(1) = YTO
        DO I = 2, N
```

```fortran
            Y2(I) = YT(I-1)
         ENDDO
         DO I = 1, N
            Y2(I) = Y2(I) + SLOPE * X2(I) + BINT
         ENDDO
         OPEN (UNIT=20,NAME=OUTFILE,TYPE='NEW')
         WRITE (20,9) TITLE(1:116)//'FOURIER/'//TITLE(125:132)
         WRITE (20,*) N
         WRITE (20,*) (X2(I), I = 1, N)
         WRITE (20,*) (Y2(I), I = 1, N)
         CLOSE (UNIT = 20)
C
C     Query to see if more Fourier smoothing is needed
C
  700       WRITE (*,30)
   30 FORMAT (1X,'$ Do you want to Fourier smooth any more data? ',
      1          '(Y or N)')
         READ (*,9,ERR=700) ANS
         IF ((ANS.EQ.'Y').OR.(ANS.EQ.'y')) GO TO 1
         WRITE (*,31)
   31 FORMAT (1X,'$ Subroutine FOURIER is ending now.')
         RETURN
         END
```

NOTE: Repeated attempts were made to obtain permission from the
copyright holder to present SUBROUTINE SIMP, SUBROUTINE SPCOEF and
FUNCTION SPLINE. The copyright holder, the publisher of the text in
which the coding appeared, chose not to respond to the requests for use.
Since the copyright holder must approve any presentation of copyrighted
material, this coding is not presented. For those who wish to know the
details of the coding, they should refer to the text in which the coding
appeared. It is NUMERICAL COMPUTING: an introduction by Lawrence F.
Shampine and Richard C. Allen, Jr. It is published by W. B. Saunders,
West Washington Square, Philadelphia PA and is copyright 1973.

APPENDIX D

EXPERIMENTAL DATA SUMMARY

In reporting peak currents at different axial positions, it should be
noted that current is recorded over a period of about 5 μs. Any current
after that time is lost. Some axial peak current data may be inaccurate
if peak current occurs near or after the end of the data. If peak axial
current occurs at the outer edge of the photographic data record, this
is noted by identifying peak current at that axial position with an
asterisk (e.g., 1.0 MA*).

The format for this experimental summary is:

Shot Number
    Applied voltage.
    Total peak transmission line current (if any) and time of
        peak after current rise.
    Total peak gun current (if any) and time of peak after current
        rise.
    Peak recorded bottom current (if any).
    Peak recorded mid-bottom current (if any).
    Peak recorded mid-top current (if any).
    Peak recorded top current (if any).
    Number of Ag detector counts/equivalent number of neutrons.
    Gas valve description.
    Comments (if any).

The actual experimental data summary follows.

357

Shot D2901

Applied voltage 60 kV.

Peak recorded bottom current 1.47 MA.

Peak recorded mid-bottom current 0.56 MA.

Peak recorded top current 0.18 MA.

221 Ag detector counts/2.8×10^6 neutrons.

One gas valve--lower gas valve, valve delay 1100 µs.

Clearing shot.

Shot D2902

Applied voltage 60 kV.

146 Ag detector counts/0 neutrons.

One gas valve--lower gas valve, valve delay 1100 µs.

Prefire.

Shot D3001

Applied voltage 60 kV.

Peak total gun current of 1.43 MA at 1.02 µs after current
rise.

Peak recorded bottom current 1.05 MA.

Peak recorded mid-bottom current 1.11 MA.

Peak recorded mid-top current 1.01 MA.

Peak recorded top current 1.00 MA.

926 Ag detector counts/1.2×10^7 neutrons.

One gas valve--lower gas valve, valve delay 1100 µs.

Clearing shot.

Shot D3002

Applied voltage 60 kV.

Peak total gun current of 1.31 MA at 2.5 μs after current
rise.

Peak recorded bottom current 0.81 MA.

Peak recorded mid-bottom current 0.62 MA.

Peak recorded mid-top current 0.40 MA.

Peak recorded top current 0.48* MA.

1092 Ag detector counts/1.4×10^7 neutrons.

One gas valve--lower gas valve, valve delay 1100 μs.

Shot SD3003

Applied voltage 60 kV.

Peak total gun current of 1.29 MA at 1.3 μs after current
rise.

Peak recorded bottom current 1.07 MA.

Peak recorded mid-bottom current 1.05 MA.

Peak recorded mid-top current 0.98 MA.

Peak recorded top current 1.06 MA*.

618 Ag detector counts/7.7×10^6 neutrons.

One gas valve--lower gas valve, valve delay 1075 μs.

Shot D3004

Applied voltage 60 kV.

Peak total transmission line current of 1.56 MA at 3.6 μs
after current rise.

Peak total gun current of 1.24 MA at 1.3 μs after current
rise.

Peak recorded bottom current 1.06 MA.

Peak recorded mid-bottom current 1.08 MA.

Peak recorded mid-top current 0.98 MA.

Peak recorded top current 1.06 MA*.

736 Ag detector counts/9.2×10^6 neutrons.

One gas valve--lower gas valve, valve delay 1075 μs.

359

Shot D3005

Applied voltage 60 kV.

Peak total transmission iine current of 1.73 MA at 3.0 μs after current rise.

Peak total gun current of 1.44 MA at 3.3 μs after current rise.

Peak recorded bottom current 0.97 MA.

Peak recorded mid-bottom currer⸴ 1.05 MA.

Peak recorded mid-top current 0.95 MA.

Peak recorded top current 0.97 MA.

884 Ag detector counts/1.1×10^7 neutrons.

One gas valve--lower gas valve, valve delay 1100 μs.

Shot D3006

Applied voltage 60 kV.

Peak total transmission line current of 2.41 MA at 3.2 μs after current rise.

Peak total gun current of 1.39 MA at 2.9 μs after current rise.

Peak recorded bottom current 1.07 MA*.

Peak recorded mid-bottom current 0.79 MA.

Peak recorded mid-top current 0.66 MA.

Peak recorded top current 0.68 MA.

1861 Ag detector counts/2.3×10^7 neutrons.

One gas valve--lower gas valve, valve delay 1125 μs.

Shot D3007

Applied voltage 60 kV.

Peak total transmission line current of 1.78 MA at 3.3 μs

after current rise.

Peak total gun current of 1.44 MA at 1.3 µs after current rise.

Peak recorded bottom current 1.10 MA.

Peak recorded mid-bottom current 1.11 MA.

Peak recorded mid-top current 0.90 MA.

Peak recorded top current 1.07 MA[*].

943 Ag detector counts/1.2×10^7 neutrons.

One gas valve--lower gas valve, valve delay 1125 µs.

Shot D3008

Applied voltage 60 kV.

Peak total transmission line current of 1.67 MA at 1.2 µs after current rise.

Peak total gun current of 1.56 MA at 1.1 µs after current rise.

Peak recorded bottom current 1.17 MA.

Peak recorded mid-bottom current 1.21 MA.

Peak recorded mid-top current 0.98 MA.

Peak recorded top current 0.97 MA[*].

2503 Ag detector counts/3.1×10^7 neutrons.

One gas valve--lower gas valve, valve delay 1150 µs.

Shot D3009

Applied voltage 60 kV.

Peak total transmission line current of 1.98 MA at 1.7 µs after current rise.

Peak total gun current of 1.65 MA at 1.4 µs after current rise.

Peak recorded bottom current 1.19 MA.

Peak recorded mid-bottom current 1.21 MA.

Peak recorded mid-top current 0.96 MA[*].

361

Peak recorded top current 0.92 MA[*].

3485 Ag detector counts/4.4×10^7 neutrons.

One gas valve--lower gas valve, valve delay 1150 μs.

Shot D3010

Applied voltage 60 kV.

Peak total transmission line current of 1.83 MA at 3.2 μs after current rise.

Peak total gun current of 1.40 MA at 1.2 μs after current rise.

Peak recorded bottom current 1.05 MA.

Peak recorded mid-bottom current 1.09 MA.

Peak recorded mid-top current 0.86 MA[*].

Peak recorded top current 0.89 MA.

2351 Ag detector counts/3.0×10^7 neutrons.

One gas valve--lower gas valve, valve delay 1150 μs.

Shot D3011

Applied voltage 60 kV.

Peak total transmission line current of 3.77 MA at 1.5 μs after current rise.

146 Ag detector counts/0 neutrons.

One gas valve--lower gas valve, valve delay 1175 μs.

Short shot.

Shot D3012

Applied voltage 70 kV.

Peak total transmission line current of 4.29 MA at 1.4 μs after current rise.

172 Ag detector counts/0 neutrons.

One gas valve--lower gas valve, valve delay 1150 μs.
Short shot.

Shot J0501

Applied voltage 70 kV.

Peak total transmission line current of 4.59 MA at 1.5 μs
after current rise.

141 Ag detector counts/0 neutrons.

One gas valve--lower gas valve, valve delay 1150 μs.

Short shot.

Shot J0601

Applied voltage 60 kV.

Peak total transmission line current of 1.81 MA at 1.0 μs
after current rise.

165 Ag detector counts/0 neutrons.

One gas valve--lower gas valve, valve delay 1200 μs.

Short shot.

Shot J0602

Applied voltage 60 kV.

Peak total transmission line current of 3.87 MA at 1.6 μs
after current rise.

144 Ag detector counts/0 neutrons.

One gas valve--lower gas valve, valve delay 1200 μs.

Short shot.

Shot J0603

Applied voltage 60 kV.

Peak total transmission line current of 3.25 MA at 1.8 μs after current rise.

155 Ag detector counts/0 neutrons.

One gas valve--lower gas valve, valve delay 1150 μs.

Short shot.

Shot J0701

Applied voltage 60 kV.

Peak total transmission line current of 1.65 MA at 1.3 μs after current rise.

Peak total gun current of 1.54 MA at 1.2 μs after current rise.

Peak recorded bottom current 1.16 MA.

Peak recorded mid-bottom current 1.12 MA.

Peak recorded mid-top current 1.01 MA*.

Peak recorded top current 0.89 MA*.

4625 Ag detector counts/5.8×10^7 neutrons.

One gas valve--lower gas valve, valve delay 1150 μs.

Clearing shot.

Shot J0702

Applied voltage 60 kV.

Peak total transmission line current of 2.24 MA at 2.5 μs after current rise.

Peak total gun current of 1.92 MA at 2.4 MA at 2.4 μs after current rise.

Peak recorded bottom current 1.02 MA.

Peak recorded mid-bottom current 1.00 MA.

Peak recorded mid-top current 0.83 MA*.

Peak recorded top current 0.61 MA.

1635 Ag detector counts/2.0×10^7 neutrons.

One gas valve--lower gas valve, valve delay 1150 µs.

Shot J0703

Applied voltage 60 kV.

Peak total transmission line current of 1.65 MA at 3.2 µs after current rise.

Peak total gun current of 1.57 MA at 3.2 after current rise.

Peak recorded bottom current 1.29 MA.

Peak recorded mid-bottom current 1.32 MA.

Peak recorded mid-top current 0.93 MA[*].

Peak recorded top current 0.64 MA[*].

12543 Ag detector counts/1.6×10^8 neutrons.

One gas valve--lower gas valve, valve delay 1150 µs.

Shot J0704

Applied voltage 60 kV.

Peak total transmission line current of 3.75 MA at 1.9 µs after current rise.

164 Ag detector counts/0 neutrons.

One gas valve--lower gas valve, valve delay 1125 µs.

Short shot.

Shot J0705

Applied voltage 60 kV.

Peak total transmission line current of 3.64 MA at 2.0 µs after current rise.

133 Ag detector counts/0 neutrons.

One gas valve--lower gas valve, valve delay 1150 µs.

Short shot.

365

Shot J0706

Applied voltage 60 kV.

Peak total transmission line current of 1.85 MA at 3.3 µs after current rise.

Peak total gun current of 1.4 MA at 1.2 µs after current rise.

Peak recorded bottom current 1.24 MA.

Peak recorded mid-bottom current 1.23 MA.

Peak recorded mid-top current 1.03 MA.

Peak recorded top current 0.85 MA.

3170 Ag detector counts/4.0×10^7 neutrons.

One gas valve--lower gas valve, valve delay 1150 µs.

Shot J0707

Applied voltage 60 kV.

Peak total transmission line current of 1.77 MA at 2.9 µs after current rise.

Peak total gun current of 1.55 MA at 1.3 µs after current rise.

Peak recorded bottom current 1.16 MA.

Peak recorded mid-bottom current 1.11 MA.

Peak recorded mid-top current 0.89 MA*.

Peak recorded top current 0.75 MA*.

5877 Ag detector counts/7.4×10^7 neutrons.

One gas valve--lower gas valve, valve delay 1200 µs.

Shot J0708

Applied voltage 60 kV.

Peak recorded bottom current 1.06 MA.

Peak recorded mid-bottom current 1.04 MA.

Peak recorded mid-top current 0.86 MA.

Peak recorded top current 0.76 MA*.

3347 Ag detector counts/4.2×10^7 neutrons.

One gas valve--lower gas valve, valve delay 1200 μs.

Shot J0709

Applied voltage 60 kV.

Peak total transmission line current of 3.58 MA at 2.1 μs
after current rise.

160 Ag detector counts/0 neutrons.

One gas valve--lower gas valve, valve delay 1250 μs.

Shot J0901

Applied voltage 60 kV.

170 Ag detector counts/0 neutrons.

One gas valve--lower gas valve, valve delay 1150 μs.

Clearing shot.

Shot J0902

Applied voltage 60 kV.

Peak total gun current of 1.76 MA at 2.6 μs after current
rise.

Peak recorded bottom current 1.03 MA.

Peak recorded mid-bottom current 1.01 MA.

Peak recorded mid-top current 0.86 MA.

Peak recorded top current 0.66 MA*.

5428 Ag detector counts/6.9×10^7 neutrons.

One gas valve--lower gas valve, valve delay 1150 μs.

Shot J0903

Applied voltage 60 kV.

Peak total transmission line current of 2.39 MA at 2.4 μs after current rise.

Peak total gun current of 2.09 MA at 1.9 μs after current rise.

Peak recorded bottom current 1.06 MA.

Peak recorded mid-bottom current 0.90 MA.

Peak recorded mid-top current 0.64 MA.

Peak recorded top current 0.56 MA.

629 Ag detector counts/7.9×10^6 neutrons.

One gas valve--lower gas valve, valve delay 1150 μs.

Shot J0904

Applied voltage 60 kV.

Peak total transmission line current of 1.90 MA at 2.9 μs after current rise.

Peak total gun current of 1.65 MA at 1.4 μs after current rise.

Peak recorded bottom current 1.11 MA.

Peak recorded mid-bottom current 1.10 MA.

Peak recorded mid-top current 0.74 MA.

Peak recorded top current 0.59 MA.

4137 Ag detector counts/5.2×10^7 neutrons.

One gas valve--lower gas valve, valve delay 1150 μs.

Shot J0905

Applied voltage 60 kV.

Peak total gun current of 2.36 MA at 2.1 μs after current rise.

Peak recorded bottom current 0.86 MA.

Peak recorded mid-bottom current 0.78 MA.

Peak recorded mid-top current 0.59 MA.

Peak recorded top current 0.41 MA.

218 Ag detector counts/2.7×10^6 neutrons.

One gas valve--lower gas valve, valve delay 1200 µs.

Shot J1001

Applied voltage 60 kV.

Peak total transmission line current of 2.34 MA at 1.8 µs
after current rise.

Peak total gun current of 2.12 MA at 1.8 µs after current
rise.

Peak recorded bottom current 1.01 MA.

Peak recorded mid-bottom current 0.85 MA.

Peak recorded mid-top current 0.70 MA.

Peak recorded top current 0.53.

237 Ag detector counts/3.0×10^6 neutrons.

One gas valve--lower gas valve, valve delay 1200 µs.

Clearing shot.

Shot J1002

Applied voltage 60 kV.

Peak total transmission line current of 1.51 MA at 2.9 µs
after current rise.

Peak total gun current of 1.48 MA at 1.1 µs after current
rise.

Peak recorded bottom current 1.24 MA.

Peak recorded mid-bottom current 1.24 MA.

Peak recorded mid-top current 1.10 MA*.

Peak recorded top current 0.95 MA*.

9196 Ag detector counts/1.2×10^8 neutrons.

One gas valve--lower gas valve, valve delay 1175 µs.

369

Shot J1003

Applied voltage 60 kV.

Peak total transmission line current of 1.68 MA at 1.3 μs after current rise.

Peak total gun current of 1.65 MA at 1.4 μs after current rise.

Peak recorded bottom current 1.20 MA.

Peak recorded mid-bottom current 1.28 MA.

Peak recorded mid-top current 1.07 MA.

Peak recorded top current 0.86 MA[*].

3145 Ag detector counts/4.0×10^7 neutrons.

One gas valve--lower gas valve, valve delay 1150 μs.

Shot J1004

Applied voltage 60 kV.

Peak total transmission line current of 3.54 MA at 2.0 μs after current rise.

160 Ag detector counts/0 neutrons.

One gas valve--lower gas valve, valve delay 1125 μs.

Short shot; plug did not fire.

Shot J1005

Applied voltage 60 kV.

Peak recorded bottom current 0.96 MA.

Peak recorded mid-bottom current 0.92 MA.

Peak recorded mid-top current 0.75 MA.

Peak recorded top current 0.55 MA[*].

5725 Ag detector counts/7.3×10^7 neutrons.

One gas valve--lower gas valve, valve delay 1125 μs.

Shot J1006

Applied voltage 60 kV.

Peak total transmission line current of 2.96 MA at 2.5 μs after current rise.

Peak total gun current of 1.53 MA at 1.6 μs after current rise.

Peak recorded bottom current 0.93 MA.

Peak recorded mid-bottom current 0.97 MA.

Peak recorded mid-top current 0.72 MA.

Peak recorded top current 0.62 MA.

351 Ag detector counts/4.4×10^6 neutrons.

One gas valve--lower gas valve, valve delay 1125 μs.

Gas regulator problems; D_2 gas pressure 925 psig.

Shot J1007

Applied voltage 60 kV.

Peak total transmission line current of 1.79 MA at 1.2 μs after current rise.

Peak total gun current of 1.46 MA at 1.3 μs after current rise.

Peak recorded bottom current 1.20 MA.

Peak recorded mid-bottom current 1.27 MA.

Peak recorded mid-top current 0.91 MA.

Peak recorded top current 0.78 MA[*].

3969 Ag detector counts/5.0×10^7 neutrons.

One gas valve--lower gas valve, valve delay 1125 μs.

Shot J1008

Applied voltage 60 kV.

Peak total transmission line current of 2.66 MA at 2.2 μs

371

after current rise.

Peak total gun current of 2.22 MA at 1.5 μs after current rise.

Peak recorded bottom current 0.81 MA.

Peak recorded mid-bottom current 0.54 MA.

Peak recorded mid-top current 0.40 MA.

Peak recorded top current 0.23 MA.

399 Ag detector counts/5.0×10^6 neutrons.

One gas valve--lower gas valve, valve delay 1125 μs.

Shot J1009

Applied voltage 60 kV.

Peak total transmission line current of 1.62 MA at 1.3 μs after current rise.

Peak total gun current of 1.52 MA at 1.3 μs after current rise.

Peak recorded bottom current 1.22 MA.

Peak recorded mid-bottom current 1.37 MA.

Peak recorded mid-top current 1.02 MA.

Peak recorded top current 0.82 MA*.

2043 Ag detector counts/1.1×10^8 neutrons.

Two gas valves--lower gas valve, valve delay 1150 μs;
upper gas valve, valve delay 3750 μs.

Shot J1101

Applied voltage 60 kV.

Peak total transmission line current of 3.93 MA at 1.7 μs after current rise.

163 Ag detector counts/0 neutrons.

Two gas valves--lower gas valve, valve delay 1150 μs;
upper gas valve, valve delay 3750 μs.

Clearing shot. Prefire. Upper gas valve did not fire.

Shot J1102

Applied voltage 60 kV.

Peak total transmission line current of 3.16 MA at 1.9 μs
after current rise.

174 Ag detector counts/0 neutrons.

Two gas valves--lower gas valve, valve delay 1150 μs;
upper gas valve, valve delay 3750 μs.

Prefire. Upper gas valve did not fire.

Shot J1103

Applied voltage 60 kV.

Peak total transmission line current of 2.62 MA at 2.4 μs
after current rise.

Peak total gun current of 1.96 MA at 2.1 μs after current
rise.

Peak recorded bottom current 0.96 MA.

Peak recorded mid-bottom current 0.78 MA.

Peak recorded mid-top current 0.57 MA.

Peak recorded top current 0.51 MA.

425 Ag detector counts/2.3×10^7 neutrons.

Two gas valves--lower gas valve, valve delay 1150 μs;
upper gas valve, valve delay 3750 μs.

Shot J1104

Applied voltage 60 kV.

Peak total transmission line current of 1.77 MA at 1.4 μs
after current rise.

Peak total gun current of 1.70 MA at 1.5 μs after current
rise.

373

Peak recorded bottom current 1.20 MA.

Peak recorded mid-bottom current 1.13 MA.

Peak recorded mid-top current 0.87 MA[*].

Peak recorded top current 0.73 MA[*].

2094 Ag detector counts/1.1×10^8 neutrons.

Two gas valves--lower gas valve, valve delay 1150 μs;

upper gas valve, valve delay 3750 μs.

Shot J1105

Applied voltage 60 kV.

Peak total transmission line current of 1.74 MA at 3.1 μs
after current rise.

Peak total gun current of 1.51 MA at 1.1 μs after current
rise.

Peak recorded bottom current 1.30 MA.

Peak recorded mid-bottom current 1.21 MA.

Peak recorded mid-top current 1.03 MA.

Peak recorded top current 0.98 MA[*].

7187 Ag detector counts/3.9×10^8 neutrons.

Two gas valves--lower gas valve, valve delay 1150 μs;

upper gas valve, valve delay 3750 μs.

Shot J1106

Applied voltage 60 kV.

Peak total transmission line current of 1.60 MA at 1.1 μs
after current rise.

Peak total gun current of 1.53 MA at 1.2 μs after current
rise.

Peak recorded bottom current 1.18 MA.

Peak recorded mid-bottom current 1.24 MA.

Peak recorded mid-top current 0.53 MA.

Peak recorded top current 0.89 MA[*].

374

3518 Ag detector counts/1.9×10^8 neutrons.

Two gas valves--lower gas valve, valve delay 1150 µs;
upper gas valve, valve delay 3800 µs.

Shot J1107

Applied voltage 60 kV.

Peak total transmission line current of 1.58 MA at 1.2 µs
after current rise.

Peak total gun current of 1.58 MA at 1.2 µs after current
rise.

Peak recorded bottom current 1.21 MA.

Peak recorded mid-bottom current 1.27 MA.

Peak recorded mid-top current 0.75 MA[*].

Peak recorded top current 0.78 MA[*].

5177 Ag detector counts/2.8×10^8 neutrons.

Two gas valves--lower gas valve, valve delay 1150 µs;
upper gas valve, valve delay 3800 µs.

Shot J1108

Applied voltage 60 kV.

Peak total transmission line current of 1.60 MA at 1.2 µs
after current rise.

Peak total gun current of 1.69 MA at 1.3 µs after current
rise.

Peak recorded bottom current 1.32 MA.

Peak recorded mid-bottom current 1.22 MA.

Peak recorded mid-top current 1.00 MA[*].

Peak recorded top current 0.78 MA[*].

5790 Ag detector counts/3.1×10^8 neutrons.

Two gas valves--lower gas valve, valve delay 1150 µs;
upper gas valve, valve delay 3850 µs.

Shot J1109

Applied voltage 60 kV.

Peak total transmission line current of 1.65 MA at 1.3 μs after current rise.

Peak total gun current of 1.51 MA at 1.2 μs after current rise.

Peak recorded bottom current 1.27 MA.

Peak recorded mid-bottom current 1.20 MA.

Peak recorded mid-top current 1.05 MA.

Peak recorded top current 0.90 MA[*].

2367 Ag detector counts/1.3×10^8 neutrons.

Two gas valves—lower gas valve, valve delay 1150 μs;
upper gas valve, valve delay 3850 μs.

Ag detector tubes changed after this shot.

Shot J1110

Applied voltage 60 kV.

Peak total transmission line current of 1.77 MA at 1.4 μs after current rise.

Peak total gun current of 1.61 MA at 1.4 μs after current rise.

Peak recorded bottom current 1.09 MA.

Peak recorded mid-bottom current 1.21 MA.

Peak recorded mid-top current 1.11 MA.

Peak recorded top current 0.85 MA.

2061 Ag detector counts/1.1×10^8 neutrons.

Two gas valves—lower gas valve, valve delay 1150 μs;
upper gas valve, valve delay 3850 μs.

Shot J1111

Applied voltage 60 kV.

Peak total transmission line current of 1.68 MA at 1.1 µs after current rise.

Peak total gun current of 1.48 MA at 1.3 µs after current rise.

Peak recorded bottom current 1.27 MA.

Peak recorded mid-bottom current 1.33 MA.

Peak recorded mid-top current 1.00 MA[*].

Peak recorded top current 0.84 MA[*].

9160 Ag detector counts/5.0×10^8 neutrons.

Two gas valves--lower gas valve, valve delay 1150 µs; upper gas valve, valve delay 3900 µs.

Shot J1201

Applied voltage 60 kV.

Peak total transmission line current of 1.66 MA at 1.2 µs after current rise.

Peak total gun current of 1.54 MA at 1.2 µs after current rise.

Peak recorded bottom current 1.32 MA.

Peak recorded mid-bottom current 1.26 MA.

Peak recorded mid-top current 0.97 MA.

Peak recorded top current 0.79 MA[*].

5514 Ag detector counts/3.0×10^8 neutrons.

Two gas valves--lower gas valve, valve delay 1150 µs; upper gas valve, valve delay 3900 µs.

Clearing shot.